hexagon:2611.00378v1

THE NUMBER OF PLANAR CENTRAL CONFIGURATIONS OF FOUR BODIES

TEJASVI SINGH TOMAR

Abstract. For four positive masses in the plane we determine the number N of central configurations, counted up to rotation, translation and scaling, in terms of one fold surface, whose certified enclosures decide N for all masses outside a closed null set. Of these configurations, 12 are collinear, by Moulton's theorem, and 6 are convex, by the existence theorem of MacMillan and Bartky and the uniqueness proved in the author's preprint arXiv:2609.35632. Through Dziobek's relations, the concave configurations with inner body i form the fibre of a proper mass map of degree 2. Their number c_i, counted up to reflection, is 1, 2, 3 or 4, and we read it off from the position of the mass ratios relative to this surface. Altogether $N = 18 + 2(c_1 + c_2 + c_3 + c_4)$, an even number with $32 \le N \le 50$. Moreover $N = 32$ exactly at Palmore's masses, and every even value in this range occurs. For four equal masses we recover Albouy's count $N = 50$. The proof shows with interval certificates that the mass map is injective where its Jacobian is not positive, obtains its degree from the restricted problem, and analyses its folds, cusps and Palmore's umbilic. A formalization in Lean also proves these results.

1. Introduction

1.1. **Central configurations of four bodies.** Consider four bodies with masses $m_1, \dots, m_4 > 0$ at positions $x_1, \dots, x_4 \in \mathbb{R}^2$. We write $r_{ij} = |x_i - x_j|$, $M = \sum_i m_i$ and $c_m = M^{-1} \sum_i m_i x_i$. A collision-free configuration $x = (x_1, \dots, x_4)$ is a *central configuration* (CC) if

$$\sum_{i \neq j} m_i \frac{x_i - x_j}{r_{ij}^3} = -\lambda (x_j - c_m), \qquad j = 1, \dots, 4, \tag{1.1}$$

for some $\lambda \in \mathbb{R}$. The planar CCs are the configurations of the relative equilibria, the solutions of the Newtonian four-body problem that rotate rigidly about their centre of mass. A non-collinear configuration is *convex* if the four bodies are the vertices of a strictly convex quadrilateral. It is *concave* if one body lies strictly inside the triangle of the other three. Each non-collinear CC is of one of these two types: by the perpendicular bisector theorem [Moe90], no four-body CC has exactly three bodies collinear [HM06, §2.2]. We count CCs modulo similarity in two ways that differ in the treatment of mirror images.

- $N(m)$ is the number of planar CCs up to rotation, translation and scaling. A configuration and its mirror image count separately. In this convention, used in [Mou10, Sim78, HM06], the collinear CCs form $4!/2 = 12$ classes.
- $c_i(m)$ is the number of concave CCs with body i strictly inside the triangle of the other three. It counts up to similarity including reflection: a configuration and its mirror image count once.

Since an orientation-reversing similarity fixes no three non-collinear points, a non-collinear CC is never equivalent, as a labelled configuration, to its mirror image under rotations, translations and scalings. Each class counted by $c_i(m)$ therefore consists of two classes in $N(m)$.

2020 *Mathematics Subject Classification.* 70F10, 70F15, 55M25, 58K05, 65G40.

Key words and phrases. Central configurations, four-body problem, relative equilibria, Dziobek configurations, mapping degree, Whitney cusp, computer-assisted proof, interval arithmetic.

Whether the number of central configurations is finite for all positive masses is a question of Chazy [Cha18] and Wintner [Win41]. Smale listed it as the sixth of his problems for this century [Sma98] (see also [ACS12, Problem 9]). For five bodies in the plane, Albouy and Kaloshin [AK12] proved finiteness except perhaps for masses in an explicit subvariety of codimension 2. For four bodies, Moeckel [Moe01] proved finiteness for almost all masses. Hampton and Moeckel [HM06] proved that $N(m)$ is finite for all positive masses and that $32 \le N(m) \le 8472$. Simó's numerical experiments [Sim78] suggest that $32 \le N(m) \le 50$. Figueras, Tucker and Zgliczyński [FTZ24] named the unrestricted four-body problem as their next challenge, expecting between 32 and 50 relative equilibria. We determine $N(m)$ for every positive mass vector in terms of one function R (Theorems 1 and 2), whose certified enclosures decide $N(m)$ for all m outside a closed null set (Remark 8.3). In particular, the range suggested by Simó's experiments holds for all masses, and every even value in it occurs.

The bound 8472 of [HM06] comes from a count of complex solutions: the mixed volume of a system of ten polynomial equations bounds their number, at most one third of them have real mutual distances, and adding the 12 collinear CCs to that third gives 8472 [HM06, §6.2]. We count real configurations directly. The concave CCs with a given inner body are the preimages of a proper map of degree 2, of which at most one has negative Jacobian. At the critical values a local analysis of the map determines their number (Section 1.3). Adding the 12 collinear and the 6 convex CCs, we obtain $N = 12 + 6 + 2\sum_i c_i$.

The term 12 of this count is Moulton's theorem [Mou10] that there are exactly 12 collinear CCs for any choice of masses. For the term 6, MacMillan and Bartky [MB32] proved that each of the three cyclic orders of the bodies is realized by a convex CC (a simpler proof is in [Xia04]). Albouy, Fu and Sun conjectured that this convex CC is unique up to similarity for all masses [AFS08]. This was known when the two ends of a diagonal carry equal masses [Lea03, AFS08]. It is Problem 10 in the list of open problems of Albouy, Cabral and Santos [ACS12]. The author proved it for all cyclic orders and all positive masses in the preprint [Tom26], where the proof, including its computer-assisted part, is also formalized in Lean.

Albouy [Alb95, Alb96] determined the CCs of four equal masses (see also [CCLM15, §1]): there are 50 of them [HM06, §6.1]. For the masses $(1, 1, 1, m_4)$, Rusu and Santoprete [RS16] computed the CCs numerically and established the fold and pitchfork bifurcations with interval methods. Their table lists the numbers D of solutions of the Dziobek equations. Since these equations are written in the mutual distances, their solutions are the non-collinear CCs up to similarity including reflection. With the 12 collinear CCs this means $N = 12 + 2D$. In the table of Rusu and Santoprete, N takes the values 32, 38, 44 and 50. Theorem 2(e) shows that the table holds exactly. Liu, Poudel, Raut and Xie [LPRX26] classified the concave kite CCs of these masses by a computer-assisted proof and treated the asymmetric ones numerically. For body 4 inside, their classification rederives a result of Shi and Xie [SX10]. For each m_4 the equilateral triangle with body 4 at its centre is a CC of these masses. Palmore found that it is degenerate for $m_4 = m^* = (81 + 64\sqrt{3})/249$ [Pal73, Pal75]. Meyer and Schmidt [MS88] showed that families of isosceles CCs bifurcate from it. For concave kites, whose two off-axis bodies have equal masses, Roberts observed numerically that the mass map on kite configurations is two-to-one [Rob25, §6.2 (arXiv version)].

In Section 12 we also compare our results with two limits of the masses. When the mass of the inner body tends to zero, the limit is the planar restricted four-body problem with equilateral primaries. It has 8, 9 or 10 relative equilibria [BL14] (see also [Bar08, BL11]). Figueras, Tucker and Zgliczyński [FTZ24] gave a computer-aided proof of this count. The limit in which the masses of the three outer bodies tend to zero is studied in [CCLM15]. Among other computer-assisted counts of CCs, all CCs of 5, 6 and 7 equal masses in the plane are listed in [MZ19] (see also [LS09]).

1.2. **Results.** For each body i we define in Section 2 a mass map F_i from an open set of spoke lengths to $\mathbb{R}^3$, whose fibre over the point $\mu^{(i)}(m)$ consists of the concave CCs with body i inside. After relabelling the bodies so that $i = 4$,

$$\mu^{(4)}(m) = \Big(\log\frac{m_1}{m_4},\ \log\frac{m_2}{m_4},\ \log\frac{m_3}{m_4}\Big).$$

For another body i and an order (j_1, j_2, j_3) of the other three, $\mu^{(i)}(m)$ is defined in the same way and has the components $\log(m_{j_k}/m_i)$. On $\mathbb{R}^3$ we use the coordinates

$$A = \tfrac{1}{3}(\mu_1+\mu_2+\mu_3), \qquad (P,Q) = \Big(\frac{\mu_1-\mu_2}{\sqrt{2}},\ \frac{\mu_1+\mu_2-2\mu_3}{\sqrt{6}}\Big) = \rho\,(\cos\Theta, \sin\Theta), \tag{1.2}$$

with $\rho \geq 0$ and Θ in the circle $S^1 = \mathbb{R}/360°$. We call the coordinates (A, ρ, Θ) of $\mu^{(i)}(m)$ the *mass coordinates* of body i. In terms of the masses, $A = \log\big((m_{j_1}m_{j_2}m_{j_3})^{1/3}/m_i\big)$; the radius ρ is the distance from the point $(\log m_{j_1}, \log m_{j_2}, \log m_{j_3})$ to the line spanned by $(1,1,1)$. Another order of the outer bodies leaves A and ρ unchanged and changes Θ by an element of the dihedral group D_3 generated by $\Theta \mapsto \Theta + 120°$ and $\Theta \mapsto 180° - \Theta$. The radius ρ vanishes exactly when the three outer masses are equal. For $\rho > 0$, $\Theta \in \{90°, 210°, 330°\}$ exactly when two outer masses are equal and the third is smaller, and $\Theta \in \{30°, 150°, 270°\}$ exactly when two outer masses are equal and the third is larger. Let $m^* = (81 + 64\sqrt{3})/249$ be Palmore's mass ratio and $A^* = -\log m^*$. Then $(A, \rho) = (A^*, 0)$ exactly when the three outer masses are equal to some m_0 and $m_i = m^* m_0$. We then call m a *Palmore mass vector*.

Theorem 1. *There is a continuous function $R : \mathbb{R} \times S^1 \to [0, \infty)$, invariant under D_3 in its second argument, with $R(A, \Theta) = 0$ if and only if $A = A^*$, such that the following holds. For every positive mass vector m and every body i, the number $c_i(m)$ is given by Table 1 in terms of the mass coordinates (A, ρ, Θ) of body i. The critical values of F_i are exactly the points of $\mathbb{R}^3$ with $\rho = R(A, \Theta)$.*

mass coordinates (A, ρ, Θ) of body i	$c_i(m)$
$\rho < R(A, \Theta)$	4
$\rho > R(A, \Theta)$	2
$\rho = R(A, \Theta)$, $A \neq A^*$, $\Theta \in \{90°, 210°, 330°\}$ (cuspidal edge)	2
$\rho = R(A, \Theta)$, $A \neq A^*$, $\Theta \notin \{90°, 210°, 330°\}$ (fold sheet)	3
$A = A^*$, $\rho = 0$ (Palmore mass vector)	1

TABLE 1. The number $c_i(m)$ of concave CCs with body i inside (Theorem 1).

For $A \neq A^*$, the critical values of F_i at the level A form the star-shaped curve $\rho = R(A, \Theta)$ around the axis $\rho = 0$. Each of them has exactly one critical point in its fibre (Section 8). In this way one surface in $\mathbb{R}^3$, the same for the four bodies, determines all the numbers $c_i(m)$. Figure 1 shows it on the rays $\Theta = 90°$ and $\Theta = 270°$. Let Z_i be the set of masses $m \in (0, \infty)^4$ for which $\mu^{(i)}(m)$ is a critical value of F_i. Each Z_i is a closed null set (Proposition 6.1 and Section 8.4).

Theorem 2. *For all positive masses m,*

$$N(m) = 12 + 6 + 2\,\big(c_1(m) + c_2(m) + c_3(m) + c_4(m)\big).$$

Here 12 counts the collinear CCs [Mou10] *and 6 the convex CCs, by the existence theorem of* [MB32, Xia04] *and the uniqueness theorem of the preprint* [Tom26]. *Moreover the following hold.*

(a) *$N(m)$ is even and $32 \leq N(m) \leq 50$.*

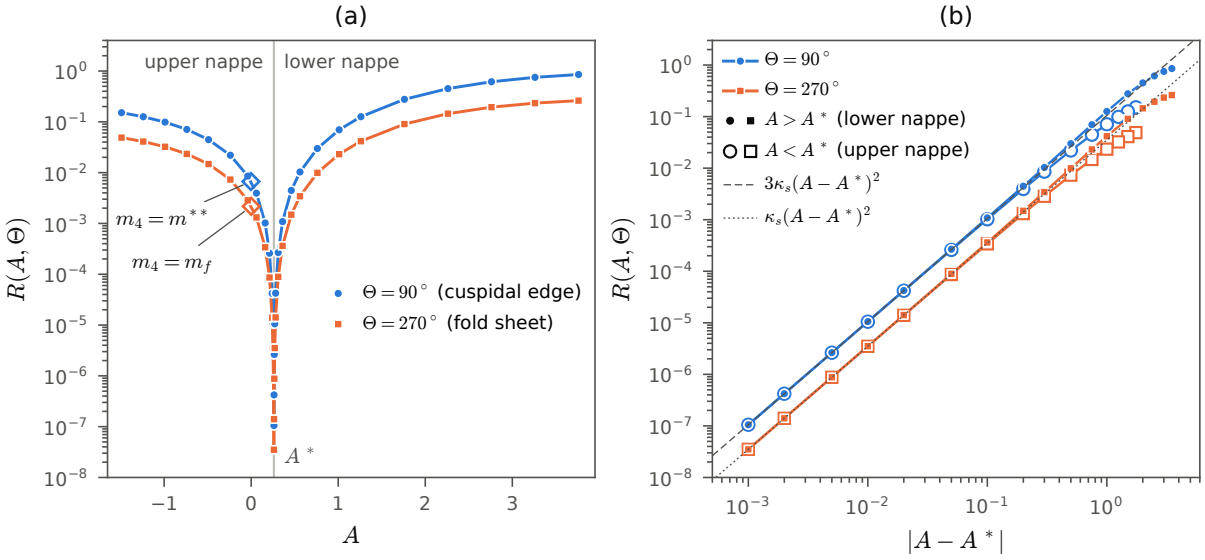


FIGURE 1. The surface of critical values $\rho = R(A, \Theta)$ of Theorem 1 on the mirror rays $\Theta = 90^\circ$ (cuspidal edge) and $\Theta = 270^\circ$ (fold sheet), at 32 levels of A from $A^* - 1.75$ to $A^* + 3.5$, against A, with R on a logarithmic axis (a), and against $|A - A^*|$ on logarithmic axes (b). The marks are circles on the ray $\Theta = 90^\circ$ and squares on the ray $\Theta = 270^\circ$. In (b) they are filled on the lower nappe ($A > A^*$) and open on the upper nappe ($A < A^*$). In (a) the ten levels with $|A - A^*| \le 0.02$ crowd near A^*, where their marks overlap; (b) separates them. All plotted values of R are certified enclosures, of radius less than 10^{-71}, from the mirror system of Section 9.1. The lines between the levels are drawn for the eye. The values of R at the other angles, which are known only in floating point, are not shown. The reference lines in (b) are $3\kappa_s(A - A^*)^2$ and $\kappa_s(A - A^*)^2$, where $\kappa_s = 0.0351137\ldots$ is computed from the closed forms of Propositions 2.4 and 2.6. They are the asymptotic radii on the two rays as $A \to A^*$ (Proposition 12.1). Near A^* the plotted values lie close to them. The open diamonds in (a) are the mass coordinates of body 1 for the masses $(1, 1, 1, m^{**})$ and $(1, 1, 1, m_f)$, which lie on the surface (Corollary 10.7).

(b) $N(m) = 32$ *if and only if* m *is a Palmore mass vector, that is, up to scaling and relabelling,* $m = (1, 1, 1, m^*)$. *For these masses* $c_4 = 1$ *and* $c_1 = c_2 = c_3 = 2$.

(c) *Let* k, f *and* p *be the numbers of bodies whose mass coordinates lie in the first, the fourth and the fifth row of Table 1. Then* $p \le 1$ *and* $N(m) = 34 + 4k + 2f - 2p$. *In particular* $N(m) = 34 + 4k$ *for* m *outside* $Z_1 \cup Z_2 \cup Z_3 \cup Z_4$.

(d) *Every even value from* 32 *to* 50 *is attained.*

(e) *For the masses* $(1, 1, 1, m_4)$ *with* $m_4 > 0$, $N = 38$ *for* $m_4 \in (0, m^*) \cup (m^*, m^{**}] \cup (m_f, \infty)$, $N = 32$ *for* $m_4 = m^*$, $N = 50$ *for* $m_4 \in (m^{**}, m_f)$ *and* $N = 44$ *for* $m_4 = m_f$, *where* $m^{**} = 0.99184227439\ldots$ *and* $m_f = 1.00266054757\ldots$ *are defined in Section 10. The masses* $(1, 1, 1, m_4)$ *lie in* $Z_1 \cup Z_2 \cup Z_3 \cup Z_4$ *exactly for* $m_4 \in \{m^*, m^{**}, m_f\}$.

(f) *A concave CC is degenerate, in the sense recalled in Section 11, if and only if the Jacobian of the mass map of its inner body vanishes there. Every degenerate concave CC has nullity* 1, *except, for each Palmore mass vector, the equilateral triangle of the three equal masses with the fourth body at its centre, which has nullity* 2. *In the coordinates given by the*

spoke lengths (Lemma 2.1), the degenerate concave CCs with a given inner body form a set homeomorphic to a double cone.

(g) $N(1,1,1,1) = 50$.

Theorem 2 follows from Theorem 1 with the collinear and convex counts of Section 1.1, certified computations of R at exact masses (Section 9), the exact treatment of the family $(1,1,1,m_4)$ in Section 10 and a lemma on degeneracy (Section 11). Section 8.4 contains the details. Through the convex count, the formula for N uses the uniqueness theorem of [Tom26]. Without it the same argument gives $N \geq 18 + 2\sum_i c_i$, because the existence theorem provides at least 6 convex CCs, and N is still even, because convex CCs come in mirror pairs. For the masses $(1,1,1,m_4)$ each cyclic order has a diagonal whose ends carry equal masses, where uniqueness was known [Lea03, AFS08]. Hence the formula for general masses, the bound $N \leq 50$ in (a) and items (c) and (d) depend on [Tom26]; the other items and Theorem 1 do not. Items (a) and (b) show that the lower bound 32 of [HM06] is sharp and is attained exactly at the Palmore mass vectors. Item (e) is the table of Rusu and Santoprete [RS16]. The values 32 and 44 of that table occur at critical values. For $m = (1,1,1,m^*)$ the point $\mu^{(4)}(m)$ is the vertex $(A^*, 0)$ of the surface and $c_4 = 1$. For $m = (1,1,1,m_f)$ the point $\mu^{(1)}(m)$ lies on a fold sheet and $c_1 = c_2 = c_3 = 3$. Item (g) is Albouy's count. For four equal masses the 32 concave CCs are the 8 equilateral configurations with a body at the centre and 24 isosceles ones (Theorem 1 and Proposition 5.2(g)). That $c_i(m) \geq 1$ for all i and m was known: by Hampton's theorem [Ham02] (see [HM06, §6.1]), for all positive masses there is a concave CC with any given body inside.

Theorem 1 also makes the count effective. Off the surface of critical values the sign of $\rho - R(A,\Theta)$ decides $c_i(m)$. An interval enclosure of $R(A,\Theta)$ can be computed by an interval Newton step at a single point of the fold, without a search for other zeros (Remark 8.3). Section 9 will use this to certify N at exactly given masses.

1.3. **The idea of the proof.** Label the inner body 4. A concave CC with body 4 inside, scaled so that $\lambda/M = 1$, is determined up to isometry by its three spoke lengths $a_i = |x_i - x_4|$. Dziobek's relations express the masses as analytic functions of $a = (a_1, a_2, a_3)$ on an open set $\Omega_4 \subset (0,1)^3$, through the angles θ_i at body 4 and an auxiliary quantity K, which a determines implicitly (Lemma 2.2). Then $c_4(m)$ is the number of preimages of the mass ratios under the mass map $F = F_4 : \Omega_4 \to \mathbb{R}^3$. Let J be its Jacobian determinant, $\mathcal{D} = \{J < 0\}$, $\overline{\mathcal{D}} = \{J \leq 0\}$ and $\Sigma = \{J = 0\}$, the *fold*. In the coordinates (1.2) on the target we write $F = (A, G)$ with $G = (P, Q)$. We proceed in six steps, of which step (2) is the main difficulty. Injectivity is a global property, whereas the fold has no closed form away from the axis and interval certificates check only local inequalities. Slicing by the levels of A turns it into statements about the angle of G along the fold curves Γ_c, which sign conditions at the points of the fold can certify.

(1) *The axis.* The symmetric group $\mathfrak{S}_3$ permutes the outer bodies. It acts in the same way on the plane orthogonal to the axis $a_1 = a_2 = a_3$ and on the plane of G. On the axis this reduces dF, in coordinates adapted to the axis, to a diagonal matrix with entries $\partial_s A$, λ_{ax}, λ_{ax}, so that $J = \partial_s A \cdot \lambda_{\mathrm{ax}}^2$ on the axis (Lemma 2.3). Both factors have closed forms (Proposition 2.4). These closed forms show that $\partial_s A < 0$ and that λ_{ax} has exactly one zero s^*, at which the mass ratio is Palmore's value m^*. The Jacobian is negative on the axis except at Palmore's configuration $p^* = s^*(1,1,1)$, the *umbilic*, where dF has rank one.

(2) *Injectivity on $\overline{\mathcal{D}}$.* We prove that F is injective on $\overline{\mathcal{D}}$ (Sections 6.3–6.8). Corbera, Cors and Roberts proposed the same strategy for convex CCs: to prove their uniqueness by showing that a suitably normalized mass map is injective [CCR19]. Interval certificates, together with the lemmas of Section 4, show that $\overline{\mathcal{D}}$ lies in an explicit neighbourhood of the axis,

the fold core, and meets every ray from the axis in an initial segment. Since $\overline{\mathcal{D}}$ meets the plane $s = s^*$ only at p^* (Proposition 5.2(e)), the umbilic splits $\overline{\mathcal{D}}$ into two nappes. On each nappe A is a proper map onto a half-line. The level sets Φ_c of A on a nappe are bounded by curves Γ_c on the fold. Each Γ_c meets each half-plane bounded by the axis exactly once. Along Γ_c the angle of G is monotone, by certified sign conditions. It makes exactly one turn, by the symmetry and a certified half-plane condition. The image of Γ_c under G is then a star-shaped curve C_c (Figure 2). Over the region bounded by C_c the map $G|_{\Phi_c}$ is a covering. A count at one point near the fold shows that it has one sheet. So G maps Φ_c homeomorphically onto the closed region bounded by C_c, and Φ_c is a closed disk. As A separates the level sets and the two nappes, F is injective on $\overline{\mathcal{D}}$.

(3) *The count at regular values.* Let $n_\pm$ be the numbers of preimages of a regular value at which $\pm J > 0$. Since F is proper (Section 6.1), n_+ and n_- are locally constant on the regular values. Step (2) shows that the regular values form three connected sets: the values inside the surface $F(\Sigma)$ with $A > A^*$, those inside it with $A < A^*$, and those outside it. We compute $n_\pm$ at a regular value with $G = 0$ and A very large, that is, for equal outer masses and an almost massless body 4 (Section 6.9). There the preimages lie close to the equilibria of the restricted problem with three equal primaries, inside their triangle. These are a minimum and three saddles of the potential. Since the passage to the limit reverses orientations, $n_- = 1$ and $n_+ = 3$. Near a fold point a normal form of F shows that $n_+ - n_-$ does not change across $F(\Sigma)$. Hence $n_+ - n_- = 2$ at all regular values, that is, F has degree 2. By injectivity $n_- \leq 1$, so $c_4 = 2 + 2n_- \in \{2, 4\}$ at regular values. Corbera, Cors, Llibre and Moeckel count the non-convex relative equilibria of the $(1 + 3)$-body problem by the same principle. The number of preimages of their proper mass map is constant on each component of its regular values, and they evaluate it at one point of each component [CCLM15, Proposition 5 and the proof of Theorem 3]. In their case the critical values form a simple closed curve with three singular points [CCLM15, Proposition 6].

(4) *Critical values.* At a critical value $\mu = F(q)$, injectivity leaves q as the only preimage in $\overline{\mathcal{D}}$. Since the other preimages have $J > 0$, $c_4(\mu) = 3 - k$, where k is the local degree of F at q (Lemma 7.4). As A is a local coordinate everywhere on Ω_4, we compute k for the planar map G on the level surface of A through q. At a fold point, where the angle of G moves along Γ_c, the normal form of step (3) shows that $k = 0$ (Proposition 7.6). On the mirrors $a_i = a_j$, where the angle of G can be stationary, a $\mathbb{Z}/2$-equivariant normal form and a quantitative version of the band lemma show that F has a cusp with $k = 1$ at all cusp points, that is, at the points of the fold other than p^* that lie on a mirror and at which the mirror determinant J_{mir} of Section 3.2 does not vanish (Proposition 7.10). At p^* the map G on the level $A = A^*$ is $c(s^*)\bar{z}^2 + O(|z|^3)$, where $z = x + iy$ is a complex coordinate orthogonal to the axis. The coefficient $c(s^*)$ has a closed form and does not vanish (Proposition 2.6). It follows that $k = 2$ (Proposition 7.11).

(5) *The surface of critical values.* Steps (2) and (4) show that for $c \neq A^*$ the image $F(\overline{\mathcal{D}}) \cap \{A = c\}$ is the closed region bounded by C_c, the curve $\rho = R(c, \Theta)$ of Theorem 1. A value inside C_c has one preimage in $\mathcal{D}$ ($c_4 = 4$), a value outside has none ($c_4 = 2$), and a value on C_c has $c_4 = 3$ or $c_4 = 2$ according as it comes from a fold point or a cusp point. On each nappe the cusp points are the points of the fold on three of the six half-mirrors, which places the cuspidal edges at $\Theta \in \{90°, 210°, 330°\}$ (Proposition 7.13). This yields Table 1 for body 4; the other bodies follow by relabelling.

(6) *Counting.* Theorem 2 then follows as described after its statement.

The interval certificates (Section 5) provide the location of $\overline{\mathcal{D}}$, the transversality of the fold, the sign conditions that make the angle of G monotone, the half-plane condition that fixes its

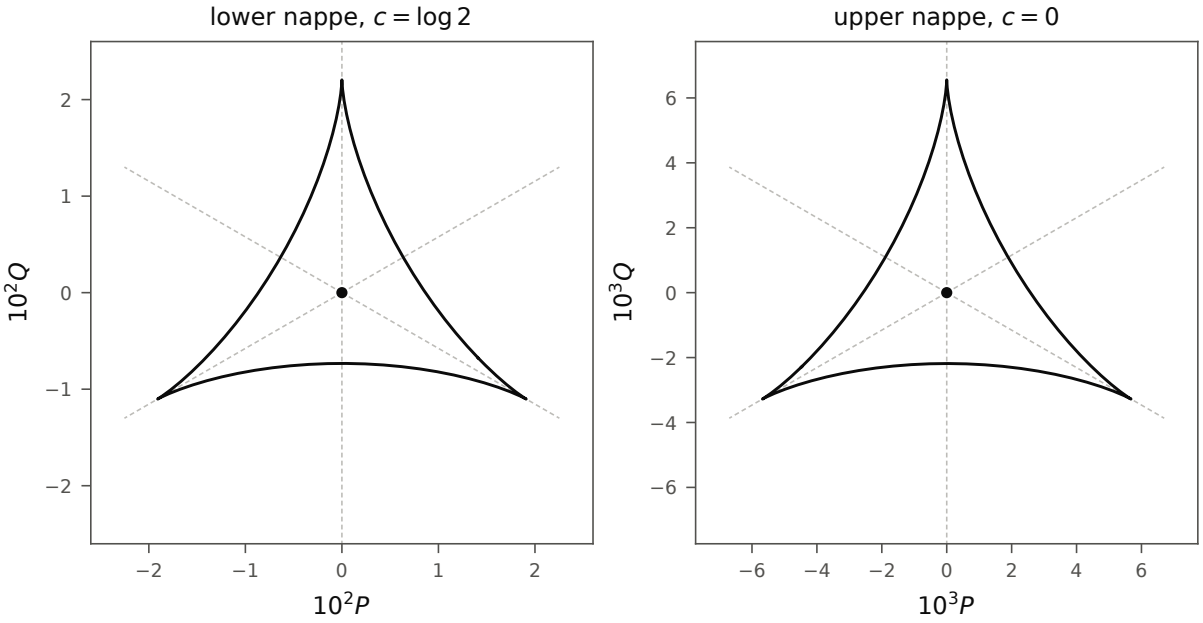


FIGURE 2. The curves $C_c = G(\Gamma_c)$ for $c = \log 2$ on the lower nappe (left) and $c = 0$ on the upper nappe (right), computed in floating point. The dot is the origin, the image of the axis point of the disk Φ_c. This point has $m_4/m = 1/2$ on the left. On the right it is the equilateral configuration of four equal masses. The dashed lines are the mirror rays $\Theta = 30° + k \cdot 60°$. Each curve meets every ray from the origin once. It has cusps on the mirror rays $\Theta = 90°$, 210° and 330° and crosses the other three mirror rays transversally, as Proposition 7.13 shows for all levels $c \neq A^*$. The two curves look alike, but the cusp points of Γ_c lie on the half-mirrors $\varphi \in \{90°, 210°, 330°\}$ on the lower nappe and on $\varphi \in \{30°, 150°, 270°\}$ on the upper nappe.

total turn, and the strict bounds behind the cusps. Inside Ω_4, box-by-box sign checks cannot succeed in two places, where quantities to be signed vanish. On the mirrors the angle of G is stationary at the cusps of C_c. Lemma 3.3 (the band lemma) handles these points. At p^*, where all first derivatives of G vanish, a separate chart certifies the quantities divided by powers of the distance to p^* (Section 5.1). The certificates are finite covers of the configuration space by boxes. Each box carries ball-arithmetic enclosures of the relevant quantities and the sign conditions derived from them.

1.4. **Ingredients of the proof.** The proof of Theorem 1 uses Dziobek's relations (Lemma 2.1). The proof of properness (Proposition 6.3) uses the absence of CCs with exactly three bodies collinear. Theorem 2 uses in addition the collinear count [Mou10] and the convex count [MB32, Xia04, Tom26]; the paragraph after its statement says which of its items depend on [Tom26]. Neither theorem uses Albouy's count [Alb95, Alb96]: we compute the degree in the limit of large A, not at equal masses. The computer-assisted parts of the proof are the certificates of Section 5, used for Theorem 1, and, for Theorem 2(b), (d) and (e), the certified computations of points of the fold in Section 9 and the exact computations behind the family theorem of Section 10. The closed forms of Propositions 2.4 and 2.6 are derived and checked by computer algebra in exact arithmetic. Data and code availability lists what the computations assume and which of the reported computations test the proof without being part of it.

Theorems 1 and 2 have two proofs, and the proof of record is the one in this paper. It rests on the computations just listed, which Data and code availability describes, and most of their certified quantities come from one implementation in C. The other proof is a formalization in Lean, also described there, whose main theorem states both theorems and takes no unproved inputs; its computer-assisted steps are certificates of its own, which the Lean kernel checks. The evaluator of Section 9, a second rigorous implementation, reproduces the values of K, $\widehat{A}$, P, Q, $\widetilde{J}$, T_1, T_2, T_3 and J_{mir} computed by the C code, but only at 100 points of chart 1 (Section 9.2). For the other quantities that the proof in this paper takes from the C code, which Data and code availability lists, the independent assurance is the formal proof, which does not depend on the C code. Data and code availability names, for each certified ingredient of Sections 6 and 7, its counterpart in the formalization, or why the formalization needs none.

1.5. **Organization.** Section 2 introduces the Dziobek reduction, the mass map, its symmetry and the axis. It also contains the closed forms on the axis and at the umbilic. Section 3 derives the formulas on the fold used in the certificates. Section 4 collects lemmas that delimit the configuration space, and Section 5 describes the certificates. In Section 6 we prove the injectivity of F on $\overline{\mathcal{D}}$ and the count at regular values. Section 7 computes the count at the critical values, and Section 8 introduces the function R and proves Theorems 1 and 2. Section 9 describes the certified examples, Section 10 treats the family $(1, 1, 1, m_4)$, and Section 11 relates degeneracy to the mass map. In Section 12 we compare the results with the literature and describe the surface of critical values near its vertex.

Notation. Some letters have more than one meaning, which the indices and the context separate. The squared length of the outer side opposite body i is R_i, and the radius function of Theorem 1 is R, with two arguments. In Section 6.2, R is a positive function on S^1; R_c and R_A are the radius functions of the curves C_c and C_A (Sections 6.7–8), and R_{d} is that of the deltoid (Section 12). The centre of mass is c_m, the counts are $c_i(m)$, a level of A is c (Sections 1.3, 3.1 and 6–9), and $c(s)$, with $c^* = c(s^*)$, is a coefficient of the 2-jet of G (Lemma 2.5). In charts 3 and 4, $\sigma = 1 - s$ (Sections 5–7); σ_m is the reflection in a mirror (Section 7), and in Section 10 σ is the transposition of the bodies 2 and 3. The angle from a mirror is $\tau = \varphi - \varphi_m$ (Sections 3.3, 7 and 8.4), and τ_1, τ_2 are tangent vectors in Section 6.9. The bracket of the band lemma is bounded by β, and that of a band certificate by β_C (Sections 3.3, 5.4 and 7.3), while β_l are barycentric coordinates (Lemma 4.5, Section 6.9 and Data and code availability). Other uses of these letters, such as τ in Appendix A and β_1, β_2 in the proof of Lemma 10.5, are local to one proof or paragraph.

2. The Dziobek reduction and the mass map

2.1. **Normalization.** Since $\sum_i m_i(x_j - x_i) = M(x_j - c_m)$, equation (1.1) is equivalent to

$$\sum_{i \neq j} m_i \, (x_i - x_j) \left(r_{ij}^{-3} - \lambda' \right) = 0, \qquad j = 1, \dots, 4, \qquad \lambda' = \lambda / M. \tag{2.1}$$

Equation (2.1) is [Moe14, (57)–(58)] with $\lambda = M\lambda'$.[1] Scaling the configuration by $t > 0$ multiplies λ' by t^{-3}. We fix $\lambda' = 1$ and write $S_{ij} = r_{ij}^{-3} - 1$.

We call bodies 1, 2, 3 the *outer* bodies, since body 4 is inside their triangle. Throughout, (i, j, k) denotes a cyclic permutation of $(1, 2, 3)$. Let

- $a_i = |x_i - x_4|$, the spoke lengths;
- θ_i the angle at x_4 between x_j and x_k;
- $R_i = r_{jk}^2 = a_j^2 + a_k^2 - 2a_j a_k \cos\theta_i$;

[1] We cite the freely available lecture notes [Moe14], on which the chapter [Moe15] is based.

- $S_i = \frac{1}{2} a_j a_k \sin\theta_i$, the area of the triangle $x_4 x_j x_k$;
- $S = S_1 + S_2 + S_3$;
- $w_i = a_i^{-3} - 1 = S_{i4}$, $q_i = R_i^{-3/2} = S_{jk} + 1$ and $k_i = w_i(q_i - 1)$.

Lemma 2.1 (Dziobek reduction)**.** *Let x be a concave CC with body 4 strictly inside the triangle of the others, normalized by $\lambda' = 1$. Then $0 < a_i < 1$, $R_i > 1$, $k_1 = k_2 = k_3 =: K < 0$, $\theta \in (0,\pi)^3$ and $\theta_1 + \theta_2 + \theta_3 = 2\pi$. If moreover $m_4 = 1$, then*

$$m_i = \frac{S_i\, w_j w_k}{(-K)\, S}, \qquad i = 1, 2, 3. \tag{2.2}$$

Conversely, let $a \in (0,1)^3$ and $\theta \in (0,\pi)^3$ with $\sum_i \theta_i = 2\pi$ and $k_1 = k_2 = k_3 = K < 0$, and place spokes of lengths a_i at x_4 with these angles. Then this configuration, with the masses (2.2) *and $m_4 = 1$, is a CC with $\lambda' = 1$ and body 4 inside.*

Proof. The configuration is planar and not collinear, that is, a Dziobek configuration. The barycentric identity $Sx_4 = \sum_{i<3} S_i x_i$ shows that the vector $\Delta = (S_1, S_2, S_3, -S)$ satisfies $\sum_l \Delta_l = 0$ and $\sum_l \Delta_l x_l = 0$. By Dziobek's relations [Dzi00], [Moe14, Prop. 26], there is a real $\kappa \neq 0$ with $m_i m_j S_{ij} = \kappa \Delta_i \Delta_j$ for all $i \neq j$. For the pairs $(i,4)$ this reads $m_i m_4 w_i = -\kappa S_i S$. For the pairs (j,k) it reads $m_j m_k (q_i - 1) = \kappa S_j S_k$. Multiplying the two gives

$$k_i = -\kappa^2 \, \frac{S_1 S_2 S_3\, S}{m_1 m_2 m_3 m_4},$$

which is the same for all i and negative.

Next, $\kappa < 0$. Otherwise $w_i < 0$ and $q_i > 1$: all spokes would be longer than 1 and all sides of the outer triangle shorter than 1. This is impossible: an interior point p of a triangle with vertices u, v, z satisfies $|p-u| < \max(|v-u|, |z-u|)$, by convexity of $|\cdot - u|$. From $\kappa < 0$ we get $w_i > 0$ (that is, $a_i < 1$) and $q_i < 1$ (that is, $R_i > 1$).

The interior position of x_4 puts the angles in $(0,\pi)$. With $m_4 = 1$ we have $m_i = -\kappa S_i S / w_i$. Substituting this and $m_4 = 1$ into the formula for $K = k_i$ gives $\kappa = w_1 w_2 w_3 / (K S^2)$ and then (2.2).

Conversely, if we define m_i by (2.2), $m_4 = 1$ and $\kappa = w_1 w_2 w_3 / (K S^2)$, a direct computation using $k_i = K$ shows that $m_i m_j S_{ij} = \kappa \Delta_i \Delta_j$ for all six pairs. Then, for each j,

$$\sum_{i \neq j} m_i S_{ij} (x_i - x_j) = \frac{\kappa \Delta_j}{m_j} \Big(\sum_i \Delta_i x_i - \Big(\sum_i \Delta_i \Big) x_j \Big) = 0,$$

which is (2.1) with $\lambda' = 1$. With $\theta \in (0,\pi)^3$ and $\sum_i \theta_i = 2\pi$, body 4 lies inside the triangle of the others. □

Lemma 2.2. *For $a \in (0,1)^3$, the system $k_1 = k_2 = k_3 = K$, with principal angles $\theta_i \in [0,\pi]$ and $\sum_i \theta_i = 2\pi$, has at most one solution (θ, K), for either sign of K. Where the solution exists and $\theta \in (0,\pi)^3$, it depends analytically on a.*

Proof. The equation $k_i = K$ gives $R_i(K) = (1 + K/w_i)^{-2/3}$, which is defined because $K = k_i > -w_i$. Since $dR_i/dK < 0$, the function $\theta_i(K) = \arccos\big((a_j^2 + a_k^2 - R_i(K))/(2a_j a_k)\big)$ decreases strictly in K where it is defined. Hence $\sum_i \theta_i(K) = 2\pi$ has at most one solution. At a solution with $\theta \in (0,\pi)^3$ the derivative $\frac{d}{dK} \sum_i \theta_i$ is negative. Analyticity there follows from the implicit function theorem. □

2.2. **The configuration space and the mass map.** Lemma 2.2 shows that the set

$$\Omega_4 = \big\{ a \in (0,1)^3 : \text{ the solution of Lemma 2.2 exists, with } \theta \in (0,\pi)^3 \text{ and } K < 0 \big\}$$

is open. We call its points *physical*. By Lemma 2.1, $a \mapsto$ (configuration) is a bijection from Ω_4 onto the set of concave CCs with body 4 inside, modulo similarity including reflection: the normalization $\lambda' = 1$ fixes the scale, and a and θ determine the configuration up to an isometry.

The *mass map* is the analytic map $F : \Omega_4 \to \mathbb{R}^3$ given by

$$F(a) = \mu = \Big(\log\frac{m_1}{m_4}, \log\frac{m_2}{m_4}, \log\frac{m_3}{m_4}\Big), \tag{2.3}$$
$$\mu_i = \hat{m}_i - \log(-K), \qquad \hat{m}_i = \log S_i + \log w_j + \log w_k - \log S,$$

and we write $J = \det \partial\mu/\partial a$ for its Jacobian determinant. Since multiplying all masses by a constant does not change the CCs, $c_4(m) = \#F^{-1}(\mu^{(4)}(m))$. It suffices to study the map $F = F_4$: for $i \neq 4$ the map F_i is defined in the same way after exchanging the labels i and 4.

2.3. **Coordinates and symmetry.** With $E_1 = (1,-1,0)/\sqrt{2}$ and $E_2 = (1,1,-2)/\sqrt{6}$ we write

$$a = s(1,1,1) + xE_1 + yE_2, \qquad x = r\cos\varphi, \quad y = r\sin\varphi.$$

Then s is the mean spoke length, r is the distance from the axis $\{a_1 = a_2 = a_3\}$, and $\det \partial a/\partial(s,x,y) = \sqrt{3}$.

- The *wedge* $W = \{a_1 \geq a_2 \geq a_3\}$ is $\{x \geq 0,\ 30^\circ \leq \varphi \leq 90^\circ\}$, whose two faces, the *mirrors*, are $\varphi = 90^\circ$ (where $a_1 = a_2$) and $\varphi = 30^\circ$ (where $a_2 = a_3$).
- The symmetric group $\mathfrak{S}_3$ permutes the outer bodies; F is $\mathfrak{S}_3$-equivariant.
- On the target we use $A = \frac{1}{3}\sum_i \mu_i$, $P = (\mu_1 - \mu_2)/\sqrt{2}$, $Q = (\mu_1 + \mu_2 - 2\mu_3)/\sqrt{6}$, $G = (P,Q)$ and $\Theta = \operatorname{atan2}(Q,P)$, for which $\det \partial(A,P,Q)/\partial\mu = 1/\sqrt{3}$.
- Since the functions (x,y) of a and (P,Q) of μ are given by the same linear formulas, the group $\mathfrak{S}_3$ acts on the angle φ and on the angle Θ by the same dihedral group.
- The functions A, K and J are $\mathfrak{S}_3$-invariant, J because the determinants of a permutation on the domain and on the target cancel.
- On the mirror $\varphi = 90^\circ$ we have $\mu_1 = \mu_2$, $P = 0$ and $\Theta \in \{90^\circ, 270^\circ\}$. On the mirror $\varphi = 30^\circ$ we have $\mu_2 = \mu_3$, $Q = P/\sqrt{3}$ and $\Theta \in \{30^\circ, 210^\circ\}$.

Any statement about W extends to Ω_4 by $\mathfrak{S}_3$-equivariance.

2.4. **The axis and the umbilic.**

Lemma 2.3. *On the axis $a = s(1,1,1)$ the following hold.*

(a) *$\theta_i = 2\pi/3$, $R_i = 3s^2$ and $K = w(q-1)$, where $w = s^{-3} - 1$ and $q = (\sqrt{3}\,s)^{-3}$.*
(b) *The point is physical if and only if $1/\sqrt{3} < s < 1$.*
(c) *With $m = m_1 = m_2 = m_3$, the mass ratio is*

$$\frac{m_4}{m} = \frac{3\big(1 - (\sqrt{3}\,s)^{-3}\big)}{s^{-3} - 1}.$$

It increases strictly from 0 to ∞ on $(1/\sqrt{3}, 1)$ and equals 1 at s_{eq}, where $s_{eq}^3 = (1+1/\sqrt{3})/4$. Moreover $A = \log(m/m_4)$ and $\partial_s A < 0$.
(d) *$P = Q = 0$, $\partial_x A = \partial_y A = 0$ and $\partial(P,Q)/\partial(x,y) = \lambda_{\mathrm{ax}}(s)\, I$, where $\lambda_{\mathrm{ax}}(s) = \partial_x P(s,0,0)$. Hence $J = \partial_s A \cdot \lambda_{\mathrm{ax}}(s)^2 \leq 0$, with $J = 0$ exactly where $\lambda_{\mathrm{ax}} = 0$.*

Proof. (a) With $a_i = s$ and $\theta_i = 2\pi/3$, the formula $R_i = a_j^2 + a_k^2 - 2a_j a_k \cos\theta_i$ gives $R_i = 3s^2$ and equal values $k_i = w(q-1)$: by Lemma 2.2 these angles form the solution. (b) Here $a_i = s$. The value $K = w(q-1)$ is negative if and only if $q < 1$, that is, $s > 1/\sqrt{3}$. (c) By (2.2), $m = w^2/(3(-K)) = w/(3(1-q))$, which is the stated formula. With $t = s^{-3} \in (1, 3^{3/2})$ and $c = 3^{-3/2}$, the ratio is $3(1-ct)/(t-1)$, whose derivative in t is $3(c-1)/(t-1)^2 < 0$. As t decreases in s, the ratio increases strictly in s. The ratio tends to 0 as $s \downarrow 1/\sqrt{3}$ and to ∞ as

$s \uparrow 1$. Setting it equal to 1 gives $s^{-3}(1+1/\sqrt{3}) = 4$. Finally $A = \frac{1}{3}\sum_i \log(m_i/m_4) = \log(m/m_4)$. (d) On the axis $\mu_1 = \mu_2 = \mu_3$ and $P = Q = 0$. It is fixed by $\mathfrak{S}_3$, which acts on the (x, y)-plane and on the (P, Q)-plane by the same irreducible two-dimensional representation. The gradient of the invariant function A in (x, y) is a fixed vector of this representation and vanishes. The matrix $\partial(P, Q)/\partial(x, y)$ commutes with the representation. Commuting with the rotation by 120° makes it a rotation-dilation. Commuting also with a reflection makes it a multiple of the identity. The matrix $\partial(A, P, Q)/\partial(s, x, y)$ is then the diagonal matrix with entries $\partial_s A$, λ_{ax}, λ_{ax}. Since its determinant is $\det \partial(A, P, Q)/\partial\mu \cdot J \cdot \det \partial a/\partial(s, x, y) = J$, we get $J = \partial_s A\, \lambda_{\mathrm{ax}}^2$. □

Both factors of J on the axis have closed forms.

Proposition 2.4 (the axis in closed form)**.** *For $1/\sqrt{3} < s < 1$,*

$$\lambda_{\mathrm{ax}}(s) = \frac{3 - (6\sqrt{3} - 2)\, s^3}{s\,(1 - s^3)}, \qquad \partial_s A = \frac{3(9 - \sqrt{3})\, s^2}{(s-1)(9s^3 - \sqrt{3})(s^2 + s + 1)} < 0.$$

The function λ_{ax} has exactly one zero s^* in $(1/\sqrt{3}, 1)$, given by $s^{*3} = 3/(6\sqrt{3} - 2)$, with $\lambda_{\mathrm{ax}} > 0$ on $(1/\sqrt{3}, s^*)$, $\lambda_{\mathrm{ax}} < 0$ on $(s^*, 1)$ and $\lambda'_{\mathrm{ax}}(s^*) = -3(6\sqrt{3} - 2)\, s^*/(1 - s^{*3}) < 0$. At s^* the mass ratio of Lemma 2.3(c) is $m_4/m = m^* = (81+64\sqrt{3})/249$, and $K = 1/9 - 44\sqrt{3}/81$. In particular $J < 0$ at every physical point of the axis other than $p^* = s^*(1, 1, 1)$, where $J = 0$.

Proof. We linearize the system of Lemma 2.2 at $a = s(1, 1, 1)$, $\theta = (2\pi/3)(1, 1, 1)$. With $R = 3s^2$, $w = s^{-3} - 1$ and $q = (\sqrt{3}\, s)^{-3}$ as in Lemma 2.3(a), the partial derivatives of $k_i = w_i(q_i - 1)$ there are

$$\eta_1 = \frac{\partial k_i}{\partial a_i} = -3s^{-4}(q - 1), \qquad \eta_2 = \frac{\partial k_i}{\partial a_j} = -\frac{9}{2}\, s\, w\, R^{-5/2}, \qquad \eta_3 = \frac{\partial k_i}{\partial \theta_i} = -\frac{3\sqrt{3}}{2}\, s^2\, w\, R^{-5/2}$$

for $j \neq i$, while k_i does not depend on θ_j for $j \neq i$. For a variation ε of a with $\sum_i \varepsilon_i = E$, the equations $\delta k_i = \delta K$ and $\sum_i \delta\theta_i = 0$ have the solution $\delta K = (\eta_1 + 2\eta_2)E/3$ and $\delta\theta_i = (\eta_1 - \eta_2)(E/3 - \varepsilon_i)/\eta_3$. On the axis the matrix $\partial\mu/\partial a$ is symmetric under $\mathfrak{S}_3$: its diagonal entries are $\alpha = \partial\mu_i/\partial a_i$ and its off-diagonal entries are $\beta = \partial\mu_i/\partial a_j$. Then $\lambda_{\mathrm{ax}} = \partial_x P = \alpha - \beta$. Differentiating (2.3) with the values above gives

$$\lambda_{\mathrm{ax}} = \frac{\eta_1 - \eta_2}{\sqrt{3}\,\eta_3} - \frac{1}{s} - \frac{w'}{w}, \qquad w' = -3s^{-4},$$

which simplifies to the stated form. The formula for $\partial_s A$ follows from $A = \log(m/m_4)$ and the mass ratio of Lemma 2.3(c); its sign follows from $s - 1 < 0 < 9s^3 - \sqrt{3}$ on $(1/\sqrt{3}, 1)$. The numerator of λ_{ax} decreases in s and vanishes at $s^{*3} = 3/(6\sqrt{3} - 2)$, which lies between $(1/\sqrt{3})^3$ and 1. With $s(1 - s^3) > 0$ this proves the statements on the zero, the signs and $\lambda'_{\mathrm{ax}}(s^*)$. Substituting s^{*3} into the mass ratio $3(1 - (\sqrt{3}\, s)^{-3})/(s^{-3} - 1)$ and into $K = w(q - 1)$ and rationalizing gives m^* and $K(p^*)$. The last assertion follows from $J = \partial_s A\, \lambda_{\mathrm{ax}}^2$ (Lemma 2.3(d)). The script `axis_lambda.py` repeats the linearization symbolically and checks these identities and evaluations in exact arithmetic. □

We call $\Sigma = \{J = 0\} \subset \Omega_4$ the *fold* and $p^* = s^*(1, 1, 1)$ the *umbilic*. By Lemma 2.3(c),(d) and Proposition 2.4, the fold meets the axis only at p^*, where dF has rank one. This point is Palmore's degenerate configuration: the equilateral triangle with body 4 at its centre and $m_4/m = m^*$ (Section 12). It is also the point where $\overline{\mathcal{D}}$ splits into two pieces. A separate chart of the certificates covers a ball around it. We set $A^* = A(p^*) = -\log m^*$. In decimals $s^* = 0.70970849110762766159\ldots$. The certificates use the two adjacent double-precision numbers

$$[s_a, s_b] = [0.70970849110762757039\ldots,\ 0.70970849110762768141\ldots].$$

Arb enclosures give $\lambda_{\mathrm{ax}}(s_a) > 0 > \lambda_{\mathrm{ax}}(s_b)$ (Proposition 5.2(a)). These signs imply $s_a < s^* < s_b$ by Proposition 2.4.

Near the umbilic we use the complex coordinate $z = x + iy$ orthogonal to the axis and write $G = P + iQ$, as a function $G(s, z)$ of the point (s, x, y).

Lemma 2.5 (the 2-jet of G near the axis)**.** *There are a real-valued real-analytic function λ and a real-analytic function c with values in $i\mathbb{R}$, both defined on a neighbourhood of s^*, and constants $\delta_s, \delta_z, C_E > 0$ such that*

$$G(s, z) = \lambda(s)\, z + c(s)\, \bar{z}^{\,2} + E(s, z), \qquad |E(s, z)| \le C_E |z|^3 \qquad (|s - s^*| \le \delta_s,\ |z| \le \delta_z).$$

Here $\lambda = \lambda_{\mathrm{ax}}$ and $\lambda(s^*) = 0$.

Proof. The map G is real-analytic near p^*, an interior point of Ω_4, and $G(s, 0) = 0$ by Lemma 2.3(d). Write $G(s, z) = \sum_{j+k\ge 1} g_{jk}(s) z^j \bar{z}^k$. A cyclic permutation of the outer bodies acts on z and on G by the same rotation $z \mapsto \omega z$, $\omega = e^{\pm 2\pi i/3}$. The resulting relation $g_{jk}\omega^{j-k} = \omega g_{jk}$ forces $g_{jk} = 0$ unless $j - k \equiv 1 \pmod 3$. Among the pairs with $j + k \le 2$ this leaves $(1, 0)$ and $(0, 2)$. The transposition of the bodies 1 and 2 acts by $z \mapsto -\bar{z}$ on the domain and by $G \mapsto -\bar{G}$ on the target, which forces g_{10} to be real and g_{02} to be imaginary. We put $\lambda = g_{10}$ and $c = g_{02}$. Then $\lambda(s) = \partial_x P(s, 0, 0) = \lambda_{\mathrm{ax}}(s)$. The bound on E follows from Taylor's theorem in (x, y), since the third derivatives are bounded on a compact neighbourhood. □

Proposition 2.6 (the umbilic)**.** *In Lemma 2.5, $c(s) = i\gamma(s)$ with*

$$\gamma(s) = \frac{\sqrt{2}\,\big[(3888 - 22032\sqrt{3})s^{12} + (22464 - 648\sqrt{3})s^9 - 2841\sqrt{3}\,s^6 + (486 + 8\sqrt{3})s^3 - 11\sqrt{3}\big]}{12\,s^2(s-1)^2(s^2+s+1)^2(3\sqrt{3}\,s^3 - 1)^2},$$

and $\gamma(s^*) = -41.5719787\ldots < 0$. In particular $c(s^*) \neq 0$. Moreover $J(p^*) = 0$, $\nabla J(p^*) = 0$ and, in the coordinates (s, x, y),

$$\operatorname{Hess} J(p^*) = \operatorname{diag}\big(2\,\partial_s A\, \lambda'_{\mathrm{ax}}(s^*)^2,\ -8\,\partial_s A\, |c(s^*)|^2,\ -8\,\partial_s A\, |c(s^*)|^2\big),$$

with $\partial_s A$ taken at s^*. This matrix has signature $(-, +, +)$.

Proof. The coefficient $c(s)$ comes from the second-order expansion of the system of Lemma 2.2 about the axis, as in the proof of Proposition 2.4. The script `axis_jet2.py` carries out this expansion in exact arithmetic. It confirms that the coefficient of $\bar{z}$ of order one and the coefficients of z^2 and $z\bar{z}$ vanish, in agreement with Lemma 2.5. It also produces λ_{ax} and $c(s)$ in the stated forms. The evaluator of Section 9.1 gives an independent check. In ball arithmetic it computes the Taylor coefficients of P and Q at the axis point $s_b(1, 1, 1)$; its coefficient of x^2 in Q agrees with the closed form of $\gamma(s^*)$ to 12 digits. The denominator of γ is positive at s^*, because $s^* \neq 0, 1$ and $3\sqrt{3}\,s^{*3} - 1 = (29 + 9\sqrt{3})/52 \neq 0$. In the field $\mathbb{Q}(\sqrt{3})$ the numerator, divided by $\sqrt{2}$, equals $-5827437/228488 - (1875095/114244)\sqrt{3} < 0$ at $s^{*3} = (3 + 9\sqrt{3})/52$. The script `s3_check.py` checks these two facts, and also $\lambda'_{\mathrm{ax}}(s^*) < 0$, in exact arithmetic. Thus $\gamma(s^*) < 0$.

For the Hessian we expand $J = \det \partial(A, P, Q)/\partial(s, x, y)$ (proof of Lemma 2.3(d)) along its first row. The derivatives $\partial_x A$ and $\partial_y A$ vanish on the axis. So do $\partial_s P$ and $\partial_s Q$, because $P = Q = 0$ on the axis. The derivatives of P and Q in (x, y) vanish at p^*, where $\lambda_{\mathrm{ax}}(s^*) = 0$. Let ϱ be the distance to p^* in the coordinates (s, x, y). The two cofactor terms are then $O(\varrho^3)$. Hence $J = \partial_s A\,(|G_z|^2 - |G_{\bar{z}}|^2) + O(\varrho^3)$. Lemma 2.5 gives the 2-jet $\lambda'_{\mathrm{ax}}(s^*)(s - s^*)z + c(s^*)\bar{z}^2$ of G at p^*, so $|G_z|^2 - |G_{\bar{z}}|^2 = \lambda'_{\mathrm{ax}}(s^*)^2(s - s^*)^2 - 4|c(s^*)|^2|z|^2 + O(\varrho^3)$. This implies $J(p^*) = 0$, $\nabla J(p^*) = 0$ and the stated Hessian, whose signature follows from $\partial_s A < 0$, $\lambda'_{\mathrm{ax}}(s^*) \neq 0$ and $c(s^*) \neq 0$. □

The proofs of Theorems 1 and 2 use only the inequality $c(s^*) \neq 0$ of Proposition 2.6, in Proposition 7.11, and the formalization proves it in Lean. Apart from the proof of this inequality, the closed form of $\gamma(s)$ and the Hessian of J are used only in remarks, in Figure 1 and in

Section 12. By the Morse lemma, $\overline{\mathcal{D}}$ is a double cone near p^* with its axis along the s-direction; in particular $\overline{\mathcal{D}} \cap \{s = s^*\} = \{p^*\}$ near p^*. The fold is asymptotic to the cone $r = |\lambda'_{\mathrm{ax}}(s^*)|\,|s - s^*|/(2|c(s^*)|)$, of slope $0.3344\ldots$. The certificates will establish the global versions of these facts (Proposition 5.2(e) and Section 6.4).

3. Formulas on the fold

3.1. **The certified quantities.** For a function f of (s, x, y) we write $\nabla f = (\partial_s f,\ \partial_r f,\ r^{-1}\partial_\varphi f)$ for its gradient in the frame (e_s, e_r, e_φ), which is orthonormal and right-handed in the (s, x, y)-space. Let $\widehat{A} = \frac{1}{3}\sum_i \hat{m}_i$. Then $A = \widehat{A} - \log(-K)$. The term $\log(-K)$ makes both A and J singular where $K = 0$, while P and Q do not contain it. We multiply ∇A by $-K$ and define

$$\mathbf{A} = (-K)\nabla A = (-K)\nabla\widehat{A} + \nabla K, \qquad \widetilde{J} = \det[\mathbf{A}; \nabla P; \nabla Q],$$
$$\mathbf{h} = P\nabla Q - Q\nabla P = (P^2 + Q^2)\nabla\Theta.$$

Note that these are analytic wherever $w_i > 0$ and $S_i > 0$, including across $K = 0$. The certificates work with $\widetilde{J}$ in place of J, since $\widetilde{J}$ has the sign of J on Ω_4 by Lemma 3.1(a). The vector $\mathbf{h}$ is the gradient of the angle Θ of G, multiplied by $P^2 + Q^2$ so that it stays analytic where $G = 0$. On the fold Σ we use

$$T_1 = \partial_r \widetilde{J}, \qquad T_2 = \mathbf{A}_s(\nabla\widetilde{J})_r - \mathbf{A}_r(\nabla\widetilde{J})_s, \qquad T_3 = \det[\mathbf{h}; \mathbf{A}; \nabla\widetilde{J}],$$

where the subscripts s, r denote the components in the frame. At a point of Σ with $T_1 > 0$ the ray crosses the fold transversally, from $J < 0$ to $J > 0$. Lemma 3.1 shows that T_2 determines the sign of the derivative of $A|_\Sigma$ in s and of $d\varphi$ along the curves $\Gamma = \Sigma \cap \{A = c\}$ and that T_3 determines the sign of $d\Theta$ along them. The signs $T_2 < 0$ and $T_3 < 0$ make $A|_\Sigma$ decrease in s and Θ increase with φ along Γ.

Lemma 3.1. (a) $\widetilde{J} = (-K)\,J$. *In particular* $\operatorname{sign}\widetilde{J} = \operatorname{sign} J$ *on* Ω_4 *and* $\Sigma = \{\widetilde{J} = 0\} \cap \Omega_4$.

(b) *At a point of* Σ *with* $T_1 \neq 0$, *the fold is locally a graph* $r = r_f(s, \varphi)$, *on which the restriction* $A|_\Sigma$ *satisfies* $\partial_s(A|_\Sigma) = T_2/((-K)\,T_1)$.

(c) *The vector* $v = \nabla A \times \nabla\widetilde{J}$ *is tangent to the curve* $\Gamma = \Sigma \cap \{A = c\}$, *and*

$$d\varphi(v) = \frac{T_2}{(-K)\,r}, \qquad d\Theta(v) = \frac{T_3}{(P^2+Q^2)(-K)}, \qquad \frac{d\Theta}{d\varphi}\Big|_\Gamma = \frac{r\,T_3}{(P^2+Q^2)\,T_2}.$$

Proof. All three parts are direct computations. (a) As $\mathbf{A} = (-K)\nabla A$ and the frame is orthonormal and right-handed, $\widetilde{J} = (-K)\det\partial(A, P, Q)/\partial(s, x, y) = (-K)\cdot\frac{1}{\sqrt{3}}\cdot J\cdot\sqrt{3}$. (b) By the implicit function theorem there is such an r_f; moreover $\partial_s r_f = -\partial_s\widetilde{J}/\partial_r\widetilde{J}$. Then $\partial_s(A|_\Sigma) = \partial_s A + \partial_r A\,\partial_s r_f = (\partial_s A\,\partial_r\widetilde{J} - \partial_r A\,\partial_s\widetilde{J})/\partial_r\widetilde{J}$, whose numerator is $T_2/(-K)$. (c) The vector v, orthogonal to ∇A and $\nabla\widetilde{J}$, is tangent to both level sets. With $d\varphi(e_\varphi) = 1/r$, its e_φ-component $(\nabla A)_s(\nabla\widetilde{J})_r - (\nabla A)_r(\nabla\widetilde{J})_s = T_2/(-K)$ gives the formula for $d\varphi(v)$. Also $d\Theta(v) = \det[\nabla\Theta; \nabla A; \nabla\widetilde{J}] = T_3/((P^2+Q^2)(-K))$. The last formula is the quotient of the first two. □

3.2. **The mirror identity.** For a mirror angle $\varphi_m \in \{30°, 90°\}$ we put

$$L = \cos\varphi_m\,P + \sin\varphi_m\,Q, \qquad L^\perp = -\sin\varphi_m\,P + \cos\varphi_m\,Q, \qquad J_{\mathrm{mir}} = \mathbf{A}_s\,\partial_r L - \mathbf{A}_r\,\partial_s L,$$

and for $\varphi_m = 90°$ we have $L = Q$ and $L^\perp = -P$.

Lemma 3.2 (mirror identity)**.** *On the mirror* $\varphi = \varphi_m$,

$$\widetilde{J} = \frac{\partial_\varphi L^\perp}{r}\,J_{\mathrm{mir}}, \qquad T_3 = L\,\frac{\partial_\varphi L^\perp}{r}\,T_2.$$

Wherever $J_{\mathrm{mir}} \neq 0$ on the mirror, $T_3 = (L\,T_2/J_{\mathrm{mir}})\,\widetilde{J}$. In particular $T_3 = 0$ at every point of Σ on the mirror at which $J_{\mathrm{mir}} \neq 0$.

Proof. As the pair $(L, L^{\perp})$ is obtained from (P, Q) by a rotation, $\widetilde{J} = \det[\mathbf{A}; \nabla L; \nabla L^{\perp}]$ and $\mathbf{h} = L\nabla L^{\perp} - L^{\perp}\nabla L$. The reflection in the mirror, which exchanges two outer bodies, fixes A, K, $\widetilde{J}$ and L and changes the sign of $L^{\perp}$. On the mirror it follows that $L^{\perp} = \partial_s L^{\perp} = \partial_r L^{\perp} = 0$ and $\partial_\varphi A = \partial_\varphi K = \partial_\varphi L = \partial_\varphi \widetilde{J} = 0$. Then $\nabla L^{\perp} = (0, 0, r^{-1}\partial_\varphi L^{\perp})$ and $\mathbf{h} = (0, 0, L\,r^{-1}\partial_\varphi L^{\perp})$, while $\mathbf{A}$, ∇L and $\nabla \widetilde{J}$ have vanishing third components. Expanding the two determinants along the third column, respectively the first row, gives the two formulas. □

3.3. **The band lemma.** Lemma 3.2 shows that $T_3 = 0$ at the points of Σ on a mirror at which $J_{\mathrm{mir}} \neq 0$. An enclosure of T_3 over a box that contains such a point cannot certify $T_3 < 0$. The band lemma replaces this test near the mirrors. The reflection in a mirror φ_m reverses orientation and changes Θ into const $- \Theta$, while it fixes A, K, $\widetilde{J}$ and $P^2 + Q^2$. These two sign changes cancel in $T_3 = (P^2 + Q^2)(-K)\det[\nabla\Theta; \nabla A; \nabla \widetilde{J}]$, making T_3 and $\widetilde{J}$ even in $\tau = \varphi - \varphi_m$ at fixed (s, r).

Lemma 3.3 (band lemma)**.** *Let C be a box in the coordinates (s, r, φ) whose φ-range contains φ_m and on which $\widetilde{J}$ and T_3 are analytic, and let $C_m = C \cap \{\varphi = \varphi_m\}$. Suppose that $J_{\mathrm{mir}} \neq 0$ and $T_1 \neq 0$ on C_m, that for every s in the s-range of C the function $\widetilde{J}(s, \cdot, \varphi_m)$ has a zero in the r-range of C, and that*

$$\partial_\varphi^2 T_3(\xi_1) - \frac{\partial_r T_3(\xi)}{T_1(\xi')}\,\partial_\varphi^2 \widetilde{J}(\xi_2) \leq \beta \qquad \text{for all } \xi_1, \xi_2 \in C \text{ and } \xi, \xi' \in C_m$$

for some $\beta < 0$. Then every zero $(s, r, \varphi_m + \tau)$ of $\widetilde{J}$ in C satisfies

$$T_3(s, r, \varphi_m + \tau) \leq \tfrac{\tau^2}{2}\,\beta. \tag{3.1}$$

In particular $T_3 < 0$ at every point of C off the mirror at which $\widetilde{J} = 0$.

Proof. Let $(s, r, \varphi_m + \tau) \in C$ with $\widetilde{J} = 0$ there. For $\tau = 0$ the claim is $T_3 \leq 0$, which holds by Lemma 3.2 because $J_{\mathrm{mir}} \neq 0$ on C_m. We assume $\tau \neq 0$. By evenness and Taylor's theorem in τ at fixed (s, r),

$$T_3(s, r, \varphi_m + \tau) = T_3(s, r, \varphi_m) + \tfrac{\tau^2}{2}\,\partial_\varphi^2 T_3(\xi_1), \qquad 0 = \widetilde{J}(s, r, \varphi_m) + \tfrac{\tau^2}{2}\,\partial_\varphi^2 \widetilde{J}(\xi_2),$$

for some $\xi_1, \xi_2 \in C$. Let $(s, r_m, \varphi_m) \in C_m$ be a zero of $\widetilde{J}$, which exists by hypothesis and at which $T_3 = 0$ by Lemma 3.2. The mean value theorem in r on C_m shows that $T_3(s, r, \varphi_m) = \partial_r T_3(\xi)\,(r - r_m)$ and $\widetilde{J}(s, r, \varphi_m) = T_1(\xi')\,(r - r_m)$ with $\xi, \xi' \in C_m$. Dividing, we get $T_3(s, r, \varphi_m) = \big(\partial_r T_3(\xi)/T_1(\xi')\big)\,\widetilde{J}(s, r, \varphi_m)$. Combining,

$$T_3(s, r, \varphi_m + \tau) = \frac{\tau^2}{2}\Big(\partial_\varphi^2 T_3(\xi_1) - \frac{\partial_r T_3(\xi)}{T_1(\xi')}\,\partial_\varphi^2 \widetilde{J}(\xi_2)\Big) \leq \frac{\tau^2}{2}\,\beta. \qquad \square$$

We verify the hypothesis on the bracket from enclosures of the four quantities over C and C_m. In exact rational arithmetic we evaluate the bracket at the corners of the enclosures and take for β the largest corner value, which must be negative. This is valid: for d of one sign, tj/d is monotone in each of t, j and d separately. So the extreme values of tj/d over a product of intervals are attained at corners. In the top chart 3 of Section 5.2 the lemma is used with $\hat{r}$ in place of r. On the ball around the umbilic (chart 2) it is applied at fixed ϱ with ψ in place of r. There the quantities $\widetilde{J}/\varrho^2$ and T_3/ϱ^4 replace $\widetilde{J}$ and T_3. For $\varrho > 0$ they have the signs of $\widetilde{J}$ and T_3. The derivative $\partial_\psi(\widetilde{J}/\varrho^2)$ replaces T_1 and is only required to be nonzero on the mirror

face. The derivative $\partial_\psi(T_3/\varrho^4)$ replaces $\partial_r T_3$. A zero of $\widetilde{J}/\varrho^2$ is required on each ψ-segment of the mirror face.

4. Lemmas on the physical region

This section collects facts about the physical points. Lemmas 4.1–4.3 bound the region that the covers of Section 5 must cover; the covers are set up on these bounds. Lemmas 4.4 and 4.5 control the face $K = 0$ of Ω_4. The proofs are elementary and by hand. The proof of Lemma 4.5(b) takes a derivative on this face from Lemma 6.22(b); the proof of Lemma 6.22 in Section 6.9 rests only on Lemmas 2.1 and 2.2.

Lemma 4.1 (a priori bounds)**.** *Every physical a satisfies $r \le \sqrt{6}\max_i(a_i - s)$, $r < \sqrt{6}\,(2s-1)$ and $r < \sqrt{6}\,(1-s)$. In particular $s > \frac{1}{2}$.*

Proof. A unit vector of the plane $\sum_i d_i = 0$ has largest coordinate at least $1/\sqrt{6}$. Applied to $(a - s(1,1,1))/r$, this proves the first inequality. Since $R_i > 1$ and $\theta_i < \pi$, we have $a_j + a_k > r_{jk} > 1$. Then $a_i = 3s - a_j - a_k < 3s - 1$ and $\max_i(a_i - s) < 2s - 1$. Finally $a_i < 1$ implies $\max_i(a_i - s) < 1 - s$. □

Lemma 4.2 (Fermat-point bound)**.** *Every physical point has $s > 1/\sqrt{3}$.*

Proof. Let L_F be the least value of the sum of the distances from a point to the vertices of the outer triangle, whose sides b_1, b_2, b_3 all exceed 1. Then $3s = \sum_i a_i \ge L_F$. If all angles of the triangle are less than 120°, then $L_F^2 = \frac{1}{2}(b_1^2 + b_2^2 + b_3^2) + 2\sqrt{3}\,\mathrm{Area}$. With β_1 the angle opposite b_1 we then have $\partial L_F^2/\partial b_1 = 2b_1 \sin(\beta_1 + 60°)/\sin\beta_1 > 0$ at fixed b_2, b_3. Shrinking the largest side to the second largest and then both to the smallest keeps all angles below 120° and decreases L_F. Thus $L_F \ge \sqrt{3}\min_l b_l > \sqrt{3}$. If some angle is at least 120°, then L_F is the sum of the two shorter sides and exceeds 2. □

Lemma 4.3 (α-test)**.** *If $a_j + a_k \le 1$ for some pair, then a is not physical. Otherwise the numbers $\zeta_i = (a_j^2 + a_k^2 - 1)/(2a_j a_k)$ exceed -1. With $\alpha_i = \arccos(\min(\zeta_i, 1))$, if $\sum_i \alpha_i \ge 2\pi$, then a is not physical.*

Proof. A physical point has $a_j + a_k > 1$ by the proof of Lemma 4.1. It also has $R_i > 1$, which is equivalent to $\cos\theta_i < \zeta_i$ and implies $\theta_i > \alpha_i$ for all i. Summing, $2\pi = \sum_i \theta_i > \sum_i \alpha_i$. □

Lemma 4.4 ($K = 0$ lemma)**.** *Let $a \in (0,1)^3$ be a point at which the solution of Lemma 2.2 exists, with $\theta \in (0,\pi)^3$ and $K = 0$. Then $1/\sqrt{3} \le s < 2/3$, and in particular $s < s^*$.*

Proof. If $K = 0$, then $q_i = 1$, that is $R_i = 1$. The outer triangle, which contains x_4 in its interior, is then the equilateral triangle with unit sides. Then $\sqrt{3} = L_F \le \sum_i a_i < 2$, with L_F as in the proof of Lemma 4.2. The upper bound holds because the convex function $\sum_i |p - x_i|$ attains its largest value 2 on the closed triangle only at the vertices. Finally $s^{*3} = 3/(6\sqrt{3} - 2) > 8/27$ by Proposition 2.4, that is, $s^* > 2/3$. □

Lemma 4.5 (angle-sum lemma)**.** *Let $g_\alpha = \sum_i \alpha_i$, with ζ_i and α_i as in Lemma 4.3.*

(a) *Let $a \in (0,1)^3$, with $a_j + a_k > 1$ for every pair, be a point at which the solution of Lemma 2.2 exists with $\theta \in (0,\pi)^3$. Then $K < 0$ if and only if $g_\alpha(a) < 2\pi$.*

(b) *Let $a = a(s, r, \varphi)$ with $r > 0$ satisfy the hypotheses of Lemma 4.4. Then there is $\epsilon > 0$ such that no point $a(s, t, \varphi)$ with $r < t < r + \epsilon$ is physical.*

Proof. (a) For $K < 0$ we have $R_i > 1$ and $\theta_i > \alpha_i$ for all i. Summing these inequalities, we obtain $g_\alpha < \sum_i \theta_i = 2\pi$. For $K \ge 0$ we have $R_i \le 1$, $\zeta_i \le \cos\theta_i \le 1$ and $\theta_i \le \alpha_i$ for all i, which implies $g_\alpha \ge 2\pi$.

(b) The point a lies on the face $\mathcal{K}$ of Section 6.9, where $K = 0$. By Lemma 6.22(a) its configuration is (v_1, v_2, v_3, p) up to an isometry, for a point p inside the unit equilateral triangle $v_1v_2v_3$ of that section, and $\theta_i = \alpha_i = \arccos\zeta_i$. Hence $|\zeta_i| < 1$, so that g_α is analytic near a. Moreover $a_j + a_k > |v_j - v_k| = 1$ for every pair, and (a) gives $g_\alpha(a) \geq 2\pi$. The barycentric coordinates $\beta_l = \frac{1}{3} + 2\,p \cdot v_l$ of p are positive, and Lemma 6.22(b) gives $\partial g_\alpha/\partial a_l = -(2/\sqrt{3})\,a_l\beta_l/(\beta_1\beta_2\beta_3)$ at a. As $|v_l|^2 = \frac{1}{3}$ and $\sum_l v_l = 0$, we have $a_l^2 = |p|^2 + \frac{1}{3} - 2\,p \cdot v_l$ and $\sum_l a_l^2 = 3|p|^2 + 1$, hence $\beta_l = \frac{1}{3}\big(\sum_i a_i^2 + 1\big) - a_l^2$.

Put $e = a - s(1,1,1)$, so that $\partial_r a = e/r$, $\sum_l e_l = 0$ and $\sum_l e_l^2 = r^2$. Since $\sum_l e_l = 0$, also $\sum_l e_l^4 = r^4/2$ and $r^6 - 6\big(\sum_l e_l^3\big)^2 = 2\prod_{j<k}(e_j - e_k)^2 \geq 0$, so that $\big|\sum_l e_l^3\big| \leq r^3/\sqrt{6}$. With $a_l = s + e_l$ we get $\sum_i a_i^2 = 3s^2 + r^2$ and $\beta_l = \frac{1}{3}(r^2 + 1) - 2se_l - e_l^2$. Expanding,

$$\sum_l a_l\beta_l e_l = -r^2\Big(2s^2 - \frac{1}{3}\Big) - \frac{r^4}{6} - 3s\sum_l e_l^3 \leq -r^2\Big(2s^2 - \frac{1}{3} + \frac{r^2}{6} - \frac{3sr}{\sqrt{6}}\Big).$$

Now $s < 2/3$ by Lemma 4.4, and $r < \sqrt{6}\,(2s - 1)$ by the proof of Lemma 4.1, which needs only $a_j + a_k > 1$. The function $t \mapsto 2s^2 - \frac{1}{3} + \frac{t^2}{6} - \frac{3st}{\sqrt{6}}$ decreases on $[0, \sqrt{6}\,(2s-1)]$, since its minimum lies at $t = 9s/\sqrt{6} > \sqrt{6}\,(2s-1)$, and it equals $\frac{2}{3} - s$ at $t = \sqrt{6}\,(2s-1)$. Therefore $\sum_l a_l\beta_l e_l < -r^2\big(\frac{2}{3} - s\big) < 0$, and

$$\partial_r g_\alpha(a) = \sum_l \frac{\partial g_\alpha}{\partial a_l}\,\frac{e_l}{r} = -\frac{2}{\sqrt{3}}\,\frac{\sum_l a_l\beta_l e_l}{r\,\beta_1\beta_2\beta_3} > 0.$$

So $g_\alpha > 2\pi$ at the points $a(s,t,\varphi)$ with $t > r$ close to r, and Lemma 4.3 shows that these points are not physical. □

5. The certificates

The certificates are finite covers of parts of the configuration space by closed boxes, the *leaves*. Each leaf carries enclosures of the quantities required for its certificate, computed in ball arithmetic. It also carries a *type*, which states the property certified on it by these enclosures. In this section we describe the enclosures, the charts, the covers, the types, the inclusion argument and the checks that we run on them. Most leaves, 1 426 826 of 1 852 313, belong to the bulk cover (Section 5.3), which certifies only that $J > 0$ or that there is no physical point. The delicate certificates are those of the umbilic chart (Section 5.1) and the band certificates (Section 5.4), where the quantities to be signed vanish. Proposition 5.2 at the end lists the computational results used in the proof of Theorem 1, together with item (g), which identifies the concave CCs of four equal masses (Section 1.2).

5.1. **Ball arithmetic and the principal branch.** We compute all enclosures of the certified quantities with the library Arb [Joh17], which is now part of FLINT [FLI25]. For interval methods and their use in proofs see [Moo66, Neu90, MKC09, Tuc11]. Arb computes with balls, intervals $[c - \varepsilon, c + \varepsilon]$ with floating-point centre c and radius ε; its operations return balls that contain the exact results for all points of the input balls. The tests below rely on the following properties of Arb, which we test on example balls (Section 5.6). The logarithm and the power with exponent $-3/2$ of a ball that meets $(-\infty, 0]$ are balls with a NaN midpoint. So is the reciprocal of a ball that contains 0. A NaN midpoint survives addition, multiplication, also by an exact zero, and intersection with a finite ball. Arb does not report a ball with a NaN midpoint as contained in a finite ball. A ball of infinite radius about a finite midpoint, however, becomes finite when it is intersected with a finite ball. This is sound, since the intersection of two enclosures is an enclosure. The principal-branch argument below uses the property of

the logarithm. The code relies on the other properties to make an evaluation fail when an intermediate value has a NaN midpoint, also at the centre of a Taylor form.

The fold-core charts. For a box in one of the charts 0–4 of Section 5.2, we compute enclosures over a ball $c \pm h$ in chart coordinates that contains the box. We use Taylor forms of order p: the jet of each quantity at the centre up to degree $p-1$, together with the coefficients of degree p of the jet computed with the whole ball as base point. The implicit angles are the solution (θ_1, θ_2) of $C(a, \theta) = (k_1 - k_2,\, k_1 - k_3) = 0$ with $\theta_3 = 2\pi - \theta_1 - \theta_2$. We set $K = (k_1 + k_2 + k_3)/3$. We enclose the angles by a Krawczyk step [Kra69]. It rests on the following criterion (see [Moo77], [Neu90, Ch. 5] and [MKC09, Ch. 8]). Let V be a box with centre $\hat{v}$ and Y an invertible matrix. If the interval evaluation of $\hat{v} - YC(a, \hat{v}) + (I - Y\,C_\theta(a, V))(V - \hat{v})$ over all a of the ball lies in the interior of V, then for each a of the ball the equation $C(a, \cdot) = 0$ has exactly one solution in V. A box is *resolved* if this step succeeds over the whole ball. Each resolved evaluation also has a finite enclosure of $\widehat{A}$, which forces the principal branch. Indeed, $\widehat{A}$ is computed from the Arb logarithms of w_i, S_i and S. A finite enclosure of $\widehat{A}$ implies $w_i > 0$ (that is, $0 < a_i < 1$) and $S_i > 0$ on the ball, hence $\sin\theta_i > 0$ for $i = 1, 2, 3$. As all quantities depend on θ only through $\cos\theta_i$ and $\sin\theta_i$, the representatives of the θ_i modulo 2π in $(0, \pi)$ solve the same equations. Their sum is a multiple of 2π in $(0, 3\pi)$, that is, 2π. By the uniqueness in Lemma 2.2, the enclosed solution is the solution of that lemma and has $\theta \in (0, \pi)^3$. On a resolved box, K, $\widehat{A}$, P, Q, $\widetilde{J}$ and the other quantities of Section 3 are therefore the analytic functions defined there. A point of the box is physical exactly when $K < 0$ there.

The umbilic chart. Since the quantities $\widetilde{J}$, T_1, T_2 and T_3 all vanish at p^*, their enclosures over boxes that contain p^* cannot have strict signs. In a separate chart we divide them by powers of the distance ϱ to p^* in the (s, x, y)-space. All first derivatives of P and Q vanish at p^*. The derivatives in s vanish on the axis, where $P = Q = 0$. The derivatives in (x, y) form the matrix $\lambda_{\mathrm{ax}}(s^*)\, I$ at p^* (Lemma 2.3(d)), which is 0. Near p^*, then, $P, Q = O(\varrho^2)$, $\nabla P, \nabla Q = O(\varrho)$, $\widetilde{J} = O(\varrho^2)$, $\mathbf{h} = O(\varrho^3)$, $T_1, T_2, J_{\mathrm{mir}} = O(\varrho)$ and $T_3 = O(\varrho^4)$. In chart 2 we certify the quantities divided by the matching power of ϱ, among them $\widetilde{J}/\varrho^2$, P/ϱ^2, Q/ϱ^2, T_1/ϱ, T_2/ϱ, T_3/ϱ^4, J_{mir}/ϱ and $\partial_\psi(\widetilde{J}/\varrho^2)$, each of which has the sign of the undivided quantity for $\varrho > 0$. We expand at p^* the base quantities K, $\widetilde{J}$, T_3, P, Q with their partial derivatives up to the orders required by the certificates, together with the vector $\mathbf{A} = (-K)\nabla A$. For a base quantity f of order ν whose jet is valid to degree n,

$$f(p^* + \varrho w)/\varrho^\nu = \sum_{\nu \le |\alpha| < n} f_\alpha(p^*)\, \varrho^{|\alpha|-\nu} w^\alpha + \varrho^{n-\nu} \sum_{|\alpha| = n} f_\alpha(\xi)\, w^\alpha, \qquad |w| = 1,$$

for some ξ on the segment from p^* to $p^* + \varrho w$. Here $f_\alpha = \partial^\alpha f/\alpha!$, and the same ξ serves for all α with $|\alpha| = n$ (Taylor's theorem for $t \mapsto f(p^* + tw)$). The coefficients $f_\alpha(p^*)$ are enclosed with s ranging over a ball that contains $[s_a, s_b]$, and the $f_\alpha(\xi)$ over a cube that contains, for each such p^*, the part of the ball $\{\varrho \le \varrho_{\mathrm{u}}\}$ over the wedge. Note that the quantities of chart 2 are assembled from these expansions, not by differentiating them. For $|\alpha| < \nu$ the coefficients $f_\alpha(p^*)$ vanish at the true p^* by the orders above. As a consistency test we check that the enclosures of these coefficients contain 0. These certificates hold on the ball around the true p^*, whose s^* lies in $[s_a, s_b]$ by Proposition 5.2(a).

The corner and fin charts. In the charts CH_{110}, $\mathrm{CH}_{\mathrm{fin}}$ and CH_{111} of Table 2, the three box coordinates u come with three implicit variables v and three equations $\Psi(u, v) = 0$. Let $d = \det \Psi_v$. Along the solution $v(u)$ the matrices $d\,\partial\mu/\partial u$ and $d\,\partial a/\partial u$ are polynomial in the partial derivatives of Ψ, μ and a. Since the factors d^3 cancel, $\operatorname{sign} J = \operatorname{sign}\det(d\,\partial\mu/\partial u) \cdot \operatorname{sign}\det(d\,\partial a/\partial u)$. Rows may be multiplied by positive factors such as $\sin\theta_1$, which leaves these signs unchanged. With a Krawczyk step in Taylor-model arithmetic [MB03] we prove that for

all u in the box the solution $v(u)$ lies in an explicit tube and is the only solution there. It is the only solution that comes from a physical point of the chart's region, either because all such solutions lie in an a priori box in which $\Psi(u,\cdot)$ has at most one zero, or, in CH_{110} and CH_{111}, where u is a function of a alone, because the solution has principal angles and Lemma 2.2 applies. Appendix A lists the equations, the regions and the tests of the three charts.

The bulk chart. In the coordinates (s,x,y) we enclose, by a Krawczyk step in Taylor-model arithmetic, a branch of θ over the box, continued analytically past $\theta_1=\pi$. With $C(a,\theta)=(k_1-k_2,k_1-k_3)$ as a function of (θ_1,θ_2) and $\theta_3=2\pi-\theta_1-\theta_2$, implicit differentiation gives $\Lambda\,\partial\mu/\partial a=\Lambda\mu_a-\mu_\theta\,\mathrm{adj}(C_\theta)C_a$, where

$$\Lambda=\det C_\theta=k_1'k_2'+k_1'k_3'+k_2'k_3', \qquad k_i'=\partial k_i/\partial\theta_i.$$

Let $\mathcal{N}'$ be this matrix with the row of μ_1 multiplied by $\sin\theta_1$, which keeps it analytic across $\theta_1=\pi$. Near $K=0$ we use instead the rows $\sin\theta_1\nabla(\mu_1-\mu_3)$, $\nabla(\mu_2-\mu_3)$ and $(-K)\nabla\mu_3$, which stay analytic across $K=0$. A box is resolved if the step succeeds. On a resolved box $0<a_i<1$, $\theta_2,\theta_3\in(0,\pi)$ and $\theta_1\in(0,2\pi)$ on the enclosed branch. The step also gives Taylor-model ranges of $\det\mathcal{N}'$ and Λ.

- Where the branch can reach $\theta_1\ge\pi$, a continuation check shows that such points are not physical. Let $K_{\pi,i}=w_i\big((a_j+a_k)^{-3}-1\big)$ be the value of K at which $\theta_i=\pi$, and let $\theta_1^{\max}$ be the largest value of θ_1 on the branch over the box. Since k_1 increases with θ_1 past $\theta_1=\pi$, at a point where the branch has $\theta_1=\theta_1^*>\pi$ and $K=K^*$ we have $0<K^*-K_{\pi,1}\le\max k_1'\cdot(\theta_1^*-\pi)$, the maximum taken over $\theta_1\in[\pi,\theta_1^{\max}]$. As K decreases from K^* to $K_{\pi,1}$, the angles θ_2 and θ_3 increase at the rates $1/|k_2'|$ and $1/|k_3'|$. This check certifies that $K_{\pi,1}>K_{\pi,2},K_{\pi,3}$ and that

  $$\bar q=\max_{[\pi,\theta_1^{\max}]}k_1'\cdot\max\Big(\frac{1}{|k_2'|}+\frac{1}{|k_3'|}\Big)<1,$$

  where the second maximum is taken over the ranges of θ_2 and θ_3 on the box, enlarged on both sides by $\delta_2\ge0$ and $\delta_3\ge0$, respectively. The check also certifies $\delta_i\ge\max_{[\pi,\theta_1^{\max}]}k_1'\cdot\max(1/|k_i'|)\cdot(\theta_1^{\max}-\pi)$ for $i=2,3$, the second maximum over the enlarged ranges, so that the enlarged ranges contain all values of θ_2 and θ_3 during the decrease. Consequently $\theta_2+\theta_3$ grows by at most $\bar q(\theta_1^*-\pi)$, which gives $\sum_i\theta_i(K_{\pi,1})\le2\pi-(1-\bar q)(\theta_1^*-\pi)<2\pi$. Since the angles $\theta_i(K)$ are all less than π only if $K>K_{\pi,1}$, the monotonicity in Lemma 2.2 leaves no solution with $\theta\in(0,\pi)^3$.
- By the continuation check, all physical points of a resolved box lie on the enclosed branch with $\theta_1<\pi$. There $k_i'<0$ and $\Lambda>0$. Moreover $\det\mathcal{N}'=\sin\theta_1\,\Lambda^3J$, or $\sin\theta_1\,(-K)\,\Lambda^3J$ with the rows used near $K=0$.
- A leaf of type P is resolved and has $\det\mathcal{N}'>0$ and $\Lambda>0$ on the box. By the previous item, $J>0$ at its physical points.
- Five tests show that a box holds no physical point. A leaf whose box passes one of them has type X.
  - (i) The branch test: the enclosed branch has $\theta_1>\pi$ throughout the box and passes the continuation check.
  - (ii) The test at $K_{\pi,1}$: throughout the box, $K_{\pi,1}>K_{\pi,2},K_{\pi,3}$ and $\theta_2+\theta_3<\pi$ at $K=K_{\pi,1}$, hence $\sum_i\theta_i(K)<2\pi$ whenever all $\theta_i(K)<\pi$.
  - (iii) The range test: throughout the box, some $a_i\ge1$ or some $a_j+a_k\le1$.
  - (iv) The test at $K=0$: throughout the box, $\sum_i\theta_i(0)\ge2\pi$, hence $\sum_i\theta_i(K)>2\pi$ for $K<0$.
  - (v) The sign test: the enclosed branch has $K\ge0$ throughout the box and passes the continuation check where it reaches $\theta_1\ge\pi$.

5.2. **The charts.** Table 2 lists the charts, in each of which all the quantities are analytic up to the faces of the chart domain that are used. In charts 3 and 4 the w_i, the k_i and K all carry a factor σ. We divide it out. The scaled equations stay regular at $\sigma = 0$. There the scaled value $\widetilde{K} = K/\sigma$ is negative. In these charts the proof uses $\widetilde{K}$ only in the test $\widetilde{K} < 0$ for physical points and in the function $A - \log\sigma = \widehat{A} - 2\log\sigma - \log(-\widetilde{K})$, which the programs compute from the scaled weights w_i/σ and from whose gradient they obtain ∇A. The frame of Section 3.1 is replaced by $(-\sigma\partial_\sigma, \partial_{\hat r}, \hat r^{-1}\partial_\varphi)$ in chart 3 and by $(-\sigma\partial_\sigma, \partial_\xi, \partial_\eta)$ in chart 4. In chart 3 this frame is $\sigma M'$ times the frame of chart 1, where M' is a shear with $\det M' = 1$. Chart 4 is related to chart 0 in the same way. With $\mathbf{A}$ replaced by ∇A, the formulas of Section 3.1 give $\widetilde{J} = \sigma^3\widetilde{J}_1/(-K)$, where $\widetilde{J}_1$ is the value in chart 1 and $K = \sigma\widetilde{K} < 0$ is the unscaled value. In particular $\operatorname{sign}\widetilde{J} = \operatorname{sign} J$. At the points of Σ, T_1, T_2 and T_3 are the values in chart 1 multiplied by positive factors. In particular $T_3 = \sigma^6 T_3^{(1)}/K^2$ at the zeros of $\widetilde{J}$, where $T_3^{(1)}$ is the value in chart 1, because the three rows of the determinant are $\sigma M'\mathbf{h}$, $\sigma M'\mathbf{A}/(-K)$ and $\sigma M'\nabla(\sigma^3\widetilde{J}_1/(-K)) = \sigma^4 M'\nabla\widetilde{J}_1/(-K)$ there. At every point $J_{\mathrm{mir}} = \sigma^2 J_{\mathrm{mir}}^{(1)}/(-K)$, where $J_{\mathrm{mir}}^{(1)}$ is the value in chart 1: the shear cancels in the 2×2 determinant.

chart	coordinates	region
0	(s, x, y)	near the axis
1	$(s,\ l = \log_2 r,\ \varphi)$	the fold core away from the axis
2	(ϱ, ψ, φ), $(s, x, y) = p^* + \varrho(\cos\psi, \sin\psi\cos\varphi, \sin\psi\sin\varphi)$	the ball around the umbilic
3	$(\sigma, \hat r, \varphi)$, $s = 1 - \sigma$, $r = \sigma\hat r$	the fold core near $a = (1,1,1)$
4	(σ, ξ, η), $s = 1 - \sigma$, $x = \sigma\xi$, $y = \sigma\eta$	the axis near $a = (1,1,1)$
CH_{110}	$u = \big(a_3,\ (1-a_2)/a_3,\ (1-a_1)/(1-a_2)\big)$	the corner $a \to (1,1,0)$
$\mathrm{CH}_{\mathrm{fin}}$	$u = (-K,\ a_3,\ \theta_1)$	the fin $a_1 + a_2 \to 2$
CH_{111}	$u = \big(1-a_3,\ (1-a_2)/(1-a_3),\ (1-a_1)/(1-a_2)\big)$	the corner $a \to (1,1,1)$ and the fin tip
bulk	(s, x, y)	the rest of the wedge

TABLE 2. The charts of the certificates. The fold core is defined in Section 5.3.

5.3. **The covers.** We use the functions r_{top} and r_{ax} defined below and the constants

$$s_{\mathrm{lo}} = \tfrac{19}{32}, \qquad s_{\mathrm{hi}} = \tfrac{31}{32}, \qquad \hat r_{\mathrm{top}} = \tfrac{3}{16}, \qquad \varrho_{\mathrm{u}} = 7.5\cdot 10^{-4}.$$

More precisely, ϱ_{u} is the smallest double-precision number not below $7.5\cdot 10^{-4}$, the double nearest to it, which the programs use. It exceeds $7.5\cdot 10^{-4}$ by $1.6\cdot 10^{-20}$. The *fold core* is the following region.

- For $s \in (\frac12, s_{\mathrm{lo}}]$: $r \le \sqrt{6}\,(2s-1)$, which holds at all physical points by Lemma 4.1.
- For $s \in [s_{\mathrm{lo}}, s_{\mathrm{hi}}]$: $r \le r_{\mathrm{top}}(s)$.
- For $s \ge s_{\mathrm{hi}}$: $\hat r \le \hat r_{\mathrm{top}}$, in the coordinates of chart 3.

At $s = s_{\mathrm{lo}}$ and $s = s_{\mathrm{hi}}$, where two descriptions apply, the fold core is their union. We write $FC(s)$ for the part of the fold core at level s. Table 3 lists the covers, and the leaves of the covers of charts 0 and 1 that meet the mirror planes are drawn in Figure 3. The *zone column* $\{s \in [0.70941162109375,\ 0.7099609375],\ r \le r_{\mathrm{top}}(s)\}$ is a neighbourhood of the umbilic, which the umbilic cover covers. In the fold-core charts, φ ranges over $[\pi/6 - 10^{-12},\ \pi/2 + 10^{-12}]$.

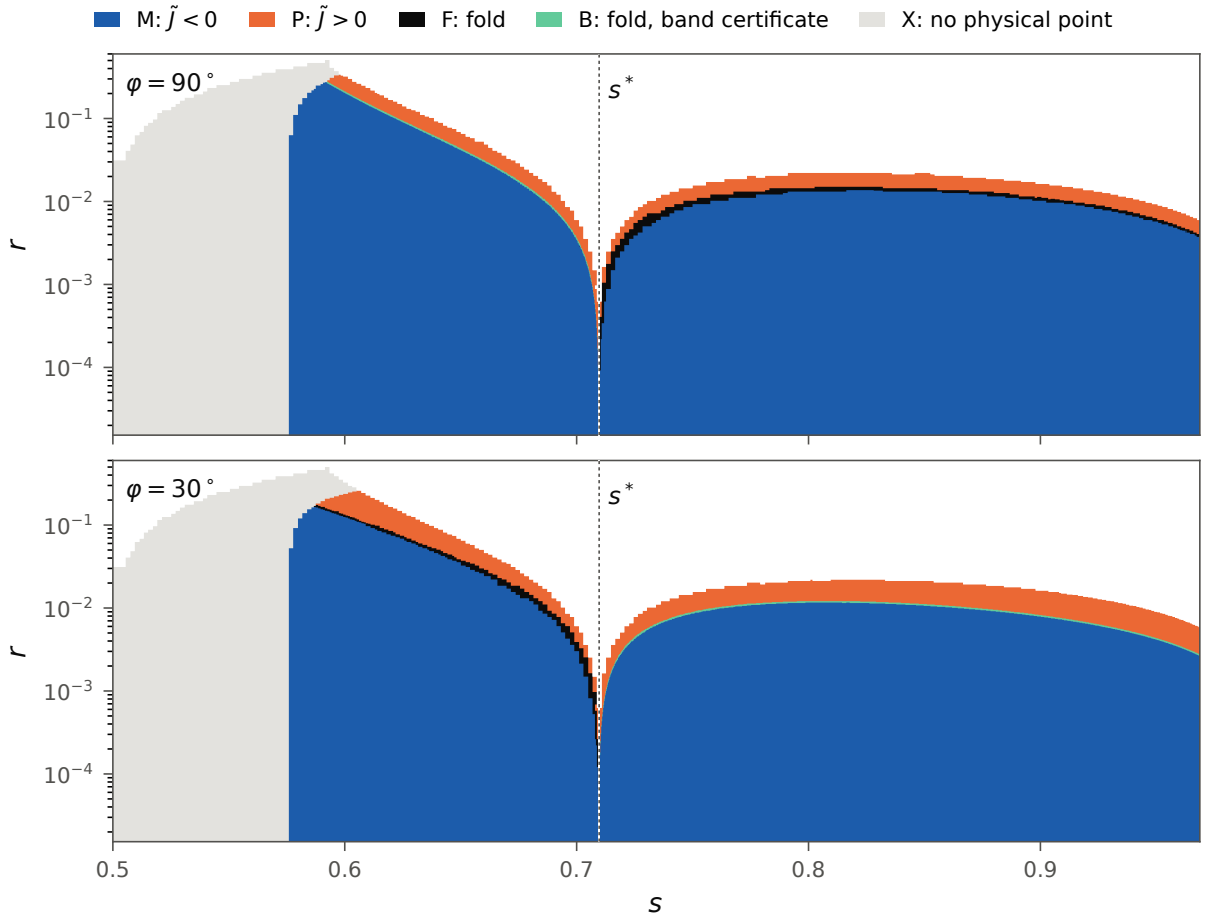


FIGURE 3. The leaves of the core, lower core, axis and lower axis covers that meet the mirror planes $\varphi = 90°$ (top) and $\varphi = 30°$ (bottom), drawn in the (s, r)-plane with r on a logarithmic scale and coloured by type (Table 4). The leaves of type U, which lie in the umbilic ball, are not drawn. The legend gives the certified signs of $\widetilde{J} = (-K)J$, which are those of J at the physical points (Lemma 3.1(a)). Leaves of type B, which are thinner than a line at this scale, are drawn one line high. The leaves of type M reach the bottom edge of the plot, $r = 2^{-16}$. They lie below the fold, except for s below about 0.59, where the rays in the mirror planes do not meet the fold (case (R2) of Corollary 6.9) and the leaves of type M lie directly below leaves of type X. Those of type X on the left contain no physical point: physical points have $s > 1/\sqrt{3}$ (Lemma 4.2). The leaves of type X above the others, for $s < 0.61$, contain no physical point either. They have $K > 0$ or are excluded by the α-test (Table 3). For $s \geq 19/32$ the region above the drawn leaves is that of the bulk cover, where $J > 0$. For $s < 19/32$ no physical point lies above $r = \sqrt{6}\,(2s - 1)$ (Lemma 4.1). Neither the zone column around s^*, covered by the umbilic cover and narrower than the dotted line at s^*, nor the strip $s \geq 31/32$, covered by the top covers, is drawn. Near $s = s^*$ the band of leaves of types F and B descends towards the axis until it reaches the edges of the zone column, where its lowest leaves lie at about $r = 10^{-4}$; inside this column the fold reaches the axis at p^*, where $\overline{\mathcal{D}}$ splits into the two nappes.

cover	chart	region	leaves
core	1	$s \in [s_{\mathrm{lo}}, s_{\mathrm{hi}}]$, $r_{\mathrm{ax}} \le r \le r_{\mathrm{top}}$, off the zone column	M 82252, P 231367, F 36031, X 2808, B 2334, U 67
axis	0	$s \in [s_{\mathrm{lo}}, s_{\mathrm{hi}}]$, $r \le r_{\mathrm{ax}}$, off the zone column	M 4576
lower core	1	$s \in [\frac{1}{2}, s_{\mathrm{lo}}]$, $r_{\mathrm{ax}} \le r \le \sqrt{6}(2s-1)$	M 12818, P 2111, F 1665, X 21661, B 25
lower axis	0	$s \in [\frac{1}{2}, s_{\mathrm{lo}}]$, $r \le r_{\mathrm{ax}}$	M 109, X 293
top core	3	$\sigma \le 2^{-5}$, $2^{-5} \le \hat{r} \le \hat{r}_{\mathrm{top}}$	M 3984, P 10607, F 1293, B 27
top axis	4	$\sigma \le 2^{-5}$, $\hat{r} \le 2^{-5}$	M 208
umbilic	2	$\varrho \le \varrho_{\mathrm{u}}$ around p^*	M 26, P 114, F 14, B 2
bulk	bulk	$s \in [s_{\mathrm{lo}}, s_{\mathrm{hi}}]$: the part of the wedge outside the core, the fin and the corner	P 443963, X 982831, D 32
corner $(1,1,0)$	CH_{110}	$u \in [0, 0.1875] \times [0,1]^2$	P 792, X 744
fin	$\mathrm{CH}_{\mathrm{fin}}$	$u \in [0, 0.08] \times [0.125, 0.9] \times [\pi/2, \pi]$	P 485, X 870
corner $(1,1,1)$	CH_{111}	$u \in [0, 0.1] \times [0,1]^2$	P 1281, X 6757, D 166

TABLE 3. The covers and the numbers of their leaves of each type (Section 5.4). Of the leaves of type X, 1195 in the core cover, 3113 in the lower core cover and 14 in the lower axis cover have $K > 0$ on a resolved box. The other 1613, 18548 and 279 are excluded by the α-test.

The region functions. The fold table is a floating-point table with 423 nodes $s \in [0.5775, 0.999]$. At each node it lists the radius of the fold at the angles $\varphi = 0°, 1°, \dots, 360°$, where one was found. Let $r_f^{\max}(s)$ and $r_f^{\min}(s)$ be the largest and the smallest of these radii, interpolated linearly in s and constant beyond the ends of the table. A missing radius counts as 0 in $r_f^{\max}$ and as 9 in $r_f^{\min}$. Then

$$r_{\mathrm{top}}(s) = (1+2^{-40}) \max\bigl(1.5\, r_f^{\max}(s),\ r_{\mathrm{fl}}(s)\bigr), \qquad r_{\mathrm{ax}}(s) = 0.4\,(1+2^{-40}) \min\bigl(r_f^{\min}(s),\ 0.3\,|s-\tilde{s}|\bigr).$$

Here the floor $r_{\mathrm{fl}}(s)$ is $6.2 \cdot 10^{-4}$ for $s \in [0.7086181640625,\ 0.7110595703125]$ and 0 otherwise. The double $\tilde{s} = 0.7097084911075526$ lies in the s-range of the zone column. In these formulas 0.4, 0.3 and $6.2 \cdot 10^{-4}$ denote the doubles nearest to them, which the programs use; the other constants are doubles. We chose the factors 1.5, 0.4 and 0.3 to split the work between the covers. This choice affects whether the certificates succeed, not their validity: off the zone column the inclusion argument of Section 5.5 works for any positive continuous r_{ax} for which the roots of the fold-core covers contain the regions that it defines. The axis and lower axis covers, which cover $r \le r_{\mathrm{ax}}$, have leaves of types M and X only, so their certificates can succeed only if $J < 0$ at all physical points with $s \le s_{\mathrm{hi}}$ and $r \le r_{\mathrm{ax}}$ off the zone column. Floating-point rounding in the programs that build the covers cannot invalidate an inclusion, since the exact check of Section 5.6 repeats in rational arithmetic all comparisons of boxes with regions; an inaccurate table could only make certificates fail.

5.4. **Leaf types.** Each leaf of a fold-core cover is a box of its chart's subdivision tree. Except for the leaves of type X excluded by the α-test and the leaves of type U, each leaf is resolved on a ball that contains it. The type of a leaf states what is certified on its box (Table 4). In the table, "physical point" means a physical point of the box and "point of Σ" a physical point of the box with $J = 0$. The types F and B use *projected enclosures*. For a box and constants $\hat{c}_1$, $\hat{c}_2$, $\hat{c}_3$ that we choose at its centre, these are enclosures over the box of $T_\ell - \hat{c}_\ell \widetilde{J}$, $\ell = 1, 2, 3$, which equal T_ℓ where $\widetilde{J} = 0$.

type	certified on the box	consequence
M	$\widetilde{J} < 0$	$J < 0$ at all physical points
P	$\widetilde{J} > 0$	$J > 0$ at all physical points
F	projected $T_1 > 0$, $T_2 < 0$ and $T_3 < 0$, plus P or Q strictly signed in the umbilic cover	at all points of Σ: $T_1 > 0$, $T_2 < 0$, $T_3 < 0$
B	band certificate (below): on the cell, projected $T_1 > 0$ and $T_2 < 0$, and the bracket of Lemma 3.3 at most $\beta_C < 0$; on the mirror face, $J_{\mathrm{mir}} \neq 0$, $(P, Q) \neq 0$ and $T_1 > 0$	at all points of Σ: $T_1 > 0$, $T_2 < 0$; off the mirror $T_3 < 0$, with the bound (3.1); on the mirror $J_{\mathrm{mir}} \neq 0$ and $T_3 = 0$
X	$K > 0$ on the resolved box, or the α-test on the box	no physical point
U	no property	lies in the umbilic ball

TABLE 4. The types of the leaves of the fold-core covers.

Further conditions depend on the chart.

- Charts 0 and 4 have leaves of types M and X only.
- Chart 2: all leaves have $K < 0$, and none is of type X.

The band certificate (charts 1 and 3). The cell of a band certificate is a ball that contains the leaf's box and has exactly one mirror angle φ_m in its φ-range. It certifies that $\widetilde{J} < 0$ on the lower r-face of the cell and $\widetilde{J} > 0$ on the upper one. Then $\widetilde{J}$ has a zero on each r-segment of the cell. The segments on the mirror provide the zeros required by Lemma 3.3. On the cell it certifies projected $T_1 > 0$ and $T_2 < 0$ and finite enclosures of $\partial_\varphi^2 T_3$ and $\partial_\varphi^2 \widetilde{J}$. On the mirror face it certifies that J_{mir} is strictly signed, that P or Q is strictly signed, and that $T_1 > 0$. Finally, it certifies a negative upper bound β_C of the bracket of Lemma 3.3. The program that builds the cover encloses the bracket with outward rounding; the separately written checking program of Section 5.6 recomputes its largest value over the corners of the enclosures in exact rational arithmetic. Lemma 3.3 then gives (3.1) with $\beta = \beta_C$ for the certified quantities of the chart. The version for chart 2 uses ψ-faces and $\partial_\psi(\widetilde{J}/\varrho^2)$.

The band certificate is used only on the mirror $\varphi = 90^\circ$ for $s < s^*$ and on the mirror $\varphi = 30^\circ$ for $s > s^*$, and for the umbilic cover only at the points with $\varrho > 0$ (Proposition 5.2(h)). Of the 2334 leaves of type B of the core cover, 980 lie below s^* and 1354 above it. All 25 leaves of type B of the lower core cover lie below s^* and all 27 of the top core cover above it; the umbilic cover has one of each kind.

The other covers. In the bulk, corner and fin covers, a leaf of type P certifies $J > 0$ at all physical points of the chart's region over the box, in the charts of Appendix A together with the uniqueness of the zero of the Krawczyk step. A leaf of type X certifies that no physical point of the region lies over the box. A leaf of type D is deferred to the fold-core covers. In the bulk cover these are 32 boxes near the umbilic that lie in the core region. In the corner cover at $(1, 1, 1)$ they are boxes in $\hat{r} < 0.184$, whose points routed to this cover in Section 5.5 lie in the top covers.

5.5. **Inclusion.** We glue the covers by the three routing statements of Lemma 5.1, whose constants we check in exact arithmetic. Let $T_{\mathrm{fin}} = 1.9499999995$, a value that satisfies the inequalities used in Lemma 5.1(a).

Lemma 5.1. *Let $a \in W$ be physical.*

(a) (Fin lemma.) *If* $a_1 + a_2 \geq T_{\text{fin}}$ *and* $a_3 \leq 0.9$*, then* $-K \leq 0.08$ *and* $\theta_1 \in [\pi/2, \pi)$*. If also* $a_3 \geq 0.125$*, then* $u = (-K, a_3, \theta_1)$ *lies in the domain of the fin cover.*

(b) (Top route.) *If* $s \geq s_{\text{hi}}$*, then* $1 - a_3 < 3\sigma \leq 3/32 < 0.1$*. If* $a_3 \geq 0.9$*, then* $1 - a_3 \leq 0.1$*. In both cases* a *lies in the domain of the corner cover at* $(1, 1, 1)$*.*

(c) (From the corner at $(1, 1, 1)$ to the top charts.) *Let* $\delta = 2 - T_{\text{fin}}$*. If* $a_1 + a_2 \geq T_{\text{fin}}$ *and* a *lies in a leaf of type D of the corner cover at* $(1, 1, 1)$*, then* $\sigma < \delta/(2 - 0.184\sqrt{6}/3) \leq 1/32$*.*

Proof. (a) As $a_1 \geq a_2$ and $a_1 < 1$, we have $a_1 \geq T_{\text{fin}}/2$ and $a_2 > T_{\text{fin}} - 1$. From the first, $0 < -K = w_1(1 - q_1) < w_1 \leq (T_{\text{fin}}/2)^{-3} - 1 \leq 0.08$. Next, $-K < w_2 < (T_{\text{fin}} - 1)^{-3} - 1$ and $w_3 \geq 0.9^{-3} - 1$, so $q_3 = 1 + K/w_3 \geq q_{lo} = 1 - \big((T_{\text{fin}} - 1)^{-3} - 1\big)/\big(0.9^{-3} - 1\big) = 0.55251\ldots > 0$. Then $R_3 = q_3^{-2/3} \leq q_{lo}^{-2/3} \leq T_{\text{fin}}^2/2 \leq a_1^2 + a_2^2$. Therefore $\cos\theta_3 \geq 0$, that is $\theta_3 \leq \pi/2$. As $\theta_2 < \pi$, it follows that $\theta_1 = 2\pi - \theta_2 - \theta_3 \geq \pi/2$, while $\theta_1 < \pi$ as a is physical. (b) We have $1 - a_3 = \sigma + 2y/\sqrt{6}$ and, by Lemma 4.1, $y \leq r < \sqrt{6}\,\sigma$. The other two coordinates of CH_{111} lie in $[0, 1]$ by $a_1 \geq a_2 \geq a_3$. (c) Since the leaves of type D of this cover lie in $\hat{r} < 0.184$ (Section 5.6), we have $y \leq r < 0.184\,\sigma$. Then $a_1 + a_2 = 2s + 2y/\sqrt{6} \geq T_{\text{fin}}$ implies $2\sigma - \delta \leq 2y/\sqrt{6} < 0.184\,\sigma\sqrt{6}/3$. □

With the exact inclusion check we verify the following statements, which together show the two coverage statements of Proposition 5.2(b).

- $\frac{1}{2} < s \leq s_{\text{lo}}$: the lower core cover where $r \geq r_{\text{ax}}$ and the lower axis cover where $r \leq r_{\text{ax}}$.
- $s_{\text{lo}} \leq s \leq s_{\text{hi}}$: the bulk cover, whose root domain contains all such points. Each point of it lies in a leaf of type P or X, in a leaf of type D (these lie in the core region, below the floor of r_{top}), or in a box that contains no leaf and lies, by the exact check,
  - outside W;
  - in the fin $a_1 + a_2 \geq T_{\text{fin}}$, which goes to the corner cover at $(1, 1, 0)$ if $a_3 \leq 0.1875$, to the fin cover if $0.1875 \leq a_3 \leq 0.9$ (by Lemma 5.1(a)), and to the corner cover at $(1, 1, 1)$ if $a_3 \geq 0.9$;
  - in the corner $a_3 \leq 0.1875$, which goes to the corner cover at $(1, 1, 0)$;
  - in the core $r \leq r_{\text{top}}$, which goes to the umbilic cover on the zone column and elsewhere to the core cover where $r \geq r_{\text{ax}}$ and to the axis cover where $r \leq r_{\text{ax}}$.
- $s \geq s_{\text{hi}}$: the corner cover at $(1, 1, 1)$, by Lemma 5.1(b). The leaves of type D of this cover lie in $\hat{r} < 0.184$. The points of these leaves that are routed to this cover have $\sigma \leq 1/32$, directly if $s \geq s_{\text{hi}}$ and by Lemma 5.1(c) if they come from the fin. They go to the top core cover where $\hat{r} \geq 2^{-5}$ and to the top axis cover where $\hat{r} \leq 2^{-5}$.
- Fold-core covers: the roots of each cover contain the chart's region, the leaves and the dropped boxes tile each root exactly, and all dropped boxes lie outside the region (in the zone column, above r_{top} or $\sqrt{6}\,(2s - 1)$, below r_{ax} in chart 1, above r_{ax} in chart 0, outside W, or in $\hat{r} \geq 2^{-5}$ in chart 4). No box of the top core cover is dropped.
- The chart domain of each of the two corner covers and of the fin cover is a box that contains the region given in Table 3. The leaves of the cover tile it exactly. In the programs the bounds 0.08, 0.9 and 0.1 of these regions are the smallest doubles not below them, while $\pi/2$ is replaced by the adjacent double below it and π by the adjacent double above it.
- The umbilic ball $\{\varrho \leq \varrho_{\text{u}}\}$ is centred at the true p^*, whose s^* lies in $[s_a, s_b]$. It contains the zone column, on which the largest value of ϱ is $6.8741 \cdot 10^{-4} < \varrho_{\text{u}}$. It also contains the 67 leaves of type U of the core cover, on which the largest value of ϱ is $3.9486 \cdot 10^{-4}$. The leaves of the umbilic cover tile its chart domain, a box that contains $[0, \varrho_{\text{u}}] \times [0, \pi] \times [\pi/6, \pi/2]$.
- The ball of each leaf contains its box.

We make these comparisons against finitely many surfaces ($r = r_{\text{ax}}(s)$, $r = r_{\text{top}}(s)$, $r = \sqrt{6}(2s - 1)$, the faces $a_1 = a_2$ and $a_2 = a_3$ of W, $a_1 + a_2 = T_{\text{fin}}$, $a_3 = 0.1875$, $a_3 = 0.9$, $s = \text{const}$,

$\hat{r} = \text{const}$), which form a closed nowhere dense set Z. It suffices to treat the physical points off Z. Indeed, since Ω_4 is open and Z is closed and nowhere dense, any physical point on Z is a limit of physical points off Z. One of the finitely many leaves contains infinitely many of them and, being closed, also their limit.

5.6. **The checks.** With one script we rebuild the compiled libraries and regenerate all covers from the sources. This reproduces the arrays of leaves of the stored covers exactly. The same script then runs the following checks.

(1) *Arb.* We test the properties of Arb listed in Section 5.1 on example balls with the installed library.
(2) *Structure of the fold-core covers.* The roots form a full grid on the root domain, the leaves and dropped boxes tile each root, the dropped boxes lie outside the region, and the leaves of type U lie in the umbilic ball. The umbilic ball contains the zone column; the leaves of the umbilic cover tile the domain of chart 2.
(3) *Band leaves.* We recertify every leaf of type B, using r-faces inside the ball of its cell. We also check in exact arithmetic that its mirror angle lies in the cell. A separate program checks, in exact arithmetic, the location in s (in ψ for chart 2) and in φ of all band certificates, as stated in Proposition 5.2(h), and that each cell is the box of its leaf widened in r (in ψ for chart 2) only. It checks 2388 leaves of type B.
(4) *Leaves of the fold-core, corner and fin covers.* We re-evaluate each leaf at its stored order outside the programs that built the covers. This reproduces the stored enclosures exactly. A separately written program derives the type of the leaf from these enclosures, including the parts not stored with the covers (the enclosures of P and Q, the band conditions, and the region and uniqueness tests of Appendix A). We retest the leaves excluded by the α-test in interval arithmetic with mpmath, independently of Arb and of the C code.
(5) *Leaves of the bulk cover.* We re-evaluate every leaf outside the program that built the cover. This reproduces its outcome and its range of $\det \mathcal{N}'$ exactly. From these we derive its type, including the condition $\Lambda > 0$, which is not stored with the cover.
(6) *Exact inclusion.* We verify all statements of Section 5.5 in rational arithmetic. Where the irrational numbers 2^l (chart 1) and π enter, we use rational bounds from Arb. The same check verifies the constants of Lemma 5.1, the parameters stored with the covers, the signs of λ_{ax} at s_a and s_b, the inclusion of each leaf's box in its ball (for the leaves of type B, in its cell: check (3)), and the stored types.
(7) *The level of the umbilic, the ends, the half-plane condition and the equal-mass check*: the checks behind Proposition 5.2(c)–(g) below.

In (3)–(5) the re-evaluations call the same compiled libraries as the programs that built the covers, so they test these programs and the stored covers, not the formulas that the libraries evaluate (see Data and code availability).

5.7. **Summary.**

Proposition 5.2. *The computations described in this section establish the following.*

(a) $\lambda_{\mathrm{ax}}(s_a) > 0 > \lambda_{\mathrm{ax}}(s_b)$, *with* s_a, s_b *as in Section 2.4.*
(b) *Every leaf of the covers of Table 3 has the properties of Section 5.4 for its type and chart. The leaves of the fold-core covers and the umbilic ball cover all points of the fold core in* W, *physical or not. Every physical point of* W *outside the fold core lies in a leaf of type* P *of the bulk, corner or fin covers.*
(c) *The umbilic ball lies in* Ω_4, *and* $K \le -0.8283$ *on it. Every leaf of the umbilic cover spans the whole range* $0 \le \varrho \le \varrho_{\mathrm{u}}$. *The leaves whose* ψ*-range contains* 0 *or* π *contain the axis*

points with $\varrho > 0$, and they are of type M. The leaves whose ψ-range contains $\pi/2$ contain the points of the plane $s = s^*$ with $\varrho > 0$, and they are of type P.

(d) *Every leaf of type M, P, F or B of the fold-core covers other than the umbilic cover is resolved and has finite enclosures of K and $\widehat{A}$ (of K/σ and $A - \log\sigma$ in charts 3 and 4).*

(e) *$J > 0$ at every physical point with $s = s^*$ other than p^*.*

(f) *Let $u_L = (\cos 75^\circ, \sin 75^\circ)$ and $u_U = (\cos 220^\circ, \sin 220^\circ)$. At every point of $\Sigma \cap W$, $u_L \cdot (P, Q) > 0$ if $s < s^*$ and $u_U \cdot (P, Q) > 0$ if $s > s^*$.*

(g) *The point $a = s_{eq}(1, 1, 1)$ has $K < 0$ and $J < 0$. There is a physical point a_{iso} on the mirror $\varphi = 90^\circ$, approximately $(0.73904, 0.73904, 0.72291)$, with $A = Q = 0$ and $J > 0$.*

(h) *For every leaf of type B one of two cases holds. Either the points with $\varrho > 0$ of its box and of its cell lie in $\{s < s^*\}$ and 90° is the only mirror angle in the φ-ranges of the box and the cell, or these points lie in $\{s > s^*\}$ and 30° is the only mirror angle in these ranges. The cells of the two leaves of type B of the umbilic cover span $0 \le \varrho \le \varrho_{\mathrm{u}}$. One has its ψ-range in $(\pi/2, \pi)$ and the mirror angle 90°. The other has its ψ-range in $(0, \pi/2)$ and the mirror angle 30°.*

We indicate how (a) and (c)–(h) are obtained, item (b) being the content of Sections 5.1–5.5. (a) Arb enclosures of λ_{ax} at the two doubles have the stated signs. (c) An evaluation over 256 boxes that cover the umbilic ball in chart 0 is resolved and shows that $K \le -0.8283$. We read off the ranges in ϱ and the types of the leaves of the umbilic cover from the stored cover. (d) We re-evaluate all leaves of type M, P, F or B of the fold-core covers other than the umbilic cover (checks (4) and (7)) and obtain the stated result. (e) In the core cover, the leaves that meet $s = s^*$ are of types P and F. Re-evaluated on the pieces that meet $[s_a, s_b]$, the F leaves have $\widetilde{J} > 0$. The axis, lower core and lower axis covers have no leaves there, the top covers lie in $s \ge s_{\mathrm{hi}}$, the leaves of type U lie in the umbilic ball, and the leaves of the umbilic cover that meet $\psi = \pi/2$ are of type P. Outside the fold core, $J > 0$ by (b). (f) All leaves of type F or B of the core, lower core, top core and umbilic covers are re-evaluated, split into pieces where necessary. Each piece either has $u \cdot (P, Q) > 0$ with the vector u of its nappe, or it has $\widetilde{J}$ of one sign or $K > 0$. In the last two cases it contains no point of Σ. The pieces that meet $s = s^*$ are settled by the signs of $\widetilde{J}$ or K alone. (g) On a box around $s_{eq}(1, 1, 1)$ the enclosures show $K < 0$ and $\widetilde{J} \in [-4.06572, -4.06571]$. The enclosure of A contains 0, in agreement with Lemma 2.3(c). On the mirror $P = 0$. Let $z_0 \approx (0.7336623572,\ 0.0131679438)$ be a floating-point zero of (A, Q) in the coordinates (s, r) of the mirror. Let $v_1 \approx (-0.0962865,\ -0.0430095)$ and $v_2 \approx (0.0817315,\ 1.5838743)$ be the columns of the inverse of a floating-point Jacobian matrix of (A, Q) near z_0. On the parallelogram $\{z_0 + t_1 v_1 + t_2 v_2 :\ |t_1|, |t_2| \le 10^{-7}\}$ the enclosures show $A < 0$ on the side $t_1 = -10^{-7}$, $A > 0$ on $t_1 = 10^{-7}$, $Q < 0$ on $t_2 = -10^{-7}$ and $Q > 0$ on $t_2 = 10^{-7}$. The Poincaré–Miranda theorem [Mir40, Kul97] then yields a zero of (A, Q) in the parallelogram. On it $\widetilde{J} \in [12.0429, 12.0438]$ and $K < 0$. (h) We compare the balls of all band certificates with the mirror angles and with $[s_a, s_b]$, in chart 2 with $\psi = \pi/2$. The comparison is in exact rational arithmetic with Arb enclosures of π. In charts 1 and 3 each such ball lies in $s < s_a$ or in $s > s_b$. Moreover $s_a \le s^* \le s_b$. The ranges in ϱ of the two cells of the umbilic cover are read off from the stored cover.

6. The count at regular values

In this section we prove the following proposition, the first step towards Theorem 1, together with the injectivity of the mass map on $\overline{\mathcal{D}}$, on which the later sections build.

Proposition 6.1 (the count at regular values)**.** *Let m be positive masses and $i \in \{1,2,3,4\}$. Then $1 \le c_i(m) \le 4$. If $\mu^{(i)}(m)$ is a regular value of the mass map F_i, then $c_i(m) \in \{2,4\}$. The critical values of F_i form a closed null subset of $\mathbb{R}^3$.*

We prove it for $i = 4$ and write $F = F_4$. The other cases follow by relabelling the bodies. Section 6.1 proves properness, and Section 6.2 collects three topological lemmas. Sections 6.3–6.8 prove that F is injective on $\overline{\mathcal{D}}$ and determine the slices $F(\overline{\mathcal{D}}) \cap \{A = c\}$. Section 6.9 computes the preimages of one regular value through the restricted problem, and Section 6.10 carries this count to all regular values and proves Proposition 6.1. The statements about W in Proposition 5.2 extend to Ω_4 by $\mathfrak{S}_3$-equivariance.

6.1. **Properness.** For a configuration x and masses m let $U(x) = \sum_{i<j} m_i m_j / r_{ij}$ and $I_m(x) = \sum_i m_i |x_i - c_m|^2$. Recall the standard identity $\lambda = U(x)/I_m(x)$, which follows from (1.1), the homogeneity of degree -1 of U and its translation invariance.

Lemma 6.2 (Shub's lemma for convergent masses)**.** *Let $m^{(k)} \to m$ in $(0,\infty)^4$, and let $x^{(k)}$ be a CC for the masses $m^{(k)}$ with $c_{m^{(k)}}(x^{(k)}) = 0$ and $I_{m^{(k)}}(x^{(k)}) = 1$. Then the mutual distances of the $x^{(k)}$ are bounded below by a positive constant.*

Proof. We adapt the standard proof of Shub's lemma [Shu71], [Moe14, Prop. 15] to convergent masses. Suppose the contrary. Since the masses are bounded below, the normalization bounds the $x^{(k)}$. Passing to a subsequence, we may assume that $\min_{i<j} r_{ij}(x^{(k)}) \to 0$ and that $x^{(k)} \to \bar{x}$. Then $c_m(\bar{x}) = 0$, $I_m(\bar{x}) = 1$, and $\bar{x}$ has a collision. Group the bodies into clusters, the classes of the relation $\bar{x}_i = \bar{x}_j$. With $\lambda_k = U(x^{(k)})$, the equations read $\nabla_j U(x^{(k)}) = -\lambda_k m_j^{(k)} x_j^{(k)}$. We sum them over the bodies j of a cluster $\mathcal{C}$. The forces between bodies of $\mathcal{C}$ cancel, while the forces exerted by the other bodies stay bounded, since the distances between different clusters stay bounded away from 0. This leaves $\lambda_k \sum_{j\in\mathcal{C}} m_j^{(k)} x_j^{(k)}$ bounded, while $\lambda_k \to \infty$ because two bodies collide and the masses are bounded below. Dividing by λ_k and letting $k \to \infty$, we get $\sum_{j\in\mathcal{C}} m_j \bar{x}_j = 0$, that is, the common position of the bodies of $\mathcal{C}$ is 0, for each cluster $\mathcal{C}$. Then $\bar{x} = 0$, which contradicts $I_m(\bar{x}) = 1$. □

Proposition 6.3. *The mass map $F : \Omega_4 \to \mathbb{R}^3$ is proper.*

Proof. We show that every sequence in the preimage of a compact set has a subsequence converging in Ω_4. Let $a^{(k)} \in \Omega_4$ with $\mu^{(k)} = F(a^{(k)}) \to \mu$, and let $m^{(k)} = (e^{\mu^{(k)}}, 1) \to m = (e^{\mu}, 1)$ be the corresponding masses. Let $x^{(k)}$ be the corresponding concave CCs, normalized as in Lemma 6.2. Their mutual distances are bounded below by that lemma and above by the normalization. The values $\lambda_k = U(x^{(k)})$ are then bounded above and below by positive constants, as is the factor that rescales $x^{(k)}$ to $\lambda' = 1$. A subsequence of the rescaled configurations converges to a CC $\bar{x}$ with masses m and $\lambda' = 1$. Body 4 lies in the closed triangle of $\bar{x}_1, \bar{x}_2, \bar{x}_3$, which leaves three cases.

- If body 4 is strictly inside a non-degenerate triangle, then $\bar{x}$ is a concave CC with body 4 inside. The spoke lengths $\bar{a}$ of $\bar{x}$ lie in Ω_4 by Lemma 2.1. Along the subsequence, $a^{(k)} \to \bar{a}$ and $F(\bar{a}) = \mu$.
- If body 4 lies on an edge of a non-degenerate triangle, then exactly three bodies are collinear. This is impossible [HM06, §2.2].
- If the triangle is degenerate, then $\bar{x}$ is collinear, which is impossible. The spokes of $\bar{x}$ are the limits of the spokes $a_i^{(k)} \in (0,1)$ of the rescaled configurations, and they are positive by Lemma 6.2, so they lie in $(0,1]$. The outer sides of $\bar{x}$ are limits of sides longer than 1 (Lemma 2.1), so they are at least 1. On the line of $\bar{x}$, two of the outer bodies lie on the same side of $\bar{x}_4$, at distances in $(0,1]$ from it; their distance is then less than 1, a contradiction.

Thus every sequence in the preimage of a compact set has a subsequence that converges in Ω_4, that is, F is proper. □

6.2. **Polar regions and fibre counts.** This subsection proves three standard topological facts directly, so that this section needs neither the Jordan curve theorem nor degree theory. The Lean formalization follows this section and so needs neither of them. We identify $\mathbb{R}^2$ with $\mathbb{C}$ and write the points of the plane as $\rho e^{i\vartheta}$ with $\rho \geq 0$ and $\vartheta \in S^1$. The slices of $F(\overline{\mathcal{D}})$ will be regions of the following kind.

Lemma 6.4 (polar regions)**.** *Let $R : S^1 \to (0, \infty)$ be continuous, and put*

$$\mathrm{In}(R) = \{0\} \cup \{\rho e^{i\vartheta} : 0 < \rho < R(\vartheta)\}, \qquad C(R) = \{R(\vartheta)e^{i\vartheta} : \vartheta \in S^1\},$$
$$\mathrm{Out}(R) = \{\rho e^{i\vartheta} : \rho > R(\vartheta)\}.$$

(a) $\mathbb{R}^2$ *is the disjoint union of* $\mathrm{In}(R)$, $C(R)$ *and* $\mathrm{Out}(R)$. *The sets* $\mathrm{In}(R)$ *and* $\mathrm{Out}(R)$ *are open, and* $C(R)$ *is compact.*
(b) $\mathrm{In}(R)$ *is bounded and star-shaped about* 0*, hence path-connected.*
(c) $\mathrm{Out}(R)$ *is unbounded and path-connected, and* $tw \in \mathrm{Out}(R)$ *for all* $w \in \mathrm{Out}(R)$ *and* $t \geq 1$.
(d) *Every point of* $C(R)$ *is a limit of points of* $\mathrm{In}(R)$ *and of points of* $\mathrm{Out}(R)$.

Proof. Each $w \neq 0$ is $\rho e^{i\vartheta}$ for exactly one pair (ρ, ϑ) with $\rho > 0$, which gives the partition. The function $\rho e^{i\vartheta} \mapsto \rho - R(\vartheta)$ is continuous on $\mathbb{R}^2 \setminus \{0\}$; the sets $\mathrm{Out}(R)$ and $\mathrm{In}(R) \setminus \{0\}$ are the open sets where it is positive and negative. The disc of radius $\min R > 0$ lies in $\mathrm{In}(R)$, so $\mathrm{In}(R)$ is open. The set $C(R)$ is the image of the compact S^1. If $\rho e^{i\vartheta} \in \mathrm{In}(R)$ and $t \in [0, 1]$, then $t\rho < R(\vartheta)$. Thus $\mathrm{In}(R)$ is star-shaped about 0. It lies in the disc of radius $\max R$. For $\rho e^{i\vartheta} \in \mathrm{Out}(R)$ and $\lambda > \max(\rho, \max R)$, the segment from $\rho e^{i\vartheta}$ to $\lambda e^{i\vartheta}$ lies in $\mathrm{Out}(R)$, and so does the circle of radius λ. This joins any two points of $\mathrm{Out}(R)$. Finally $R(\vartheta)e^{i\vartheta}$ is the limit of $(R(\vartheta) \pm \epsilon)e^{i\vartheta}$ as $\epsilon \downarrow 0$. □

Lemma 6.5 (fibre counts)**.** *Let X be a Hausdorff space, $f : X \to \mathbb{R}^m$ a continuous proper map and $Y \subset \mathbb{R}^m$ an open set. Suppose that each $x \in f^{-1}(Y)$ has an open neighbourhood U such that $f(U)$ is open and $f|_U : U \to f(U)$ is a homeomorphism. Then for each $y \in Y$ the fibre $f^{-1}(y) = \{x_1, \ldots, x_k\}$ is finite. Given pairwise disjoint neighbourhoods $U_i \ni x_i$ of this kind, there is an open set $\mathcal{V} \subset Y$ containing y such that each $y' \in \mathcal{V}$ has exactly one preimage in each U_i and none outside $U_1 \cup \cdots \cup U_k$. In particular the number of preimages is locally constant on Y, hence constant on each connected subset of Y.*

Proof. The fibre is compact, since f is proper. It is discrete, since f is injective on each U. Hence it is finite. Pairwise disjoint neighbourhoods U_i exist since X is Hausdorff. Let $B \subset Y$ be a closed ball around y. The set $X_B = f^{-1}(B) \setminus (U_1 \cup \cdots \cup U_k)$ is compact; $f(X_B)$ does not contain y. The open set $\mathcal{V} = \operatorname{int} B \cap f(U_1) \cap \cdots \cap f(U_k) \setminus f(X_B)$ contains y and has the stated property. □

Lemma 6.6 (planar covering lemma)**.** *Let X be a compact Hausdorff space, $X^\circ \subset X$ an open subset and $\partial X = X \setminus X^\circ$, and let $f : X \to \mathbb{R}^2$ be continuous. Let $R : S^1 \to (0, \infty)$ be continuous. Suppose that*

(i) *each $x \in X^\circ$ has an open neighbourhood $U \subset X^\circ$ such that $f(U)$ is open and $f|_U : U \to f(U)$ is a homeomorphism, and*
(ii) *$f(\partial X) \subset C(R)$.*

Then the following hold.

(a) *$f(X^\circ) \subset \mathrm{In}(R)$. In particular $f^{-1}(\mathrm{Out}(R)) = \emptyset$ and $f^{-1}(C(R)) = \partial X$.*
(b) *The number of preimages of y is finite and does not depend on $y \in \mathrm{In}(R)$.*

(c) *Suppose moreover that* (iii) f *maps* ∂X *bijectively onto* $C(R)$*, and that* (iv) *some point of* $\mathrm{In}(R)$ *has exactly one preimage. Then* f *is a homeomorphism of* X *onto* $\mathrm{In}(R) \cup C(R)$*, which maps* X° *onto* $\mathrm{In}(R)$*.*

Proof. The set $Y = \mathbb{R}^2 \setminus C(R) = \mathrm{In}(R) \cup \mathrm{Out}(R)$ is open. By (ii), $f^{-1}(Y) \subset X^\circ$. Since X is compact, f is proper. By (i), every point of $f^{-1}(Y) \subset X^\circ$ has an open neighbourhood that f maps homeomorphically onto an open set, so Lemma 6.5 applies to f and Y. Thus $n(y) = \#f^{-1}(y)$ is finite and locally constant on Y. It is therefore constant on the path-connected sets $\mathrm{In}(R)$ and $\mathrm{Out}(R)$ (Lemma 6.4). As $f(X)$ is compact and $\mathrm{Out}(R)$ is unbounded, $n = 0$ at some point of $\mathrm{Out}(R)$, hence on all of $\mathrm{Out}(R)$. Suppose that a point $x \in X^\circ$ had $f(x) \in C(R)$. With U as in (i), $f(U)$ would be an open neighbourhood of $f(x)$. It contains points of $\mathrm{Out}(R)$ by Lemma 6.4(d). These would have preimages in U, which is impossible. Therefore $f(X^\circ) \subset \mathrm{In}(R)$, which proves (a) and (b). Under (iv), $n = 1$ on $\mathrm{In}(R)$, so f maps $X^\circ = f^{-1}(\mathrm{In}(R))$ bijectively onto $\mathrm{In}(R)$. Under (iii) it maps ∂X bijectively onto $C(R)$. As $\mathrm{In}(R) \cap C(R) = \emptyset$, f is then a continuous bijection of the compact space X onto the Hausdorff space $\mathrm{In}(R) \cup C(R)$, hence a homeomorphism. □

6.3. **Rays.** Sections 6.3–6.5 derive from the certificates the shape of $\overline{\mathcal{D}}$: it meets every ray from the axis in an initial segment, the umbilic splits it into two nappes, and we determine the limit points of these nappes. Sections 6.6 and 6.7 use these facts, the signs of T_1, T_2 and T_3 on the fold and the half-plane condition to describe the level sets of A on the nappes and the fold curves Γ_c in them. Section 6.8 then counts the sheets of G over each level set at one point near the fold. We now study $\overline{\mathcal{D}}$ along the rays from the axis. For $s \in (\frac{1}{2}, 1)$ and $\varphi \in [30°, 90°]$, the *ray* $\{a(s, r, \varphi) : r \geq 0\}$ meets the part $FC(s)$ of the fold core in a segment $\{0 \leq r \leq r_{\max}(s)\}$.

Lemma 6.7. (a) $J > 0$ *at every physical point of* W *outside the fold core.*
(b) *On the axis,* $J < 0$ *at the physical points other than* p^**, while* $J(p^*) = 0$*.*
(c) *For each ray, the physical points of* $FC(s)$ *on the ray form an initial segment of* $FC(s) \cap \mathrm{ray}$*.*
(d) *Every physical point of* W *with* $J = 0$*, other than* p^**, has* $T_1 = \partial_r \widetilde{J} > 0$ *and lies in a leaf of type F or B. In particular, for* $s \neq s^*$*,* J *has at most one zero on the physical part of* $FC(s) \cap \mathrm{ray}$*, and such a zero is a transverse crossing from* $J < 0$ *to* $J > 0$*.*

Proof. (a) By Proposition 5.2(b), every physical point of W outside the fold core lies in a leaf of type P of the bulk, corner or fin covers, and such a leaf certifies $J > 0$ there (Section 5.4).

(b) This is the last assertion of Proposition 2.4. The covers certify it independently. The axis lies in the regions of the covers of charts 0 and 4 (the lower axis, axis and top axis covers), whose leaves are of types M and X. On the zone column it lies in the umbilic ball, where the axis points with $\varrho > 0$ lie in leaves of type M of the umbilic cover (Proposition 5.2(c)). Since the quantity certified in chart 2 is $\widetilde{J}/\varrho^2$, these leaves give $J < 0$ at the axis points with $\varrho > 0$. Since a physical axis point lies in none of the leaves of type X, the covers imply $J < 0$ there unless it is p^*.

(c) We argue by contradiction and suppose that a physical point $a(r_2) \in FC(s)$ lies beyond a non-physical point $a(r_1) \in FC(s)$, $r_1 < r_2$. Let r_0 be the supremum of the non-physical parameters in $[r_1, r_2]$. Since Ω_4 is open, $a(r_0)$ is not physical, $r_0 < r_2$, and $a(r)$ is physical for $r \in (r_0, r_2]$. The leaves of the fold-core covers, together with the umbilic ball, cover $FC(s) \cap W$ (Proposition 5.2(b)). Since finitely many of them meet the plane of level s, one of them, a leaf L, contains points $a(r_n)$ with $r_n \downarrow r_0$ and, being closed, also $a(r_0)$.

If L is a leaf of the umbilic cover or of type U, it lies in the umbilic ball, which is contained in Ω_4 (Proposition 5.2(c)). Then $a(r_0)$ is physical, a contradiction. Otherwise L contains physical points. It is then not of type X but a resolved leaf of type M, P, F or B (Section 5.4 and Proposition 5.2(b),(d)). Since the leaves of charts 0, 1, 3 and 4 meet each ray in an interval, L

contains the segment from $a(r_0)$ to $a(r_n)$. On L the solution of Lemma 2.2 exists with $\theta \in (0,\pi)^3$ and $0 < a_i < 1$, by the principal-branch argument of Section 5.1; there K is analytic. As $a(r_0)$ is not physical while $K(r) < 0$ for $r \in (r_0, r_n]$, we get $K(r_0) = 0$. If $r_0 = 0$, then $a(r_0) = s(1,1,1)$ and $K = w(q-1)$ there (Lemma 2.3(a)), so $K(r_0) = 0$ forces $s = 1/\sqrt{3}$; but the physical point $a(r_n)$ has the same s, against Lemma 4.2. Hence $r_0 > 0$, and Lemma 4.5(b) shows that the points $a(r)$ with $r > r_0$ close to r_0 are not physical, against the choice of r_0.

(d) By (a) and Proposition 5.2(b), a physical point of W with $J = 0$ lies in the fold core, hence in a leaf of a fold-core cover or in the umbilic ball. We go through the types of leaves. The leaves of types M and P have $J \neq 0$ at their physical points, those of type X contain none, and the leaves of type U lie in the umbilic ball. This ball is tiled by the leaves of the umbilic cover, of which those of types M and P have $\widetilde{J}/\varrho^2 \neq 0$. Unless the point is p^*, it lies in a leaf of type F or B. At such a point $T_1 = \partial_r \widetilde{J} > 0$, also in charts 2 and 3, where T_1 is the value in chart 1 multiplied by a positive factor. For $s \neq s^*$, each zero of J on the physical part of $FC(s) \cap \mathrm{ray}$ is then a transverse crossing from $J < 0$ to $J > 0$. Since this physical part is an interval by (c), there is at most one such zero. □

Let $\mathcal{D} = \{J < 0\} \subset \Omega_4$ and $\overline{\mathcal{D}} = \{J \leq 0\} \subset \Omega_4$. Then $\overline{\mathcal{D}}$ is the closure of $\mathcal{D}$ in Ω_4. Indeed, $\partial_r \widetilde{J} > 0$ at all zeros of J other than p^* (Lemma 6.7(d), extended to Ω_4 in Lemma 6.10), and p^* is a limit of axis points with $J < 0$ by Lemma 6.7(b).

Lemma 6.8. *For $s \in (1/\sqrt{3}, 1) \setminus \{s^*\}$, on each ray at level s either $\overline{\mathcal{D}} \cap \mathrm{ray} = \{0 \leq r \leq r_f\}$ with $J(a(r_f)) = 0$, or $\overline{\mathcal{D}} \cap \mathrm{ray} = \{0 \leq r < r_1\}$ is the whole physical part of $FC(s) \cap \mathrm{ray}$. In the second case $a(r_1)$ is not physical, $K(a(r_1)) = 0$, and $s < 2/3$.*

Proof. By Lemma 2.3(b) the axis point is physical, and by Lemma 6.7(b) it has $J < 0$. By Lemma 6.7(c) the physical points of $FC(s)$ on the ray form an initial segment I, and J has at most one zero on I by Lemma 6.7(d). Outside $FC(s)$ all physical points of the ray have $J > 0$ by Lemma 6.7(a). If J has a zero r_f on I, then $\overline{\mathcal{D}} \cap \mathrm{ray} = \{0 \leq r \leq r_f\}$. Otherwise $J < 0$ on I. If I were the whole segment $FC(s) \cap \mathrm{ray}$, then, since Ω_4 is open, the points just beyond it would be physical points outside $FC(s)$. For $s \leq s_{\mathrm{lo}}$ there are no such points, by Lemma 4.1. For $s \geq s_{\mathrm{lo}}$ they would have $J > 0$ by Lemma 6.7(a), against the continuity of J. Therefore $I = \{0 \leq r < r_1\}$ with $a(r_1) \in FC(s)$ not physical. As in the proof of Lemma 6.7(c), some leaf contains $a(r_1)$ and points $a(r)$ with $r \uparrow r_1$. It is not in the umbilic ball, which lies in Ω_4, so it is a resolved leaf of type M, P, F or B (Section 5.4 and Proposition 5.2(b),(d)). On it K is continuous. Thus $K(a(r_1)) = 0$; hence $s < 2/3$ by Lemma 4.4. □

By $\mathfrak{S}_3$-equivariance the same holds on all rays from the axis. For $s \in \mathbb{R}$ and $\varphi \in S^1$ we write $\mathrm{ray}(s,\varphi) = \{a(s,r,\varphi) : r \geq 0\}$.

Corollary 6.9. *Let $s \in (1/\sqrt{3}, 1) \setminus \{s^*\}$ and $\varphi \in S^1$. Exactly one of the following holds.*

(R1) *$\overline{\mathcal{D}} \cap \mathrm{ray}(s,\varphi) = \{a(s,r,\varphi) : 0 \leq r \leq r_f\}$ for some $r_f > 0$, and $\Sigma \cap \mathrm{ray}(s,\varphi)$ is the single point $a(s,r_f,\varphi)$.*

(R2) *$s < 2/3$ and $\Sigma \cap \mathrm{ray}(s,\varphi) = \emptyset$.*

Proof. The group $\mathfrak{S}_3$ preserves s, $\overline{\mathcal{D}}$ and Σ. For each φ one of its elements maps $\mathrm{ray}(s,\varphi)$ onto a ray whose angle lies in $[30°, 90°]$. So we may assume $\varphi \in [30°, 90°]$. Each zero of J on the ray is a transverse crossing from $J < 0$ to $J > 0$, by Lemma 6.7(d). Such a zero lies in $\Sigma \subset \overline{\mathcal{D}}$, but the points just beyond it lie outside $\overline{\mathcal{D}}$. As $\overline{\mathcal{D}} \cap \mathrm{ray}(s,\varphi)$ is an interval (Lemma 6.8), the zero is its right end. In the first case of Lemma 6.8 this yields (R1). Here $r_f > 0$, since $J < 0$ on the axis (Lemma 6.7(b)). In the second case the interval $\{0 \leq r < r_1\}$ contains no zero of J, and $s < 2/3$, which is (R2). The ray meets Σ in (R1) and not in (R2), so the two cases exclude each other. □

Lemma 6.10. *At every point of $\Sigma \setminus \{p^*\}$, $T_1 > 0$ and $T_2 < 0$. At every point of $\Sigma \cap W$ off the two mirrors of W, $T_3 < 0$.*

Proof. By Lemma 6.7(d), each point of $\Sigma \cap W$ other than p^* lies in a leaf of type F or B. Table 4 and Lemma 3.3 show that $T_1 > 0$ and $T_2 < 0$ at the points of Σ in such a leaf and that $T_3 < 0$ at those off the mirrors. In charts 2 and 3 the certified quantities are positive multiples of T_1, T_2 and T_3 at these points (Sections 5.1 and 5.2). The group $\mathfrak{S}_3$ fixes s and acts on (x, y) by orthogonal maps. It therefore preserves r and maps e_s and e_r at a point to e_s and e_r at the image point. As A, K and $\widetilde{J}$ are invariant, so are $T_1 = \partial_r \widetilde{J}$ and $T_2 = \mathbf{A}_s(\nabla \widetilde{J})_r - \mathbf{A}_r(\nabla \widetilde{J})_s$. Each point of Ω_4 is the image of a point of W. □

6.4. **Nappes.** We split $\overline{\mathcal{D}}$ at p^*: by Proposition 5.2(e), $\overline{\mathcal{D}} \cap \{s = s^*\} = \{p^*\}$, and

$$\overline{\mathcal{D}} = \overline{\mathcal{D}}_L \sqcup \{p^*\} \sqcup \overline{\mathcal{D}}_U, \qquad \overline{\mathcal{D}}_L = \overline{\mathcal{D}} \cap \{s < s^*\}, \quad \overline{\mathcal{D}}_U = \overline{\mathcal{D}} \cap \{s > s^*\}.$$

We call $\overline{\mathcal{D}}_L$ and $\overline{\mathcal{D}}_U$ the lower and upper *nappes*. Put $\mathcal{D}_L = \mathcal{D} \cap \overline{\mathcal{D}}_L$, $\mathcal{D}_U = \mathcal{D} \cap \overline{\mathcal{D}}_U$, $\Sigma_L = \Sigma \cap \overline{\mathcal{D}}_L$ and $\Sigma_U = \Sigma \cap \overline{\mathcal{D}}_U$. By Lemmas 2.3(b) and 6.7(b), the axis points $s(1,1,1)$ with $1/\sqrt{3} < s < s^*$ lie in $\mathcal{D}_L$, and those with $s^* < s < 1$ lie in $\mathcal{D}_U$. In Figure 3, which shows how the nappes meet the mirror planes, the fold is the thin band of leaves of types F and B, below which the leaves of type M fill $\overline{\mathcal{D}}$ down to the axis, except for s below about 0.59, where the band has not begun and leaves of type X bound $\overline{\mathcal{D}}$ from above. This band descends towards the axis as $s \to s^*$ and ends at the edges of the zone column, which the figure does not show; inside this column the fold reaches the axis at p^*, where the two nappes meet.

6.5. **Ends.** We next determine the limit points of the nappes. Let $\mathcal{U}$ be the union of the leaves of types M, F and B of the fold-core covers, of their images under $\mathfrak{S}_3$, and of the umbilic ball. By Lemma 6.7(a) and Proposition 5.2(b), this compact set contains the closure of $\mathcal{D}$ in $\mathbb{R}^3$. By Proposition 5.2(c),(d), K and $\widehat{A}$ are finite and continuous on each of these leaves, and in charts 3 and 4 the scaled K/σ and $A - \log\sigma$ take their place. Also $0 < a_i < 1$ and $\theta \in (0, \pi)^3$ there, except at $\sigma = 0$ in charts 3 and 4. These functions agree where leaves overlap, by the uniqueness in Lemma 2.2. Hence K is continuous on $\mathcal{U} \cap \{\sigma > 0\}$.

Lemma 6.11. *If $\bar{a} \in \mathbb{R}^3$ is a limit of points $a^{(n)} \in \overline{\mathcal{D}}_L$ with $\bar{a} \notin \overline{\mathcal{D}}_L$, then either $\bar{a} = p^*$ and $A(a^{(n)}) \to A^*$, or $K(\bar{a}) = 0$, $s(\bar{a}) < 2/3$ and $A(a^{(n)}) \to +\infty$. If $\bar{a}$ is a limit of points $a^{(n)} \in \overline{\mathcal{D}}_U$ with $\bar{a} \notin \overline{\mathcal{D}}_U$, then either $\bar{a} = p^*$ and $A(a^{(n)}) \to A^*$, or $\bar{a}$ has $\sigma = 0$ in chart 3 or 4 and $A(a^{(n)}) \to -\infty$.*

Proof. We treat $\overline{\mathcal{D}}_L$ first and let $a^{(n)} \in \overline{\mathcal{D}}_L$. If $\bar{a} \in \Omega_4$, then $\bar{a} \in \overline{\mathcal{D}}$ ($\overline{\mathcal{D}}$ is closed in Ω_4) and $s(\bar{a}) = s^*$ ($s(\bar{a}) \le s^*$ and $\bar{a} \notin \overline{\mathcal{D}}_L$). Then $\bar{a} = p^*$ and $A(a^{(n)}) \to A^*$. If $\bar{a} \notin \Omega_4$, then $\bar{a}$ must lie in a leaf of $\mathcal{U}$ outside the umbilic ball, since this ball is contained in Ω_4. From $s(\bar{a}) \le s^* < s_{\mathrm{hi}}$ we get $\sigma(\bar{a}) > 0$. Hence the solution of Lemma 2.2 exists at $\bar{a}$ with $\theta \in (0, \pi)^3$ and $0 < a_i < 1$. As $\bar{a}$ is not physical, $K(\bar{a}) \ge 0$. As a limit of points with $K < 0$, it has $K(\bar{a}) = 0$. Then $s(\bar{a}) < 2/3$ by Lemma 4.4, while $A = \widehat{A} - \log(-K) \to +\infty$ because $\widehat{A}$ stays bounded.

For $a^{(n)} \in \overline{\mathcal{D}}_U$ the case $\bar{a} \in \Omega_4$ is the same. If $\bar{a} \notin \Omega_4$ and $\sigma(\bar{a}) > 0$, the argument above shows that $K(\bar{a}) = 0$ and $s(\bar{a}) < 2/3$, which is impossible: $s(\bar{a}) \ge s^* > 2/3$. The remaining limits must have $\sigma = 0$ in chart 3 or 4. There $A - \log\sigma$ is finite and continuous up to $\sigma = 0$; hence $A = (A - \log\sigma) + \log\sigma \to -\infty$. □

6.6. **The levels of A on the nappes.** We put $\Phi_c = \overline{\mathcal{D}}_L \cap A^{-1}(c)$ for $c > A^*$ and $\Phi_c = \overline{\mathcal{D}}_U \cap A^{-1}(c)$ for $c < A^*$, and in both cases

$$\Phi_c^\circ = \Phi_c \cap \mathcal{D}, \qquad \Gamma_c = \Phi_c \cap \Sigma,$$

so that Φ_c is the disjoint union of Φ_c° and Γ_c.

Lemma 6.12. (a) *$A > A^*$ on $\overline{\mathcal{D}}_L$ and $A < A^*$ on $\overline{\mathcal{D}}_U$.*
(b) *The maps $A : \overline{\mathcal{D}}_L \to (A^*, \infty)$ and $A : \overline{\mathcal{D}}_U \to (-\infty, A^*)$ are proper and surjective.*
(c) *If $a_n \in \overline{\mathcal{D}}$ and $A(a_n) \to A^*$, then $a_n \to p^*$.*

Proof. (a) We first show that A has no local extremum on $\overline{\mathcal{D}}_L$. At a point of the open set $\mathcal{D}_L$, dF is invertible and $dA \neq 0$, so the point is not a local extremum. Let $a \in \Sigma_L$ have coordinates (s, r, φ). Then $r > 0$, since p^* is the only point of Σ on the axis. Since $T_1(a) > 0$ and $T_2(a) < 0$ (Lemma 6.10), Lemma 3.1(b) shows that the fold is a graph $r = r_f(s, \varphi)$ near a and that $t \mapsto A(s + t, r_f(s + t, \varphi), \varphi)$ has the derivative $T_2/((-K)T_1) < 0$ at $t = 0$. For small $|t|$ these points lie in $\Sigma \cap \{s < s^*\} \subset \overline{\mathcal{D}}_L$, so A takes values above and below $A(a)$ on $\overline{\mathcal{D}}_L$ near a.

Next let $a_n \in \overline{\mathcal{D}}_L$ with $A(a_n) \to m_0 = \inf_{\overline{\mathcal{D}}_L} A$, which is less than $+\infty$ since $\overline{\mathcal{D}}_L$ is not empty. A subsequence converges to some $\bar{a}$ in the compact set $\mathcal{U}$ of Section 6.5. If $\bar{a} \in \overline{\mathcal{D}}_L$, then A attains its minimum on $\overline{\mathcal{D}}_L$ at $\bar{a}$, which is impossible. So $\bar{a} \notin \overline{\mathcal{D}}_L$. By Lemma 6.11, either $\bar{a} = p^*$ and $m_0 = A^*$, or $A(a_n) \to +\infty$, which is excluded. Thus $m_0 = A^*$ and the infimum is not attained. On the upper nappe we argue in the same way with the supremum and the limits A^* and $-\infty$ of Lemma 6.11.

(b) Let $a_n \in \overline{\mathcal{D}}_L$ with $A(a_n) \in [\alpha, \beta] \subset (A^*, \infty)$. A subsequence converges in $\mathcal{U}$. By Lemma 6.11 its limit lies in $\overline{\mathcal{D}}_L$, since the other possible limits have $A \to A^*$ or $A \to +\infty$. The set $\overline{\mathcal{D}}_L \cap A^{-1}[\alpha, \beta]$ is therefore compact, which proves properness. By Lemma 2.3(c) and Proposition 2.4, A decreases strictly from $+\infty$ to A^* on the axis segment $\{s(1, 1, 1) : 1/\sqrt{3} < s < s^*\}$, which lies in $\overline{\mathcal{D}}_L$. In particular A maps $\overline{\mathcal{D}}_L$ onto (A^*, ∞). The upper nappe is the same.

(c) Otherwise a subsequence stays at a distance at least $\epsilon > 0$ from p^*, lies in one nappe and converges in $\mathcal{U}$ to some $\bar{a} \neq p^*$. If the nappe is $\overline{\mathcal{D}}_L$, then $\bar{a} \notin \overline{\mathcal{D}}_L$, since $A(\bar{a}) = A^*$ would contradict (a), and Lemma 6.11 gives $A(a_n) \to +\infty$. For $\overline{\mathcal{D}}_U$ it gives $A(a_n) \to -\infty$. Both contradict $A(a_n) \to A^*$. □

Corollary 6.13. *For every compact interval $I \subset \mathbb{R}$, the set $\overline{\mathcal{D}} \cap A^{-1}(I)$ is compact, and G is bounded on it. Moreover $\overline{\mathcal{D}} \cap A^{-1}(c) = \Phi_c$, $\mathcal{D} \cap A^{-1}(c) = \Phi_c^\circ$ and $\Sigma \cap A^{-1}(c) = \Gamma_c$ for $c \neq A^*$, and $\overline{\mathcal{D}} \cap A^{-1}(A^*) = \{p^*\}$. In particular Φ_c is compact for $c \neq A^*$.*

Proof. The identities follow from Lemma 6.12(a), since $A(p^*) = A^*$. Let $a_n \in \overline{\mathcal{D}} \cap A^{-1}(I)$, and pass to a subsequence with $A(a_n) \to c \in I$. If $c > A^*$, we choose $\epsilon > 0$ with $c - \epsilon > A^*$. Eventually a_n lies in $\overline{\mathcal{D}}_L \cap A^{-1}[c - \epsilon, c + \epsilon]$, which is compact by Lemma 6.12(b). The case $c < A^*$ is the same. If $c = A^*$, then $a_n \to p^*$ by Lemma 6.12(c), and $p^* \in \overline{\mathcal{D}} \cap A^{-1}(I)$. In each case a subsequence converges in $\overline{\mathcal{D}} \cap A^{-1}(I)$. □

6.7. **The fold curves.** For $\varphi \in S^1$ let $H_\varphi = \{a(s, r, \varphi) : s \in \mathbb{R},\ r > 0\}$ be the open half-plane of angle φ bounded by the axis.

Lemma 6.14. *Let $\varphi \in S^1$.*
(a) *There are $s_{\min}(\varphi) \in [1/\sqrt{3}, 2/3]$ and a C^1 function $r_f : (s_{\min}(\varphi), s^*) \to (0, \infty)$ such that $\Sigma_L \cap H_\varphi = \{a(s, r_f(s), \varphi) : s_{\min}(\varphi) < s < s^*\}$. The function $\alpha(s) = A(a(s, r_f(s), \varphi))$ decreases strictly. It tends to $+\infty$ as $s \downarrow s_{\min}(\varphi)$ and to A^* as $s \uparrow s^*$.*
(b) *There is a C^1 function $r_f^U : (s^*, 1) \to (0, \infty)$ such that $\Sigma_U \cap H_\varphi = \{a(s, r_f^U(s), \varphi) : s^* < s < 1\}$. The function $\alpha^U(s) = A(a(s, r_f^U(s), \varphi))$ decreases strictly. It tends to A^* as $s \downarrow s^*$ and to $-\infty$ as $s \uparrow 1$.*

Proof. (a) Let S_φ be the set of $s \in (1/\sqrt{3}, s^*)$ for which $\mathrm{ray}(s, \varphi)$ meets Σ. For $s \in \mathsf{S}_\varphi$ let $r_f(s)$ be the radius of the intersection point, which is unique by Corollary 6.9. Since physical points have $s > 1/\sqrt{3}$ (Lemma 4.2), $\Sigma_L \cap H_\varphi$ consists of the points $a(s, r_f(s), \varphi)$ with $s \in \mathsf{S}_\varphi$.

By Corollary 6.9, $(2/3, s^*) \subset \mathsf{S}_\varphi$, since case (R2) needs $s < 2/3$. Here $s^* > 2/3$ because $s^{*3} = 3/(6\sqrt{3}-2) > 8/27$ (Proposition 2.4).

Let $s_1 \in \mathsf{S}_\varphi$. The point $q_1 = a(s_1, r_f(s_1), \varphi)$ lies in $\Sigma \setminus \{p^*\}$, so $\partial_r \widetilde{J}(q_1) = T_1(q_1) > 0$ by Lemma 6.10. The implicit function theorem solves $\widetilde{J}(a(s,r,\varphi)) = 0$ near q_1 by a C^1 function $r = \tilde{r}(s)$ of s near s_1. The points $a(s, \tilde{r}(s), \varphi)$ are physical, since Ω_4 is open. They lie in Σ by Lemma 3.1(a). So $s \in \mathsf{S}_\varphi$ and $r_f(s) = \tilde{r}(s)$ for s near s_1. Thus S_φ is open and r_f is C^1. By Lemmas 3.1(b) and 6.10, $\alpha' = T_2/((-K)T_1) < 0$ on S_φ.

Let (s_-, s_+) be a component of S_φ, and let $s_n \in (s_-, s_+)$ tend to s_+ or to s_-. The points $q_n = a(s_n, r_f(s_n), \varphi)$ lie in $\overline{\mathcal{D}}_L$. A subsequence converges to some $\bar{q} \in \mathcal{U}$. Suppose that $\bar{q} \in \overline{\mathcal{D}}_L$. Then $\bar{q} \in \Sigma$, since Σ is closed in Ω_4. It is not on the axis, because $s(\bar{q}) < s^*$ and p^* is the only point of Σ on the axis. So $\bar{q} \in H_\varphi$ and $s(\bar{q}) \in \mathsf{S}_\varphi$, which is false for an end of a component. Thus $\bar{q} \notin \overline{\mathcal{D}}_L$. Lemma 6.11 leaves two cases: either $\bar{q} = p^*$, $s(\bar{q}) = s^*$ and $\alpha(s_n) \to A^*$, or $K(\bar{q}) = 0$, $s(\bar{q}) < 2/3$ and $\alpha(s_n) \to +\infty$. At the left end $s(\bar{q}) = s_- < s^*$, so $\alpha \to +\infty$ as $s \downarrow s_-$. If $s_+ < s^*$, the right end also gives $\alpha \to +\infty$, which contradicts the strict decrease of α. Therefore $s_+ = s^*$. Then $\bar{q} = p^*$, since the second alternative needs $s(\bar{q}) < 2/3 < s^*$. Thus $\alpha \to A^*$ as $s \uparrow s^*$. Each component of S_φ therefore has the right end s^*. So S_φ is a single interval $(s_{\min}(\varphi), s^*)$ for some $s_{\min}(\varphi) \in [1/\sqrt{3}, 2/3]$.

(b) For $s \in (s^*, 1)$ case (R2) of Corollary 6.9 is impossible, so $\mathrm{ray}(s, \varphi)$ meets Σ in exactly one point. Smoothness and $(\alpha^U)' < 0$ follow as in (a). As $s \downarrow s^*$, the limit points in $\mathcal{U}$ of $a(s, r_f^U(s), \varphi)$ have $s = s^*$, so they do not lie in $\overline{\mathcal{D}}_U$. They equal p^* by Lemma 6.11, since the other limits have $\sigma = 0$, that is $s = 1$. Hence $\alpha^U \to A^*$. As $s \uparrow 1$ the limit points have $s = 1$ and are not physical; hence $\alpha^U \to -\infty$ by Lemma 6.11. □

Proposition 6.15. *Let $c \neq A^*$. For every $\varphi \in S^1$, the set Γ_c meets H_φ in exactly one point $\gamma_c(\varphi) = a(s_c(\varphi), r_c(\varphi), \varphi)$, and $\Gamma_c = \gamma_c(S^1)$. The functions s_c and r_c are C^1 on S^1, and $r_c > 0$. The map $\gamma_c : S^1 \to \Gamma_c$ is a homeomorphism, with inverse $\varphi|_{\Gamma_c}$.*

Proof. Let $c > A^*$. Then $\Gamma_c = \Sigma_L \cap A^{-1}(c)$, a set that does not meet the axis. By Lemma 6.14(a), α is a continuous, strictly decreasing bijection of $(s_{\min}(\varphi), s^*)$ onto (A^*, ∞), which yields the existence and the uniqueness of $\gamma_c(\varphi)$. At $\gamma_c(\varphi_0)$ the system $(\widetilde{J}, A - c) = 0$ in the unknowns (s, r) has the Jacobian determinant $\partial_s \widetilde{J}\, \partial_r A - \partial_r \widetilde{J}\, \partial_s A = -T_2/(-K) \neq 0$, so the implicit function theorem yields a C^1 solution $(s(\varphi), r(\varphi))$ for φ near φ_0. The corresponding points are physical and lie in $\Sigma_L \cap A^{-1}(c) \cap H_\varphi$, so they are the points $\gamma_c(\varphi)$. Thus s_c and r_c are C^1. A continuous bijection of the compact space S^1 onto the Hausdorff space Γ_c is a homeomorphism. For $c < A^*$ we use Lemma 6.14(b) in the same way. □

Since $s \neq s^*$ on $\Sigma \setminus \{p^*\}$ (Proposition 5.2(e)), Proposition 5.2(f) shows that $G \neq 0$ at the points of $\Sigma \cap W$ other than p^*. As $|G|$ is $\mathfrak{S}_3$-invariant, $G \neq 0$ on $\Sigma \setminus \{p^*\}$. For $c \neq A^*$ we put $\theta_c(\varphi) = \Theta(G(\gamma_c(\varphi)))$, a continuous function on S^1. We write $\mathsf{A}_k = [30^\circ + 60^\circ k,\ 90^\circ + 60^\circ k] \subset S^1$ for $k = 0, \dots, 5$. The points of W are those with $\varphi \in \mathsf{A}_0$.

Proposition 6.16. *Let $c \neq A^*$ and $k \in \{0, \dots, 5\}$. If $c > A^*$, the function θ_c maps the arc A_k increasingly and homeomorphically onto A_k, and it fixes the endpoints. If $c < A^*$, it maps A_k increasingly and homeomorphically onto $\mathsf{A}_k + 180^\circ$, and it adds 180° to the endpoints. Consequently θ_c is a homeomorphism of S^1, and $\Theta \circ G$ maps Γ_c homeomorphically onto S^1. The function $R_c : S^1 \to (0, \infty)$ defined by $R_c(\vartheta) = |G(x)|$ for the point $x \in \Gamma_c$ with $\Theta(G(x)) = \vartheta$ is continuous. Finally $G(\Gamma_c) = C(R_c)$, and G is injective on Γ_c.*

Proof. Let $c > A^*$. *The arc* A_0. For $\varphi \in \mathsf{A}_0$ the point $\gamma_c(\varphi)$ lies in $\Sigma \cap W$ and has $s < s^*$, so $u_L \cdot G > 0$ there by Proposition 5.2(f). That is, G lies in the open half-plane of the angles in $(-15^\circ, 165^\circ)$. On this half-plane Θ has a continuous determination with values in $(-15^\circ, 165^\circ)$.

We write $\tilde\theta(\varphi)$ for its value at $G(\gamma_c(\varphi))$. At $\varphi = 30^\circ$ we have $\Theta \in \{30^\circ, 210^\circ\}$ (Section 2.3), so $\tilde\theta(30^\circ) = 30^\circ$. Likewise $\tilde\theta(90^\circ) = 90^\circ$. Since $\widetilde J$ and A are constant along γ_c, the tangent vector $\gamma_c'(\varphi)$ is orthogonal to ∇A and $\nabla\widetilde J$, hence a multiple of $v = \nabla A \times \nabla\widetilde J$. Because γ_c is parametrized by φ, we have $d\varphi(\gamma_c'(\varphi)) = 1$. For $30^\circ < \varphi < 90^\circ$, Lemma 3.1(c) gives

$$\tilde\theta'(\varphi) = \frac{d\Theta(v)}{d\varphi(v)} = \frac{r\,T_3}{(P^2+Q^2)\,T_2} > 0,$$

since $T_2 < 0$ and $T_3 < 0$ off the mirrors (Lemma 6.10). Thus $\tilde\theta$ increases strictly from 30° to 90°; hence θ_c maps A_0 increasingly and homeomorphically onto A_0.

The other arcs. Let $g \in \mathfrak{S}_3$ be the cyclic permutation that acts on (x, y) as the rotation through 120°. It acts on G by the same rotation (Section 2.3) and preserves s, A and Σ. It therefore maps $\Gamma_c \cap H_\varphi$ onto $\Gamma_c \cap H_{\varphi+120^\circ}$. The uniqueness in Proposition 6.15 then gives $g\gamma_c(\varphi) = \gamma_c(\varphi + 120^\circ)$ and $\theta_c(\varphi + 120^\circ) = \theta_c(\varphi) + 120^\circ$. In the same way the transposition that fixes the mirror $\varphi = 90^\circ$ gives $\theta_c(180^\circ - \varphi) = 180^\circ - \theta_c(\varphi)$. The group generated by these two maps of S^1 carries A_0 onto each A_k. Under the rotation both φ and Θ increase by 120°. Under the reflection both are replaced by 180° minus themselves, which reverses both orders. In either case θ_c is again increasing on the image arc, maps it onto itself and fixes its endpoints.

Consequences. The arcs cover S^1 and overlap only at their endpoints, where θ_c is the identity. So θ_c is a continuous bijection of S^1, hence a homeomorphism. Proposition 6.15 then shows that $\Theta \circ G$ is a continuous bijection of the compact set Γ_c onto S^1 and therefore a homeomorphism. Hence $R_c = |G| \circ (\Theta \circ G|_{\Gamma_c})^{-1}$ is continuous. It is positive since $G \neq 0$ on Γ_c. Each $x \in \Gamma_c$ satisfies $G(x) = R_c(\Theta(G(x)))\, e^{i\Theta(G(x))}$. This shows that $G(\Gamma_c) = C(R_c)$ and that G is injective on Γ_c.

For $c < A^*$ the vector u_U replaces u_L. The half-plane is that of the angles in $(130^\circ, 310^\circ)$; the values at the endpoints of A_0 are 210° and 270°. So $\theta_c - 180^\circ$ maps A_0 increasingly and homeomorphically onto A_0 and fixes the endpoints. It satisfies the two relations of the second step modulo 360°; the rest of the proof therefore applies to it in place of θ_c. □

At a point of Γ_c on a mirror where $J_{\mathrm{mir}} \neq 0$, for instance in a leaf of type B, $T_3 = 0$ by Lemma 3.2; hence the angle of G is stationary there. Proposition 7.13 will show that $C(R_c)$ has a cusp at the image of such a point (Figure 2).

6.8. **Injectivity.** We call a point $q \in \Sigma \setminus \{p^*\}$ a *fold point* if $T_3(q) \neq 0$. For every $c \neq A^*$ the point $\gamma_c(60^\circ)$ is a fold point, by Lemma 6.10. For $c \in \mathbb{R}$ and $w \in \mathbb{R}^2$ we write $F^{-1}(c, w)$ for the fibre of F over the point with coordinates $(A, G) = (c, w)$, and $w^\perp$ for w turned through 90°. The following normal form is local: it uses neither the injectivity of F nor a count of preimages.

Lemma 6.17 (fold normal form)**.** *Let q be a fold point and $c = A(q)$. There are orthonormal affine coordinates $w = G(q) + U\,e + V\,e'$ on $\mathbb{R}^2$ with the following property. For every neighbourhood $\mathcal{N}_0$ of q there are an open neighbourhood $\mathcal{N} \subset \mathcal{N}_0$ of q, numbers $\varepsilon_1, \varepsilon_2 > 0$ and a continuous function $M : (-\varepsilon_1, \varepsilon_1) \to (-\varepsilon_2, \varepsilon_2)$ with $M(0) = 0$ such that the following holds for $|U| < \varepsilon_1$, $|V| < \varepsilon_2$ and $w = G(q) + Ue + Ve'$.*

(a) *If $V < M(U)$, then $F^{-1}(c, w) \cap \mathcal{N} = \emptyset$.*
(b) *If $V = M(U)$, then $F^{-1}(c, w) \cap \mathcal{N}$ is one point, at which $J = 0$.*
(c) *If $V > M(U)$, then $F^{-1}(c, w) \cap \mathcal{N}$ consists of two points, with $J < 0$ at one of them and $J > 0$ at the other.*

Proof. Step 1: independence. At q we have $K < 0$ and, by Lemma 6.10, $T_2 \neq 0$. The e_φ-component of $v = \nabla A \times \nabla\widetilde J$ is $(\nabla A)_s(\nabla\widetilde J)_r - (\nabla A)_r(\nabla\widetilde J)_s = T_2/(-K) \neq 0$. Thus $\nabla A(q)$ and

$\nabla\widetilde{J}(q)$ are independent. Lemma 3.1(a) and the implicit function theorem show that the set $\Sigma\cap A^{-1}(c)=\{\widetilde{J}=0,\ A=c\}$ is a C^1 curve near q whose tangent line at q is $\mathbb{R}v(q)$.

Step 2: rank. By the definitions of Section 3.1, $T_3=\det[\mathbf{h};\mathbf{A};\nabla\widetilde{J}]=(-K)\,\mathbf{h}\cdot v$, where $\mathbf{h}\cdot v=P\,dQ(v)-Q\,dP(v)$. As $T_3(q)\neq 0$, we get $dG(q)v\neq 0$. Since $J(q)=0$, the restriction of $dG(q)$ to $\ker dA(q)$ is not injective, for otherwise $dF(q)=(dA,dG)(q)$ would be injective. As $v\in\ker dA(q)$ and $dG(q)v\neq 0$, this restriction has rank 1. Let e be a unit vector that spans its image.

Step 3: coordinates. Put $u=e\cdot(G-G(q))$. Then $du(q)v=e\cdot dG(q)v\neq 0=dA(q)v$, so $dA(q)$ and $du(q)$ are independent. We choose an affine function ζ of a with $\zeta(q)=0$ and $d\zeta\notin\operatorname{span}(dA(q),du(q))$. By the inverse function theorem, (A,u,ζ) are coordinates on a connected open neighbourhood $\Omega_q\subset\Omega_4$ of q, in which $q=(c,0,0)$. With $e'=e^{\perp}$ and $h=e'\cdot(G-G(q))$, the map F reads $(A,u,\zeta)\mapsto(A,u,h(A,u,\zeta))$ in the target coordinates (A,U,V).

Step 4: the sign of J. By the chain rule, $\partial_\zeta h=\det\partial(A,U,V)/\partial(A,u,\zeta)=\pm J\,D_0$, where $D_0=\det\partial(s,x,y)/\partial(A,u,\zeta)$ does not vanish on Ω_q. Here we used $\det\partial(A,P,Q)/\partial(s,x,y)=J$ (proof of Lemma 2.3(d)). It follows that $\Sigma\cap\Omega_q=\{\partial_\zeta h=0\}$ and that $\operatorname{sign}J=\epsilon_0\operatorname{sign}\partial_\zeta h$ on Ω_q for a constant $\epsilon_0\in\{1,-1\}$.

Step 5: nondegeneracy. Put $h_c(u,\zeta)=h(c,u,\zeta)$. At q, where $J=0$, we have $d(\partial_\zeta h)=\pm D_0\,dJ$ and $\nabla\widetilde{J}=(-K)\nabla J$. Step 1 shows that $dJ(q)$ is not a multiple of $dA(q)$, so $(\partial_u\partial_\zeta h_c,\partial_\zeta^2 h_c)(0,0)\neq(0,0)$. Near 0 the curve $\Sigma\cap A^{-1}(c)$ is $\{\partial_\zeta h_c=0\}$; its tangent at 0 is spanned by $(du(v),d\zeta(v))$, which is not parallel to ∂_ζ since $du(v)\neq 0$. If $\partial_\zeta^2 h_c(0,0)$ vanished, then $\partial_u\partial_\zeta h_c(0,0)\neq 0$, and the curve would be a graph $u=g_1(\zeta)$ with $g_1'(0)=0$, tangent to ∂_ζ. Therefore $\partial_\zeta^2 h_c(0,0)\neq 0$. Replacing e' by $-e'$, and h by $-h$, we may assume $\partial_\zeta^2 h_c(0,0)>0$.

Step 6: one variable. Given $\mathcal{N}_0$, we choose $\delta>0$ such that the closed coordinate box $\{|A-c|\le\delta,\ |u|\le\delta,\ |\zeta|\le\delta\}$ lies in $\mathcal{N}_0\cap\Omega_q$ and $\partial_\zeta^2 h_c\ge\nu$ on $[-\delta,\delta]^2$ for some $\nu>0$. We choose $\varepsilon\in(0,\delta]$ with $|\partial_\zeta h_c(u,0)|\le\nu\delta/2$ for $|u|\le\varepsilon$. For $|u|\le\varepsilon$ the function $\partial_\zeta h_c(u,\cdot)$ increases strictly on $[-\delta,\delta]$, it is at most $-\nu\delta/2$ at $-\delta$ and at least $\nu\delta/2$ at δ, and it has exactly one zero $\zeta^*(u)$, located in $[-\delta/2,\delta/2]$. The function ζ^* is continuous. We put $M(u)=h_c(u,\zeta^*(u))$, so that $M(0)=h_c(0,0)=0$. The function $h_c(u,\cdot)$ decreases strictly on $[-\delta,\zeta^*(u)]$ and increases strictly on $[\zeta^*(u),\delta]$. Moreover $h_c(u,\zeta)\ge M(u)+\frac{\nu}{2}(\zeta-\zeta^*(u))^2$, so $h_c(u,\pm\delta)\ge M(u)+\nu\delta^2/8$. We choose $\varepsilon_1\in(0,\varepsilon]$ with $|M(u)|<\nu\delta^2/16$ for $|u|<\varepsilon_1$. We put $\varepsilon_2=\nu\delta^2/16$ and $\mathcal{N}=\{|A-c|<\delta,\ |u|<\varepsilon,\ |\zeta|<\delta\}$. For $|U|<\varepsilon_1$ and $|V|<\varepsilon_2$ we have $V<M(U)+\nu\delta^2/8$; hence the equation $h_c(U,\zeta)=V$ has 0, 1 or 2 solutions $\zeta\in(-\delta,\delta)$ according as $V<M(U)$, $V=M(U)$ or $V>M(U)$. In the second case the solution is $\zeta^*(U)$, where $J=0$. In the third case one solution has $\partial_\zeta h_c<0$ and the other $\partial_\zeta h_c>0$, so J has opposite signs there by Step 4. The preimages of (c,w) in $\mathcal{N}$ are exactly the points (c,U,ζ) with these ζ. □

Lemma 6.18. *Let $c\neq A^*$. The map $f=G|_{\Phi_c}$ satisfies the hypotheses* (i)–(iii) *of Lemma 6.6 with $X=\Phi_c$, $X^\circ=\Phi_c^\circ$, $\partial X=\Gamma_c$ and $R=R_c$. Some point of* $\operatorname{In}(R_c)$ *has exactly one preimage in Φ_c.*

Proof. Hypothesis (i). By Corollary 6.13, $\Phi_c^\circ=\mathcal{D}\cap A^{-1}(c)$, which is open in Φ_c since $\mathcal{D}$ is open. For $x\in\Phi_c^\circ$, the inverse function theorem yields an open set $U\ni x$ in $\mathcal{D}$ such that $F|_U$ is a homeomorphism onto an open set. Then $U\cap A^{-1}(c)$ is an open neighbourhood of x in Φ_c, contained in Φ_c°; G maps it homeomorphically onto the open set $\{w:(c,w)\in F(U)\}$. *Hypotheses (ii) and (iii)* hold by Proposition 6.16.

The base point. By Lemma 6.6(a), no point of Φ_c° is mapped into $C(R_c)$. Let $q=\gamma_c(60^\circ)$, a fold point. Since $G(q)\in C(R_c)$ and G is injective on Γ_c, the point q is the only point of Φ_c that G maps to $G(q)$. We apply Lemma 6.17 at q with $\mathcal{N}_0=\Omega_4$. It yields $\mathcal{N}$, ε_1, ε_2 and M. The

compact set $G(\Phi_c \setminus \mathcal{N})$ does not contain $G(q)$, so $G(q)$ has a neighbourhood Y_1 that does not meet it. Take $y_0 = G(q) + V_0 e' \in Y_1$ with $0 < V_0 < \varepsilon_2$. Since $V_0 > M(0) = 0$, Lemma 6.17(c) shows that $F^{-1}(c, y_0) \cap \mathcal{N} = \{x_-, x_+\}$ with $J(x_-) < 0 < J(x_+)$. The preimages of y_0 in Φ_c lie in $\mathcal{N} \cap A^{-1}(c)$, so they are among x_- and x_+. Here $x_+ \notin \overline{\mathcal{D}}$, while $x_- \in \mathcal{D} \cap A^{-1}(c) = \Phi_c^\circ$. Thus y_0 has exactly one preimage x_- in Φ_c, and $y_0 = G(x_-) \in \mathrm{In}(R_c)$ by Lemma 6.6(a). □

Theorem 6.19. (a) *F is injective on $\overline{\mathcal{D}}$.*

(b) *Let $c \neq A^*$. Then Φ_c is compact, and Γ_c is the image of the C^1 embedding $\gamma_c : S^1 \to \Omega_4$ of Proposition 6.15. The map G restricts to a homeomorphism of Φ_c onto $\mathrm{In}(R_c) \cup C(R_c)$, which maps Φ_c° onto $\mathrm{In}(R_c)$ and Γ_c onto $C(R_c)$.*

(c) $\overline{\mathcal{D}} \cap A^{-1}(A^*) = \{p^*\}$.

Proof. Let $c \neq A^*$. By Corollary 6.13, Φ_c is compact; γ_c is an embedding since $d\varphi(\gamma_c') = 1$ (Proposition 6.15). By Lemmas 6.6 and 6.18, G is a homeomorphism of Φ_c onto $\mathrm{In}(R_c) \cup C(R_c)$ with $G(\Phi_c^\circ) = \mathrm{In}(R_c)$. Moreover $G(\Gamma_c) = C(R_c)$ by Proposition 6.16. This proves (b). Item (c) is the last identity of Corollary 6.13: $A > A^*$ on $\overline{\mathcal{D}}_L$ and $A < A^*$ on $\overline{\mathcal{D}}_U$ (Lemma 6.12(a)), while $A(p^*) = A^*$. Let $a, a' \in \overline{\mathcal{D}}$ with $F(a) = F(a')$, and let $c = A(a) = A(a')$. For $c \neq A^*$ both points lie in $\overline{\mathcal{D}} \cap A^{-1}(c) = \Phi_c$ (Corollary 6.13), on which G is injective. For $c = A^*$ both equal p^* by (c). □

Corollary 6.20. *For $c \neq A^*$,*

$$F(\mathcal{D}) \cap \{A = c\} = \{c\} \times \mathrm{In}(R_c), \qquad F(\Sigma) \cap \{A = c\} = \{c\} \times C(R_c),$$
$$F(\overline{\mathcal{D}}) \cap \{A = c\} = \{c\} \times \big(\mathrm{In}(R_c) \cup C(R_c)\big).$$

Moreover $F(\overline{\mathcal{D}}) \cap \{A = A^*\} = \{F(p^*)\}$, and $F(p^*)$ has the coordinates $(A, P, Q) = (A^*, 0, 0)$.

Proof. Since $F = (A, G)$, and $\Phi_c^\circ = \mathcal{D} \cap A^{-1}(c)$ and $\Gamma_c = \Sigma \cap A^{-1}(c)$ by Corollary 6.13, the first three identities are Theorem 6.19(b). The last statement follows from Theorem 6.19(c) and $G(p^*) = 0$ (Lemma 2.3(d)). □

Corollary 6.21. *Let $c \neq A^*$, and let Π_c be the map of $\mathrm{In}(R_c) \cup C(R_c)$ onto the closed unit disk given by $\Pi_c(0) = 0$ and $\Pi_c(\rho e^{i\vartheta}) = (\rho / R_c(\vartheta))\, e^{i\vartheta}$ for $\rho > 0$. Then $\Pi_c \circ G$ is a homeomorphism of Φ_c onto the closed unit disk, which maps Γ_c onto the unit circle and Φ_c° onto the open disk. In particular Φ_c is a closed disk with boundary circle Γ_c.*

Proof. Theorem 6.19(b) shows that G is a homeomorphism of Φ_c onto $\mathrm{In}(R_c) \cup C(R_c)$. The map Π_c is a bijection onto the closed unit disk: its inverse is $\rho e^{i\vartheta} \mapsto \rho R_c(\vartheta) e^{i\vartheta}$. Both maps are continuous, because R_c is continuous and $0 < \min R_c \leq \max R_c < \infty$. □

6.9. **The restricted problem and the base value.** We now compute the preimages of the points with coordinates $(A, P, Q) = (A_0, 0, 0)$ for A_0 large. Since $A = \log\big((m_1 m_2 m_3)^{1/3} / m_4\big)$, body 4 is almost massless in this limit. The preimages lie near the face $K = 0$ of Ω_4, where they correspond to the relative equilibria of the restricted four-body problem inside the triangle of the primaries. At $G = 0$ the three primaries have equal masses. These equilibria are then a minimum and three saddles of the potential; the passage from the restricted problem to F reverses the signs. The value $(A_0, 0, 0)$ therefore has one preimage with $J < 0$ and three with $J > 0$ (Proposition 6.30). A base value at equal masses would need Albouy's count of the CCs of four equal masses and the signs of Proposition 5.2(g), but the limit of large A needs neither of these. Theorem 2(g) then recovers Albouy's count. Of the earlier results the proofs of Lemmas 6.22–6.28 and Propositions 6.29 and 6.30 use only Lemmas 2.1, 2.2 and 2.3(a). In particular they use none of the certificates of Section 5 and none of Sections 6.1–6.8. The

supplementary file `deg_restricted.py` checks identities of this subsection by exact symbolic computation. We cite its checks by their labels.

The barycentric form. Let $\mathcal{A} \subset (0,1)^3$ be the set of points at which the solution of Lemma 2.2 exists with $\theta \in (0,\pi)^3$, so that $\Omega_4 = \{a \in \mathcal{A} : K(a) < 0\}$. Lemma 2.2 shows that $\mathcal{A}$ is open and that K is analytic on it. On $\mathcal{A}$ we have $w_i > 0$ and $S_i > 0$. We write $\beta_i = S_i/S$ for the barycentric coordinates of x_4 in the outer triangle, and

$$\ell_i = \log \frac{\beta_i}{w_i}, \qquad \bar{\ell} = \tfrac{1}{3}(\ell_1 + \ell_2 + \ell_3).$$

Then $\hat{m}_i = \ell_i + \log(w_1 w_2 w_3)$ in (2.3). For the vectors E_1 and E_2 of Section 2.3, let $\varpi : \mathbb{R}^3 \to \mathbb{R}^2$ be the linear map $\varpi(\xi) = (\xi \cdot E_1, \xi \cdot E_2)$; its kernel is spanned by $(1,1,1)$. Since E_1 and E_2 form an orthonormal basis of the plane $\xi_1 + \xi_2 + \xi_3 = 0$, the restriction of ϖ to this plane is an isometry onto $\mathbb{R}^2$. With $G = \varpi(\mu)$ we obtain

$$G = \varpi(\ell), \qquad A = \widehat{A} - \log(-K), \qquad \widehat{A} = \bar{\ell} + \log(w_1 w_2 w_3), \tag{6.1}$$

where $\widehat{A}$ is as in Section 3.1. The functions $\varpi(\ell)$ and $\bar{\ell} + \log(w_1 w_2 w_3)$ are analytic on all of $\mathcal{A}$. Through (6.1) we regard G and $\widehat{A}$ as analytic functions on $\mathcal{A}$. In this subsection ∇f denotes the Euclidean gradient of a function f on $\mathcal{A}$ with respect to $a = (a_1, a_2, a_3)$, and of a function on the plane with respect to p, not the gradient in the frame (e_s, e_r, e_φ) of Section 3.1. Dot products and determinants of vectors of $\mathbb{R}^3$ are taken in the coordinates a.

The face $K = 0$. Let $\mathcal{K} = \{a \in \mathcal{A} : K(a) = 0\}$. We fix the unit equilateral triangle with the positively oriented vertices

$$v_1 = \Big(\frac{1}{2}, \frac{1}{2\sqrt{3}}\Big), \qquad v_2 = \Big(-\frac{1}{2}, \frac{1}{2\sqrt{3}}\Big), \qquad v_3 = \Big(0, -\frac{1}{\sqrt{3}}\Big),$$

that is, $v_i = \varpi(e_i)/\sqrt{2}$, where e_1, e_2, e_3 is the standard basis of $\mathbb{R}^3$. Let $\mathcal{T}$ be its open interior. For $p \in \mathcal{T}$ let $a(p) = (|p - v_1|, |p - v_2|, |p - v_3|)$ and $w_i(p) = |p - v_i|^{-3} - 1$. The barycentric coordinates of p are the affine functions $\beta_i(p) = \frac{1}{3} + 2\, p \cdot v_i$. The *restricted map* is

$$g : \mathcal{T} \to \mathbb{R}^2, \qquad g(p) = \varpi(\ell(p)), \qquad \ell_i(p) = \log \frac{\beta_i(p)}{w_i(p)}.$$

Lemma 6.22. (a) *The map $p \mapsto a(p)$ is a bijection from $\mathcal{T}$ onto $\mathcal{K}$, and its differential has rank 2 at every point. At $a(p)$ the configuration is (v_1, v_2, v_3, p) up to an isometry, and $\theta_i = \alpha_i = \arccos \zeta_i$ with ζ_i as in Lemma 4.3.*

(b) *At every point of $\mathcal{K}$, for $l = 1, 2, 3$,*

$$\frac{\partial}{\partial a_l}(\alpha_1 + \alpha_2 + \alpha_3) = -\frac{2}{\sqrt{3}} \frac{a_l \beta_l}{\beta_1 \beta_2 \beta_3} < 0 \qquad \text{and} \qquad \frac{\partial K}{\partial a_l} < 0.$$

In particular $\mathcal{K}$ is an analytic surface with normal vector ∇K, and $\nabla K \cdot (1,1,1) < 0$ on $\mathcal{K}$.

(c) *$G(a(p)) = g(p)$ for every $p \in \mathcal{T}$.*

Proof. (a) Let $a \in \mathcal{K}$. From $k_i = w_i(q_i - 1) = 0$ and $w_i > 0$ we get $q_i = 1$, that is $R_i = 1$: the outer triangle is equilateral with unit sides. Since $\theta \in (0,\pi)^3$ and $\sum_i \theta_i = 2\pi$, body 4 lies strictly inside it. An isometry that maps x_i to v_i for $i \le 3$ maps x_4 to a point $p \in \mathcal{T}$; then $a = a(p)$. Conversely, let $p \in \mathcal{T}$. Then $|p - v_i| < 1$: an interior point of a triangle is closer to each vertex than the farther of the two other vertices (proof of Lemma 2.1). The angles α_i at p between $v_j - p$ and $v_k - p$ lie in $(0,\pi)$ and add up to 2π, and the law of cosines gives $\cos \alpha_i = \zeta_i$, since $|v_j - v_k| = 1$. With $R_i = 1$, these angles and $K = 0$ solve the system of Lemma 2.2 at $a(p)$. They are its solution by the uniqueness in that lemma, so $a(p) \in \mathcal{K}$. The map $p \mapsto a(p)$ is injective: a point of the plane is determined by its distances to three non-collinear points.

The differential of $p \mapsto a(p)$ has the unit vectors $(p-v_i)/|p-v_i|$ as rows. Any two of them are independent, since p does not lie on a line through two vertices.

(b) Let $\theta_i(a,K) = \arccos\big((a_j^2+a_k^2-R_i)/(2a_ja_k)\big)$ with $R_i = (1+K/w_i)^{-2/3}$, as in the proof of Lemma 2.2. Differentiating $\sum_i \theta_i(a,K(a)) = 2\pi$ on $\mathcal{A}$ gives

$$\nabla K = -\frac{\nabla_a \sum_i \theta_i}{\partial_K \sum_i \theta_i},$$

where $\partial_K \theta_i < 0$ as in that proof. At $K=0$ we have $R_i = 1$ and $\partial R_i/\partial a = 0$, so $\nabla_a \theta_i = \nabla \alpha_i$ on $\mathcal{K}$. We compute $\nabla\alpha_i$ with the configuration of (a). The triangle pv_jv_k has area $S_i = \frac{\sqrt{3}}{4}\beta_i$. For $\{l,j,k\} = \{1,2,3\}$ we have $p - v_l = \beta_j(v_j - v_l) + \beta_k(v_k - v_l)$. It follows that $a_l^2 = \beta_j^2 + \beta_j\beta_k + \beta_k^2$ and, since $\sum_i \beta_i = 1$,

$$a_l^2 - a_k^2 + 1 = \beta_j + 2\beta_k.$$

Differentiating $\cos\alpha_i = (a_j^2+a_k^2-1)/(2a_ja_k)$ and using $2S_i = a_ja_k\sin\alpha_i$ gives $\partial\alpha_i/\partial a_j = -(a_j^2 - a_k^2 + 1)/(4a_jS_i)$. As α_l does not depend on a_l,

$$\frac{\partial}{\partial a_l}\sum_i \alpha_i = -\frac{\beta_j + 2\beta_k}{\sqrt{3}\,a_l\beta_j} - \frac{\beta_k + 2\beta_j}{\sqrt{3}\,a_l\beta_k} = -\frac{2(\beta_j^2 + \beta_j\beta_k + \beta_k^2)}{\sqrt{3}\,a_l\beta_j\beta_k} = -\frac{2a_l}{\sqrt{3}\,\beta_j\beta_k}$$

(check E6). With $\partial_K \sum_i \theta_i < 0$, the formula for ∇K shows that all the partial derivatives $\partial K/\partial a_l$ are negative. In particular $\nabla K \neq 0$ on $\mathcal{K} = \mathcal{A} \cap \{K=0\}$, which is thus an analytic surface with normal vector ∇K.

(c) By (a), $\beta_i(a(p)) = \beta_i(p)$ and $w_i(a(p)) = w_i(p)$. Statement (c) then follows from (6.1). □

The restricted problem. For $m = (m_1,m_2,m_3) \in (0,\infty)^3$ and $p \in \mathbb{R}^2 \setminus \{v_1,v_2,v_3\}$ let

$$V_m^{\mathrm{r}}(p) = \sum_{i=1}^3 m_i\Big(\frac{1}{|p-v_i|} + \frac{|p-v_i|^2}{2}\Big).$$

Since the gradient of $|p-v_i|^{-1} + \frac{1}{2}|p-v_i|^2$ is $-w_i(p)(p-v_i)$,

$$\nabla V_m^{\mathrm{r}}(p) = -\sum_{i=1}^3 m_i w_i(p)\,(p-v_i). \tag{6.2}$$

Thus $\nabla V_m^{\mathrm{r}}(p) = 0$ is the equation of body 4 in (2.1) for the configuration (v_1,v_2,v_3,p), an equation that does not involve m_4; the critical points of V_m^{r} are therefore the relative equilibria of the restricted problem with primaries of masses m_i at the points v_i. We write $\log m = (\log m_1, \log m_2, \log m_3)$.

Lemma 6.23. *Let $m \in (0,\infty)^3$. A point $p \in \mathcal{T}$ is a critical point of V_m^{r} if and only if $g(p) = \varpi(\log m)$, and then m is a positive multiple of $m(p) = (\beta_i(p)/w_i(p))_i$.*

Proof. The vectors $\xi \in \mathbb{R}^3$ with $\sum_i \xi_i(p-v_i) = 0$ form a line, since $p-v_1$ and $p-v_2$ are independent for $p \in \mathcal{T}$. It contains $(\beta_i(p))_i$, since $\sum_i \beta_i(p)(p-v_i) = p - p = 0$. Equation (6.2) shows that p is a critical point of V_m^{r} if and only if $(m_iw_i(p))_i$ is a multiple of $(\beta_i(p))_i$, that is, if and only if m is a positive multiple of $m(p)$. As the kernel of ϖ is spanned by $(1,1,1)$, this holds if and only if $\varpi(\log m) = \varpi(\log m(p)) = g(p)$. □

Equal primaries. We write $V = V_{(1,1,1)}^{\mathrm{r}}$; its critical points in $\mathcal{T}$ are the relative equilibria of the restricted problem with three equal primaries inside their triangle. That there are exactly four of them is known [Bar08, Teor. 45] (see the references there). We include a short proof, which also gives the signs of the Hessians. For $p = (x,y)$ we put $p^\perp = (-y,x)$.

Lemma 6.24 (equal primaries)**.** *The function V has exactly four critical points in $\mathcal{T}$: the centre 0, where* $\operatorname{Hess} V(0) = (3 + \frac{9}{2}\sqrt{3})\, I$*, and three points p_1, p_2, p_3, which the rotation through 120° about 0 permutes and at which* $\det \operatorname{Hess} V(p_k) < 0$*. The point p_3 lies on the open segment from 0 to the midpoint of $v_1 v_2$.*

Proof. We write $u_i = |p - v_i|^2$, $f_0(u) = u^{-3/2}$, $w_i = f_0(u_i) - 1$ and, as in (6.2), $Y = -\nabla V = \sum_i w_i\,(p - v_i)$. Differentiating once more and using $\nabla w_i = -3u_i^{-5/2}(p - v_i)$, we get

$$\operatorname{Hess} V = \sum_{i=1}^{3} \Big(-w_i\, I + 3u_i^{-5/2}\,(p - v_i)(p - v_i)^{\mathsf{T}} \Big).$$

At the centre $u_i = \frac{1}{3}$. With $\sum_i v_i v_i^{\mathsf{T}} = \frac{1}{2} I$ this yields $\operatorname{Hess} V(0) = -3(3\sqrt{3} - 1)\, I + \frac{27\sqrt{3}}{2}\, I = (3 + \frac{9}{2}\sqrt{3})\, I$ (check E2).

Step 1: the critical points lie on the medians. Let (i, j, k) be a cyclic permutation of $(1, 2, 3)$ and $t_i = p \cdot v_i$. As $|v_i|^2 = \frac{1}{3}$, we have $u_i = |p|^2 + \frac{1}{3} - 2t_i$. Moreover $v_j - v_k = \sqrt{3}\, v_i^{\perp}$, so that $\det[v_i, p] = p \cdot v_i^{\perp} = (t_j - t_k)/\sqrt{3} = (u_k - u_j)/(2\sqrt{3})$. Since $(p - v_i) \cdot p^{\perp} = \det[v_i, p]$, we obtain

$$Y \cdot p^{\perp} = \frac{w_1(u_3 - u_2) + w_2(u_1 - u_3) + w_3(u_2 - u_1)}{2\sqrt{3}} = \frac{1}{2\sqrt{3}} \det \begin{pmatrix} 1 & 1 & 1 \\ u_1 & u_2 & u_3 \\ f_0(u_1) & f_0(u_2) & f_0(u_3) \end{pmatrix}.$$

The constants -1 in the w_i drop out. The determinant is alternating in its three columns. If $u_1 < u_2 < u_3$, it equals $(u_2 - u_1)(u_3 - u_2)\big(f_0[u_2, u_3] - f_0[u_1, u_2]\big)$, where $f_0[a, b] = (f_0(b) - f_0(a))/(b - a)$. This is positive, because f_0 is strictly convex on $(0, \infty)$. Thus $Y(p) \neq 0$ whenever u_1, u_2 and u_3 are pairwise distinct. The sets $\{u_j = u_k\}$ are the perpendicular bisectors of the edges. They meet $\mathcal{T}$ in its three medians.

Step 2: the median through v_3. The reflection $(x, y) \mapsto (-x, y)$ exchanges v_1 and v_2 and preserves V, so $Y_x(0, y) = 0$. We parametrize the median $\{x = 0\} \cap \mathcal{T}$ by the distance $d = \frac{1}{2\sqrt{3}} - y \in (0, \frac{\sqrt{3}}{2})$ to the edge $v_1 v_2$. Then $u_1 = u_2 = \frac{1}{4} + d^2$, $|p - v_3| = \frac{\sqrt{3}}{2} - d$ and

$$Y_y\big(0, \tfrac{1}{2\sqrt{3}} - d\big) = \psi(d) := -2d\Big(\big(\tfrac{1}{4} + d^2\big)^{-3/2} - 1 \Big) + \Big(\tfrac{\sqrt{3}}{2} - d \Big)^{-2} - \Big(\tfrac{\sqrt{3}}{2} - d \Big).$$

The function ψ is strictly convex on $[0, \frac{\sqrt{3}}{2})$. Indeed

$$\psi''(d) = 2d\big(\tfrac{9}{4} - 6d^2\big)\big(\tfrac{1}{4} + d^2\big)^{-7/2} + 6\Big(\tfrac{\sqrt{3}}{2} - d \Big)^{-4}.$$

For $d^2 \le \frac{3}{8}$ both terms are nonnegative, and the second is positive. For $d \in [\frac{\sqrt{6}}{4}, \frac{\sqrt{3}}{2})$ we have $\frac{\sqrt{3}}{2} - d \le \frac{2\sqrt{3} - \sqrt{6}}{4} < 0.26$. Then the second term exceeds $6/0.26^4 > 1304$, while the first has absolute value at most $\sqrt{3} \cdot \frac{9}{4} \cdot (\frac{8}{5})^{7/2} < 1.75 \cdot 2.25 \cdot 5.2 < 21$. Next, $\psi(0) = \frac{4}{3} - \frac{\sqrt{3}}{2} > 0$. At the centre, where $d = d_0 = \frac{1}{2\sqrt{3}}$, we have $\psi(d_0) = 0$ and $\psi'(d_0) = \partial_y^2 V(0) = 3 + \frac{9}{2}\sqrt{3} > 0$. Thus $\psi < 0$ just below d_0; hence ψ has a zero $d_s \in (0, d_0)$ by the intermediate value theorem. A strictly convex function has at most two zeros. The zeros of ψ on $(0, \frac{\sqrt{3}}{2})$ are therefore d_s and d_0. By convexity, $\psi'(d_s) < (\psi(d_0) - \psi(d_s))/(d_0 - d_s) = 0$. Thus the critical points of V on this median are 0 and $p_3 = (0, y_s)$, where $y_s = d_0 - d_s > 0$. The rotations through $\pm 120^\circ$ about 0 preserve V and $\mathcal{T}$ and map this median onto the other two. This yields p_1 and p_2, and with Step 1 the four critical points.

Step 3: the Hessian at p_3. By the reflection symmetry, $\operatorname{Hess} V(p_3)$ is diagonal. Moreover $\partial_y^2 V(p_3) = \psi'(d_s) < 0$. On the median, $p - v_1 = (-\frac{1}{2}, y - \frac{1}{2\sqrt{3}})$, $p - v_2 = (\frac{1}{2}, y - \frac{1}{2\sqrt{3}})$ and

$p - v_3 = (0,\, y + \frac{1}{\sqrt{3}})$, so the formula for $\operatorname{Hess} V$ gives

$$\partial_x^2 V(0,y) = -2f_0(u_1) - f_0(u_3) + 3 - f_0'(u_1), \qquad u_3 - u_1 = \sqrt{3}\, y.$$

The equation $Y_y(0,y) = 0$ reads $E(y) = 0$, where $E(y) = \sqrt{3}\, Y_y(0,y) = (1+\sqrt{3}y)\big(f_0(u_3)-1\big) - (1-2\sqrt{3}y)\big(f_0(u_1)-1\big)$. Expanding both sides, we find

$$\sqrt{3}\, y\, \partial_x^2 V(0,y) - \big[f_0(u_3) - f_0(u_1) - f_0'(u_1)(u_3-u_1)\big] = -E(y).$$

At a critical point $(0,y)$ the right side vanishes. At p_3 we have $y_s > 0$ and $u_3 > u_1$, so the bracket is positive, since a strictly convex function lies above its tangent lines. Therefore $\partial_x^2 V(p_3) > 0$ and $\det \operatorname{Hess} V(p_3) = \partial_x^2 V(p_3)\, \partial_y^2 V(p_3) < 0$. The rotations carry this to p_1 and p_2. □

Numerically $d_s = 0.0497168\ldots$, $p_3 = (0, 0.238958\ldots)$, $\partial_x^2 V(p_3) = 32.2297\ldots$ and $\partial_y^2 V(p_3) = -8.6257\ldots$

The signs of the critical points are the signs of the Jacobian of g, by the following identity.

Lemma 6.25 (sign identity)**.** *For $p \in \mathcal{T}$ let $C(p)$ be the linear map of $\mathbb{R}^2$ with $C(p)\varpi(e_l) = \beta_l(p)(v_l - p)$ for $l = 1,2,3$. Then*

$$\operatorname{Hess} V^{\mathrm{r}}_{m(p)}(p) = -C(p)\, Dg(p), \qquad \det C(p) = \tfrac{3}{2}\, \beta_1(p)\beta_2(p)\beta_3(p) > 0.$$

In particular $\operatorname{sign}\det Dg(p) = \operatorname{sign}\det \operatorname{Hess} V^{\mathrm{r}}_{m(p)}(p)$.

Proof. The map $C(p)$ is well defined: $\varpi(e_1)$ and $\varpi(e_2)$ form a basis of $\mathbb{R}^2$, $\sum_l \varpi(e_l) = 0$ and $\sum_l \beta_l(p)(v_l - p) = 0$. We omit the argument p and write $a_l = |p - v_l|$. Differentiating (6.2) and using $\nabla w_l = -3a_l^{-5}(p - v_l)$ and $m_l w_l = \beta_l$ for $m = m(p)$, we get

$$\operatorname{Hess} V^{\mathrm{r}}_{m(p)} = \sum_l \Big(-\beta_l I + \frac{3\beta_l}{a_l^5 w_l}\, (p - v_l)(p - v_l)^{\mathsf{T}} \Big).$$

From $\beta_l = \frac{1}{3} + 2\, p \cdot v_l$ we get $\nabla \ell_l = 2v_l/\beta_l + 3a_l^{-5} w_l^{-1}(p - v_l)$. With $Dg = \sum_l \varpi(e_l) \nabla \ell_l^{\mathsf{T}}$ this gives

$$C\, Dg = \sum_l \Big(2(v_l - p) v_l^{\mathsf{T}} - \frac{3\beta_l}{a_l^5 w_l}\, (p - v_l)(p - v_l)^{\mathsf{T}} \Big).$$

With $\sum_l \beta_l = 1$, $\sum_l v_l v_l^{\mathsf{T}} = \frac{1}{2} I$ and $\sum_l v_l = 0$, the sum of the two matrices is $-I + 2\sum_l v_l v_l^{\mathsf{T}} - 2p\big(\sum_l v_l\big)^{\mathsf{T}} = 0$. This identity does not use the relation $a_l = |p - v_l|$ (check E8b). Finally, C maps the basis $\varpi(e_1), \varpi(e_2)$, of determinant $1/\sqrt{3}$, to the vectors $\beta_1(v_1 - p), \beta_2(v_2 - p)$, whose determinant is $\beta_1\beta_2$ times twice the area $\frac{\sqrt{3}}{4}\beta_3$ of the positively oriented triangle pv_1v_2. So $\det C = \frac{3}{2}\beta_1\beta_2\beta_3$ (check E8c). The last assertion holds as $\det(-C\, Dg) = \det C \det Dg$ for 2×2 matrices. □

The collar. For $A_0 \in \mathbb{R}$ and $G_0 \in \mathbb{R}^2$ we write $F^{-1}(A_0, G_0)$ for the set of $a \in \Omega_4$ with $A(a) = A_0$ and $G(a) = G_0$, which is the fibre of F over the point with coordinates $(A, P, Q) = (A_0, G_0)$. We show that for A_0 large this fibre corresponds to $g^{-1}(G_0)$. The first step locates it near $\mathcal{K}$.

Lemma 6.26. *Let $B \geq 0$, and let $a^{(n)} \in \Omega_4$ satisfy $|G(a^{(n)})| \leq B$ and $A(a^{(n)}) \to +\infty$. Then a subsequence of $(a^{(n)})$ converges to a point of $\mathcal{K}$.*

Proof. We scale the masses of $a^{(n)}$ so that $m_1 + m_2 + m_3 = 1$. Since (2.1) is linear in the masses, this does not change the CC. The vector $\mu - A(1,1,1)$ lies in the plane $\xi_1 + \xi_2 + \xi_3 = 0$, on which ϖ is an isometry. Therefore $|\mu_i - A| \leq |G| \leq B$ for each i. It follows that $m_i/m_j \leq e^{2B}$ and $m_i \geq e^{-2B}/3$ for $i, j \leq 3$. Moreover $m_4 = (m_1 m_2 m_3)^{1/3} e^{-A} \leq e^{-A} \to 0$. With x_4 at the origin, $|x_i| = a_i < 1$; the positions are therefore bounded.

First, all spokes are bounded below. Since $R_i > 1$ by Lemma 2.1 and $R_i = r_{jk}^2 \le (a_j + a_k)^2$, we have $a_j + a_k > 1$ for all pairs: at most one spoke is shorter than $1/2$. The equation of body 4 in (2.1) reads $\sum_{i\le 3} m_i w_i (x_i - x_4) = 0$. The i-th term of this sum has length $m_i(a_i^{-2} - a_i)$, which is at most $7m_i/2$ if $a_i \ge 1/2$. Let a_i be the shortest spoke. The two other terms, whose spokes are at least $1/2$, have total length at most $7/2$. Then $m_i(a_i^{-2} - a_i) \le 7/2$ and $a_i^{-2} \le 1 + \frac{21}{2}e^{2B}$. So $c_B = (1 + \frac{21}{2}e^{2B})^{-1/2}$ is a lower bound for all spokes.

We pass to a subsequence along which the masses converge to $\bar m$ and the positions to $\bar x$. Then $\bar m_4 = 0$, $\bar m_i \ge e^{-2B}/3$ for $i \le 3$, $a^{(n)} \to \bar a$ and $\bar a_i \ge c_B$. In the equation of an outer body j, the term of body 4 has length $m_4(a_j^{-2} - a_j) \le m_4 c_B^{-2} \to 0$, while the other terms depend continuously on the positions, since $r_{ij} > 1$. In the limit,

$$\sum_{i\le 3,\ i\ne j} \bar m_i\,(\bar x_i - \bar x_j)\,(\bar r_{ij}^{-3} - 1) = 0, \qquad j = 1,2,3, \qquad \text{with } \bar r_{ij} \ge 1.$$

If $\bar x_1, \bar x_2, \bar x_3$ were collinear, then at an end body j the two vectors $\bar x_i - \bar x_j$ would have the same direction and coefficients $\bar m_i(\bar r_{ij}^{-3} - 1) \le 0$. Both coefficients would vanish, and the two other bodies would coincide, a contradiction. For each j the two vectors $\bar x_i - \bar x_j$ are then independent, so all coefficients vanish. Hence the limit outer triangle is equilateral with unit sides. It contains $\bar x_4$, a limit of interior points, which is not a vertex, since all $\bar a_l$ are positive. As the only points of a closed unit equilateral triangle at distance 1 from a vertex are the two other vertices, all $\bar a_i$ are less than 1; hence $w_i \to \bar a_i^{-3} - 1 > 0$. The equation of body 4 shows that the barycentric coordinates of x_4 in the outer triangle are $\beta_i = m_i w_i / \sum_l m_l w_l$. These converge to positive limits. Hence $\bar x_4$ lies inside the limit triangle, so $\bar a = a(p)$ for some $p \in \mathcal{T}$. Lemma 6.22(a) then gives $\bar a \in \mathcal{K}$. □

Lemma 6.27. *For $p \in \mathcal{T}$ let $\tau_1(p)$ and $\tau_2(p)$ be the partial derivatives of a at p with respect to the two Cartesian coordinates of the plane. Then*

$$\det[\nabla K(a(p)), \tau_1(p), \tau_2(p)] < 0 \qquad \textit{for every } p \in \mathcal{T}.$$

Proof. Lemma 6.22 shows that $\tau_1(p)$ and $\tau_2(p)$ span the tangent plane of $\mathcal{K}$ at $a(p)$ and that $\nabla K(a(p))$ is a nonzero normal vector. The determinant is then a continuous function on $\mathcal{T}$ without zeros. Since $\mathcal{T}$ is connected, its sign is constant. We may evaluate it at $p = 0$, where $a(0) = 3^{-1/2}(1,1,1)$ and $\beta_l = \frac13$. Lemma 6.22(b) shows that the three partial derivatives of K are equal there: $\nabla K = \frac13 K_s(1,1,1)$, where K_s is the derivative of K along $s \mapsto s(1,1,1)$ at $s = 1/\sqrt3$. By Lemma 2.2, the symmetric solution $\theta_i = 2\pi/3$, $R_i = 3s^2$ yields $K = (s^{-3}-1)\big((\sqrt3\,s)^{-3}-1\big)$ on the axis (Lemma 2.3(a)). Differentiating at $s = 1/\sqrt3$ gives $K_s = -3\sqrt3\,(3\sqrt3 - 1)$. Also $\tau_k(0) = -\sqrt3\,(v_{1,k}, v_{2,k}, v_{3,k})$, where $v_{l,k}$ is the k-th coordinate of v_l. Hence $\det[(1,1,1), \tau_1(0), \tau_2(0)]$ is 3 times twice the area $\frac{\sqrt3}{4}$ of the positively oriented triangle $v_1v_2v_3$, that is $\frac{3\sqrt3}{2}$. At $p = 0$ we obtain

$$\det[\nabla K, \tau_1, \tau_2] = \frac{K_s}{3}\cdot\frac{3\sqrt3}{2} = -\frac92\,(3\sqrt3 - 1) < 0$$

(check E7). □

Collar coordinates. Let $p_0 \in \mathcal{T}$. Since $\nabla K \cdot (1,1,1) < 0$ on $\mathcal{K}$, by the implicit function theorem there is an analytic function $t(K,p)$ near $(0,p_0)$ with $t(0,p) = 0$ and $K\big(a(p) + t(K,p)(1,1,1)\big) = K$. Let $\Xi(K,p) = a(p) + t(K,p)(1,1,1)$; its differential at $(0,p)$ has the columns $(1,1,1)/(\nabla K \cdot (1,1,1))$, $\tau_1(p)$ and $\tau_2(p)$. It is invertible: $\tau_1(p)$ and $\tau_2(p)$ span the tangent plane of $\mathcal{K}$ at $a(p)$ (Lemma 6.22) and $(1,1,1)$ is not tangent to $\mathcal{K}$. By the inverse function theorem, Ξ maps a neighbourhood $(-\eta,\eta)\times D$ of $(0,p_0)$ diffeomorphically onto a neighbourhood of $a(p_0)$ in $\mathcal{A}$. It

maps $(-\eta, 0) \times D$ into Ω_4 and $\{0\} \times D$ into $\mathcal{K}$. In the coordinates (K, p) the functions G and $\widehat{A}$ are analytic, and $G(0, p) = g(p)$ by Lemma 6.22(c).

Lemma 6.28. *Let $p_0 \in \mathcal{T}$ with $\det Dg(p_0) \neq 0$. As $a \to a(p_0)$ in Ω_4,*

$$(-K)\, J \;\to\; \sqrt{3}\, \frac{|\nabla K|^2 \det Dg(p_0)}{\det[\nabla K, \tau_1, \tau_2]},$$

where ∇K, τ_1 and τ_2 are taken at $a(p_0)$ and p_0. In particular $J \neq 0$ and $\operatorname{sign} J = -\operatorname{sign} \det Dg(p_0)$ at the points of Ω_4 close to $a(p_0)$.

Proof. We use the collar coordinates at p_0 and put $\omega = -\log(-K)$ for $K < 0$. Then $A = \widehat{A} + \omega$ and $\partial_\omega = (-K)\, \partial_K$. As $(K, p) \to (0, p_0)$ with $K < 0$,

$$D_{(\omega,p)}(A, P, Q) = \begin{pmatrix} 1 + (-K)\, \partial_K \widehat{A} & \partial_p \widehat{A} \\ (-K)\, \partial_K G & D_p G \end{pmatrix} \;\to\; \begin{pmatrix} 1 & \partial_p \widehat{A} \\ 0 & Dg(p_0) \end{pmatrix},$$

because $\widehat{A}$ and G are analytic in (K, p) and $G(0, p) = g(p)$. With $\det \partial(A, P, Q)/\partial\mu = 1/\sqrt{3}$ and $d\omega/dK = 1/(-K)$,

$$(-K)\, J = \sqrt{3}\, \frac{\det D_{(\omega,p)}(A, P, Q)}{\det D\Xi(K, p)} \;\to\; \sqrt{3}\, \frac{\det Dg(p_0)}{\det D\Xi(0, p_0)}.$$

Differentiating $K(\Xi(K, p)) = K$ gives $\nabla K \cdot \partial_K \Xi = 1$. At $K = 0$ the column $\partial_K \Xi$ is then $\nabla K/|\nabla K|^2$ plus a vector tangent to $\mathcal{K}$, that is, plus a combination of τ_1 and τ_2. Therefore $\det D\Xi(0, p_0) = \det[\nabla K, \tau_1, \tau_2]/|\nabla K|^2$, which is negative by Lemma 6.27. □

Proposition 6.29 (collar)**.** *Let $G_0 \in \mathbb{R}^2$, and suppose that $g^{-1}(G_0) = \{q_1, \dots, q_n\}$ is finite and that $\det Dg(q_l) \neq 0$ for $l = 1, \dots, n$. For every A_0 large enough, $F^{-1}(A_0, G_0)$ consists of exactly n points, one near each point $a(q_l)$. At the point near $a(q_l)$ we have $J \neq 0$ and $\operatorname{sign} J = -\operatorname{sign} \det Dg(q_l)$.*

Proof. For each l we take collar coordinates (K, p) at q_l on $(-\eta, \eta) \times D_l$ and choose the discs D_l so small that the sets $\Xi((-\eta, \eta) \times D_l)$ are disjoint. Since $D_p G(0, q_l) = Dg(q_l)$ is invertible, the implicit function theorem gives, after shrinking η and D_l, a unique solution $p = q_l(K) \in D_l$ of $G(K, p) = G_0$ for each $K \in (-\eta, \eta)$. At $K = 0$ the solution is $q_l(0) = q_l$. For $K \in (-\eta, 0)$ let $\chi_l(K) = \widehat{A}(K, q_l(K)) - \log(-K)$, the value of A at this solution. Since the derivative of χ_l is a bounded function minus $1/K$, there is $\eta' \in (0, \eta)$ such that χ_l increases strictly on $(-\eta', 0)$. It tends to $+\infty$ as $K \to 0$. A point of $F^{-1}(A_0, G_0)$ in $\Xi((-\eta', \eta') \times D_l)$ has $K < 0$, $p = q_l(K)$ and $\chi_l(K) = A_0$. Conversely, such a K determines the point $\Xi(K, q_l(K))$ of $F^{-1}(A_0, G_0)$. For $A_0 > \max_l \chi_l(-\eta'/2)$ the equation $\chi_l(K) = A_0$ has exactly one solution in $(-\eta', 0)$, by monotonicity and the intermediate value theorem. Each of the n sets $\Xi((-\eta', \eta') \times D_l)$ then contains exactly one point of $F^{-1}(A_0, G_0)$. This point tends to $a(q_l)$ as $A_0 \to +\infty$.

It remains to show that, for A_0 large, $F^{-1}(A_0, G_0)$ lies in the union $\mathcal{V}$ of these sets. Otherwise there are $A^{(n)} \to +\infty$ and points $a^{(n)} \in F^{-1}(A^{(n)}, G_0) \setminus \mathcal{V}$. By Lemma 6.26 with $B = |G_0|$, a subsequence converges to a point $\bar{a} = a(\bar{p})$ of $\mathcal{K}$. Since G is continuous on $\mathcal{A}$, $g(\bar{p}) = G(\bar{a}) = G_0$, so $\bar{a}$ is one of the points $a(q_l)$. This is impossible because $\mathcal{V}$ is a neighbourhood of these points. The signs follow from Lemma 6.28. □

We now take $G_0 = 0$.

Proposition 6.30 (base value)**.** *For every sufficiently large A_0, the point with coordinates $(A, P, Q) = (A_0, 0, 0)$ is a regular value of F with exactly four preimages. At one of them $J < 0$, and at the other three $J > 0$.*

Proof. Let $m = (1,1,1)$, so that $\varpi(\log m) = 0$. Lemma 6.23 shows that $g^{-1}(0)$ is the set of critical points of $V = V_m^{\mathrm{r}}$ in $\mathcal{T}$ and that at each of them $m(p)$ is a positive multiple of m. This set is $\{0, p_1, p_2, p_3\}$ by Lemma 6.24. As $\operatorname{Hess} V_{tm}^{\mathrm{r}} = t \operatorname{Hess} V_m^{\mathrm{r}}$ for $t > 0$, Lemma 6.25 implies $\operatorname{sign}\det Dg(p) = \operatorname{sign}\det \operatorname{Hess} V(p)$ at these points. This sign is $+$ at the centre and $-$ at p_1, p_2 and p_3 (Lemma 6.24). Therefore $g^{-1}(0)$ is finite and $\det Dg \neq 0$ at each of its four points. Proposition 6.29 with $G_0 = 0$ shows that for A_0 large the set $F^{-1}(A_0, 0)$ consists of exactly four points, at which $J \neq 0$ and $\operatorname{sign} J = -\operatorname{sign}\det Dg$, that is, $-$, $+$, $+$, $+$. □

The preimage with $J < 0$ is the axis point at which $A = A_0$: this point has $G = 0$ and $J < 0$ by Lemma 2.3(c),(d) and Proposition 2.4.

6.10. **Counting.** For $\mu \in \mathbb{R}^3$ let $n_\pm(\mu)$ be the number of points of $F^{-1}(\mu)$ at which $\pm J > 0$. The critical values of F form the set $F(\Sigma)$; the other points of $\mathbb{R}^3$ are the regular values. We show that $n_+ - n_- = 2$ at all regular values and then count the preimages. The proof combines the injectivity of Section 6.8, the base value of Section 6.9 and the fold normal form at one fold point on each nappe.

Lemma 6.31. *The set $\mathbb{R}^3 \setminus F(\Sigma)$ of regular values is open, and n_+ and n_- are locally constant on it.*

Proof. The set $F(\Sigma)$ is closed, since Σ is closed in Ω_4 and the proper map F is closed. Let $Y = \mathbb{R}^3 \setminus F(\Sigma)$. The points of $F^{-1}(Y)$ have $J \neq 0$, so by the inverse function theorem they have neighbourhoods U on which F is a homeomorphism onto an open set. We may assume that each U is connected and that J has one sign on it. Let $\mu \in Y$. Lemma 6.5, applied with $X = \Omega_4$ and $f = F$, shows that the fibre $F^{-1}(\mu) = \{x_1, \dots, x_k\}$ is finite. For pairwise disjoint such neighbourhoods $U_i \ni x_i$ there is an open set $\mathcal{V} \ni \mu$ such that each $\mu' \in \mathcal{V}$ has exactly one preimage in each U_i and no other preimage. This preimage has the sign of $J(x_i)$, so $n_\pm(\mu') = n_\pm(\mu)$. □

Lemma 6.32 (fold crossing)**.** *Let q be a fold point and $c = A(q)$. Then $F^{-1}(F(q)) = \{q, p_1, \dots, p_n\}$ is finite, and $J(p_j) > 0$ for each j. Moreover $G(q)$ has an open neighbourhood $Y_2 \subset \mathbb{R}^2$ such that $n_+(c,w) - n_-(c,w) = n$ for every $w \in Y_2$ for which (c,w) is a regular value.*

Proof. Theorem 6.19(a) shows that q is the only point of the fibre in $\overline{\mathcal{D}}$. All other points have $J > 0$. They are isolated in the fibre by the inverse function theorem. Lemma 6.17(b), applied with $\mathcal{N}_0 = \Omega_4$ and $(U,V) = (0,0)$, shows that q is isolated in the fibre. The fibre is compact (Proposition 6.3), hence finite.

We choose pairwise disjoint open sets $\mathcal{N}_0 \ni q$ and $\mathcal{N}_j \ni p_j$ such that $F|_{\mathcal{N}_j}$ is a homeomorphism onto an open set and $J > 0$ on $\mathcal{N}_j$. Lemma 6.17 with this $\mathcal{N}_0$ yields $\mathcal{N} \subset \mathcal{N}_0$, ε_1, ε_2 and M. As in the proof of Lemma 6.5, properness yields an open set $\mathcal{V} \ni F(q)$ with $F^{-1}(\mathcal{V}) \subset \mathcal{N} \cup \mathcal{N}_1 \cup \dots \cup \mathcal{N}_n$. Let Y_2 be the set of points $w = G(q) + Ue + Ve'$ with $|U| < \varepsilon_1$, $|V| < \varepsilon_2$ and $(c,w) \in \mathcal{V} \cap F(\mathcal{N}_1) \cap \dots \cap F(\mathcal{N}_n)$. It is an open neighbourhood of $G(q)$.

Let $w \in Y_2$. The fibre of (c,w) consists of one point in each $\mathcal{N}_j$, at which $J > 0$, and of the points of $F^{-1}(c,w) \cap \mathcal{N}$. If $V > M(U)$, there are two of the latter, one with $J < 0$ and one with $J > 0$ (Lemma 6.17(c)), so $n_+ - n_- = (n+1) - 1 = n$. If $V < M(U)$, there is none (Lemma 6.17(a)), so again $n_+ - n_- = n$. If $V = M(U)$, then (c,w) is a critical value by Lemma 6.17(b). □

We put

$$\mathcal{I}_L = F(\mathcal{D}) \cap \{A > A^*\}, \qquad \mathcal{I}_U = F(\mathcal{D}) \cap \{A < A^*\}, \qquad \mathcal{O} = \mathbb{R}^3 \setminus F(\overline{\mathcal{D}}).$$

Proposition 6.33. (a) *The set $\mathbb{R}^3 \setminus F(\Sigma)$ of regular values is the disjoint union of $\mathcal{I}_L$, $\mathcal{I}_U$ and $\mathcal{O}$, and these three sets are open.*

(b) *In the coordinates* (A, G), $\mathcal{I}_L = \{(c, w) : c > A^*,\ w \in \mathrm{In}(R_c)\}$, $\mathcal{I}_U = \{(c, w) : c < A^*,\ w \in \mathrm{In}(R_c)\}$ *and* $\mathcal{O} = \{(c, w) : c \neq A^*,\ w \in \mathrm{Out}(R_c)\} \cup \{(A^*, w) : w \neq 0\}$.
(c) *Each of the sets* $\mathcal{I}_L$, $\mathcal{I}_U$ *and* $\mathcal{O}$ *is path-connected.*

Proof. (a) We have $F(\overline{\mathcal{D}}) = F(\mathcal{D}) \cup F(\Sigma)$, a disjoint union by Theorem 6.19(a). By Corollary 6.20, $F(\overline{\mathcal{D}}) \cap \{A = A^*\} = \{F(p^*)\} \subset F(\Sigma)$, so $F(\mathcal{D})$ does not meet $\{A = A^*\}$. Hence $\mathbb{R}^3 \setminus F(\Sigma)$ is the disjoint union of $F(\mathcal{D}) = \mathcal{I}_L \sqcup \mathcal{I}_U$ and $\mathcal{O}$. The set $F(\mathcal{D})$ is open by the inverse function theorem, since $\mathcal{D}$ is open and $J \neq 0$ on it. The set $\mathcal{O}$ is open because $F(\overline{\mathcal{D}})$ is closed: $\overline{\mathcal{D}}$ is closed in Ω_4, and F is a closed map.

(b) This follows from Corollary 6.20 and Lemma 6.4(a).

(c) Let $(c, w) \in \mathcal{I}_L$. The segment $t \mapsto (c, (1-t)w)$, $t \in [0, 1]$, stays in $\mathcal{I}_L$ by Lemma 6.4(b) and ends on the half-line $\{(c, 0) : c > A^*\} \subset \mathcal{I}_L$, which is connected. The same argument applies to $\mathcal{I}_U$. Now let (c_1, w_1) and (c_2, w_2) be points of $\mathcal{O}$ with $c_1 \leq c_2$. Then $w_1 \neq 0$ and $w_2 \neq 0$, since $(c, 0) \in F(\overline{\mathcal{D}})$ for all c by Corollary 6.20. By Corollary 6.13, $B = \max\{|G(a)| : a \in \overline{\mathcal{D}},\ c_1 \leq A(a) \leq c_2\}$ is finite. Moreover $R_c \leq B$ for $c \in [c_1, c_2] \setminus \{A^*\}$ because $C(R_c) = G(\Gamma_c)$. Fix $\lambda > \max(B, |w_1|, |w_2|)$, and put $\hat{w}_k = w_k/|w_k|$. Consider the path that runs from (c_1, w_1) radially to $(c_1, \lambda\hat{w}_1)$, then at constant G to $(c_2, \lambda\hat{w}_1)$, then along the circle of radius λ to $(c_2, \lambda\hat{w}_2)$, and finally radially to (c_2, w_2). The radial parts of the path lie in $\mathcal{O}$ by Lemma 6.4(c), or since $w \neq 0$ when $c = A^*$. The other two parts consist of points (c, w) with $|w| = \lambda > B$. These lie in $\mathrm{Out}(R_c)$ for $c \neq A^*$, and they have $w \neq 0$ for $c = A^*$. The whole path therefore lies in $\mathcal{O}$. □

Theorem 6.34. *At every regular value* μ *of* F, $n_+(\mu) - n_-(\mu) = 2$. *More precisely,* $n_- = 1$ *and* $n_+ = 3$ *on* $F(\mathcal{D})$, *and* $n_- = 0$ *and* $n_+ = 2$ *on* $\mathbb{R}^3 \setminus F(\overline{\mathcal{D}})$. *These two sets make up the regular values.*

Proof. Lemma 6.31 shows that n_+ and n_- are locally constant on the regular values. By Proposition 6.33, the regular values form the three open path-connected sets $\mathcal{I}_L$, $\mathcal{I}_U$ and $\mathcal{O}$, so n_+ and n_- are constant on each of them. Let d_L, d_U and $d_{\mathcal{O}}$ be the values of $n_+ - n_-$ on these three sets. For A_0 large the point $(A_0, 0, 0)$ is a regular value with $n_- = 1$ and $n_+ = 3$, by Proposition 6.30. Since the preimage of $(A_0, 0, 0)$ with $J < 0$ lies in $\mathcal{D}$ and $A_0 > A^*$, the point lies in $\mathcal{I}_L$. Hence $d_L = 2$.

Fix $c > A^*$ and the fold point $q_c = \gamma_c(60°)$. Lemma 6.32 yields a neighbourhood Y_2 of $G(q_c)$. As $G(q_c) \in C(R_c)$, there are points $w_{in} \in Y_2 \cap \mathrm{In}(R_c)$ and $w_{out} \in Y_2 \cap \mathrm{Out}(R_c)$ by Lemma 6.4(d). By Proposition 6.33(b), $(c, w_{in}) \in \mathcal{I}_L$ and $(c, w_{out}) \in \mathcal{O}$. These two regular values have the same value of $n_+ - n_-$ by Lemma 6.32, so $d_{\mathcal{O}} = d_L$. The same argument with $c < A^*$ yields $d_U = d_{\mathcal{O}}$. Hence $n_+ - n_- = 2$ at all regular values.

By Theorem 6.19(a), a value in $F(\mathcal{D})$ has exactly one preimage in $\overline{\mathcal{D}}$, a point of $\mathcal{D}$. Thus $n_- = 1$ and $n_+ = 3$ there. A value in $\mathcal{O}$ has no preimage in $\overline{\mathcal{D}}$, so $n_- = 0$ and $n_+ = 2$. The last assertion is Proposition 6.33(a). □

Thus F has degree 2, in the sense that $n_+ - n_- = 2$ at all regular values.

Proof of Proposition 6.1. At a regular value $c_4 = n_+ + n_-$, which is 4 on $F(\mathcal{D})$ and 2 on $\mathcal{O}$ by Theorem 6.34. Now let μ be a critical value. Exactly one point of $F^{-1}(\mu)$ lies in $\overline{\mathcal{D}}$, by injectivity. All others have $J > 0$. Any k distinct points of the fibre with $J > 0$ persist, by the inverse function theorem, to k distinct preimages with $J > 0$ of any μ' near μ. The point μ is a limit of points of $\mathcal{O}$. Indeed, if $\mu = (c, w)$ with $c \neq A^*$, then $w \in C(R_c)$ by Corollary 6.20, and Lemma 6.4(d) applies. Otherwise $\mu = F(p^*)$, the limit of the points $(A^*, w) \in \mathcal{O}$ as $w \to 0$. As $n_+ = 2$ on $\mathcal{O}$, we get $k \leq 2$, so $1 \leq c_4(\mu) \leq 3$. Finally, the critical values form a closed set (proof of Lemma 6.31), and a null set by Sard's theorem [Sar42]. This proves Proposition 6.1. □

7. The count at critical values

In this section we compute $c_4(\mu) = \#F^{-1}(\mu)$, for $\mu \in \mathbb{R}^3$, at the critical values μ of $F = F_4$. Off the mirrors the points of $\Sigma \setminus \{p^*\}$ are fold points (Proposition 7.13), the generic case in Whitney's theory of planar maps [Whi55]. At fold points the count follows from the fold normal form and Theorem 6.34 (Section 7.2). But at the cusp points on the mirrors and at the umbilic the certified signs alone do not determine the local degree. There we will combine them with a normal form (Section 7.3) and with the closed form of the 2-jet at p^* (Section 7.4). We keep the notation of Section 6. As a set, $\Sigma = \Sigma_L \sqcup \{p^*\} \sqcup \Sigma_U$. For $c \neq A^*$, $\Phi_c = A^{-1}(c) \cap \overline{\mathcal{D}}$ is a closed disk (Corollaries 6.13 and 6.21), which lies in $\overline{\mathcal{D}}_L$ if $c > A^*$ and in $\overline{\mathcal{D}}_U$ if $c < A^*$. The boundary circle of Φ_c is $\Gamma_c = \Phi_c \cap \Sigma$. We write $C_c = G(\Gamma_c) = C(R_c)$, $V_{in}(c) = \mathrm{In}(R_c)$ and $V_{out}(c) = \mathrm{Out}(R_c)$, with R_c as in Proposition 6.16. By Lemma 6.4, $V_{in}(c)$ and $V_{out}(c)$ are the bounded and the unbounded component of $\mathbb{R}^2 \setminus C_c$. On the target we use the coordinates (A, ρ, Θ) of (1.2).

The planes $a_j = a_k$ are the six half-planes $\varphi \equiv 30^\circ \pmod{60^\circ}$, which we call *half-mirrors*. A *mirror point* is a point of $\Sigma \setminus \{p^*\}$ on a half-mirror. For a mirror angle $\varphi_m \in \{30^\circ, 90^\circ\}$ the functions L, $L^\perp$ and J_{mir} are those of Section 3.2. With $e_m = (\cos\varphi_m, \sin\varphi_m)$ and $e_m^\perp = (-\sin\varphi_m, \cos\varphi_m)$ we have $G = L\, e_m + L^\perp e_m^\perp$. The reflection $\sigma_m : (s, r, \varphi) \mapsto (s, r, 2\varphi_m - \varphi)$ is the action of the transposition of the two outer bodies whose spokes are equal on the mirror. It fixes A, K, J, $\widetilde{J}$ and L, it changes the sign of $L^\perp$ (proof of Lemma 3.2), and on the target it reflects G in the line $\mathbb{R}e_m$, mapping Θ to $2\varphi_m - \Theta$. The group $\mathfrak{S}_3$ acts on (x, y) and on (P, Q) by the same orthogonal matrices O_g (Section 2.3), hence on φ and on Θ through D_3. The functions A, K, J, $\widetilde{J}$, r, T_1, T_2 and T_3 are $\mathfrak{S}_3$-invariant. For $T_3 = (P^2 + Q^2)(-K)\det[\nabla\Theta; \nabla A; \nabla\widetilde{J}]$ the two signs cancel, as in Section 3.3: a reflection reverses the orientation and changes Θ into a constant minus Θ. By equivariance, the statements proved below for points of W extend to Ω_4. In particular, at a mirror point outside W the functions L, $L^\perp$ and J_{mir} are those of its image in W under an element of $\mathfrak{S}_3$. This does not depend on the choice: the two elements that map a mirror point into W differ by σ_m, which fixes J_{mir} and $\partial_\varphi L^\perp$ on the mirror.

7.1. Reduction to a local count.

We recall the facts from Sections 5 and 6 that we will use.

Lemma 7.1. (a) *At a regular value with $n_\pm$ preimages at which $\pm J > 0$, we have $n_+ - n_- = 2$.*
(b) *F is injective on $\overline{\mathcal{D}}$.*
(c) *$A > A^*$ on $\overline{\mathcal{D}}_L$ and $A < A^*$ on $\overline{\mathcal{D}}_U$, and $A : \overline{\mathcal{D}}_L \to (A^*, \infty)$ and $A : \overline{\mathcal{D}}_U \to (-\infty, A^*)$ are proper and surjective. In particular $\overline{\mathcal{D}} \cap A^{-1}(c) = \Phi_c$ for $c \neq A^*$, and $\overline{\mathcal{D}} \cap A^{-1}(A^*) = \{p^*\}$.*
(d) *Let $c \neq A^*$. The restriction of φ to Γ_c is a bijection onto the circle. The angle $\Theta \circ G$ increases strictly along Γ_c in the direction of increasing φ, by 360° in total. The map G maps Φ_c° bijectively onto $V_{in}(c)$ and Γ_c bijectively onto C_c. At the two points of Γ_c on the mirrors of W, $\Theta = \varphi$ if $c > A^*$ and $\Theta = \varphi + 180^\circ$ if $c < A^*$. The axis point a_c of Φ_c lies in Φ_c°, $G(a_c) = 0$, $0 \in V_{in}(c)$ and $G \neq 0$ on Γ_c.*
(e) *The fibre of a critical value has at most two points with $J > 0$.*
(f) *Every point of $\Sigma \cap W$ other than p^* lies in a leaf of type F or B of the core, lower core, top core or umbilic cover. At every point of $\Sigma \setminus \{p^*\}$, $T_1 > 0$ and $T_2 < 0$. At every point of $\Sigma \cap W$ in a leaf of type F, and at every point of $\Sigma \cap W$ off the mirrors in a leaf of type B, $T_3 < 0$.*

Proof. Part (a) is Theorem 6.34, and (b) is Theorem 6.19(a). Part (c) is Lemma 6.12(a),(b) with Corollary 6.13. For (d), the first statement is Proposition 6.15, and the third is Theorem 6.19(b). The second statement and the values of Θ at the mirrors are Proposition 6.16: over the wedge Θ runs from 30° to 90° on the lower nappe and from 210° to 270° on the upper nappe. The axis meets $\overline{\mathcal{D}}_L$ in the segment $1/\sqrt{3} < s < s^*$, on which $J < 0$ and A decreases strictly from $+\infty$ to A^* (Section 6.4 and the proof of Lemma 6.12(b)). So for $c > A^*$ it meets Φ_c in exactly one point

a_c, which lies in Φ_c°. Because $P = Q = 0$ on the axis, $G(a_c) = 0$. The case $c < A^*$ is the same, with the segment $s^* < s < 1$. Finally $0 \in \mathrm{In}(R_c) = V_{in}(c)$, and $G \neq 0$ on Γ_c (Section 6.7). Part (e) is shown in Section 6.10, in the proof of Proposition 6.1: the points of the fibre with $J > 0$ persist as preimages with $J > 0$ of all nearby values, among them points of $\mathcal{O}$, where $n_+ = 2$. Part (f) follows from Lemma 6.7(d), Table 4 and Lemma 3.3. Lemma 6.10 extends its second statement to Ω_4. The leaves of types F and B occur only in the four covers listed (Table 3). □

Lemma 7.2. *$dA \neq 0$ at every point of Ω_4.*

Proof. Where $J \neq 0$, dF is invertible and $dA \neq 0$. At a point of $\Sigma \setminus \{p^*\}$, $T_2 < 0$ by Lemma 7.1(f). The formula $T_2 = \mathbf{A}_s(\nabla \widetilde{J})_r - \mathbf{A}_r(\nabla \widetilde{J})_s$ then shows that the vector $\mathbf{A} = (-K)\nabla A$ is nonzero there. As $K < 0$, it follows that $dA \neq 0$. At p^*, $\partial_s A < 0$ by Lemma 2.3(c). □

Lemma 7.3. (a) *For $c \neq A^*$, $\Sigma \cap A^{-1}(c) = \Gamma_c$ and $F(\overline{\mathcal{D}}) \cap \{A = c\} = \{c\} \times (V_{in}(c) \cup C_c)$.*
(b) *$F(\overline{\mathcal{D}}) \cap \{A = A^*\} = \{F(p^*)\} = \{(A^*, 0, 0)\}$.*
(c) *If $\mu' \notin F(\overline{\mathcal{D}})$, then μ' is a regular value of F with exactly two preimages, at both of which $J > 0$. This applies to $\mu' = (c, w)$ with $c \neq A^*$ and $w \in V_{out}(c)$, and to $\mu' = (A^*, w)$ with $w \neq 0$.*

Proof. (a) We have $\Sigma \subset \overline{\mathcal{D}}$, $\overline{\mathcal{D}} \cap A^{-1}(c) = \Phi_c$ by Lemma 7.1(c), and $\Phi_c \cap \Sigma = \Gamma_c$. Lemma 7.1(d) shows that $G(\Phi_c) = V_{in}(c) \cup C_c$. (b) follows from Lemma 7.1(c), because $P = Q = 0$ on the axis. (c) A preimage with $J \leq 0$ would lie in $\overline{\mathcal{D}}$. Then $n_-(\mu') = 0$, so $\#F^{-1}(\mu') = n_+(\mu') = 2$ by Lemma 7.1(a). □

Lemma 7.4 (local count)**.** *Let $q \in \Sigma$ and $\mu = F(q)$.*
(a) *$F^{-1}(\mu) = \{q\} \cup \{p_1, \dots, p_n\}$ with $n \leq 2$ and $J(p_j) > 0$. In particular $c_4(\mu) = n + 1$.*
(b) *Let $\mathcal{N}_0$ be an open neighbourhood of q whose closure contains none of the p_j. There is a neighbourhood $\mathcal{V}$ of μ such that $\#F^{-1}(\mu') = n + \#(F^{-1}(\mu') \cap \mathcal{N}_0)$ for every $\mu' \in \mathcal{V}$.*
(c) *If some $\mu' \in \mathcal{V} \setminus F(\overline{\mathcal{D}})$ has exactly k preimages in $\mathcal{N}_0$, then $c_4(\mu) = 3 - k$.*

Proof. (a) By Lemma 7.1(b), the points of $F^{-1}(\mu)$ other than q lie outside $\overline{\mathcal{D}}$ and have $J > 0$. There are at most two of them by Lemma 7.1(e). (b) By the inverse function theorem there are pairwise disjoint open sets $\mathcal{N}_j \ni p_j$, disjoint from $\mathcal{N}_0$, such that F maps each $\mathcal{N}_j$ diffeomorphically onto an open neighbourhood $\mathcal{V}_j$ of μ. Let B be a closed ball around μ. As F is proper (Proposition 6.3), the set $F^{-1}(B) \setminus (\mathcal{N}_0 \cup \mathcal{N}_1 \cup \dots \cup \mathcal{N}_n)$ is compact; its image does not contain μ. Let $\mathcal{V} \subset B \cap \mathcal{V}_1 \cap \dots \cap \mathcal{V}_n$ be an open ball around μ that avoids this image. For $\mu' \in \mathcal{V}$ all preimages lie in $\mathcal{N}_0 \cup \mathcal{N}_1 \cup \dots \cup \mathcal{N}_n$, exactly one in each $\mathcal{N}_j$. (c) By (b) and Lemma 7.3(c), $n + k = 2$. Then $c_4(\mu) = n + 1 = 3 - k$ by (a). □

The number k is the local degree of F at q. At cusp points and at p^* we compute it with $\mu' = (A(q), w)$, where $w \in V_{out}(A(q))$ is close to $G(q)$, or $w \neq 0$ is small if $q = p^*$. With A as a coordinate near q (Lemma 7.2), the preimages of μ' near q are the preimages of w near q under the planar map $g_c = G|_{\{A=c\}}$, where $c = A(q)$. At fold points the count follows from Lemma 6.32 and Theorem 6.34 instead.

7.2. **Fold points.** Recall from Section 6.8 that a point $q \in \Sigma \setminus \{p^*\}$ is a fold point if $T_3(q) \neq 0$.

Lemma 7.5. *At a fold point q, $\dim \ker dF(q) = 1$, and $\ker dF(q)$ is transverse to $\Gamma_{A(q)}$.*

Proof. Put $c = A(q)$. Since $J(q) = 0$ and $dA(q) \neq 0$, the kernel $\ker dF(q) = \ker dA(q) \cap \ker dG(q)$ has dimension 1 or 2. By Lemma 3.1(c), the vector $v = \nabla A \times \nabla \widetilde{J}$ is tangent to Γ_c at q. It is nonzero, since its e_φ-component is $T_2/(-K) \neq 0$. If $\dim \ker dF(q) = 2$, then $\ker dF(q) = \ker dA(q) \ni v$. If $\ker dF(q)$ is a line that is not transverse to Γ_c, it is spanned

by v. In both cases $dG(q)v = 0$, hence $d\Theta(v) = 0$, since $G(q) \neq 0$ by Lemma 7.1(d). Then $T_3(q) = (P^2 + Q^2)(-K)\, d\Theta(v) = 0$ by Lemma 3.1(c), a contradiction. □

Proposition 7.6. *If q is a fold point, then $c_4(F(q)) = 3$.*

Proof. Put $c = A(q)$, and let n be the number of points of $F^{-1}(F(q))$ other than q, so that $c_4(F(q)) = n+1$. Lemma 6.32 provides an open neighbourhood Y_2 of $G(q)$ such that $n_+(c,w) - n_-(c,w) = n$ for each $w \in Y_2$ for which (c,w) is a regular value. As $q \neq p^*$, we have $c \neq A^*$ and $G(q) \in C(R_c)$ (Theorem 6.19). By Lemma 6.4(d), Y_2 contains a point w of $\mathrm{Out}(R_c)$. The point (c,w) is a regular value by Proposition 6.33. Theorem 6.34 gives $n_+ - n_- = 2$ at (c,w). Hence $n = 2$ and $c_4(F(q)) = 3$. □

Lemma 6.17 shows that the values (c,w) near $F(q)$ with $V > M(U)$ have exactly two preimages near q, one with $J < 0$ and one with $J > 0$, while those with $V < M(U)$ have none. This is a fold in the sense of Whitney [Whi55]; the local degree of F at q is 0.

7.3. **Cusp points.** A mirror point q is a *cusp point* if $J_{\mathrm{mir}}(q) \neq 0$ for the mirror through q. Cusp points are the delicate case of the local analysis. Since $T_3 = 0$ there (Lemma 7.7(a)), the sign condition behind the count at fold points is not available. Instead we combine a $\mathbb{Z}/2$-equivariant normal form with the quantitative bound (3.1) of the band lemma.

For a leaf of type B with cell C, Lemma 3.3 and the band certificate give (3.1) with $\beta = \beta_C$ for the certified quantities of its chart (Section 5.4). In chart 2, where the certified quantity is T_3/ϱ^4, this means $T_3 \le \frac{\tau^2}{2}\beta_C \varrho^4$. In chart 3 the certified quantity is $\sigma^6 T_3/K^2$ at the zeros of $\widetilde{J}$, with T_3 and K the values in chart 1 (Section 5.2). There the bound reads $T_3 \le \frac{\tau^2}{2}\beta_C K^2/\sigma^6$. Combining the three cases, we have in all charts

$$T_3 \le \tfrac{\tau^2}{2}\, \beta_C\, \kappa_C \tag{7.1}$$

at the zeros of $\widetilde{J}$ in C off the mirror, where $\kappa_C = 1$, ϱ^4 or K^2/σ^6 according to the chart of the leaf, a continuous function that is positive away from p^* and from $\sigma = 0$.

Lemma 7.7 (normal form at a cusp point)**.** *Let $q \in W$ be a cusp point with mirror angle φ_m, and put $c = A(q)$. Then the following hold.*

(a) *$L(q) \neq 0$, $\partial_\varphi L^\perp(q) = 0$ and $T_3(q) = 0$.*

(b) *There is a σ_m-invariant open neighbourhood Ω_q of q on which (A, L, φ) are coordinates.*

(c) *In these coordinates and in the target coordinates $(A, L, L^\perp)$,*

$$F(A,l,\varphi) = \big(A,\ l,\ (\varphi - \varphi_m)\, H(A,l,\varphi-\varphi_m)\big),$$

with H real-analytic and even in its last argument. With $u = l - L(q)$ and $\tau = \varphi - \varphi_m$, there is a real-analytic function $\widetilde{H}$ with $H(c, L(q)+u, \tau) = \widetilde{H}(u, \tau^2)$.

(d) *Let $D_1 = \partial_s A\, \partial_r L - \partial_r A\, \partial_s L$, which does not vanish on Ω_q. On $A^{-1}(c) \cap \Omega_q$ we have $\partial_\tau\big[\tau \widetilde{H}(u,\tau^2)\big] = rJ/D_1$, and $\Gamma_c \cap \Omega_q = \{A = c,\ \partial_\tau[\tau\widetilde{H}(u,\tau^2)] = 0\}$.*

(e) *$\widetilde{H}(0,0) = 0$ and*

$$\hat{a} := \partial_u \widetilde{H}(0,0) = \frac{r\, T_2}{J_{\mathrm{mir}}^2}(q) < 0.$$

Proof. (a) By Lemma 7.1(d), $G(q) \neq 0$. As $L^\perp = 0$ on the mirror, $L(q) \neq 0$. By Lemma 3.2, $0 = \widetilde{J}(q) = (\partial_\varphi L^\perp(q)/r)\, J_{\mathrm{mir}}(q)$. As $J_{\mathrm{mir}}(q) \neq 0$, this forces $\partial_\varphi L^\perp(q) = 0$, so $T_3(q) = L\,(\partial_\varphi L^\perp/r)\, T_2 = 0$.

(b) Since $r(q) > 0$, the coordinates (s, r, φ) are valid near q. In them the Jacobian determinant of (A, L, φ) is $\partial_s A\, \partial_r L - \partial_r A\, \partial_s L = D_1$. At q it equals $J_{\mathrm{mir}}(q)/(-K(q)) \neq 0$, by $J_{\mathrm{mir}} = \mathbf{A}_s \partial_r L - \mathbf{A}_r \partial_s L$ and $\mathbf{A} = (-K)\nabla A$. The inverse function theorem shows that (A, L, φ) are

coordinates on a neighbourhood of q. We shrink it to a box centred at q in these coordinates on which $D_1 \neq 0$. This box is σ_m-invariant.

(c) As A and L are σ_m-invariant, σ_m reads $(A, l, \varphi) \mapsto (A, l, 2\varphi_m - \varphi)$ in these coordinates. From $L^\perp \circ \sigma_m = -L^\perp$, the function $h(A, l, \varphi) = L^\perp$ is odd in $\tau = \varphi - \varphi_m$. Hence $h = \tau H$ with $H(A, l, \tau) = \int_0^1 \partial_\tau h(A, l, t\tau)\, dt$, where the box contains the segments of integration. This function is analytic and even in τ. An analytic function that is even in τ is an analytic function of τ^2, which defines $\widetilde{H}$.

(d) The determinant of $\partial(A, L, L^\perp)/\partial(A, l, \varphi)$ is $\partial_\varphi h$. By the chain rule it equals rJ/D_1: the determinants of $\partial(A, L, L^\perp)/\partial(A, P, Q)$ (a rotation), $\partial(A, P, Q)/\partial(s, x, y)$, $\partial(s, x, y)/\partial(s, r, \varphi)$ and $\partial(s, r, \varphi)/\partial(A, l, \varphi)$ are 1, J, r and $1/D_1$. The last statement follows from Lemma 7.3(a).

(e) At the points of the mirror, $\partial_\varphi A = \partial_\varphi L = 0$. Since $D_1 \neq 0$, implicit differentiation gives $\partial s/\partial\varphi = \partial r/\partial\varphi = 0$ at fixed (A, l), that is, $\partial_\varphi|_{(A,l)} = \partial_\varphi|_{(s,r)}$ there. In particular $\widetilde{H}(0, 0) = H(c, L(q), 0) = \partial_\tau h(q) = \partial_\varphi L^\perp(q) = 0$. Next, let ω denote the second argument of $\widetilde{H}$ and put $j(u, \tau) := \partial_\tau[\tau\widetilde{H}(u, \tau^2)] = \widetilde{H}(u, \tau^2) + 2\tau^2\partial_\omega\widetilde{H}(u, \tau^2)$. By (d), $j = rJ/D_1$ on the level surface. Moreover $j(u, 0) = \widetilde{H}(u, 0)$. In particular $\hat{a} = \partial_u j(0, 0)$. At fixed (A, φ) the coordinate field is $\partial_l = (-\partial_r A\, \partial_s + \partial_s A\, \partial_r)/D_1$. At q, where $J = 0$, we have $\nabla\widetilde{J}(q) = (-K)\nabla J(q)$ and $T_2(q) = K^2(\partial_s A\, \partial_r J - \partial_r A\, \partial_s J)(q)$. Then

$$\hat{a} = \frac{r}{D_1}\, \partial_l J(q) = \frac{r}{D_1^2}\, \frac{T_2}{K^2}(q) = \frac{r\, T_2}{J_{\mathrm{mir}}^2}(q),$$

using $J_{\mathrm{mir}} = (-K)D_1$. This is negative because $T_2(q) < 0$ (Lemma 7.1(f)). □

Lemma 7.8 (the cusp is of order three)**.** *In the situation of Lemma 7.7,* $\hat{b} := \partial_\omega\widetilde{H}(0, 0) \neq 0$*, and in fact* $\hat{b}\, L(q) < 0$*.*

Proof. We first expand along Γ_c. Put $\hat{j}(u, \omega) = \widetilde{H}(u, \omega) + 2\omega\, \partial_\omega\widetilde{H}(u, \omega)$. Lemma 7.7(d) shows that Γ_c is $\{\hat{j}(u, \tau^2) = 0\}$ near q. As $\partial_u\hat{j}(0, 0) = \hat{a} \neq 0$ and $\partial_\omega\hat{j}(0, 0) = 3\hat{b}$, the implicit function theorem gives an analytic function χ with $\chi(0) = 0$ and $\chi'(0) = -3\hat{b}/\hat{a}$ such that $\Gamma_c = \{u = \chi(\tau^2)\}$ near q. This is the parametrization of Γ_c by φ (Lemma 7.1(d)). Along it

$$U(\tau) := L - L(q) = \chi(\tau^2) = -\tfrac{3\hat{b}}{\hat{a}}\tau^2 + O(\tau^4), \qquad V(\tau) := L^\perp = \tau\, \widetilde{H}(\chi(\tau^2), \tau^2) = -2\hat{b}\tau^3 + O(\tau^5),$$

since $\widetilde{H}(\chi(\omega), \omega) = \hat{a}\chi(\omega) + \hat{b}\omega + O(\omega^2) = -2\hat{b}\omega + O(\omega^2)$. From $G = L\, e_m + L^\perp e_m^\perp$ we get $\Theta - \Theta_m = \arctan\big(V/(L(q) + U)\big)$ near q, where $\Theta_m = \varphi_m$ if $L(q) > 0$ and $\Theta_m = \varphi_m + 180°$ if $L(q) < 0$. The function $\Theta(\tau)$ is analytic, and

$$\Theta(\tau) - \Theta_m = -\frac{2\hat{b}}{L(q)}\tau^3 + O(\tau^5), \qquad \frac{d\Theta}{d\tau} = -\frac{6\hat{b}}{L(q)}\tau^2 + O(\tau^4). \tag{7.2}$$

Next we bound $d\Theta/d\tau$ from below. Let $\mathcal{L}$ be the finite set of leaves of type F or B of the four covers of Lemma 7.1(f). As these are closed sets, there is $\epsilon > 0$ such that each member of $\mathcal{L}$ that meets the ball $B_\epsilon(q)$ contains q. No leaf of type F contains q: $T_3(q) = 0$ by Lemma 7.7(a), whereas Lemma 7.1(f) would imply $T_3(q) < 0$. Lemma 7.1(f) and the choice of ϵ show that each point $p \in \Sigma \cap W \cap B_\epsilon(q)$ lies in a leaf of type F or B that contains q, hence in a leaf of type B. The cell C of this leaf contains p and q. Hence the mirror angle of C is $\varphi_m = \varphi(q)$. If $p = (s, r, \varphi_m + \tau)$ with $\tau \neq 0$, then $T_3(p) \leq \frac{\tau^2}{2}\beta_C\kappa_C(p)$ by (7.1). We shrink ϵ so that on $\overline{B_\epsilon(q)}$ the functions r, $P^2 + Q^2$ and the κ_C lie between positive constants and $|T_2|$ is bounded. Let $\beta < 0$ be the largest of the finitely many β_C of the leaves of type B that contain q, and $\kappa_0 > 0$ the smallest value on $\overline{B_\epsilon(q)}$ of the finitely many functions κ_C of their charts. Then $T_3(p) \leq \frac{\tau^2}{2}\beta\kappa_0$.

At the points of Σ, $T_2 < 0$, and $T_3 < 0$ off the mirror (Lemma 7.1(f)). Along Γ_c on the side of W, Lemma 3.1(c) yields

$$\frac{d\Theta}{d\tau} = \frac{r\,T_3}{(P^2+Q^2)\,T_2} \;\geq\; C_0\tau^2, \qquad C_0 = \frac{\min r\cdot|\beta|\cdot\kappa_0}{2\max(P^2+Q^2)\cdot\max|T_2|} > 0.$$

Since the reflection σ_m maps Γ_c to itself, reverses τ and maps Θ to $2\varphi_m - \Theta$, the function $\Theta(\tau) - \Theta_m$ is odd. So $d\Theta/d\tau$ is even; hence the bound holds on both sides of the mirror.

With (7.2) this yields $-6\hat{b}/L(q) + O(\tau^2) \geq C_0 > 0$ for small $\tau \neq 0$. Hence $\hat{b} \neq 0$ and $\hat{b}L(q) < 0$. □

As $\hat{a} < 0$ and $\hat{b}L(q) < 0$, the function $U = -\frac{3\hat{b}}{\hat{a}}\tau^2 + O(\tau^4)$ along Γ_c has the sign of $-L(q)$, or equivalently $|L| < |L(q)|$ on $\Gamma_c \setminus \{q\}$ near a cusp point: the cusp of C_c at $G(q)$ points away from the origin.

Lemma 7.9 (one-variable lemma)**.** *Let $\delta > 0$, $\hat{a} \neq 0$ and $\hat{b} > 0$, and let $\widetilde{H}$ be a C^2 function on $[-\delta,\delta]\times[0,\delta^2]$ with $\widetilde{H}(0,0) = 0$, $\partial_u\widetilde{H}(0,0) = \hat{a}$ and $\partial_\omega\widetilde{H}(0,0) = \hat{b}$ such that, on the whole rectangle,*

(H1) $\partial_\omega\widetilde{H} \geq \hat{b}/2$,
(H2) $3\,\partial_\omega\widetilde{H} + 2\omega\,\partial_\omega^2\widetilde{H} > 0$,
(H3) $\partial_u\widetilde{H}(u,0)$ has the sign of $\hat{a}$ for $|u| \leq \delta$.

For $|u| \leq \delta$ and $|\tau| \leq \delta$ put $f_u(\tau) = \tau\widetilde{H}(u,\tau^2)$. There is $\varepsilon \in (0,\delta]$ such that for every u with $|u| \leq \varepsilon$ the following hold.

(a) *$f_u(\delta) = -f_u(-\delta) \geq \hat{b}\delta^3/4$ and $f_u'(\pm\delta) > 0$.*
(b) *If $\hat{a}u \geq 0$, then f_u is strictly increasing on $[-\delta,\delta]$ and $f_u' > 0$ except at $\tau = 0$ when $u = 0$.*
(c) *If $\hat{a}u < 0$, there is $\tau_+(u) \in (0,\delta)$ with $f_u' > 0$ on $[-\delta,-\tau_+)\cup(\tau_+,\delta]$, $f_u' < 0$ on $(-\tau_+,\tau_+)$ and $f_u'(\pm\tau_+) = 0$, and $M(u) := f_u(-\tau_+(u)) = -f_u(\tau_+(u)) > 0$.*
(d) *For $|V| < \hat{b}\delta^3/4$, the number of $\tau \in (-\delta,\delta)$ with $f_u(\tau) = V$ is 3 if $\hat{a}u < 0$ and $|V| < M(u)$, 2 if $\hat{a}u < 0$ and $|V| = M(u)$, and 1 otherwise. When it is 3, exactly one solution has $|\tau| < \tau_+(u)$.*
(e) *The functions τ_+ and M are continuous on $\{0 < |u| \leq \varepsilon,\ \hat{a}u < 0\}$, and $\tau_+(u) \to 0$ and $M(u) \to 0$ as $u \to 0$.*

Proof. The derivative $f_u'(\tau) = \widetilde{H}(u,\tau^2) + 2\tau^2\partial_\omega\widetilde{H}(u,\tau^2)$ is even. The second derivative $f_u''(\tau) = 2\tau\big(3\partial_\omega\widetilde{H} + 2\tau^2\partial_\omega^2\widetilde{H}\big)(u,\tau^2)$ has the sign of τ by (H2). Thus f_u' decreases strictly on $[-\delta,0]$ and increases strictly on $[0,\delta]$. The minimum of f_u', $f_u'(0) = \widetilde{H}(u,0) = \int_0^u \partial_u\widetilde{H}(t,0)\,dt$, has the sign of $\hat{a}u$ by (H3) and vanishes for $u = 0$. By (H1), $\widetilde{H}(0,\omega) \geq \hat{b}\omega/2$. Then $f_0(\delta) \geq \hat{b}\delta^3/2$ and $f_0'(\delta) \geq \hat{b}\delta^2/2 + 2\delta^2\cdot\hat{b}/2 = 3\hat{b}\delta^2/2$. Continuity then yields ε with (a). Then (b) and (c) follow from the monotonicity of f_u' and from (a). Moreover $M(u) > 0$ because f_u is odd and decreases strictly on $[-\tau_+,\tau_+]$. For (d), in case (c) the function f_u maps $[-\delta,-\tau_+]$ increasingly onto $[f_u(-\delta),M]$, $[-\tau_+,\tau_+]$ decreasingly onto $[-M,M]$ and $[\tau_+,\delta]$ increasingly onto $[-M,f_u(\delta)]$, while $|V| < \hat{b}\delta^3/4 \leq f_u(\delta)$. In case (b) it maps $[-\delta,\delta]$ increasingly onto $[f_u(-\delta),f_u(\delta)]$. For (e), $\tau_+(u)$ is a simple zero of f_u', since $f_u''(\tau_+) \neq 0$, hence continuous by the implicit function theorem. Given $\eta \in (0,\delta)$, $f_0' \geq f_0'(\eta) > 0$ on $[\eta,\delta]$. It follows by continuity that $\tau_+(u) < \eta$ for $|u|$ small. Finally $M(u) = \tau_+(u)\,|\widetilde{H}(u,\tau_+(u)^2)| \to 0$. □

Proposition 7.10. *If q is a cusp point, then $c_4(F(q)) = 2$.*

Proof. By equivariance we may assume $q \in W$. Let c, φ_m, $\hat{a}$, $\hat{b}$, $\widetilde{H}$, u and τ be as in Lemmas 7.7 and 7.8. These lemmas show that $\hat{a} \neq 0$ and $\hat{b} \neq 0$. Replacing the target coordinate $L^\perp$ by $-L^\perp$ if

necessary, which changes $\widetilde{H}$ into $-\widetilde{H}$ and $(\hat{a},\hat{b})$ into $(-\hat{a},-\hat{b})$, we may assume $\hat{b}>0$. Continuity yields $\delta>0$ such that (H1)–(H3) hold, the rectangle lies in the chart of Lemma 7.7, and the corresponding closed set avoids the other points of $F^{-1}(F(q))$. Let ε be given by Lemma 7.9, and put $\mathcal{N}=\{|u|<\varepsilon,\ |\tau|<\delta\}\subset A^{-1}(c)$ and $\mathcal{N}_0=\{|A-c|<\eta,\ (u,\tau)\in\mathcal{N}\}$ for a small $\eta>0$.

In the target coordinates $(U,V)=(L-L(q),L^{\perp})$, the preimages in $\mathcal{N}$ of a point (U,V) with $|U|<\varepsilon$ are the points (U,τ) with $f_U(\tau)=V$. Let $Y_0=\{|U|<\varepsilon,\ |V|<\hat{b}\delta^3/4\}$ and

$$E_3=\{(U,V):\ |U|<\varepsilon,\ \hat{a}U<0,\ |V|<M(U)\}.$$

Lemma 7.9(d) shows that a point of Y_0 has three preimages in $\mathcal{N}$ if it lies in E_3, and one if it lies neither in E_3 nor on the set $\mathcal{C}=\{(U,\pm M(U)):\hat{a}U<0\}\cup\{(0,0)\}$. Lemma 7.7(d) shows that the critical set of g_c in $\mathcal{N}$ is $\Gamma_c\cap\mathcal{N}=\{(u,\pm\tau_+(u)):\hat{a}u<0\}\cup\{(0,0)\}$; $\mathcal{C}$ is its image.

We show that the middle sheet lies in $\overline{\mathcal{D}}$. Let $\mathcal{N}_{mid}=\{(u,\tau)\in\mathcal{N}:\ \hat{a}u<0,\ |\tau|<\tau_+(u)\}$. By Lemma 7.9, $\partial_\tau(\tau\widetilde{H})<0$ exactly on $\mathcal{N}_{mid}$ and $\partial_\tau(\tau\widetilde{H})>0$ on $\mathcal{N}\setminus\overline{\mathcal{N}_{mid}}$. As $J=D_1\,\partial_\tau(\tau\widetilde{H})/r$ with D_1/r of constant sign, J has one strict sign on $\mathcal{N}_{mid}$ and the opposite one on $\mathcal{N}\setminus\overline{\mathcal{N}_{mid}}$. Suppose that $J<0$ on $\mathcal{N}\setminus\overline{\mathcal{N}_{mid}}$. A point $(U,0)$ with $0<|U|<\varepsilon$ and $\hat{a}U<0$ lies in E_3. Two of its three preimages, those with $|\tau|>\tau_+(U)$, lie in $\mathcal{N}\setminus\overline{\mathcal{N}_{mid}}$. They are two distinct points of $\overline{\mathcal{D}}$ with the same image under F, which contradicts Lemma 7.1(b). Hence $J<0$ on $\mathcal{N}_{mid}$, so the points of $\mathcal{N}_{mid}$ lie in Φ_c°. Lemmas 7.9(c) and 7.1(d) then give $E_3=g_c(\mathcal{N}_{mid})\subset V_{in}(c)$.

Since G is injective on Γ_c (Lemma 7.1(d)), the compact set $G(\Gamma_c\setminus\mathcal{N})$ does not contain $G(q)$. Let $Y\subset Y_0$ be an open box around $G(q)$ that avoids it. Then $C_c\cap Y=\mathcal{C}\cap Y$. A point $w\in Y\cap V_{out}(c)$ lies neither on C_c nor in $V_{in}(c)\supset E_3$, so by the count above it has exactly one preimage in $\mathcal{N}$. Points $w\in Y\cap V_{out}(c)$ exist arbitrarily close to $G(q)$. For them $(c,w)\notin F(\overline{\mathcal{D}})$ by Lemma 7.3(c). Lemma 7.4(c) with $k=1$ now shows that $c_4(F(q))=2$. □

The proof shows that near a cusp point the map F is a Whitney cusp [Whi55]. The points of E_3, inside C_c, have three preimages near q, one of them with $J<0$. The points of $V_{out}(c)$ near $G(q)$ have one, at which $J>0$. The local degree is $+1$.

7.4. **The umbilic.**

Proposition 7.11. $c_4(F(p^*))=1$. *That is, for the masses* $(1,1,1,m^*)$ *the only concave CC with body* 4 *inside, up to similarity, is the equilateral triangle with body* 4 *at its centre.*

Proof. We put $c^*=c(s^*)$. Recall that $c^*\neq 0$ by Proposition 2.6.

We first restrict G to the level of p^*. Since $\partial_s A(p^*)<0$, near p^* the level set $A^{-1}(A^*)$ is the graph $s=s_A(z)$ of an analytic function s_A. Like A, the function s_A is $\mathfrak{S}_3$-invariant. The differential of s_A at 0, an invariant linear form on the irreducible representation on (x,y), vanishes. Hence $|s_A(z)-s^*|\le C_s|z|^2$ for small $|z|$. For $g_*(z)=G(s_A(z),z)$, Lemma 2.5 and $\lambda(s^*)=0$ imply

$$g_*(z)=c^*\bar{z}^{\,2}+E_*(z),\qquad |E_*(z)|\le C_*|z|^3\qquad (|z|\le\delta_*).$$

Here we use $|\lambda(s_A(z))z|\le\sup|\lambda'|\,C_s|z|^3$ and $|c(s_A(z))-c^*|\,|z|^2\le\sup|c'|\,C_s|z|^4$.

We also need a bound on the derivative of E_*. For real-linear and real-multilinear maps on $\mathbb{C}$, $|\cdot|$ denotes the operator norm. The map g_* is real-analytic, as G and s_A are. Shrinking δ_* if necessary, we may assume that g_* is real-analytic on a neighbourhood of the closed disk $|z|\le\delta_*$. The Taylor polynomial of order 2 of E_* at 0 is the only polynomial of degree at most 2 that agrees with E_* up to $o(|z|^2)$. As $E_*(z)=O(|z|^3)$, the zero polynomial has this property. It follows that E_* and its first and second derivatives vanish at 0. Since $c^*\bar{z}^2$ is quadratic in (x,y), we have $D^3E_*=D^3g_*$. Taylor's formula with integral remainder, applied to DE_*, now gives

$$|DE_*(z)|\le C'_*|z|^2\qquad (|z|\le\delta_*),$$

where C'_* is half the maximum of $|D^3 g_*|$ on the disk $|z| \le \delta_*$.

In the coordinates (A, x, y) near p^* (Lemma 7.2), F reads $(A, x, y) \mapsto (A, \widetilde{G}(A, x, y))$ with $\widetilde{G}(A^*, \cdot) = g_*$. We fix $\rho_0 \in (0, \delta_*]$ with $16C_*\rho_0 \le |c^*|$ and $3C'_*\rho_0 \le |c^*|$, and we fix $\eta > 0$. We take both so small that the coordinates are defined on the closed box $\{|A - A^*| \le \eta,\ |z| \le \rho_0\}$ and that this box contains none of the points p_j of Lemma 7.4(a). Let $\mathcal{N}_0$ be the open box $\{|A - A^*| < \eta,\ |z| < \rho_0\}$. The preimages in $\mathcal{N}_0$ of a point $\mu' = (A^*, w)$ are the points (A^*, z) with $|z| < \rho_0$ and $g_*(z) = w$. We show that there are exactly two of them if $0 < |w| < |c^*|\rho_0^2/4$.

Let $0 < |w| < |c^*|\rho_0^2/4$, let ζ_+ be a square root of w/c^*, and put $\zeta_- = -\zeta_+$, $z_\pm = \zeta_\pm$, $t = |\zeta_+|$. Then $|w| = |c^*|t^2$ and $0 < t < \rho_0/2$. Since $c^*\bar z^2 - w = c^*(\bar z - \zeta_+)(\bar z - \zeta_-)$ and $|\bar z - \zeta_\pm| = |z - z_\pm|$, the roots of $c^*\bar z^2 = w$ are z_+ and z_-, and

$$|c^*\bar z^{\,2} - w| = |c^*|\,|z - z_+|\,|z - z_-|.$$

Let $B_\pm$ be the closed disk of radius $t/2$ about $z_\pm$. The two disks are disjoint, as $|z_+ - z_-| = 2t$. They lie in the disk $|z| \le 3t/2$, and hence in $\{|z| < \rho_0\}$.

We first show that each disk $B_\pm$ contains exactly one solution of $g_*(z) = w$. For $z \in B_\pm$ we put $u(z) = E_*(z)/w$. As $|z| \le 3t/2$, $2t < \rho_0$ and $16C_*\rho_0 \le |c^*|$,

$$|u(z)| \le \frac{27C_*t^3}{8|c^*|t^2} \le \frac{27C_*\rho_0}{16|c^*|} \le \frac{27}{256} < \frac{1}{8}.$$

For $\operatorname{Re} v > 0$ the principal square root $\sqrt{v}$ satisfies $\operatorname{Re}\sqrt{v} > 0$ and $(\operatorname{Re}\sqrt{v})^2 - (\operatorname{Im}\sqrt{v})^2 = \operatorname{Re} v$. Hence $\operatorname{Re}\sqrt{v} \ge (\operatorname{Re} v)^{1/2}$ for $\operatorname{Re} v > 0$; in particular $\operatorname{Re}\sqrt{1-u} > 1/2$ for $|u| < 1/8$. For $|u|, |u'| < 1/8$ the denominators in

$$\sqrt{1-u} - 1 = \frac{-u}{\sqrt{1-u}+1}, \qquad \sqrt{1-u} - \sqrt{1-u'} = \frac{u'-u}{\sqrt{1-u}+\sqrt{1-u'}}$$

have real parts greater than 1. Therefore all u, u' with $|u|, |u'| < 1/8$ satisfy $|\sqrt{1-u} - 1| \le |u|$, $|\sqrt{1-u} - \sqrt{1-u'}| \le |u - u'|$ and $|\sqrt{1-u} + 1| > 1$.

A point $z \in B_\pm$ solves $g_*(z) = w$ if and only if $\bar z^2 = (w - E_*(z))/c^* = \zeta_\pm^2(1 - u(z))$, that is, if and only if $\bar z = \zeta_\pm\sqrt{1-u(z)}$ or $\bar z = -\zeta_\pm\sqrt{1-u(z)}$. The second case does not occur in $B_\pm$, since it gives $|z - z_\pm| = |\bar z - \zeta_\pm| = t\,|\sqrt{1-u(z)} + 1| > t$. The solutions in $B_\pm$ are thus the fixed points of the map

$$f_\pm : B_\pm \to \mathbb{C}, \qquad f_\pm(z) = \overline{\zeta_\pm\sqrt{1-u(z)}}.$$

The map $f_\pm$ sends $B_\pm$ into itself, because $|f_\pm(z) - z_\pm| = t\,|\sqrt{1-u(z)} - 1| \le t\,|u(z)| < t/8$ for $z \in B_\pm$. It is also a contraction. Let $z_1, z_2 \in B_\pm$. Since the segment from z_1 to z_2 lies in $B_\pm$, where $|DE_*| \le \frac{9}{4}C'_*t^2$, we have $|E_*(z_1) - E_*(z_2)| \le \frac{9}{4}C'_*t^2\,|z_1 - z_2|$. As $|w| = |c^*|t^2$, $2t < \rho_0$ and $3C'_*\rho_0 \le |c^*|$, it follows that

$$|f_\pm(z_1) - f_\pm(z_2)| \le t\,|u(z_1) - u(z_2)| \le \frac{9C'_*t}{4|c^*|}\,|z_1 - z_2| \le \frac{3}{8}\,|z_1 - z_2|.$$

Banach's fixed point theorem yields exactly one fixed point of $f_\pm$ in the closed disk $B_\pm$.

Next we show that there is no other solution with $|z| < \rho_0$. Let $|z| < \rho_0$ and $z \notin B_+ \cup B_-$. If $|z| \ge 2t$, then $|w| = |c^*|t^2 \le |c^*|\,|z|^2/4$, and

$$|c^*\bar z^{\,2} - w| \ge \tfrac{3}{4}|c^*|\,|z|^2 > \tfrac{1}{16}|c^*|\,|z|^2 \ge C_*\rho_0|z|^2 \ge C_*|z|^3 \ge |E_*(z)|.$$

If $|z| < 2t$, then $|z - z_\pm| > t/2$ for both signs, and

$$|c^*\bar z^{\,2} - w| = |c^*|\,|z - z_+|\,|z - z_-| > \tfrac{1}{4}|c^*|t^2 \ge 4C_*\rho_0t^2 \ge 8C_*t^3 \ge C_*|z|^3 \ge |E_*(z)|.$$

In both cases $g_*(z) - w = (c^*\bar z^2 - w) + E_*(z) \ne 0$. We conclude that for $0 < |w| < |c^*|\rho_0^2/4$ the equation $g_*(z) = w$ has exactly two solutions with $|z| < \rho_0$, one in B_+ and one in B_-.

Let $\mathcal{V}$ be the neighbourhood of $F(p^*)$ given by Lemma 7.4(b). For $w \neq 0$ small enough, the point $\mu' = (A^*, w)$ lies in $\mathcal{V}$ and has exactly two preimages in $\mathcal{N}_0$. Moreover $\mu' \notin F(\overline{\mathcal{D}})$ by Lemma 7.3(b),(c). Lemma 7.4(c), applied with $q = p^*$ and $k = 2$, shows that $c_4(F(p^*)) = 1$. By Proposition 2.4, $F(p^*) = \mu^{(4)}(1, 1, 1, m^*)$, and p^* is the equilateral configuration with body 4 at its centre. □

The local degree of F at p^* is $+2$. All values inside C_c for c near A^* have four preimages near p^*, which is the coalescence of four solutions into one observed in [RS16].

7.5. **Classification of the fold and location of the cusps.**

Lemma 7.12. *The map $\Sigma_L \to (A^*, \infty) \times S^1$, $q \mapsto (A(q), \Theta(G(q)))$, is a homeomorphism, and so is the map $\Sigma_U \to (-\infty, A^*) \times S^1$ defined in the same way. We write ι_L and ι_U for their inverses, and $\iota(A, \Theta)$ for $\iota_L(A, \Theta)$ or $\iota_U(A, \Theta)$ according as $A > A^*$ or $A < A^*$.*

Proof. The map is a bijection: Σ_L is the disjoint union of the circles Γ_c, $c > A^*$ (Lemma 7.1(c)), and $\Theta \circ G$ maps each Γ_c bijectively onto S^1 (Lemma 7.1(d)). Since $G \neq 0$ on Σ_L (Lemma 7.1(d)), the map is continuous. It is also proper: the preimage of $[\alpha, \beta] \times S^1$ is $\Sigma \cap \overline{\mathcal{D}}_L \cap A^{-1}[\alpha, \beta]$, a closed subset of a compact set (Lemma 7.1(c)). A proper continuous map into a locally compact Hausdorff space is closed. A closed continuous bijection is a homeomorphism. The same holds for Σ_U. □

Proposition 7.13. (a) *Every point $q \in \Sigma \setminus \{p^*\}$ is either a fold point or a cusp point, and not both. Points off the mirrors are fold points. At a mirror point exactly one of $J_{\mathrm{mir}}(q)$ and $\partial_\varphi L^\perp(q)$ vanishes. A mirror point $q \in W$ is a cusp point if and only if it lies in a leaf of type B, if and only if $\partial_\varphi L^\perp(q) = 0$. It is a fold point if and only if it lies in a leaf of type F, if and only if $J_{\mathrm{mir}}(q) = 0$.*

(b) *For each nappe and each of the six half-mirrors, the mirror points of that nappe on that half-mirror form a connected set, and they are either all fold points or all cusp points.*

(c) *The cusp points are the mirror points of Σ_L on the half-mirrors $\varphi \in \{90°, 210°, 330°\}$ and the mirror points of Σ_U on the half-mirrors $\varphi \in \{30°, 150°, 270°\}$. At all mirror points of Σ_L, $\Theta = \varphi$, and at all mirror points of Σ_U, $\Theta = \varphi + 180°$. In particular, for every $c \neq A^*$, Γ_c has exactly three cusp points, those where $\Theta \circ G \in \{90°, 210°, 330°\}$, and C_c has a cusp at each of their images, pointing away from the origin. All other points of Γ_c, including the other three mirror points, are fold points.*

Proof. (a) Let $q \in W$, which lies in a leaf of type F or B by Lemma 7.1(f). If q is not on a mirror, then $T_3(q) < 0$ in both cases: q is a fold point and not a cusp point. If q is a mirror point, then $0 = \widetilde{J}(q) = (\partial_\varphi L^\perp(q)/r)\, J_{\mathrm{mir}}(q)$ by Lemma 3.2. If $J_{\mathrm{mir}}(q) \neq 0$, then q is a cusp point, $\partial_\varphi L^\perp(q) = 0$ and $T_3(q) = 0$ (Lemma 7.7(a)). It is not a fold point. It lies in no leaf of type F, hence in a leaf of type B. If $J_{\mathrm{mir}}(q) = 0$, then q lies in no leaf of type B, since the band certificate ensures $J_{\mathrm{mir}} \neq 0$ on the mirror face of the cell. The leaf of q is then of type F, where $T_3(q) < 0$ by Table 4. Then $T_3 = L\,(\partial_\varphi L^\perp / r)\, T_2$ implies $\partial_\varphi L^\perp(q) \neq 0$, so q is a fold point and not a cusp point. Part (a) holds on Ω_4 by invariance.

(b) By Lemma 7.1(d), each circle Γ_c meets each half-mirror $\varphi = \varphi_0$ in exactly one point, at which $\Theta = \varphi_0$ if $c > A^*$ and $\Theta = \varphi_0 + 180°$ if $c < A^*$. For the half-mirrors of W this is Lemma 7.1(d). For the others it follows by equivariance: the rotation by 120° adds 120° to both φ and Θ, and the reflection in the line $\varphi = 90°$ maps both to 180° minus themselves. This point is $\iota_L(c, \varphi_0)$, respectively $\iota_U(c, \varphi_0 + 180°)$, by the definition of ι. The mirror points of Σ_L on the half-mirror form the connected set $\{\iota_L(c, \varphi_0) : c > A^*\}$, those of Σ_U the connected set $\{\iota_U(c, \varphi_0 + 180°) : c < A^*\}$ (Lemma 7.12). On such a set the subsets where $J_{\mathrm{mir}} \neq 0$ and where

$\partial_\varphi L^\perp \neq 0$ are relatively open, disjoint and, by (a), they cover it. As the set is connected, one of them is empty.

(c) The formulas for Θ follow from Lemma 7.1(d) and the equivariance just described. Proposition 5.2(h) shows that no leaf of type B contains a point of Σ_L on the half-mirror $\varphi = 30°$ or a point of Σ_U on $\varphi = 90°$: by (a) these points are fold points. The cell of the leaf of type B of the umbilic cover with mirror angle 90° contains, for each $\varrho \in (0, \varrho_{\mathrm{u}}]$, a zero of $\widetilde{J}$ on its mirror face, by the band certificate and Proposition 5.2(h). This zero is physical by Proposition 5.2(c) and lies in Σ. As the cell has $\psi > \pi/2$, the zero has $s < s^*$ and lies in Σ_L. By the band certificate, $J_{\mathrm{mir}} \neq 0$ at this zero. The mirror points of Σ_L on $\varphi = 90°$ thus include a cusp point, so by (b) they are all cusp points. In the same way the cell with mirror angle 30°, which has $\psi < \pi/2$, shows that the mirror points of Σ_U on $\varphi = 30°$ are cusp points. Equivariance carries these four statements to the six half-mirrors. On Σ_L the cusp half-mirrors are $\varphi \in \{90°, 210°, 330°\}$, where $\Theta = \varphi$. On Σ_U they are $\varphi \in \{30°, 150°, 270°\}$, where $\Theta = \varphi + 180° \in \{210°, 330°, 90°\}$. By Lemma 7.8, C_c has a cusp at the image of a cusp point: along Γ_c, $\Theta - \Theta_m$ vanishes to the third order while U has the exact order τ^2. By the remark after Lemma 7.8, this cusp of C_c points away from the origin. □

The location agrees with the leading-order model $G \approx \lambda_{\mathrm{ax}}(s)z + i\gamma(s^*)\bar{z}^2$ of Lemma 2.5. In this model $\gamma(s^*) < 0$ (Proposition 2.6). On the circle $|z| = |\lambda_{\mathrm{ax}}(s)|/(2|\gamma(s^*)|)$, where this model is singular, its image is a deltoid. The cusps of the deltoid are the images of the points of this circle with $\varphi \in \{90°, 210°, 330°\}$ when $\lambda_{\mathrm{ax}} > 0$, that is, for $s < s^*$, and with $\varphi \in \{30°, 150°, 270°\}$ when $\lambda_{\mathrm{ax}} < 0$. Proposition 12.1 shows that the curves C_c, scaled by $(c - A^*)^{-2}$, converge to such a deltoid as $c \to A^*$.

8. The surface of critical values and the proofs of the theorems

In this section we define the function R of Theorem 1, show that certified points of the fold determine it, and prove Theorems 1 and 2. We keep the notation of Section 7.

8.1. **The radius function.**

Lemma 8.1. (a) *If $q_n \in \Sigma \setminus \{p^*\}$ and $A(q_n) \to A^*$, then $q_n \to p^*$.*

(b) *Put $R(A, \Theta) = |G(\iota(A, \Theta))|$ for $A \neq A^*$ and $R(A^*, \Theta) = 0$, with ι as in Lemma 7.12. Then R is continuous on $\mathbb{R} \times S^1$, positive for $A \neq A^*$, and invariant under D_3 in Θ. For $A \neq A^*$,*

$$C_A = \{R(A, \Theta)e^{i\Theta}\}, \qquad V_{in}(A) = \{\rho e^{i\Theta} : \rho < R(A, \Theta)\}, \qquad V_{out}(A) = \{\rho e^{i\Theta} : \rho > R(A, \Theta)\},$$

and every point of C_A is a boundary point of both $V_{in}(A)$ and $V_{out}(A)$.

(c) *The sets $\Sigma_L \cup \{p^*\}$ and $\Sigma_U \cup \{p^*\}$ are homeomorphic to the open cone over a circle, with vertex p^*. Hence Σ is homeomorphic to a double cone with vertex p^*.*

Proof. (a) This is Lemma 6.12(c), since $\Sigma \subset \overline{\mathcal{D}}$.

(b) Let $A \neq A^*$. By the definitions of ι and of R_A (Proposition 6.16), $R(A, \Theta) = R_A(\Theta)$. So $R(A, \cdot)$ is positive, and $C_A = C(R_A)$, $V_{in}(A) = \mathrm{In}(R_A)$ and $V_{out}(A) = \mathrm{Out}(R_A)$ are the three sets of the statement. Each point of C_A is a boundary point of both $V_{in}(A)$ and $V_{out}(A)$ by Lemma 6.4(d). Continuity off $A = A^*$ follows from Lemma 7.12. If $(A_n, \Theta_n) \to (A^*, \Theta_0)$ with $A_n \neq A^*$, then $q_n = \iota(A_n, \Theta_n)$ satisfies $A(q_n) \to A^*$. Part (a) gives $q_n \to p^*$, so $R(A_n, \Theta_n) = |G(q_n)| \to |G(p^*)| = 0$. For the invariance, let $g \in \mathfrak{S}_3$. Then $F \circ g = \hat{g} \circ F$ with $\hat{g}(A, G) = (A, O_g G)$, and g preserves Σ_L, Σ_U and A. Therefore $O_g C_A = C_A$. As O_g preserves lengths and acts on angles through D_3, $R(A, \cdot)$ is D_3-invariant.

(c) By Lemma 7.12, the map $q \mapsto (A(q), \Theta(G(q)))$, extended by sending p^* to the vertex, is a bijection of $\Sigma_L \cup \{p^*\}$ onto the cone $([A^*, \infty) \times S^1)/(\{A^*\} \times S^1)$. It is continuous at p^* because A is continuous; its inverse is continuous at the vertex by (a). Elsewhere we use Lemma 7.12. The

same holds for $\Sigma_U \cup \{p^*\}$. These two sets are the closed subsets $\Sigma \cap \{s \le s^*\}$ and $\Sigma \cap \{s \ge s^*\}$ of Σ (recall $\Sigma \subset \overline{\mathcal{D}}$). Since they meet only at p^*, their union Σ is a double cone. □

Near p^* the double cone is also the smooth picture. By Proposition 2.6, $J(p^*) = 0$, $\nabla J(p^*) = 0$ and $\operatorname{Hess} J(p^*)$ has signature $(-,+,+)$. By the Morse lemma, Σ is then a quadratic cone at p^* up to a diffeomorphism. In particular Σ is not a 2-manifold at p^*.

8.2. **Certified points of the fold.**

Lemma 8.2 (certified points of the fold determine R)**.** *Let $c \neq A^*$ and $\Theta_0 \in S^1$. If $q \in \Omega_4$ satisfies $J(q) = 0$, $A(q) = c$ and $G(q) \in (0,\infty) \cdot e^{i\Theta_0}$, then $q = \iota(c,\Theta_0)$ and $R(c,\Theta_0) = |G(q)|$. Consequently, let X be a box on which physicality is certified, and let S be a set of parameters (c,Θ_0) with $c \neq A^*$. If for each $(c,\Theta_0) \in S$ the box X contains a point q with $\widetilde{J}(q) = 0$, $A(q) = c$ and $G(q) \in (0,\infty)\cdot e^{i\Theta_0}$, then $R(c,\Theta_0) \in |G|(X)$ for all $(c,\Theta_0) \in S$. Such a point is, for instance, a zero of $(\widetilde{J},\ A-c,\ \Theta\circ G - \Theta_0)$ or, at a mirror angle Θ_0, a zero of $(\widetilde{J},\ A-c)$ on the mirror plane at which L has the sign that selects the ray.*

Proof. We have $q \in \Sigma \cap A^{-1}(c) = \Gamma_c$ by Lemma 7.3(a), and $\Theta(G(q)) = \Theta_0$. The injectivity in Lemma 7.12 implies $q = \iota(c,\Theta_0)$, so $R(c,\Theta_0) = |G(q)|$ by definition. On a box where physicality is certified, $K < 0$ and $\widetilde{J} = (-K)J$ vanishes exactly where J does (Lemma 3.1(a)). □

In other words, an interval enclosure of a physical zero of either system is an enclosure of the point $\iota(c,\Theta_0)$ itself, so no search for other zeros is needed.

Remark 8.3 (effectivity). Off the surface of critical values, $c_i(m)$ is decided by the sign of $\rho - R(A,\Theta)$ (Theorem 1), and by Lemma 8.2 an enclosure of $R(A,\Theta)$ can be obtained from an interval Newton or Krawczyk enclosure of one physical zero. Two systems are needed.

- For Θ off the six mirror rays, the point $q = \iota(A,\Theta)$ is not a mirror point, hence a fold point. The system $(\widetilde{J},\ A-c,\ \Theta\circ G - \Theta)$ in (s,x,y) has Jacobian determinant $\det[\nabla\widetilde{J};\nabla A;\nabla\Theta] = -T_3/((P^2+Q^2)(-K)) \neq 0$ at q.
- For Θ on a mirror ray, q is a mirror point. On the cusp rays $\Theta \in \{90°, 210°, 330°\}$ we have $T_3(q) = 0$, and the first system degenerates. On every mirror ray we use instead the system $(\widetilde{J},\ A-c)$ on the mirror plane, where G lies on the mirror line. In the coordinates (s,r) of the plane its Jacobian determinant is $\partial_s\widetilde{J}\,\partial_r A - \partial_r\widetilde{J}\,\partial_s A = -T_2/(-K) \neq 0$ at q. The sign of $L(q)$ decides which of the two opposite mirror rays is reached.

Near a regular zero the Krawczyk test succeeds on small boxes centred near it, at sufficient precision: with centred forms, the enclosures over a box converge as the box shrinks and the precision grows, so that the Krawczyk operator maps the box into its interior (see [Neu90, §2.3 and Ch. 5]). These enclosures rest on the Krawczyk step for the implicit angles, which succeeds on small boxes since $\Lambda > 0$ at physical points (Section 5.1), and on jets of K and μ up to order two, which $\nabla\widetilde{J}$ involves. As $|G(\iota(A,\Theta))| = R(A,\Theta) > 0$, the angle $\Theta\circ G$ is defined near $\iota(A,\Theta)$. Since $\rho \neq R(A,\Theta)$ off the critical surfaces, four enclosures of values of R at sufficient precision decide $N(m)$ for any m outside $Z_1 \cup \cdots \cup Z_4$ whose masses are given exactly (for instance as rational or algebraic numbers). If $\rho = 0$ no solve is needed: then $\rho < R(A,\Theta)$ exactly when $A \neq A^*$. If $\rho > 0$ and $A = A^*$ (an algebraic condition on m, which rational masses never satisfy, since m^{*3} is irrational), then $\rho > R(A,\Theta) = 0$. If $\rho > 0$ and $A \neq A^*$, a starting box comes from a floating-point solve (Section 9.1) or, in principle, from an enumeration. Going through all pairs of a box with rational corners and a precision, one reaches a box on which the Krawczyk test succeeds and on which physicality and, for Θ on a mirror ray, the sign of L that selects the ray are certified, since all of this holds, at sufficient precision, on small boxes centred near the regular zero $\iota(A,\Theta)$. By Lemma 8.2 every such box encloses $\iota(A,\Theta)$.

8.3. **Proof of Theorem 1.** Let R be the function of Lemma 8.1. It has the properties stated in Theorem 1 by Lemma 8.1(b). Consider first $i = 4$, and let (A, ρ, Θ) be the coordinates of $\mu = \mu^{(4)}(m)$.

- If $\rho < R(A, \Theta)$, then $A \neq A^*$ and $\mu \in \{A\} \times V_{in}(A) \subset F(\overline{\mathcal{D}})$. Recall that F is injective on $\overline{\mathcal{D}}$ and that G maps Φ_A° onto $V_{in}(A)$ (Lemma 7.1(b),(d)). Hence μ has exactly one preimage in $\overline{\mathcal{D}}$, a point of Φ_A°, where $J < 0$. The other preimages have $J > 0$. Thus μ is a regular value with $n_- = 1$ and, by Lemma 7.1(a), $n_+ = 3$, so $c_4 = 4$.
- If $\rho > R(A, \Theta)$ (this includes the case $A = A^*$, $\rho > 0$), then $c_4 = 2$ by Lemmas 8.1(b) and 7.3(c).
- If $\rho = R(A, \Theta)$ and $A \neq A^*$, then $\mu = F(q)$ with $q = \iota(A, \Theta) \in \Gamma_A \subset \Sigma \setminus \{p^*\}$. By Proposition 7.13, q is a cusp point if $\Theta \in \{90°, 210°, 330°\}$ and a fold point otherwise. Then $c_4 = 2$ and $c_4 = 3$, respectively, by Propositions 7.10 and 7.6.
- If $A = A^*$ and $\rho = 0$, then $\mu = F(p^*)$ and $c_4 = 1$ by Proposition 7.11.

The points with $\rho = R(A, \Theta)$ form $F(\Sigma)$, the set of critical values. For another body i, the map F_i is F_4 after the labels i and 4 are exchanged. Then $c_i(m) = c_4(m')$, where m' is m with m_i and m_4 exchanged. Also $\mu^{(4)}(m') = \mu^{(i)}(m)$ for the order of the outer bodies induced by the exchange. Another order replaces (A, G) by $(A, O_g G)$ for some $g \in \mathfrak{S}_3$. This leaves A and ρ unchanged and acts on Θ through D_3, which preserves R (Lemma 8.1(b)) and the set $\{90°, 210°, 330°\}$. This proves Theorem 1. □

8.4. **Proof of Theorem 2.** Section 1.1 and [HM06, §2.2] show that a non-collinear CC is convex or concave with exactly one body inside the triangle of the other three. We count each type in classes up to rotation, translation and scaling. Mirror images are counted separately.

- Collinear: exactly $4!/2 = 12$ [Mou10].
- Convex: for each of the 3 cyclic orders, up to reversal, exactly one class up to similarity, by [MB32, Xia04] for existence and [Tom26] for uniqueness. In total $3 \cdot 2 = 6$.
- Concave with body i inside: $2c_i$.

Adding, $N = 12 + 6 + 2(c_1 + c_2 + c_3 + c_4)$. Since the map $m \mapsto \mu^{(i)}(m)$ is a linear surjection onto $\mathbb{R}^3$ in the coordinates $\log m_1, \dots, \log m_4$, each set Z_i, the preimage of the set of critical values of F_i, is closed and null by Proposition 6.1.

For the examples of item (d) we use the following lemma, which locates critical values on segments of masses.

Lemma 8.4 (crossing lemma)**.** *Let $m : [0, 1] \to (0, \infty)^4$ be continuous, and let X be a nonempty set of bodies whose mass coordinates $(A(t), \rho(t), \Theta(t))$ at $m(t)$ are the same for all $i \in X$ and all t, for suitable orders of their outer bodies. This holds, for instance, if $|X| = 1$, or if the bodies of X have the same mass and the same multiset of outer masses. Suppose that the following hold.*

1. *$\rho(t) > 0$, $A(t) \neq A^*$ and $\Theta(t) \notin \{90°, 210°, 330°\}$ for all $t \in [0, 1]$.*
2. *$\rho(0) < R(A(0), \Theta(0))$ and $\rho(1) > R(A(1), \Theta(1))$, or the reverse.*
3. *For every body $j \notin X$, $c_j(m(t))$ does not depend on t. This holds if $\rho^{(j)} - R(A^{(j)}, \Theta^{(j)})$ has a constant strict sign on $[0, 1]$, where $(A^{(j)}, \rho^{(j)}, \Theta^{(j)})$ are the mass coordinates of body j, or if $\rho^{(j)} \equiv 0$ and $A^{(j)}(t) \neq A^*$ for all t.*

Then there is $t^* \in (0, 1)$ with $c_i(m(t^*)) = 3$ for all $i \in X$, and $N(m(t^*)) = \frac{1}{2}\big(N(m(0)) + N(m(1))\big)$.

Proof. As $\rho > 0$, the angle $\Theta(t)$ is continuous; hence $h(t) = \rho(t) - R(A(t), \Theta(t))$ is continuous by Lemma 8.1(b). It changes sign between 0 and 1 and vanishes at some $t^* \in (0, 1)$. There $\rho = R(A, \Theta)$ with $A \neq A^*$ and Θ off the cusp rays: by the fourth row of Table 1, $c_i(m(t^*)) = 3$ for $i \in X$. The two sufficient conditions in (3) follow from the first two rows, and from the first

row with $\rho = 0 < R$. The counts of the bodies of X are 4 at one end and 2 at the other. Those of the other bodies are constant. It follows that $N(m(t^*)) = 18+2\big(\sum_{j\notin X} c_j + 3|X|\big)$ is the mean of $N(m(0))$ and $N(m(1))$. □

Proof of Theorem 2. The formula for N was shown above. (a) Theorem 1 shows that $c_i \in \{1,2,3,4\}$ and that $c_i = 1$ if and only if the masses of the three bodies other than i are equal to some m_0 and $m_i = m^* m_0$. This happens for at most one i. Indeed, if it happened for $i \neq j$, the two triples of equal masses would share two bodies, making all four masses equal, whereas $m_i = m^* m_0 \neq m_0$. Hence $\sum_i c_i \geq 7$, so $N = 18 + 2\sum_i c_i$ is even and satisfies $32 \leq N \leq 50$.

(b) If m is not a Palmore mass vector, then $c_i \geq 2$ for all i and $N \geq 34$. Let $m = (1,1,1,m^*)$, up to scaling and relabelling. Then $c_4 = 1$ by Proposition 7.11. As the permutations of the bodies 1, 2, 3 preserve the masses, $c_1 = c_2 = c_3$. The outer masses of body 1 are 1, 1 and $m^* < 1$. Hence the mass coordinates of body 1 are $A = \frac{1}{3}\log m^* = -A^*/3 \neq A^*$, $\rho = \frac{2}{\sqrt{6}}A^* > 0$ and $\Theta = 90°$. Proposition 9.1 shows that $\rho > R(-A^*/3, 90°)$, so Theorem 1 gives $c_1 = 2$. Then $N(1,1,1,m^*) = 18+2(1+2+2+2) = 32$. Item (e) yields the same value without Proposition 9.1 (Corollary 10.7).

(c) By Table 1, $c_i = 2 + 2[\text{row } 1] + [\text{row } 4] - [\text{row } 5]$, where $[\cdot]$ is 1 if the mass coordinates of body i lie in the given row and 0 otherwise. Summing over i gives $N = 18+2(8+2k+f-p) = 34+4k+2f-2p$; by the proof of (a), $p \leq 1$. Outside $Z_1 \cup \cdots \cup Z_4$, where no mass coordinates lie in rows 3–5, $f = p = 0$.

(d) This is proved in Section 9 (Proposition 9.2).

(e) This is Corollary 10.7.

(f) The nullity of a CC does not change under similarities (including reflections), under relabellings of the bodies or under scalings of the masses. Indeed, between CCs normalized by $\lambda' = 1$ a similarity is an isometry. These operations compose V_m with an affine isometry of $(\mathbb{R}^2)^4$ or multiply it by a positive constant, which preserves the dimension of the kernel of its Hessian at corresponding critical points. Hence, by Lemma 11.1, a concave CC with body 4 inside and spokes a has nullity $\dim\ker dF(a)$. It is degenerate exactly when $J(a) = 0$. At a fold point $\dim\ker dF = 1$ by Lemma 7.5. At a cusp point q, in the coordinates (A, l, φ) of Lemma 7.7, the first two components of F have independent differentials that vanish on ∂_φ, and the derivative of the third along ∂_φ is $\partial_\tau(\tau\widetilde{H})(0,0) = \widetilde{H}(0,0) = 0$. It follows that $\ker dF(q)$ is the line spanned by ∂_φ. Each point of $\Sigma \setminus \{p^*\}$ is a fold point or a cusp point (Proposition 7.13(a)), and $\dim\ker dF(p^*) = 2$ by Lemma 2.3(d) and Proposition 2.4. Proposition 2.4 identifies p^* with the configuration named in (f). The configurations of Σ form the degenerate concave CCs with body 4 inside; Σ is a double cone by Lemma 8.1(c). The other inner bodies follow by relabelling.

(g) At equal masses the four points $\mu^{(i)}(1,1,1,1) = 0$ have $A = 0 \neq A^*$ and $\rho = 0 < R(0,\Theta)$. They lie in the first row of Table 1. Then $c_i = 4$ for all i, so $N(1,1,1,1) = 12+6+32 = 50$. □

The cusp points form six arcs, the mirror points with $\Theta \in \{90°, 210°, 330°\}$ of each nappe. Each arc is homeomorphic to an interval and ends at p^*, by Lemmas 7.12 and 8.1(a). These points are symmetric (isosceles) concave CCs whose two equal outer masses are larger than the third.

9. Certified examples

In this section we certify the count N at exact masses and prove Theorem 2(d). Theorem 1 reduces the task to a decision for each body i: whether $\rho < R(A,\Theta)$ or $\rho > R(A,\Theta)$, where (A,ρ,Θ) are its mass coordinates. Lemma 8.2 reduces this to the enclosure of one point of the fold.

9.1. **The decision procedure.** For a body i of an exactly given mass vector, a program computes ball enclosures of the mass coordinates from the exact masses and then proceeds as follows. All enclosures are computed in Arb ball arithmetic at 256 bits, through `python-flint`, by an evaluator of the mass map independent of the C code of Section 5. This evaluator encloses the implicit angles of Lemma 2.2 by a Krawczyk step valid for all spokes of a box. From them it computes the jets of K, μ, A, P, Q and $\widetilde{J}$, and from these the quantities T_1, T_2, T_3 and J_{mir} of Section 3. Physicality is certified on a box when all a_i lie in $(0,1)$, the three angles lie in $(0,\pi)$ and $K<0$, by certified comparisons. Lemma 2.2 then shows that all points of the box are physical and carry the solution of that lemma.

- If the three outer masses are equal, then $\rho=0$ and the program certifies $A\neq A^*$. Then $\rho<R(A,\Theta)$ and $c_i=4$ by Theorem 1. As a check, it also encloses the axis point with the given A and certifies $\widetilde{J}<0$ there.
- If exactly two outer masses are equal, Θ lies on a mirror ray, and the program uses the system $(\widetilde{J},\ A-c)$ in the coordinates (s,y) of the mirror plane $x=0$ ($a_1=a_2$), on which $P=0$ exactly by the symmetry of Lemma 2.2. The program certifies that Q has at the solution the sign of the body's ray ($Q>0$ for $\Theta=90^\circ$, $Q<0$ for $\Theta=270^\circ$), as Lemma 8.2 requires; the enclosure of R is then $|Q|$.
- Otherwise Θ lies off the mirror rays. Let (P_t,Q_t) be the target point in the (P,Q)-plane. The program uses the system $(\widetilde{J},\ A-c,\ -Q_tP+P_tQ)$ in (s,x,y) and certifies $P_tP+Q_tQ>0$ at the solution. The enclosure of R is $(P_tP+Q_tQ)/|(P_t,Q_t)|$.

In both systems a Krawczyk test with centred forms, built from jets of order three at the centre and over the box, proves that the system has exactly one zero in a box on which physicality is certified. By Lemma 8.2 this zero is $\iota(A,\Theta)$, so its enclosure of $|G|$ is an enclosure of $R(A,\Theta)$. These are the two systems of Remark 8.3, except that $-Q_tP+P_tQ$ replaces $\Theta\circ G-\Theta$. Where $P_tP+Q_tQ>0$, the two functions have the same zeros. The program then certifies a strict inequality between the enclosures of ρ and of $R(A,\Theta)$, or, if it cannot, reports the body as undecided. Floating-point computations enter only to find starting points.

For a segment of masses the program works with interval parameters. It covers the segment by subintervals on which the masses are balls containing $m(t)$ for all t in the subinterval, encloses the mass coordinates over each subinterval, and solves the systems above with these balls as parameters. This enclosure of R holds for all parameter values. A subinterval is decided if the enclosures of ρ and of R are strictly ordered. Undecided subintervals are bisected.

9.2. **The examples.**

Proposition 9.1. *For the masses $(1,1,1,m^*)$, $c_1=c_2=c_3=2$. The mass coordinates of body 1 are $A=-A^*/3$, $\rho=\frac{2}{\sqrt{6}}A^*=0.2128872401074461921835\ldots$ and $\Theta=90^\circ$, and*

$$R(-A^*/3,90^\circ)\in[0.011287144197733611\pm1.3\cdot10^{-19}],$$
$$\rho-R(-A^*/3,90^\circ)\in[0.2016000959097125813062817\pm2.9\cdot10^{-26}].$$

Proof. Since the outer masses of body 1 are 1, 1 and $m^*<1$, we have $P=0$, $\Theta=90^\circ$ and $A=\frac{1}{3}\log m^*$. The program of Section 9.1 treats the masses $(m^*,1,1,1)$, which are $(1,1,1,m^*)$ after the labels 1 and 4 are exchanged. It encloses m^* in a ball that contains $(81+64\sqrt{3})/249$. For each of the three bodies of mass 1 its mirror solve finds the point of the fold near $(s,x,y)=(0.74168,0,-0.00759)$, a cusp point on the half-mirror $\varphi=270^\circ$ of the upper nappe (Proposition 7.13(c)). It returns an enclosure of $|Q|$ at this point and the stated enclosure of $\rho-R(-A^*/3,90^\circ)$. By Lemma 8.2, the enclosure of $|Q|$ is one of $R(-A^*/3,90^\circ)$ itself. Hence $c_1=c_2=c_3=2$ by Theorem 1. Both enclosures are computed in ball arithmetic

at 256 bits, and the stated radii round up those of the program's log, which prints R with 17 significant digits and $\rho - R$ with 25. □

Proposition 9.2. *For the mass vectors and segments of Table 5, the counts c_i and N are as stated. In particular every even value of N from 32 to 50 is attained.*

N	masses (m_1, m_2, m_3, m_4)	(c_1, c_2, c_3, c_4)	kind
32	$(1, 1, 1, m^*)$	$(2, 2, 2, 1)$	Palmore (Proposition 9.1)
34	$(1, 2, 3, 4)$	$(2, 2, 2, 2)$	regular
	$(1, 51/50, 26/25, 53/50)$	$(2, 2, 2, 2)$	regular
36	$(1006, 1000, 994, 500) \to (1007, 1000, 993, 500)$	$(2, 2, 2, 3)$	body 4 crosses, $\Theta \approx 60.1°$
38	$(1, 1, 1, 1/2)$	$(2, 2, 2, 4)$	regular
	$(1000, 1001, 1002, 500)$	$(2, 2, 2, 4)$	regular
40	$(8000, 8020, 8041, 8039) \to$ $(8000, 8020, 8044, 8036)$	$(4, 3, 2, 2)$	body 2 crosses, Θ from $207.5°$ to $200.2°$
	$(10000, 10004, 10038, 10019) \to$ $(10000, 10004, 10040, 10020)$	$(3, 2, 4, 2)$	body 1 crosses, $\Theta \approx 176.1°$–$176.4°$
42	$(200, 200, 201, 201)$	$(4, 4, 2, 2)$	regular
	$(2000, 2001, 2010, 2011)$	$(4, 4, 2, 2)$	regular
44	$(1, 1, 1, 1001/1000) \to (1, 1, 1, 1003/1000)$	$(3, 3, 3, 4)$	bodies 1, 2, 3 cross at $\Theta = 270°$
	$(10000, 10004, 10036, 10018) \to$ $(10000, 10004, 10038, 10019)$	$(4, 3, 4, 2)$	body 2 crosses, $\Theta \approx 180.03°$
46	$(2000, 2000, 2006, 2003)$	$(4, 4, 4, 2)$	regular
	$(125231/125000,\ 1002873/1000000,$ $24989/25000, 1)$	$(2, 4, 4, 4)$	regular
48	$(10000, 10000, 10024, 10012) \to$ $(10000, 10000, 10028, 10014)$	$(4, 4, 4, 3)$	body 4 crosses at $\Theta = 270°$
	$(10000, 10001, 10026, 10013) \to$ $(10000, 10001, 10028, 10014)$	$(4, 4, 4, 3)$	body 4 crosses, $\Theta \approx 268.1°$
50	$(1, 1, 1, 1)$	$(4, 4, 4, 4)$	regular
	$(10000, 10001, 10002, 10004)$	$(4, 4, 4, 4)$	regular

TABLE 5. Certified examples. A regular example has all four statuses certified strictly. For a segment $m(t) = (1-t)m_a + tm_b$, $0 \le t \le 1$, the counts are those at a parameter $t^* \in (0, 1)$ given by Lemma 8.4, and the angle is the value of Θ for the crossing body along the segment, with its outer bodies ordered as $j_1 < j_2 < j_3$.

Proof. For the value 32, $c_1 = c_2 = c_3 = 2$ by Proposition 9.1 and $c_4 = 1$ by Theorem 1. For each regular example and each body i, the program of Section 9.1 certifies the strict inequality between ρ and $R(A, \Theta)$ that determines the stated c_i, or it certifies $\rho = 0$ and $A \neq A^*$. In the first case R is identified by Lemma 8.2. Among the regular examples the smallest relative margin $|\rho/R(A, \Theta) - 1|$ is 4.5%, for body 2 of $(2000, 2001, 2010, 2011)$, while the enclosures of ρ and R printed in the program's log have relative radii below 10^{-16}.

For each segment we apply Lemma 8.4 with the set X of crossing bodies. The program certifies the following. (i) The statuses at both ends, inside at one end and outside at the other for the bodies of X, and equal at the two ends for the others. (ii) Hypothesis (3) of the lemma, by strict inequalities between $\rho^{(j)}$ and $R(A^{(j)}, \Theta^{(j)})$ on subintervals that cover $[0, 1]$, or by $\rho^{(j)} = 0$ and $A^{(j)} \neq A^*$ on the whole segment, as for body 4 of the first segment for $N = 44$. (iii) Hypothesis

(1) for the bodies of X on 64 subintervals that cover $[0,1]$: $A \neq A^*$, $G \neq 0$, and G is not a positive multiple of any of the three unit vectors at the cusp angles. (iv) For the first segment for $N = 44$ ($X = \{1,2,3\}$), that the three bodies have the same mass and the same multiset of outer masses along the segment, and therefore the same mass coordinates. Lemma 8.4 then provides t^* with the stated counts and $N(m(t^*)) = \frac{1}{2}(N(m_a) + N(m_b))$. The values at the ends are $(38+34)/2$, $(42+38)/2$, $(50+38)/2$ and $(50+46)/2$ for the first segments for $N = 36$, 40, 44 and 48, and $(42+38)/2$, $(46+42)/2$ and $(50+46)/2$ for the second segments for $N = 40$, 44 and 48. □

The program also brackets the crossing parameters by bisection on rationals, for instance $t^* \in [509/4096, 2037/16384]$ for $N = 36$. For the first segment for $N = 44$ the bracket is $m_4 \in [1642759/1638400, 2053449/2048000]$, which contains the value m_f of Section 10. The evaluator agrees with the C library of Section 5. At 100 physical points, in chart 1, it reproduces the library's midpoints of K, $\widehat{A}$, P, Q, $\widetilde{J}$, T_1, T_2, T_3 and of J_{mir} for both mirror angles; the library's enclosures of these quantities contain its own. It also agrees with an independent floating-point solver of Lemma 2.2 and with finite differences. A separately written program re-certifies all of Table 5. It shares with the computations above only the ball arithmetic, the formulas of Section 2 and the results of Sections 2.4 and 8 that turn enclosures into counts. It uses its own evaluator (with symbolic derivatives and an interval Newton step for K), its own fold solvers and its own subdivisions of the segments. It certifies again all 92 points of the fold used in the examples, each with an enclosure of R inside the enclosure printed in the log. It also certifies again all statuses, all vectors (c_1, c_2, c_3, c_4) and all values of N, the hypotheses of Lemma 8.4 on the whole of each segment, and the statuses at the ends of the brackets of the crossing parameters.

10. The family $(1, 1, 1, m_4)$

In this section $m = (1, 1, 1, m_4)$ with $m_4 > 0$. The point $\mu^{(4)}(m) = -(\log m_4)(1,1,1)$ lies on the axis $\rho = 0$, where Theorem 1 gives c_4 directly. As the permutations of the bodies 1, 2, 3 preserve m, $c_1 = c_2 = c_3$. For body 1 inside, the point $\mu^{(1)}(m) = (0, 0, \log m_4)$ lies on a mirror of the target of F_1. Theorem 1 determines c_1 once the position of this point relative to the surface of critical values is known. Certified computations as in Section 9 decide it for one m_4 at a time, but for all m_4 at once we use the symmetry. The count c_1 depends on the concave CCs with body 1 inside that are symmetric under the exchange of the bodies 2 and 3. These CCs depend on one parameter, which reduces the question to functions of one variable. Theorem 10.1 shows that they form one analytic arc, along which the mass has exactly one critical point and the Jacobian of F_1 has exactly two zeros. Corollary 10.7 gives the counts for all m_4, which are those of Table 6.

10.1. **Setting.** We take the outer bodies of F_1 in the order $2, 3, 4$. Thus F_1 is defined on an open set Ω_1 of spoke vectors $a = (a_2, a_3, a_4)$, $a_j = |x_j - x_1|$. Here $F_1(a) = (\mu_2, \mu_3, \mu_4)$ with $\mu_j = \log(m_j/m_1)$. After a relabelling of the bodies, F_1 is the map F of Section 2, to which the results of Sections 2–6 apply. On Ω_1 we use the coordinates (s, x, y) of Section 2.3, and on the target the coordinates (A, P, Q). In this section J is the Jacobian determinant of F_1, and $\overline{\mathcal{D}} = \{J \leq 0\} \subset \Omega_1$.

The transposition σ of the bodies 2 and 3 acts on Ω_1 by $(s, x, y) \mapsto (s, -x, y)$ and on the target by $(A, P, Q) \mapsto (A, -P, Q)$. We have $F_1 \circ \sigma = \sigma \circ F_1$ and $J \circ \sigma = J$. The fixed points of σ form the mirror

$$\Omega_1^\sigma = \{a \in \Omega_1 :\ a_2 = a_3\} = \Omega_1 \cap \{x = 0\}.$$

At a point of Ω_1^σ, exchanging the labels 2 and 3 maps the solution of Lemma 2.2 to a solution with the same spokes. By uniqueness the configuration is symmetric under the reflection that exchanges the bodies 2 and 3. Conversely, a configuration with this symmetry has $a_2 = a_3$. Thus the points of Ω_1^σ correspond to the symmetric concave CCs with body 1 inside, and $m_2 = m_3$ there. As A and Q are even in x and P is odd, the derivatives $\partial_x A$, $\partial_x Q$, $\partial_s P$ and $\partial_y P$ vanish on Ω_1^σ. The determinant of $\partial(A,P,Q)/\partial(s,x,y)$ is J (proof of Lemma 2.3(d)). Expanding it on Ω_1^σ, we find

$$J = J_{\mathrm{sym}} \cdot \frac{\partial P}{\partial x}, \qquad J_{\mathrm{sym}} = \det \frac{\partial(A,Q)}{\partial(s,y)}. \tag{10.1}$$

We call $\partial(A,Q)/\partial(s,y)$ the *symmetric block*.

In this section we do not normalize λ'. Instead we place the bodies 2 and 3 at $(\mp 1, 0)$. We write $S_{ij} = r_{ij}^{-3} - \lambda'$. Equation (2.1) shows that a configuration is a CC with multiplier λ' if and only if

$$\mathsf{E}_j := \sum_{i \neq j} m_i S_{ij}(x_i - x_j) = 0, \qquad j = 1, \dots, 4.$$

Scaling a configuration by $t > 0$ multiplies λ' by t^{-3}. For $0 < b < h$ let $x(b,h)$ be the configuration with the bodies 2, 3 at $(\mp 1, 0)$, body 1 at $(0, b)$ and body 4 at $(0, h)$. With $\hat{p} = \sqrt{1+b^2}$, $\hat{q} = \sqrt{1+h^2}$ and $d = h - b$ we have $r_{12} = r_{13} = \hat{p}$, $r_{23} = 2$, $r_{24} = r_{34} = \hat{q}$ and $r_{14} = d$. Let

$$\begin{gathered} \mathsf{G}(b,h) = 2h\hat{q}^{-3} + d^{-2} - \frac{h}{4} - d\hat{p}^{-3}, \qquad \mathsf{L}(b,h) = \frac{h/4 + d\hat{p}^{-3}}{2h+d}, \\ \mathsf{M}(b,h) = -\frac{b\,(\hat{p}^{-3} - \mathsf{L})}{h\,(\hat{q}^{-3} - \mathsf{L})}. \end{gathered} \tag{10.2}$$

For $m_4, \lambda' > 0$ let $\mathsf{H} = (\mathsf{H}_{ij})$ be the symmetric 2×2 matrix with

$$\begin{aligned} \mathsf{H}_{11} &= 3\lambda' m_4 - 2m_4\hat{q}^{-3} + 6m_4\hat{q}^{-5} - m_4 d^{-3}, \qquad \mathsf{H}_{12} = -6hm_4\hat{q}^{-5}, \\ \mathsf{H}_{22} &= 2\lambda' m_4 + 6\lambda' + 6b^2\hat{p}^{-5} + 6h^2 m_4\hat{q}^{-5} - 2m_4\hat{q}^{-3} - \tfrac{1}{2} - 2\hat{p}^{-3}, \end{aligned} \tag{10.3}$$

and let $\mathsf{D}(b,h) = \det \mathsf{H} = \mathsf{H}_{11}\mathsf{H}_{22} - \mathsf{H}_{12}^2$ with $m_4 = \mathsf{M}(b,h)$ and $\lambda' = \mathsf{L}(b,h)$. Lemma 10.5 below shows that H is the Hessian of the potential on two antisymmetric displacements of $x(b,h)$. We call D the *pitchfork determinant*.

Theorem 10.1. (1) The arc. *The set $\{\mathsf{G} = 0,\ 0 < b < h\}$ is the graph of an analytic function $b(h)$ on (h_c, ∞) ($h_c = 1.1394\ldots$). On it $\mathsf{M} > 0$ exactly for $h \in (h_c, h_1)$ ($h_1 = 2.9373\ldots$). Every concave CC of the masses $(1,1,1,m_4)$ with body 1 inside that is symmetric under the reflection exchanging the bodies 2 and 3 is, up to similarity including reflection, the configuration $x(b,h)$ of exactly one point (b,h) of the arc, and $\mathsf{M}(b,h) = m_4$ there. Conversely, for every point of the arc with $\mathsf{M} > 0$ the configuration $x(b,h)$ is such a CC of the masses $(1,1,1,\mathsf{M}(b,h))$, with $\lambda' = \mathsf{L}(b,h) > 0$.*

(2) Monotonicity and degenerate points. *For $h_c < h < h_1$ write $\mathsf{M}(h) = \mathsf{M}(b(h),h)$, $\mathsf{D}(h) = \mathsf{D}(b(h),h)$, and $a(h) \in \Omega_1^\sigma$ for the spoke vector of $x(b(h),h)$ scaled to $\lambda' = 1$. The function $\mathsf{M}(h)$ increases strictly from 0 to m_f on $(h_c, h_f]$ and decreases strictly to 0 on $[h_f, h_1)$. The Jacobian J vanishes at $a(h)$ exactly when $h \in \{h^{**}, h_f\}$, where $h^{**} < \sqrt{3} < h_f$. In (10.1), $J_{\mathrm{sym}}(a(h))$ is the product of $d\mathsf{M}/dh$ and a continuous nonvanishing function of h, and $\partial P/\partial x\,(a(h))$ is the product of $\mathsf{D}(h)$ and a continuous nonvanishing function of h. These two factors vanish only at h_f, respectively h^{**}, and change sign there. At $h = \sqrt{3}$ the configuration is the equilateral triangle with body 1 at its centre and $m_4 = 1$, where $J < 0$. Hence $J(a(h)) > 0$ for $h \in (h_c, h^{**}) \cup (h_f, h_1)$, and $J(a(h)) < 0$ for $h \in (h^{**}, h_f)$.*

(3) Values. *The masses* $m^{**} = \mathsf{M}(h^{**})$ *and* $m_f = \mathsf{M}(h_f)$ *satisfy*

$$m^{**} = 0.99184227439094091554349694436440902909455904 2 \pm 4 \cdot 10^{-46},$$
$$m_f = 1.00266054757261000068580350218611540512511700 \pm 5 \cdot 10^{-46}.$$

In particular $m^* < m^{**} < 1 < m_f < (m^*)^{-3}$.

The proofs in Sections 10.2 and 10.3 are by hand. They reduce Theorem 10.1 to statements about the zeros of two functions of h, namely $d\mathsf{M}/dh$ and $\mathsf{D}(h)$, and to the bounds in (3). Section 10.4 proves these by exact computation and ball arithmetic.

10.2. **The arc.**

Lemma 10.2. *Let* $0 < b < h$ *and* $m_4 > 0$.

(a) *The configuration* $x(b,h)$ *is a CC of the masses* $(1,1,1,m_4)$ *if and only if* $\mathsf{G}(b,h) = 0$ *and* $m_4 = \mathsf{M}(b,h)$. *The multiplier of this CC is then* $\lambda' = \mathsf{L}(b,h)$, *and* $\mathsf{L} > 0$.

(b) *If* $\mathsf{G}(b,h) = 0$, *then*

$$\hat{q}^{-3} - \mathsf{L} = \frac{d\,(\hat{q}^{-3} - d^{-3})}{2h+d} < 0, \qquad \mathsf{M}(b,h) = -\frac{2b\,(\hat{p}^{-3} - \frac{1}{8})}{(2h+d)(\hat{q}^{-3} - \mathsf{L})}.$$

In particular M *has no pole on* $\{\mathsf{G} = 0\}$, *and it has the sign of* $\sqrt{3} - b$ *there.*

(c) *Every concave CC with body* 1 *inside that is symmetric under the reflection exchanging the bodies* 2 *and* 3 *is similar to* $x(b,h)$ *for exactly one pair* $0 < b < h$, *by a similarity that may reverse the orientation.*

Proof. (a) The reflection $(u,v) \mapsto (-u,v)$ maps $x(b,h)$ to itself with the bodies 2 and 3 exchanged. Hence, for the masses $(1,1,1,m_4)$, the first components of E_1 and E_4 vanish, and E_3 is the mirror image of E_2. The remaining components are

$$\mathsf{E}_2 = \big(2S_{23} + S_{12} + m_4 S_{24},\ bS_{12} + m_4 h S_{24}\big), \quad \mathsf{E}_{1,2} = -2bS_{12} + m_4 d S_{14}, \quad \mathsf{E}_{4,2} = -dS_{14} - 2hS_{24},$$

where $\mathsf{E}_{j,2}$ denotes the second component of E_j. The sum $\sum_j m_j \mathsf{E}_j$ vanishes identically: its terms $m_i m_j S_{ij}(x_i - x_j)$ are antisymmetric in (i,j). The second component of this identity, $\mathsf{E}_{1,2} + 2\mathsf{E}_{2,2} + m_4 \mathsf{E}_{4,2} = 0$, shows that $x(b,h)$ is a CC if and only if $\mathsf{E}_2 = 0$ and $\mathsf{E}_{4,2} = 0$. As $h \neq 0$, this holds if and only if $\mathsf{E}_{2,2} = 0$ and

$$\text{(I)} \quad h\mathsf{E}_{2,1} - \mathsf{E}_{2,2} = 2hS_{23} + dS_{12} = 0, \qquad \text{(II)} \quad -\mathsf{E}_{4,2} = 2hS_{24} + dS_{14} = 0.$$

Both equations are linear in λ'. Equation (I) holds if and only if $\lambda' = \mathsf{L}(b,h)$. Equation (II) holds if and only if $\lambda' = (2h\hat{q}^{-3} + d^{-2})/(2h+d)$. Together they hold if and only if $\lambda' = \mathsf{L}$ and

$$\mathsf{G} = (2h+d)\Big(\frac{2h\hat{q}^{-3} + d^{-2}}{2h+d} - \mathsf{L}\Big) = 0.$$

At such a point $S_{24} \neq 0$. Otherwise (II) gives $S_{14} = 0$ and then $d^{-3} = \lambda' = \hat{q}^{-3}$, which is impossible for $d < h < \hat{q}$. Then $\mathsf{E}_{2,2} = 0$ if and only if $m_4 = -bS_{12}/(hS_{24}) = \mathsf{M}(b,h)$. Finally $\mathsf{L} > 0$: its numerator and its denominator are positive.

(b) On $\{\mathsf{G} = 0\}$ the two expressions for λ' in (a) agree. Then $\hat{q}^{-3} - \mathsf{L} = \hat{q}^{-3} - (2h\hat{q}^{-3} + d^{-2})/(2h+d) = d(\hat{q}^{-3} - d^{-3})/(2h+d)$. This is negative because $d < \hat{q}$. The formula for M follows from $\hat{p}^{-3} - \mathsf{L} = 2h(\hat{p}^{-3} - \frac{1}{8})/(2h+d)$. The denominator $(2h+d)(\hat{q}^{-3} - \mathsf{L})$ of this formula is negative; $\hat{p}^{-3} - \frac{1}{8}$ has the sign of $2 - \hat{p}$, that is, of $\sqrt{3} - b$.

(c) Let x be such a CC. A similarity maps the bodies 2 and 3 to $(\mp 1, 0)$. The reflection that exchanges them becomes the reflection in the vertical axis. The bodies 1 and 4 are fixed by it and lie on this axis, at $(0,b)$ and $(0,h)$. As body 1 is strictly inside the triangle of the other three, $h \neq 0$. Since c_1 counts up to similarity including reflection, we may compose with the

reflection $(u,v)\mapsto(u,-v)$ if necessary. Then $h>0$ and $0<b<h$. The only similarities that fix $(-1,0)$ and $(1,0)$ are the identity and this reflection. This makes the pair (b,h) with $h>0$ unique. □

Lemma 10.3. (a) *For $0<b<h$, $\partial\mathsf{G}/\partial b = 2d^{-3}+\hat p^{-3}+3bd\hat p^{-5}>0$, and $\mathsf{G}(b,h)\to+\infty$ as $b\to h^-$. The function $g_0(h)=\mathsf{G}(0,h)=2h(1+h^2)^{-3/2}+h^{-2}-\frac54 h$ decreases strictly from $+\infty$ to $-\infty$ on $(0,\infty)$. Let h_c be its zero. Then $h_c<\sqrt3$, and $\{\mathsf{G}=0,\ 0<b<h\}$ is the graph of an analytic function $b(h)$ on (h_c,∞) with $b(h)\to0$ as $h\to h_c$.*

(b) *There is exactly one $h_1>h_c$ with $b(h_1)=\sqrt3$. Moreover $b(h)<\sqrt3$ for $h_c<h<h_1$, and $b(h)>\sqrt3$ for $h>h_1$.*

Proof. (a) The formula for $\partial\mathsf{G}/\partial b$ follows by direct computation; its three terms are positive. As $b\to h^-$, the term d^{-2} tends to $+\infty$ while the other terms stay bounded. Next,

$$g_0'(h)=2(1-2h^2)(1+h^2)^{-5/2}-2h^{-3}-\tfrac54.$$

For $h\ge1/\sqrt2$ the first term is at most 0. For $0<h<1/\sqrt2$ it is less than 2, while $-2h^{-3}<-4\sqrt2$. In both cases $g_0'(h)<0$. Moreover $g_0\to+\infty$ as $h\to0^+$, $g_0\to-\infty$ as $h\to\infty$, and $g_0(\sqrt3)=\frac13-\sqrt3<0$. Hence g_0 has exactly one zero h_c, $h_c<\sqrt3$, and $g_0<0$ exactly on (h_c,∞). For fixed $h>0$ the function $\mathsf{G}(\cdot,h)$ increases strictly on $[0,h)$ from $g_0(h)$ to $+\infty$. It has a zero in $(0,h)$ if and only if $g_0(h)<0$, that is, $h>h_c$; the zero $b(h)$ is then unique. It is analytic in h by the implicit function theorem. Given $\epsilon>0$, we have $\mathsf{G}(\epsilon,h_c)>g_0(h_c)=0$. Continuity gives $\mathsf{G}(\epsilon,h)>0$ for h close to h_c, so $b(h)<\epsilon$ for these h.

(b) For $h>\sqrt3$ put $g_1(h)=\mathsf{G}(\sqrt3,h)=2h\hat q^{-3}+(h-\sqrt3)^{-2}-\frac h4-\frac18(h-\sqrt3)$. Then

$$g_1'(h)=2(1-2h^2)(1+h^2)^{-5/2}-2(h-\sqrt3)^{-3}-\tfrac38<0,$$

because each term is negative for $h>\sqrt3$. Since $g_1\to+\infty$ for $h\to\sqrt3{}^+$ and $g_1\to-\infty$ for $h\to\infty$, the function g_1 has exactly one zero $h_1>\sqrt3$, and $g_1>0$ on $(\sqrt3,h_1)$, $g_1<0$ on (h_1,∞). As G increases in b, for $h>\sqrt3$ we have $b(h)<\sqrt3$, $b(h)=\sqrt3$ or $b(h)>\sqrt3$ according as $g_1(h)>0$, $g_1(h)=0$ or $g_1(h)<0$. For $h_c<h\le\sqrt3$ we have $b(h)<h\le\sqrt3$. With $h_c<\sqrt3<h_1$, this proves (b). □

Proof of Theorem 10.1(1). The first statement is Lemma 10.3(a). Lemmas 10.2(b) and 10.3(b) show that $\mathsf{M}>0$ on the arc exactly for $h_c<h<h_1$. Let x be a symmetric concave CC of the masses $(1,1,1,m_4)$ with body 1 inside. Lemma 10.2(c) shows that it is similar to $x(b,h)$ for exactly one pair $0<b<h$. By Lemma 10.2(a), $\mathsf{G}(b,h)=0$ and $\mathsf{M}(b,h)=m_4$. Conversely, let (b,h) be a point of the arc with $\mathsf{M}(b,h)>0$. Then $x(b,h)$ is a CC of the masses $(1,1,1,\mathsf{M}(b,h))$ with $\lambda'=\mathsf{L}(b,h)>0$, by Lemma 10.2(a). It is symmetric. Body 1 lies strictly inside the triangle of the others because $0<b<h$. □

Scaled by $\mathsf{L}^{1/3}$, the configuration $x(b(h),h)$ has $\lambda'=1$. By Lemma 2.1 the point $a(h)=\mathsf{L}^{1/3}(\hat p,\hat p,d)$, evaluated at $(b(h),h)$, lies in Ω_1^σ. It depends analytically on $h\in(h_c,h_1)$, and $F_1(a(h))=(0,0,\log\mathsf{M}(h))$.

10.3. **The degenerate points of the arc.**

Lemma 10.4. *For $h\in(h_c,h_1)$, $h\ne\sqrt3$, we have $J_{\rm sym}(a(h))=\chi_{\rm s}(h)\,\mathsf{M}'(h)$, where $\mathsf{M}'=d\mathsf{M}/dh$ and $\chi_{\rm s}$ is continuous and nonvanishing on $(h_c,\sqrt3)$ and on $(\sqrt3,h_1)$.*

Proof. Let $0<b<h$ with $h\ne\sqrt3$, and let $\alpha,\nu>0$. The computation in the proof of Lemma 10.2(a), with the masses $(1,\alpha,\alpha,\nu)$ in place of $(1,1,1,m_4)$, shows that $x(b,h)$ is a CC of these masses with multiplier λ' if and only if

$$2\alpha hS_{23}+dS_{12}=0,\qquad 2\alpha hS_{24}+dS_{14}=0,\qquad bS_{12}+\nu hS_{24}=0.$$

The first two equations give $\lambda' = \lambda_I(\alpha) := (\alpha h/4 + d\hat{p}^{-3})/(2\alpha h + d)$ and $\lambda' = (2\alpha h\hat{q}^{-3} + d^{-2})/(2\alpha h + d)$. These agree if and only if $\alpha\, e(h) = d^{-2} - d\hat{p}^{-3}$, where $e(h) = h/4 - 2h\hat{q}^{-3}$. As $e(h) = 0$ only for $\hat{q} = 2$, that is, $h = \sqrt{3}$, this means $\alpha = \tilde{\alpha}(b,h) := 1 + \mathsf{G}(b,h)/e(h)$. Then $\lambda' = \tilde{\lambda}(b,h) := \lambda_I(\tilde{\alpha}(b,h))$. If $\hat{q}^{-3} \neq \tilde{\lambda}$, the third equation determines $\nu = \tilde{\nu}(b,h) := \mathsf{N}(b,h,\tilde{\lambda}(b,h))$ with $\mathsf{N}(b,h,\lambda') = -b(\hat{p}^{-3} - \lambda')/(h(\hat{q}^{-3} - \lambda'))$.

Fix $h_0 \in (h_c, h_1) \setminus \{\sqrt{3}\}$ and let $b_0 = b(h_0)$. At (b_0, h_0) we have $\mathsf{G} = 0$, $\tilde{\alpha} = 1$, $\tilde{\lambda} = \mathsf{L} > 0$, $\hat{q}^{-3} - \tilde{\lambda} < 0$ and $\tilde{\nu} = \mathsf{M} > 0$, by Lemma 10.2. Hence on a neighbourhood U of (b_0, h_0) these functions are analytic and $\tilde{\alpha}$, $\tilde{\lambda}$ and $\tilde{\nu}$ are positive. There $x(b,h)$ is a concave CC with body 1 inside of the masses $(1, \tilde{\alpha}, \tilde{\alpha}, \tilde{\nu})$ and with multiplier $\tilde{\lambda}$. By the computation above, these are the only masses of the form $(1, \alpha, \alpha, \nu)$, and $\tilde{\lambda}$ is the only multiplier, for which $x(b,h)$ is a CC. Scaling by $\tilde{\lambda}^{1/3}$ gives the point

$$\Upsilon(b,h) = \tilde{\lambda}(b,h)^{1/3}\,(\hat{p}, \hat{p}, d) \in \Omega_1^\sigma, \qquad F_1(\Upsilon(b,h)) = (\log\tilde{\alpha}, \log\tilde{\alpha}, \log\tilde{\nu}).$$

Conversely, by Lemma 10.2(c) a point a of Ω_1^σ is similar to $x(b,h)$ for a unique pair (b,h). This pair depends analytically on a through the solution of Lemma 2.2 and lies in U if a is close to $a(h_0)$. Then $x(b,h)$ is a CC for the masses of a. These masses have $m_2 = m_3$, because $F_1 \circ \sigma = \sigma \circ F_1$ and $\sigma a = a$. By the uniqueness of the masses and of the multiplier noted above, these masses are $(1, \tilde{\alpha}, \tilde{\alpha}, \tilde{\nu})$, the multiplier of $x(b,h)$ is $\tilde{\lambda}$, and $a = \Upsilon(b,h)$. Thus Υ maps a neighbourhood of (b_0, h_0) bijectively onto a neighbourhood of $a(h_0)$ in Ω_1^σ; the inverse map is analytic. The Jacobian determinant $k(b,h)$ of Υ in the coordinates (s,y) of Ω_1^σ does not vanish.

At $\Upsilon(b,h)$ we have $A = (2\log\tilde{\alpha} + \log\tilde{\nu})/3$ and $Q = 2(\log\tilde{\alpha} - \log\tilde{\nu})/\sqrt{6}$; the linear map $(u,w) \mapsto ((2u+w)/3,\, 2(u-w)/\sqrt{6})$ has determinant $-2/\sqrt{6}$. By the chain rule,

$$J_{\mathrm{sym}}(\Upsilon(b,h))\, k(b,h) = -\frac{2}{\sqrt{6}}\, \det \frac{\partial(\log\tilde{\alpha}, \log\tilde{\nu})}{\partial(b,h)}.$$

On the arc we have $\mathsf{G} = 0$, hence $\tilde{\alpha} = 1$ and $d\tilde{\alpha} = d\mathsf{G}/e$. The difference $\tilde{\lambda} - \mathsf{L} = \lambda_I(1 + \mathsf{G}/e) - \lambda_I(1)$ is G times an analytic function. So is $\tilde{\nu} - \mathsf{M} = \mathsf{N}(b,h,\tilde{\lambda}) - \mathsf{N}(b,h,\mathsf{L})$. It follows that on the arc $\tilde{\nu} = \mathsf{M}$ and $d\tilde{\nu} = d\mathsf{M} + f\, d\mathsf{G}$ for an analytic function f, and

$$\det \frac{\partial(\log\tilde{\alpha}, \log\tilde{\nu})}{\partial(b,h)} = \frac{\mathsf{G}_b\mathsf{M}_h - \mathsf{G}_h\mathsf{M}_b}{e\,\mathsf{M}} = \frac{\mathsf{G}_b}{e\,\mathsf{M}}\, \mathsf{M}'(h),$$

using $\mathsf{M}'(h) = \mathsf{M}_h + \mathsf{M}_b\, b'(h) = \mathsf{M}_h - \mathsf{M}_b\mathsf{G}_h/\mathsf{G}_b$. Thus $J_{\mathrm{sym}}(a(h)) = \chi_{\mathrm{s}}(h)\mathsf{M}'(h)$ with $\chi_{\mathrm{s}} = -2\mathsf{G}_b/(\sqrt{6}\, e\, \mathsf{M}\, k)$, evaluated at $(b(h), h)$. Since the formula for Υ defines k as an analytic function near each point of the arc with $h \neq \sqrt{3}$, the function χ_{s} is continuous on $(h_c, \sqrt{3})$ and on $(\sqrt{3}, h_1)$. It does not vanish because $\mathsf{G}_b > 0$, $e \neq 0$, $\mathsf{M} > 0$ and $k \neq 0$. □

Lemma 10.5. *For $h \in (h_c, h_1)$ we have $\partial P/\partial x\,(a(h)) = \chi_{\mathrm{a}}(h)\, \mathsf{D}(h)$, where χ_{a} is continuous and nonvanishing on (h_c, h_1).*

Proof. For masses m and $\lambda' > 0$ let $V_{m,\lambda'}(x) = \sum_{i<j} m_i m_j \big(r_{ij}^{-1} + \frac{1}{2}\lambda' r_{ij}^2\big)$ on $(\mathbb{R}^2)^4$. Then $\partial V_{m,\lambda'}/\partial x_j = m_j \mathsf{E}_j$: the CCs with multiplier λ' are the critical points of $V_{m,\lambda'}$. For $\phi(r) = r^{-1} + \frac{1}{2}\lambda' r^2$ we have $\phi''(r) - \phi'(r)/r = 3r^{-3}$ and $\phi'(r)/r = -(r^{-3} - \lambda')$. These give

$$\text{(10.4)}\quad \operatorname{Hess} V_{m,\lambda'}[\xi,\xi] = \sum_{i<j} m_i m_j \Big(3r_{ij}^{-5}\big((x_i - x_j)\cdot(\xi_i - \xi_j)\big)^2 - S_{ij}\,|\xi_i - \xi_j|^2\Big), \qquad \xi \in (\mathbb{R}^2)^4.$$

Fix $h \in (h_c, h_1)$, and let $b = b(h)$, $m_4 = \mathsf{M}(h)$, $\lambda' = \mathsf{L}(b,h)$ and $x^0 = x(b,h)$, a critical point of $V_{m,\lambda'}$ for $m = (1,1,1,m_4)$. The reflection $(u,v) \mapsto (-u,v)$ combined with the exchange of the bodies 2 and 3 is an orthogonal map σ_* of $(\mathbb{R}^2)^4$ that fixes x^0 and $V_{m,\lambda'}$; its (-1)-eigenspace, the space of antisymmetric displacements, consists of the ξ with $\xi_1 = (\xi_{1,1}, 0)$,

$\xi_4 = (\xi_{4,1}, 0)$, $\xi_2 = (u, v)$ and $\xi_3 = (u, -v)$. It contains the displacement $\mathbf{u}$, in which body 4 moves by $(1, 0)$ and the others are fixed, the displacement $\mathbf{w}$, in which the bodies 2 and 3 move by $(0, 1)$ and $(0, -1)$ and the others are fixed, the translation $\mathbf{t}$, in which all bodies move by $(1, 0)$, and the rotation $\mathbf{r}$, $\mathbf{r}_j = (-x^0_{j,2}, x^0_{j,1})$. Since $b \neq 0$, these four vectors form a basis. They depend continuously on h. Since $V_{m,\lambda'}$ is invariant under translations and rotations and x^0 is a critical point, $\operatorname{Hess} V_{m,\lambda'}(x^0)\,\mathbf{t} = \operatorname{Hess} V_{m,\lambda'}(x^0)\,\mathbf{r} = 0$. A direct computation with (10.4), in which only the pairs that contain body 4 contribute to the entries with $\mathbf{u}$, shows that $\operatorname{Hess} V_{m,\lambda'}(x^0)[\mathbf{u},\mathbf{u}] = \mathsf{H}_{11}$, $\operatorname{Hess} V_{m,\lambda'}(x^0)[\mathbf{u},\mathbf{w}] = \mathsf{H}_{12}$ and $\operatorname{Hess} V_{m,\lambda'}(x^0)[\mathbf{w},\mathbf{w}] = \mathsf{H}_{22}$, with H as in (10.3).

Next we differentiate along $\partial/\partial x$. For small τ let X^τ be the configuration of the point $a(h) + \tau E_1$ of Ω_1, placed with body 1 at the origin, body 4 on the positive vertical half-axis and body 2 to its left, then scaled by $\mathsf{L}^{-1/3}$ and translated so that $X^0 = x^0$. It is a CC with multiplier L for the masses $m(\tau) = (1, e^{F_1(a(h)+\tau E_1)})$: $\nabla V_{m(\tau),\lambda'}(X^\tau) = 0$. Differentiating at $\tau = 0$ gives

$$\operatorname{Hess} V_{m,\lambda'}(x^0)\,\dot X + \sum_k \dot m_k \,\frac{\partial \nabla V_{m,\lambda'}}{\partial m_k}(x^0) = 0.$$

Here $\dot m_1 = 0$, and $\dot m_4 = m_4\,\partial_x \mu_4 = 0$ because μ_4 is σ-invariant. Since $m_2 = m_3 = 1$ and $\partial_x \mu_3 = -\partial_x \mu_2$ on Ω_1^σ, we have $\dot m_2 = -\dot m_3 = \partial_x \mu_2 = \frac{1}{\sqrt2}\,\partial P/\partial x$. The point $a(h) - \tau E_1$ is $\sigma(a(h) + \tau E_1)$. Thus $X^{-\tau} = \sigma_* X^\tau$ and $\dot X$ is antisymmetric:

$$\dot X = z_1\mathbf{u} + z_2\mathbf{w} + z_3\mathbf{t} + z_4\mathbf{r}.$$

We have $(z_1, z_2) \neq 0$. Otherwise $\dot X$ would be an infinitesimal isometry, and the spokes $\mathsf{L}^{-1/3}(a(h) + \tau E_1)$ of X^τ would be stationary at $\tau = 0$. Taking the inner product with $\mathbf{u}$ and $\mathbf{w}$ gives

$$\mathsf{H}\begin{pmatrix} z_1 \\ z_2 \end{pmatrix} + \dot m_2 \begin{pmatrix} \beta_1 \\ \beta_2 \end{pmatrix} = 0, \quad \beta_1 = \Big\langle \mathbf{u}, \Big(\frac{\partial}{\partial m_2} - \frac{\partial}{\partial m_3}\Big)\nabla V_{m,\lambda'} \Big\rangle, \quad \beta_2 = \Big\langle \mathbf{w}, \Big(\frac{\partial}{\partial m_2} - \frac{\partial}{\partial m_3}\Big)\nabla V_{m,\lambda'} \Big\rangle.$$

At x^0 and for arbitrary m_2, m_3, the formulas for E_2, E_3 and E_4 give $\langle \mathbf{u}, \nabla V_{m,\lambda'}\rangle = m_4 \mathsf{E}_{4,1} = m_4\,(m_3 - m_2) S_{24}$ and $\langle \mathbf{w}, \nabla V_{m,\lambda'}\rangle = m_2 \mathsf{E}_{2,2} - m_3 \mathsf{E}_{3,2} = (m_2 - m_3)(bS_{12} + m_4 h S_{24})$. Hence $\beta_1 = -2m_4 S_{24}$ and $\beta_2 = 2(bS_{12} + m_4 h S_{24}) = 2\mathsf{E}_{2,2} = 0$. By Lemma 10.2, $\beta_1 > 0$. Moreover $\mathsf{H}_{12} = -6hm_4\hat q^{-5} < 0$. The second row of the system, $\mathsf{H}_{12} z_1 + \mathsf{H}_{22} z_2 = 0$, shows that $z_2 \neq 0$. Multiplying the first row, $\mathsf{H}_{11} z_1 + \mathsf{H}_{12} z_2 = -\beta_1 \dot m_2$, by H_{12} and substituting $\mathsf{H}_{12} z_1 = -\mathsf{H}_{22} z_2$ gives $(\mathsf{H}_{11}\mathsf{H}_{22} - \mathsf{H}_{12}^2)\, z_2 = \mathsf{H}_{12}\beta_1 \dot m_2$, that is,

$$\frac{\partial P}{\partial x}\,(a(h)) = \sqrt2\,\dot m_2 = \frac{\sqrt2\, z_2}{\mathsf{H}_{12}\,\beta_1}\,\mathsf{D}(h).$$

Adding an infinitesimal isometry to $\dot X$ does not change (z_1, z_2), and both $\dot X$ and the basis depend continuously on h. Thus z_2 is a continuous nonvanishing function of h, so $\chi_{\mathrm{a}} = \sqrt2\, z_2/(\mathsf{H}_{12}\beta_1)$ is continuous and nonvanishing. □

10.4. **The certified computations.**

Proposition 10.6. (a) $h_c = 1.139428224956\ldots$ *and* $h_1 = 2.937347078968\ldots$
(b) M' *has exactly one zero* h_f *in* (h_c, h_1), *and* $h_f = 1.774177389967\ldots$
(c) D *has exactly one zero* h^{**} *in* (h_c, h_1), *and* $h^{**} = 1.690172438713\ldots$ *Moreover* $\mathsf{D}(1.60) > 0 > \mathsf{D}(1.75)$.
(d) m^{**} *and* m_f *satisfy the bounds of Theorem 10.1*(3).

Proof. The existence of the zero of M' is elementary. Lemma 10.2(b) shows that $(2h+d)(\hat{q}^{-3}-\mathsf{L}) = d(\hat{q}^{-3}-d^{-3})$ on the arc. As $h \to h_c$, this tends to $h_c(\hat{q}(h_c)^{-3} - h_c^{-3}) \neq 0$, while $b(h) \to 0$. The formula for M in Lemma 10.2(b) then implies $\mathsf{M}(h) \to 0$ as $h \to h_c$. Also $\mathsf{M}(h_1) = 0$ and $\mathsf{M} > 0$ on (h_c, h_1). Rolle's theorem then yields a zero of M' in (h_c, h_1). The zero of D exists by the signs in (c). The rest is computed. All ball arithmetic uses Arb [Joh17] in FLINT [FLI25] through python-flint and starts from exact rational constants.

(a) Interval Newton steps [Moo66, Neu90] for g_0 and for g_1 of Lemma 10.3 give $h_c \in 1.13942822495620091451485 3 \pm 2 \cdot 10^{-25}$ and $h_1 \in 2.9373470789684912304 \pm 2 \cdot 10^{-20}$.

Polynomial form. The substitution $b = (t^2-1)/(2t)$, $\hat{p} = (t^2+1)/(2t)$, $h = (v^2-1)/(2v)$, $\hat{q} = (v^2+1)/(2v)$ maps $\{1 < t < v\}$ onto $\{0 < b < h\}$, and $b < \sqrt{3}$ if and only if $t < 2+\sqrt{3}$. It turns G, L, M and D into rational functions of (t, v) with rational coefficients, which we compute exactly with SymPy. We write $\mathsf{M} = M_n/M_d$ in lowest terms. Then $(2h+d)(\hat{q}^{-3}-\mathsf{L}) = -M_d/\big(8tv(t^2+1)^3(v^2+1)^3\big)$. Lemma 10.2(b) shows that M_d does not vanish on the arc. Let $\mathcal{G}$ be the numerator of G, a polynomial of bidegree $(10, 12)$ in (t, v). The denominator $8v(t-v)^2(t^2+1)^3(v^2+1)^3(tv+1)^2$ of G does not vanish for $1 < t < v$: the arc is $\{\mathcal{G} = 0,\ 1 < t < v\}$, and $\partial_t \mathcal{G} \neq 0$ there by Lemma 10.3(a). By the chain rule, at a point of the arc $\mathsf{M}'(h) = 0$ if and only if

$$(\partial_t M_n\, M_d - M_n\, \partial_t M_d)\, \partial_v \mathcal{G} - (\partial_v M_n\, M_d - M_n\, \partial_v M_d)\, \partial_t \mathcal{G} = 0.$$

For $1 < t < v$ the zeros of this polynomial are those of a factor $\mathcal{F}$ of bidegree $(25, 22)$: its other irreducible factors are among t, v, $t \pm 1$, $v \pm 1$, t^2+1, v^2+1, $tv+1$ and $v-t$, none of which vanishes there. The numerator of D is $-12v(t-1)^2(t+1)^2(t^2-4t+1)(t^4+4t^3+18t^2+4t+1)\,\mathcal{P}$ for a polynomial $\mathcal{P}$ of bidegree $(29, 25)$. The denominator of D is a product of powers of $t-v$, $tv+1$, t^2+1, v^2+1, M_d and $t^2v - 3tv^2 + 3t - v = -2tv(3h-b)$. On the arc with $1 < t < 2+\sqrt{3}$, that is, $h_c < h < h_1$, all these factors except $\mathcal{P}$ are nonzero: there $\mathsf{D}(h) = 0$ if and only if $\mathcal{P} = 0$.

Resultants and root isolation. We prove the uniqueness of these zeros in two independent ways. The first, below, uses resultants of degree up to 550, computed with Singular. The second, the certificate without resultants at the end of this proof, works along the arc in the variables (b, h), independently of the resultants. If (t_0, v_0) is a common zero of $\mathcal{G}$ and of $\mathcal{X} \in \{\mathcal{F}, \mathcal{P}\}$, then v_0 is a root of the resultant $\mathrm{Res}_t(\mathcal{G}, \mathcal{X}) \in \mathbb{Z}[v]$ and t_0 is a root of $\mathrm{Res}_v(\mathcal{G}, \mathcal{X}) \in \mathbb{Z}[t]$: each resultant lies in the ideal generated by $\mathcal{G}$ and $\mathcal{X}$. We compute the four resultants exactly with Singular. Their degrees are 474 and 484 for $\mathcal{F}$, and 502 and 550 for $\mathcal{P}$. We factor them over $\mathbb{Z}$. The routine `arb_fmpz_poly_complex_roots` of FLINT, called through `python-flint` with target precision 800 bits, encloses the complex roots of each irreducible factor in disjoint balls, each certified to be real (imaginary part exactly 0) or nonreal (imaginary part excluding 0). For $\mathcal{F}$ there are 6 real roots $v > 1$ and 6 real roots $t > 1$, and for $\mathcal{P}$ there are 3 and 2. The real roots equal to 1 are exact roots of the factors $t-1$ or $v-1$, that is, $b = 0$ or $h = 0$, outside the open domain. For each pair of a t-ball and a v-ball we evaluate $\mathcal{G}$ and $\mathcal{X}$ on their product in ball arithmetic at 800 bits. We discard the pair if one of the two enclosures excludes 0 or if $t > v$ on the product. The only pair whose order is not decided is $t = v = 2+\sqrt{3}$ for $\mathcal{F}$, the same root of the factor t^2-4t+1 of both resultants, which lies on the boundary $b = h$. Exactly one pair with $1 < t < v$ survives for each $\mathcal{X}$. Hence M' has at most one zero on the whole arc $h > h_c$, and D has at most one zero on (h_c, h_1). These zeros lie in the surviving boxes, at $(b, h) = (0.61349\ldots, 1.77417\ldots)$ for $\mathcal{F}$ and $(0.54129\ldots, 1.69017\ldots)$ for $\mathcal{P}$. With the existence shown above, this proves (b) and the first part of (c).

The values. The coordinates of the surviving pairs are simple roots of irreducible factors of the resultants, of degree 240 for $\mathcal{F}$ and 126 for $\mathcal{P}$. These are the degrees of the coordinates t and v, not of m_f and m^{**}. An interval Newton step on these factors at 400 bits encloses the coordinates in balls of radius less than 10^{-100}. Evaluating M_n/M_d on these balls proves (d).

The signs. Bisection with certified signs of $\mathcal{G}(\cdot, v)$ encloses the points of the arc at $h = 1.60$ and $h = 1.75$. On these enclosures $\mathcal{P}$ has opposite strict signs. As the other factors of D do not vanish on the arc, D changes sign between $h = 1.60$ and $h = 1.75$. The certificate without resultants below certifies the signs themselves, $\mathsf{D}(1.60) > 0 > \mathsf{D}(1.75)$, which is the second part of (c).

A certificate without resultants. The program `arc_cert.py` encloses the arc by interval Newton steps for $\mathsf{G}(\cdot, h)$ on subintervals of $[h_c - 10^{-4}, h_1 + 10^{-4}]$ and, by certified signs and monotonicity along the arc, verifies the uniqueness of the zeros in (b) and (c) a second time, in the variables (b, h) (README of the supplement). It also shows that $\widehat{\mathsf{D}} = \mathsf{D}/(b\,\mathsf{M})$, which has the sign of D on (h_c, h_1), satisfies $\widehat{\mathsf{D}}(1.60) > 0 > \widehat{\mathsf{D}}(1.75)$.

Checks. msolve solves the systems $\mathcal{G} = \mathcal{F} = 0$ and $\mathcal{G} = \mathcal{P} = 0$ without resultants. Each has 21 real solutions, isolated in boxes with rational endpoints. Comparing these endpoints exactly with the domain shows that exactly one box of each system lies in $\{1 < t < v\}$, at the point found above, and that the others lie outside, except for one box of the second system that meets the line $t = 1$. This box contains the end $b = 0$, $h = h_c$ of the arc, which is a common zero of $\mathcal{G}$ and $\mathcal{P}$. A floating-point computation at 70 digits with the mass map of Section 2, which uses neither G nor M, locates the zeros of J_{sym} and of $\partial P/\partial x$ along the arc and reproduces m_f and m^{**} to within $5 \cdot 10^{-46}$. □

10.5. **End of the proof.** *Proof of Theorem 10.1*(2) *and* (3). By the proof of Proposition 10.6, $\mathsf{M}(h) \to 0$ as $h \to h_c$, $\mathsf{M}(h_1) = 0$ and $\mathsf{M} > 0$ on (h_c, h_1). Proposition 10.6(b) adds that M' vanishes only at h_f. Hence $\mathsf{M}' > 0$ on (h_c, h_f) and $\mathsf{M}' < 0$ on (h_f, h_1). This is the monotonicity; the maximum is $m_f = \mathsf{M}(h_f)$.

The point $(b, h) = (1/\sqrt{3}, \sqrt{3})$ has $\hat{p} = d = 2/\sqrt{3}$, $\hat{q} = 2$, $\mathsf{G} = 0$, $\mathsf{L} = (3 + 3\sqrt{3})/32$ and $\mathsf{M} = 1$. Then $b(\sqrt{3}) = 1/\sqrt{3}$ and $\mathsf{M}(\sqrt{3}) = 1$. The configuration $x(1/\sqrt{3}, \sqrt{3})$ is the equilateral triangle of side 2 with body 1 at its centre; $a(\sqrt{3})$ is the point of the axis of Ω_1 for four equal masses. As $1 \neq m^*$, it is not the umbilic, so $J(a(\sqrt{3})) < 0$ by Proposition 2.4. Equation (10.1) then gives $J_{\mathrm{sym}}(a(\sqrt{3})) \neq 0$. Since $\sqrt{3} \in (h_c, h_f)$ (Lemma 10.3(a) and Proposition 10.6(b)), also $\mathsf{M}'(\sqrt{3}) \neq 0$. Hence the quotient $J_{\mathrm{sym}}(a(h))/\mathsf{M}'(h)$ is continuous and nonvanishing near $\sqrt{3}$. It agrees with χ_{s} of Lemma 10.4 for $h \neq \sqrt{3}$ and extends it to a continuous nonvanishing function on (h_c, h_1) with $J_{\mathrm{sym}}(a(h)) = \chi_{\mathrm{s}}(h)\mathsf{M}'(h)$.

Equation (10.1) and Lemmas 10.4 and 10.5 show that $J(a(h)) = \chi_{\mathrm{s}}(h)\chi_{\mathrm{a}}(h)\,\mathsf{M}'(h)\,\mathsf{D}(h)$ on (h_c, h_1). Here $\chi_{\mathrm{s}}\chi_{\mathrm{a}}$ is continuous and nonvanishing. The factor M' vanishes only at h_f and changes sign there. The factor D vanishes only at h^{**} and changes sign there, by Proposition 10.6(c) and $1.60 < h^{**} < 1.75$. Proposition 10.6(b),(c) shows that $h^{**} < \sqrt{3} < h_f$. It follows that $J(a(h))$ vanishes exactly at h^{**} and h_f and changes sign at both. As $J(a(\sqrt{3})) < 0$, we get $J < 0$ on (h^{**}, h_f) and $J > 0$ on (h_c, h^{**}) and on (h_f, h_1). This proves (2).

The bounds of (3) are Proposition 10.6(d). Finally $m^* = (81 + 64\sqrt{3})/249 = 0.7704\ldots$ and $(m^*)^{-3} = 2.1862\ldots$ □

10.6. **The counts.**

Corollary 10.7. *Let* $m_4 > 0$.

(a) $c_4(1, 1, 1, m_4) = 4$ *for* $m_4 \neq m^*$, *and* $c_4(1, 1, 1, m^*) = 1$.
(b) $c_1 = c_2 = c_3$, *and this number is* 2 *for* $m_4 \in (0, m^{**}]$, 4 *for* $m_4 \in (m^{**}, m_f)$, 3 *for* $m_4 = m_f$, *and* 2 *for* $m_4 \in (m_f, \infty)$.
(c) $N(1, 1, 1, m_4)$ *is* 38 *on* $(0, m^*)$, 32 *at* m^*, 38 *on* $(m^*, m^{**}]$, 50 *on* (m^{**}, m_f), 44 *at* m_f, *and* 38 *on* (m_f, ∞). *These are the values of Table 6.*

(d) $(1,1,1,m_4) \in Z_4$ *if and only if* $m_4 = m^*$, *and for* $i \in \{1,2,3\}$, $(1,1,1,m_4) \in Z_i$ *if and only if* $m_4 \in \{m^{**}, m_f\}$.

Proof. As the permutations of the bodies 1, 2, 3 preserve the masses, $c_1 = c_2 = c_3$, and $(1,1,1,m_4)$ lies either in all of Z_1, Z_2, Z_3 or in none of them. We consider body 1 and the map F_1 of Section 10.1. Then $\mu' := \mu^{(1)}(m) = (0, 0, \log m_4)$ has the coordinates $P = 0$, $A = \frac{1}{3}\log m_4$, $Q = -\frac{2}{\sqrt{6}}\log m_4$ and $\rho = |Q|$, with $\Theta = 90°$ for $m_4 < 1$ and $\Theta = 270°$ for $m_4 > 1$.

Step 1: the fibre. Recall that F_1, like F, is injective on $\overline{\mathcal{D}}$ (Theorem 6.19). As σ fixes μ', it maps $F_1^{-1}(\mu')$ to itself. Let $p \in F_1^{-1}(\mu')$ with $\sigma p \neq p$. Then $J(\sigma p) = J(p)$, and $J(p) > 0$: otherwise p and σp would be two points of $\overline{\mathcal{D}}$ with the same image. The points of the fibre off Ω_1^σ form pairs $\{p, \sigma p\}$ with $J > 0$. The points of the fibre on Ω_1^σ are the symmetric concave CCs of the masses $(1,1,1,m_4)$ with body 1 inside, that is, by Theorem 10.1(1), the points $a(h)$ with $\mathsf{M}(h) = m_4$. By Theorem 10.1(2) there are two of them for $0 < m_4 < m_f$ (one with $h < h_f$ and one with $h > h_f$), one for $m_4 = m_f$ and none for $m_4 > m_f$.

Step 2: the critical values. The point μ' is a critical value of F_1 if and only if $m_4 \in \{m^{**}, m_f\}$. Indeed, $a(h^{**})$ and $a(h_f)$ are preimages of $\mu^{(1)}(1,1,1,m^{**})$ and $\mu^{(1)}(1,1,1,m_f)$ with $J = 0$, by Theorem 10.1(2). Conversely, let $q \in F_1^{-1}(\mu')$ with $J(q) = 0$. Then q and σq lie in $\overline{\mathcal{D}}$ and have the same image, forcing $q = \sigma q$ by injectivity. By Step 1, $q = a(h)$ with $\mathsf{M}(h) = m_4$. Then, by Theorem 10.1(2), $J(a(h)) = 0$ implies $h \in \{h^{**}, h_f\}$. This proves (d) for $i = 1$.

Step 3: the regular values. Let $m_4 \notin \{m^{**}, m_f\}$. Step 2 shows that μ' is a regular value. Recall from Theorem 6.34 that at a regular value $c_1 = 2 + 2n_-$, where n_- is the number of preimages with $J < 0$. Step 1 identifies n_- with the number of points $a(h)$ with $\mathsf{M}(h) = m_4$ and $J(a(h)) < 0$. For $0 < m_4 < m^{**}$, Theorem 10.1(2) shows that the two such points have $h < h^{**}$ and $h > h_f$, so $J > 0$ at both and $c_1 = 2$. For $m^{**} < m_4 < m_f$ they have $h^{**} < h < h_f$ and $h > h_f$. Then $n_- = 1$ and $c_1 = 4$. For $m_4 > m_f$ there are none, so $c_1 = 2$.

Step 4: the critical values. At $m_4 = m^{**}$ we have $A = \frac{1}{3}\log m^{**} < 0 < A^*$ and $\Theta = 90°$. As μ' is a critical value, $\rho = R(A, \Theta)$ by Theorem 1. This is the cuspidal edge, where $c_1 = 2$ by Theorem 1. At $m_4 = m_f$ we have $0 < A = \frac{1}{3}\log m_f < -\log m^* = A^*$ by Theorem 10.1(3), $\Theta = 270°$, and again $\rho = R(A, \Theta)$. This is the fold sheet, where Theorem 1 gives $c_1 = 3$.

Step 5: body 4, and N. The point $\mu^{(4)}(m) = -(\log m_4)(1,1,1)$ has $\rho = 0$ and $A = -\log m_4$. For $m_4 \neq m^*$ we have $A \neq A^*$ and $\rho = 0 < R(A, \Theta)$ for all Θ. Theorem 1 then gives $c_4 = 4$ and shows that $\mu^{(4)}$ is a regular value. For $m_4 = m^*$ we have $(A, \rho) = (A^*, 0)$, so $c_4 = 1$ by Theorem 1 (Proposition 7.11). This value is critical: it is the image of the umbilic p^*, where $J = 0$. This proves (a) and (d). Finally $N = 12 + 6 + 2(c_1 + c_2 + c_3 + c_4)$ by Theorem 2, and $m^* < m^{**}$ by Theorem 10.1(3). Substituting the counts, we obtain (c): $18 + 2(6 + 4) = 38$, $18 + 2(6 + 1) = 32$, $18 + 2(12 + 4) = 50$ and $18 + 2(9 + 4) = 44$. □

Theorem 10.1(3) rests on the resultants of Section 10.4. The certificate without resultants does not give these values, but the decimals of m^{**} and m_f printed in Theorem 2(e) also follow without resultants. The program `family.py` (README of the supplement) certifies, by the procedure of Section 9.1, opposite statuses of body 1 at the two ends of each of two intervals of width $5.4 \cdot 10^{-25}$. Steps 1–3 of the proof above do not use Theorem 10.1(3). These steps show that c_1 changes only at m^{**} and m_f, so one interval contains m^{**} and the other m_f.

As a check, floating-point counts of all concave CCs with body 1 inside, by Newton's method from many starting points, both in the variables of the mass map and in Cartesian coordinates, agree with Corollary 10.7(b) at all sampled values of m_4, including the signs of J.

10.7. **Relation to earlier work.** Bernat, Llibre and Pérez-Chavela [BLP09] computed numerically the number of kite CCs of the masses $(1,1,1,m_4)$ and the values of m_4 at which it changes.

Rusu and Santoprete counted all CCs of these masses numerically and obtained the values of N in Table 6 [RS16, §4.2]. They note [RS16, §4.3] that their value of the fold bifurcation differs slightly from that of [BLP09]. In [RS16, §§4.3–4.4] they certified the two degenerate CCs by a Krawczyk computation [Kra69] on the full system of Dziobek equations together with the determinant of its Jacobian matrix. Their enclosures, printed as 1.00266054757261000068580350? and 0.99184227439094091554349?, contain the values of Theorem 10.1(3). They also proved that the bifurcations at m_f and at m^{**} are a fold and a supercritical pitchfork. Liu, Poudel, Raut and Xie [LPRX26] classify the concave kite CCs of three equal masses by a computer-assisted proof with interval arithmetic and the Krawczyk operator. For a unit body inside, which is their outer case, they show that the symmetric CCs form a one-parameter family [LPRX26, Lemmas 3.1–3.2], by the argument of Lemma 10.3(a) in other coordinates. They show that there are two such CCs for $m_4 < m_f$, one for $m_4 = m_f$ and none for $m_4 > m_f$ [LPRX26, Theorem 1.2]. They also show that the mass has a unique maximum m_f along the family (their m_O) and that this maximum is a fold in the reduced symmetric space [LPRX26, §§3.2–3.3]. For the body of mass m_4 inside, which is their inner case, the kite CCs with a given axis are the equilateral one and one isosceles family. Shi and Xie [SX10, Theorem 1.4] obtained this description of the inner case, as [LPRX26, Remark 1.3] points out. The computer-assisted proof of [LPRX26] rederives it in other variables. It finds two CCs for $m_4 \neq m^*$, one for $m_4 = m^*$ and a transcritical bifurcation at m^* in the reduced space [LPRX26, Theorem 1.2 and §4.3]. The asymmetric CCs and the pitchfork at m^{**} are treated numerically in [LPRX26, §5]. In [LPRX26, §3.2] the value of m_f is printed as 1.00266054757261000068580350216? and stated to lie in $[1.\cdots21,\ 1.\cdots22]$. In SageMath's convention the printed value denotes $[1.\cdots350215,\ 1.\cdots350217]$, which excludes m_f (its 29th decimal is 8); read at 28 decimals, the stated interval contains m_f. Relative to [RS16], the uniqueness of the fold point and of the pitchfork point on the whole arc is new here, and relative to [LPRX26] the uniqueness of the pitchfork point. The counts of Corollary 10.7, which include the asymmetric CCs, are new as theorems.

m_4	N	c_4; $c_1 = c_2 = c_3$
$(0, m^*)$	38	4; 2
m^*	32	1; 2
$(m^*, m^{**}]$, $m^{**} = 0.99184227\ldots$	38	4; 2
(m^{**}, m_f), $m_f = 1.00266054\ldots$	50	4; 4
m_f	44	4; 3
(m_f, ∞)	38	4; 2

TABLE 6. The counts for the masses $(1, 1, 1, m_4)$, which Corollary 10.7 proves, with $m^* = (81 + 64\sqrt{3})/249$ and m^{**}, m_f as in Theorem 10.1. The table of [RS16] lists, in place of N, the number $(N - 12)/2$ of solutions of the Dziobek equations; its column of geometrically different CCs counts a configuration and its mirror image once.

11. Degenerate concave central configurations

In this section we relate the degeneracy of a concave CC to the mass map and prove the lemma used for Theorem 2(f). Let $\varphi_0(r) = r^{-1} + r^2/2$ and $V_m(x) = \sum_{i<j} m_i m_j \varphi_0(r_{ij})$ on $(\mathbb{R}^2)^4$. From $\varphi_0'(r)/r = -(r^{-3} - 1)$ we get

$$\frac{\partial V_m}{\partial x_j} = m_j \sum_{i \neq j} m_i S_{ij}(x_i - x_j),$$

and the critical points of V_m are the solutions of (2.1) with $\lambda' = 1$. As V_m is invariant under the isometries of the plane, at a critical point x the tangent space $\mathfrak{o}_x$ of the orbit of the group $SE(2)$, of dimension 3, lies in $\ker \operatorname{Hess} V_m(x)$. We call x *nondegenerate* if $\ker \operatorname{Hess} V_m(x) = \mathfrak{o}_x$. We call $\dim \ker \operatorname{Hess} V_m(x) - 3$ its *nullity*. This is the usual notion. Indeed $V_m = U + \frac{M}{2} I_m$, with I_m the moment of inertia about the centre of mass. At a critical point x the Hessian of V_m on configurations with centre of mass 0 is block diagonal for the splitting $\mathbb{R}x \oplus T_x\{I_m = I_m(x)\}$. The radial entry is $2U(x) + MI_m(x) > 0$; the tangential block is the Hessian of U restricted to the sphere $\{I_m = I_m(x)\}$. The mixed terms vanish: $dV_m(tx) = t^{-2} dU(x) + \frac{M}{2} t\, dI_m(x)$ vanishes on $T_x\{I_m = I_m(x)\}$ for all t.

Moeckel states that a Dziobek configuration is a nondegenerate critical point if and only if it has a smooth continuation to nearby masses and the map to mass space is a local diffeomorphism [Moe14, §14]. He justifies this by the implicit function theorem, an argument that covers the direction from nondegeneracy to the local diffeomorphism. The following lemma gives a complete proof of both directions for concave configurations, through the transversality of the CC equations, and adds the identity between the nullity and $\dim \ker dF$.

Lemma 11.1. *Let x be a concave CC with body 4 inside, normalized by $\lambda' = 1$, with spokes $a \in \Omega_4$ and masses $m = (e^{F(a)}, 1)$. Then the nullity of x equals $\dim \ker dF(a)$. In particular, x is degenerate if and only if $J(a) = 0$.*

Proof. We first pass to a slice. Let $\mathcal{Y} = \{x \in (\mathbb{R}^2)^4 : \ x_4 = 0, \ x_1 \in (0, \infty) \times \{0\}\}$, an open subset of a linear subspace of dimension 5, which is transverse to the orbits of $SE(2)$ at the configurations with $x_1 \neq x_4$ and meets each of them once. Each point of Ω_4 determines a configuration $y(a) \in \mathcal{Y}$ in which body 2 lies on the counterclockwise side of x_1, say. This map $a \mapsto y(a)$ is analytic and injective. It is an immersion, since the spokes are functions of y. Put $m' = (m_1, m_2, m_3)$ with $m_4 = 1$, and $\mathcal{E}(y, m') = \nabla(V_m|_{\mathcal{Y}})(y) \in \mathbb{R}^5$. Then $\mathcal{E}(y(a), m'(a)) = 0$ with $m'(a) = e^{F(a)}$ (Lemma 2.1). As $\mathbb{R}^8 = T_y\mathcal{Y} \oplus \mathfrak{o}_y$ and V_m is invariant, the critical points of $V_m|_{\mathcal{Y}}$ are those of V_m, and $\ker \operatorname{Hess} V_m(y) = \ker \operatorname{Hess}(V_m|_{\mathcal{Y}})(y) \oplus \mathfrak{o}_y$. The nullity of x is then $\dim \ker \mathcal{H}$, where $\mathcal{H} = \operatorname{Hess}(V_m|_{\mathcal{Y}})(y_0)$ and $y_0 = y(a)$.

Next we show that $D\mathcal{E}$ is onto. We have $D\mathcal{E}(y_0, m_0') = [\mathcal{H} \mid \mathcal{B}]$ with $\mathcal{B}e_k = \nabla_y U_k$, where $U_k = \partial V_m / \partial m_k = \sum_{j \neq k} m_j \varphi_0(r_{kj})$. Let $\dot{x} \in T_{y_0}\mathcal{Y}$ be orthogonal to the image of $D\mathcal{E}$. Then $\mathcal{H}\dot{x} = 0$, which puts $\dot{x}$ in $\ker \operatorname{Hess} V_m(y_0)$. Moreover $dU_k(\dot{x}) = 0$ for $k = 1, 2, 3$. Since $\sum_k m_k U_k = 2V_m$ and $dV_m(y_0) = 0$, also $dU_4(\dot{x}) = 0$. Write $Z_{kj} = (x_k - x_j) \cdot (\dot{x}_k - \dot{x}_j)$, a symmetric matrix with zero diagonal. Recall Dziobek's relations $m_k m_j S_{kj} = \kappa \Delta_k \Delta_j$ from the proof of Lemma 2.1, where $\kappa \neq 0$ and $\Delta = (S_1, S_2, S_3, -S)$. They give

$$dU_k(\dot{x}) = -\sum_{j \neq k} m_j S_{kj} Z_{kj} = -\frac{\kappa \Delta_k}{m_k} (Z\Delta)_k,$$

and since $\kappa \Delta_k / m_k \neq 0$, we get $Z\Delta = 0$. The linear map $Z \mapsto Z\Delta$ from symmetric matrices with zero diagonal to $\mathbb{R}^4$ has rank 4. Indeed, with $f_k = e_k / \Delta_k$, the six elementary matrices have the images $\Delta_j e_k + \Delta_k e_j = \Delta_j \Delta_k (f_k + f_j)$. They span $\mathbb{R}^4$ because the vectors $f_k + f_j$ do, the complete graph on four vertices not being bipartite. The kernel $\{Z : Z\Delta = 0\}$ has dimension $6 - 4 = 2$. For a symmetric 2×2 matrix M, the infinitesimal deformation $\dot{x}_j = Mx_j$ has $Z_{kj} = (x_k - x_j) \cdot M(x_k - x_j)$ and $(Z\Delta)_k = \sum_j \Delta_j x_j \cdot Mx_j =: c_M$, independent of k by $\sum_j \Delta_j = 0$ and $\sum_j \Delta_j x_j = 0$. The map $M \mapsto Z$ is injective: the six vectors $x_k - x_j$ of a configuration with no three bodies collinear have at least three pairwise independent directions, and a quadratic form on $\mathbb{R}^2$ that vanishes on three such directions is zero. Also $c_I = \sum_{i \leq 3} S_i a_i^2 > 0$ because $x_4 = 0$. Hence $\{M : c_M = 0\}$ has dimension 2, so its image is all of $\{Z : Z\Delta = 0\}$. Each $\dot{x}$ with $Z\Delta = 0$ is then of the form $\dot{x} = Mx + \zeta$ with $c_M = 0$ and $Z(\zeta) = 0$. Such a ζ is an infinitesimal

isometry: the framework of the six segments on a configuration with no three bodies collinear is infinitesimally rigid in the plane, since the triangle $x_1x_2x_3$ is and x_4 is joined to it by three bars that are not all parallel. Now

$$\operatorname{Hess} V_m[\xi,\xi] = \sum_{i<j} m_i m_j \big(3r_{ij}^{-3}(u_{ij}\cdot\xi_{ij})^2 - S_{ij}|\xi_{ij}|^2\big), \qquad \xi_{ij}=\xi_i-\xi_j, \quad u_{ij}=\frac{x_i-x_j}{r_{ij}},$$

by $\varphi_0'' - \varphi_0'/r = 3r^{-3}$. For $\xi = Mx$ the second sum is $-\kappa\sum_{i<j}\Delta_i\Delta_j|\xi_i-\xi_j|^2 = \kappa\big|\sum_i \Delta_i\xi_i\big|^2 = \kappa\big|M\sum_i\Delta_i x_i\big|^2 = 0$, by $\sum_i\Delta_i=0$ and $\sum_i\Delta_i x_i = 0$. Hence

$$\operatorname{Hess} V_m[\dot x,\dot x] = \operatorname{Hess} V_m[Mx,Mx] = 3\sum_{i<j} m_i m_j\, r_{ij}^{-1}(u_{ij}\cdot Mu_{ij})^2,$$

which vanishes only for $M=0$. As $\dot x \in \ker \operatorname{Hess} V_m(y_0)$, we get $M=0$ and $\dot x = \zeta \in T_{y_0}\mathcal{Y}\cap \mathfrak{o}_{y_0} = 0$. Thus $D\mathcal{E}$ has rank 5.

By the implicit function theorem, $\mathcal{E}^{-1}(0)$ is, near (y_0, m_0'), an analytic 3-manifold with tangent space $\ker D\mathcal{E}$. It contains the image of $a\mapsto (y(a), m'(a))$ near a. This image is an injectively immersed 3-manifold, hence an open subset of $\mathcal{E}^{-1}(0)$. The tangent spaces of this image give $\ker D\mathcal{E} = \{(dy(w), dm'(w)) : w\in\mathbb{R}^3\}$. Now $\ker\mathcal{H}\times\{0\} = \ker D\mathcal{E}\cap(\mathbb{R}^5\times\{0\})$. Since $dm' = \operatorname{diag}(m')\,dF$, the vector $(dy(w), dm'(w))$ lies in $\mathbb{R}^5\times\{0\}$ if and only if $dF(a)w = 0$. With dy injective, $\dim\ker\mathcal{H} = \dim\ker dF(a)$. □

Together with Theorem 2(f), Lemma 11.1 implies that Palmore's configuration has nullity 2, in agreement with [Pal75, MS88]. Recent work treats the degeneracy of planar CCs from other points of view. Sun, Xie and You [SXY25] compare four formulations of degeneracy in the full configuration space and show, among other examples, that the equilateral triangle with a central mass is degenerate exactly at Palmore's mass ratio. Zhou and Xia [ZX26] split the Hessian at a regular n-gon with a central mass into blocks by the dihedral symmetry and find the degenerate central masses, recovering Palmore's value for $n=3$. For kites, Roberts [Rob25, §6.2 (arXiv version)] noted that the derivative of the mass map restricted to concave kites has rank one at the degenerate kites.

12. Comparison with known results

We compare our results with Palmore's degeneracy, known lower bounds and two limiting problems, and we describe the surface of critical values near its vertex. Section 10.7 compares Corollary 10.7 with earlier work on the masses $(1,1,1,m_4)$.

For all m_4, the equilateral triangle with body 4 at its centre is a CC of the masses $(1,1,1,m_4)$. Each physical point of the axis is this triangle (Lemma 2.3(a)). These points correspond one-to-one to the values of m_4 by Lemma 2.3(c). Palmore [Pal73, Pal75] showed that m^* is the only value of the central mass for which this configuration is degenerate, and that its nullity there is 2. Meyer and Schmidt reproduced the uniqueness [MS88, (4.6)]. Proposition 2.4 and Lemma 11.1 recover both facts from our mass map. On the axis $J = \partial_s A\cdot\lambda_{\mathrm{ax}}^2$ vanishes only at s^*, where $m_4/m = m^*$. The nullity there is $\dim\ker dF(p^*) = 2$. The square λ_{ax}^2 matches the squared factor $(249m_4 - 64\sqrt{3} - 81)^2$ of the Jacobian determinant that Meyer and Schmidt compute along the same family in other coordinates [MS88, (4.6)]. The same squared factor appears in the determinants of Sun, Xie and You [SXY25]. In our coordinates the square has a direct reason: by the symmetry, $\partial(P,Q)/\partial(x,y) = \lambda_{\mathrm{ax}} I$ on the axis (Lemma 2.3(d)). At p^*, where $\lambda_{\mathrm{ax}}=0$, both directions orthogonal to the axis lie in the kernel of $dF(p^*)$. The bracket $[s_a, s_b]$ that the certificates use (Section 2.4) has width $1.1\cdot10^{-16}$ and contains s^*. At s_a the mass ratio of Lemma 2.3(c) is $m_4/m = 0.7704869545558552025\ldots$, at s_b it is $0.7704869545558561869\ldots$, and $m^* = 0.7704869545558560111\ldots$ lies between them. This agreement also tests on the axis

the formulas for P and Q of the fold-core certificates, since we compute λ_{ax} at s_a and s_b with these formulas. Finally $A^* = -\log m^* = 0.2607325555063045247\ldots$

Hampton and Moeckel proved that there are always at least 14 concave relative equilibria, and at least 16 unless exactly three of the masses are equal [HM06, Prop. 4], refining the main result of Hampton's thesis [Ham02]. Theorem 2(b) sharpens these bounds: the number $N-18 = 2\sum_i c_i$ of concave CCs is 14 exactly at the Palmore mass vectors and at least 16 for all other masses, also when exactly three masses are equal. With Theorem 2(a), the lower bound 32 of [HM06] is attained exactly at the Palmore mass vectors.

When the mass of the inner body tends to 0, the limit is the planar restricted problem with equilateral primaries. It has 8, 9 or 10 relative equilibria [BL14, FTZ24]. Off its bifurcation curve, 4 or 2 of them lie inside the triangle of the primaries [Bar08, §5.2 and Teor. 45–46], since the 6 outside it are nondegenerate [Bar08, Teor. 18–19], so that their number is constant. The base value of Section 6.9 lies in this limit. For A large, the concave CCs with body 4 inside correspond one-to-one to the interior equilibria of the restricted problem with the outer masses given by G_0, if these equilibria are finitely many and nondegenerate (Proposition 6.29). When the inner mass tends to ∞, the limit is the (1+3)-body problem. There the number of non-convex relative equilibria, counted with mirror images identified, is 4 or 2 off the bifurcation curve, under the assumption of distinct limiting positions for the small masses [CCLM15, Theorem 3 and its proof]. In both limits these are the two values that Theorem 1 allows for c_4 off the surface of critical values.

Near its vertex $(A^*, 0)$ the surface of critical values is thin. Proposition 12.1 shows that, as $A \to A^*$, the curve C_A is close to a deltoid of size proportional to $(A-A^*)^2$, as the leading-order model $G \approx \lambda_{\mathrm{ax}}(s) z + i\gamma(s^*)\bar{z}^2$ of Section 7.5 suggests. The cusps of this deltoid, at $\Theta = 90^\circ$, 210° and 330°, are three times as far from the axis as its closest points. We compute R in floating point at all integer degrees of Θ and certify its values at $\Theta = 90^\circ$ and 270° with the mirror system of Section 9.1. Numerically, these values agree with the deltoid (Figure 1 shows the certified ones). At $|A - A^*| = 10^{-3}$ the certified ratio $R(A, 90^\circ)/R(A, 270^\circ)$ is 3.00000004. At the same levels the floating-point profile $R(A,\Theta)/(A-A^*)^2$ differs by at most $3.6 \cdot 10^{-4}$, relative, from that of the deltoid with smallest radius $\kappa_s = \lambda'_{\mathrm{ax}}(s^*)^2/(4|\gamma(s^*)|\,\partial_s A(s^*)^2) = 0.0351137\ldots$. The certified values $R(A, 90^\circ)$ and $R(A, 270^\circ)$ exceed $3\kappa_s(A-A^*)^2$ and $\kappa_s(A-A^*)^2$, respectively, by the relative amount $3.12 \cdot 10^{-4}$ at $A = A^* + 10^{-3}$. They fall short of these values by the same relative amount at $A = A^* - 10^{-3}$.

Proposition 12.1 (deltoid limit)**.** *Let $\nu^* = \lambda'_{\mathrm{ax}}(s^*)/\partial_s A(s^*)$ and $\gamma^* = \gamma(s^*)$, so that $\kappa_s = (\nu^*)^2/(4|\gamma^*|)$. The image of the circle $|\zeta| = \nu^*/(2|\gamma^*|)$ under the map $f(\zeta) = \nu^*\zeta + i\gamma^*\bar{\zeta}^2$ of $\mathbb{C}$ is a deltoid that meets every ray from the origin exactly once. Let $R_{\mathrm{d}}(\Theta)$ be the distance from the origin to the point of this deltoid on the ray of angle Θ. Then $\kappa_s \le R_{\mathrm{d}} \le 3\kappa_s$. The maximum $3\kappa_s$ is attained at $\Theta \in \{90^\circ, 210^\circ, 330^\circ\}$ and the minimum κ_s at $\Theta \in \{30^\circ, 150^\circ, 270^\circ\}$. Moreover $R(A,\Theta)/(A-A^*)^2 \to R_{\mathrm{d}}(\Theta)$ as $A \to A^*$, uniformly in $\Theta \in S^1$.*

Proof. The deltoid. Propositions 2.4 and 2.6 show that $\nu^* > 0$ and $\gamma^* < 0$. Put $r_0 = \nu^*/(2|\gamma^*|)$ and $w(\varphi) = 2e^{i\varphi} - ie^{-2i\varphi}$. Then $f(r_0 e^{i\varphi}) = \kappa_s\, w(\varphi)$, and $w(\varphi) = e^{-i\pi/6}(2e^{it} + e^{-2it})$ for $t = \varphi + \pi/6$. So the image of the circle is the deltoid $\{2e^{it} + e^{-2it} : t \in \mathbb{R}\}$, scaled by κ_s and turned through -30°. Moreover

$$|w(\varphi)|^2 = 5 - 4\sin 3\varphi, \qquad \operatorname{Im}\bigl(w'(\varphi)\,\overline{w(\varphi)}\bigr) = 2 + 2\sin 3\varphi.$$

So $1 \le |w| \le 3$. The derivative $\operatorname{Im}(w'\bar{w})/|w|^2$ of the argument of w is positive except at three points. The argument increases by 360° in total, since $|2e^{i\varphi}| > |e^{-2i\varphi}|$. It is therefore a homeomorphism of S^1. Thus the deltoid meets every ray from the origin once, and R_{d} is continuous. Where $\sin 3\varphi = -1$ we have $w(\varphi) = 3e^{i\varphi}$, and where $\sin 3\varphi = 1$ we have $w(\varphi) = e^{i\varphi}$.

As R_{d} takes the value $\kappa_s|w(\varphi)|$ at the argument of $w(\varphi)$, this gives the extreme values of R_{d} and their positions.

The level sets near p^*. Put $\delta = A - A^*$. As $\partial_s A < 0$ on the axis (Lemma 2.3(c)), near p^* the level set $\{A = A^* + \delta\}$ is the graph $s = s(A^* + \delta, z)$ of a function analytic in (δ, z). For ζ in a compact set and small $\delta \neq 0$ put $\widehat{G}_\delta(\zeta) = \delta^{-2} G(s(A^* + \delta, \delta\zeta), \delta\zeta)$. As a function of (δ, ζ) it extends real-analytically to $\delta = 0$, where it equals $f(\zeta)$. Indeed, write $G = \lambda z + c\bar{z}^{\,2} + E$ as in Lemma 2.5. First, $\lambda(s)$ is $s - s^*$ times an analytic function that equals $\lambda'_{\mathrm{ax}}(s^*)$ at s^*. Second, $s(A^* + \delta, \delta\zeta) - s^*$ is δ times an analytic function of (δ, ζ) that equals $1/\partial_s A(s^*)$ at $\delta = 0$, since $\partial_x A = \partial_y A = 0$ at p^* (Lemma 2.3(d)). Third, the Taylor coefficients of E of order at most 2 in (x, y) vanish, since $|E| \le C_E|z|^3$. So E is a sum of cubic monomials in (x, y) with analytic coefficients; therefore $\delta^{-2}E(s(A^* + \delta, \delta\zeta), \delta\zeta)$ is δ times an analytic function. Hence $\widehat{G}_\delta(\zeta) - \nu^*\zeta - c(s^*)\bar{\zeta}^{\,2}$ is δ times an analytic function of (δ, ζ), where $c(s^*) = i\gamma^*$ by Proposition 2.6. In particular $\widehat{G}_\delta \to f$ in C^1 on compact sets as $\delta \to 0$.

The fold curves near p^*. By the chain rule and the proof of Lemma 2.3(d), $J = \partial_s A \cdot \det D_z g_A(z)$ at the point $(s(A, z), z)$, where $g_A(z) = G(s(A, z), z)$ and D_z is the derivative in (x, y). As $g_A(\delta\zeta) = \delta^2 \widehat{G}_\delta(\zeta)$, this determinant is $\delta^2 j_\delta(\zeta)$, where j_δ is the Jacobian determinant of $\widehat{G}_\delta$. So $j_\delta(z/\delta) = 0$ at the points $(s(A, z), z)$ of Γ_A near p^*.

The fold curves shrink at the rate $|\delta|$. Lemma 8.1(a) shows that Γ_A lies in any given neighbourhood of p^* when $|\delta|$ is small. Near p^* the proof of Proposition 2.6 gives

$$J = \partial_s A \left(\lambda'_{\mathrm{ax}}(s^*)^2 (s - s^*)^2 - 4|c(s^*)|^2 |z|^2\right) + O(\varrho^3), \qquad \varrho = \left((s - s^*)^2 + |z|^2\right)^{1/2}.$$

Since $J = 0$ on Σ and $\partial_s A \neq 0$ near p^*, the bracket is $O(\varrho^3)$ on Σ. Let $C_1 = |\lambda'_{\mathrm{ax}}(s^*)|/|c(s^*)|$. At a point of Σ with $|z| > C_1|s - s^*|$ the bracket is less than $-3|c(s^*)|^2|z|^2$ while $\varrho < (1 + C_1^{-1})|z|$. This is impossible near p^*. So $|z| \le C_1|s - s^*|$ on Σ near p^*. As $A - A^* = \partial_s A(s^*)\,(s - s^*) + O(\varrho^2)$, also $|s - s^*| \le C_2|\delta|$ on Γ_A near p^* for a constant C_2. Hence $|z| \le C|\delta|$ on Γ_A for $C = C_1 C_2$ and small $|\delta|$.

Convergence of the fold curves. The Jacobian determinant of f is $j_0(\zeta) = |f_\zeta|^2 - |f_{\bar{\zeta}}|^2 = (\nu^*)^2 - 4(\gamma^*)^2|\zeta|^2$. As $(\nu^*)^2 = 4(\gamma^*)^2 r_0^2$, we have $|j_0(\zeta)| \ge 4(\gamma^*)^2 r_0 \left||\zeta| - r_0\right|$. Let ϵ_δ be the maximum of $|j_\delta - j_0|$ on the disk $|\zeta| \le C$, divided by $4(\gamma^*)^2 r_0$. Then $\epsilon_\delta \to 0$, and $\left||\zeta| - r_0\right| \le \epsilon_\delta$ for $\zeta = z/\delta$ at every point $(s(A, z), z)$ of Γ_A. In particular $\zeta \neq 0$ for small $|\delta|$.

Convergence of the radius functions. Let C_f be a Lipschitz constant of f on the disk $|\zeta| \le C + r_0$, and put $\eta_\delta = \max_{|\zeta| \le C} |\widehat{G}_\delta - f| + C_f\epsilon_\delta$. Then $\eta_\delta \to 0$. Let $\Theta \in S^1$ and let $(s(A, z), z)$ be the point $\iota(A, \Theta)$ of Γ_A. Put $\zeta = z/\delta$. By the definition of R (Lemma 8.1(b)), $\delta^{-2} R(A, \Theta) e^{i\Theta} = \delta^{-2} G(\iota(A, \Theta)) = \widehat{G}_\delta(\zeta)$. This point lies within η_δ of the point $f(r_0\zeta/|\zeta|)$ of the deltoid, whose modulus is at least κ_s. So the arguments of the two points differ by at most $\arcsin(\eta_\delta/\kappa_s)$ once $\eta_\delta < \kappa_s$. Hence $|\delta^{-2} R(A, \Theta) - R_{\mathrm{d}}(\Theta)|$, the distance from $\delta^{-2} R(A, \Theta) e^{i\Theta}$ to $R_{\mathrm{d}}(\Theta) e^{i\Theta}$, is at most η_δ plus the oscillation of $\vartheta \mapsto R_{\mathrm{d}}(\vartheta) e^{i\vartheta}$ on intervals of length $\arcsin(\eta_\delta/\kappa_s)$. As this map is uniformly continuous, the bound tends to 0, uniformly in Θ. □

One question remains open: whether Theorem 1 has a proof without computer assistance. The obstacle is that the fold has no closed form away from the axis: the sign of J near it is known only box by box. In our proof the interval certificates supply the facts listed at the end of Section 1.3. The closed forms of Section 2.4 replace them only on the axis and at the umbilic.

Appendix A. The corner and fin charts

In each of the charts CH_{110}, $\mathrm{CH}_{\mathrm{fin}}$ and CH_{111} the box coordinates u and the implicit variables v determine a and a solution (θ, K) of $k_1 = k_2 = k_3 = K$ with $\theta_3 = 2\pi - \theta_1 - \theta_2$. The three equations $\Psi(u, v) = 0$ are these equations divided by positive factors. Conversely, each physical

point a of the chart's region, defined below, determines a point $u(a)$ of the chart domain and a solution $v(a)$. With $d = \det \Psi_v$, implicit differentiation gives $d\,\partial\mu/\partial u = \mu_u\, d - \mu_v \operatorname{adj}(\Psi_v)\Psi_u$ and the same formula for a. We evaluate these with the rows of μ and of a multiplied by positive factors or combined by row operations of determinant 1, using logarithmic derivatives in the coordinates of u that tend to 0, none of which changes the signs of the two determinants. By the chain rule, $J = \det(\partial\mu/\partial u)/\det(\partial a/\partial u)$. We write $\mathfrak{g}(t) = (1 + t + t^2)/t^3$, so that $t^{-3} - 1 = (1 - t)\,\mathfrak{g}(t)$.

Uniqueness. For a box of u, we compute an a priori box V^{big} that contains $v(a)$ for all points a of the region with $u(a)$ in the box, or prove that there is no such point. Uniqueness holds if each sub-box of an adaptive subdivision of the box either has an empty a priori box or satisfies $\|I - Y\Psi_v\|_\infty < 1$ over the interval hull of its own a priori box and Krawczyk tube, with Y the inverse of Ψ_v at its centre. Then $\Psi(u, \cdot)$ has at most one zero in that hull, so that the zero of the Krawczyk step is the only point of the region over u. In CH_{110} and CH_{111}, where u is a function of a alone, uniqueness also holds if the angles of the Krawczyk tube are principal, $0 < \theta_1, \theta_2 < \pi < \theta_1 + \theta_2$, because by Lemma 2.2 the solution with principal angles is unique for each a.

Types. A leaf is of type P if the Krawczyk step succeeds over its box, $\det(d\,\partial\mu/\partial u)$ and $\det(d\,\partial a/\partial u)$ are of definite signs on the box with positive product, and uniqueness holds. Then $J > 0$ at all physical points of the region over the box. A leaf is of type X if the a priori box is empty, or if uniqueness holds and the zero of the Krawczyk step lies outside the region throughout the box, by the tests listed below. Then no physical point of the region lies over the box.

$\mathrm{CH}_{\mathrm{fin}}$*, the fin* $a_1 + a_2 \to 2$. Here $u = (t, a_3, \theta_1)$ with $t = -K$. The implicit variables are $v = (\omega_1, \omega_2, \theta_2)$ with $w_i = t\,\omega_i$ for $i = 1, 2$, so that $a_i = (1 + t\omega_i)^{-1/3}$. The equations are

$$\Psi = \big(\omega_1(q_1 - 1) + 1,\ \omega_2(q_2 - 1) + 1,\ w_3(q_3 - 1) + t\big),$$

and $\mu_1 = \log S_1 + \log\omega_2 + \log w_3 - \log S$, $\mu_2 = \log S_2 + \log\omega_1 + \log w_3 - \log S$, $\mu_3 = \log t + \log S_3 + \log\omega_1 + \log\omega_2 - \log S$. We multiply the row of μ_1 by $\sin\theta_1$ and divide the rows of a_1 and a_2 by t. The region is the set of physical a with $a_1 \geq a_2$, $a_1 + a_2 \geq T_{\mathrm{fin}}$ and $u(a)$ in the domain of the fin cover. We compute the a priori box from bounds valid on this region, as the exact check confirms. The tests for type X are $\omega_1 > \omega_2$ (that is $a_1 < a_2$), $\theta_2 > \pi$, and $a_1 + a_2 < D_X$ for a constant $D_X \leq T_{\mathrm{fin}}$. The last test excludes only points outside the fin.

CH_{110}*, the corner* $a \to (1, 1, 0)$. Here $u = (\varepsilon, \lambda, b)$ with $a_1 = 1 - \varepsilon\lambda b$, $a_2 = 1 - \varepsilon\lambda$ and $a_3 = \varepsilon$. The implicit variables are $v = (\tau, \theta_1, \theta_2)$ with $K = -\varepsilon^2\lambda\tau$. With $H(R) = (1 + R + R^2)/\big(R^{3/2}(1 + R^{3/2})\big)$ and $\Pi(z, \theta) = 2(z + \cos\theta) - \varepsilon(z^2 + 1 + 2z\cos\theta)$, so that $R_1 = 1 - \varepsilon\,\Pi(\lambda, \theta_1)$ and $R_2 = 1 - \varepsilon\,\Pi(\lambda b, \theta_2)$, the equations are

$$\Psi = \big(b\,\mathfrak{g}(a_1)\Pi(\lambda, \theta_1)H(R_1) + \tau,\ \mathfrak{g}(a_2)\Pi(\lambda b, \theta_2)H(R_2) + \tau,\ (1 - \varepsilon^3)(q_3 - 1) + \varepsilon^5\lambda\tau\big),$$

the equations $k_i = K$ divided by $\varepsilon^2\lambda$, $\varepsilon^2\lambda$ and ε^{-3}. The rows of μ are $\sin\theta_1\nabla(\mu_1 - \mu_3)$, $\sin\theta_2\nabla(\mu_2 - \mu_3)$ and $\tau\nabla\mu_3$; the rows of a are divided by $\varepsilon\lambda b$, $\varepsilon\lambda$ and ε. Since no logarithm of ε, λ, b or τ is evaluated, the chart is regular where these vanish. The region is the set of physical a with $a_3 \leq 0.1875$ and $a_1 \geq a_2$. The tests for type X are $\tau \leq 0$ (that is $K \geq 0$), $\theta_1 > \pi$, $\theta_2 > \pi$, and $\theta_1 + \theta_2 < \pi$ (that is $\theta_3 > \pi$).

CH_{111}*, the corner* $a \to (1, 1, 1)$ *and the fin tip.* Here $u = (\varsigma, \lambda, b)$ with $a_1 = 1 - \varsigma\lambda b$, $a_2 = 1 - \varsigma\lambda$ and $a_3 = 1 - \varsigma$. The implicit variables are $v = (\kappa, \theta_1, \theta_2)$ with $K = -\varsigma\lambda\kappa$. The equations are

$$\Psi = \big(b\,\mathfrak{g}(a_1)(q_1 - 1) + \kappa,\ \mathfrak{g}(a_2)(q_2 - 1) + \kappa,\ \mathfrak{g}(a_3)(q_3 - 1) + \lambda\kappa\big),$$

the equations $k_i = K$ divided by $\varsigma\lambda$, $\varsigma\lambda$ and ς. The rows of μ are $\sin\theta_1\nabla(\mu_1 - \mu_3)$, $\sin\theta_2\nabla(\mu_2 - \mu_3)$ and $\kappa\nabla\mu_3$; the rows of a are divided by $\varsigma\lambda b$, $\varsigma\lambda$ and ς. The chart is regular at $\varsigma = 0$, $\lambda = 0$ and

$b = 0$. The region is the set of physical a with $a_3 \geq 1 - 0.1$ and $a_1 \geq a_2 \geq a_3$. The tests for type X are those of CH_{110} with κ in place of τ. A leaf of type D is not evaluated. It is a box in $\hat{r} < 0.184$, where $\hat{r} = |a - s(1,1,1)|/(1-s)$ is the coordinate of chart 3. The points of such a box routed to this cover in Section 5.5 have $1 - s \leq 1/32$ and lie in the top covers.

Data and code availability

The supplement to this paper on Zenodo (doi:10.5281/zenodo.23256905) contains the following parts. The README lists the SHA-256 hashes of the files of the first four parts, directly or through the hash lists of their directories.

- The C and Python sources of the certificates of Section 5, the floating-point fold table of Section 5.3 and the logs of the run described in Section 5.6. The list `cert/runs/SHA256SUMS` contains the hashes of the 80 files of that run, among them 12 arrays that are not included: the 11 covers and the array of pieces of the check of Proposition 5.2(f).
- The programs and logs of the certified computations of Section 9 and of the separately written program of Section 9.2 that re-certifies them. The script `exact/cert/run_all.sh` regenerates the logs of the certified computations in about 20 minutes, and `exact/judge/run_judge.sh` reruns the re-certification.
- The exact computations behind the family theorem of Section 10. The script `analytic1/exact/run_all.sh` reruns the polynomial and resultant computations. It reads the factor $\mathcal{F}$ of Section 10.4 from the file `fold_cache.pkl` if that file is present; after the file is deleted, it recomputes $\mathcal{F}$, with the same result. The program `exact/ref_family/arc_cert.py` is the certificate without resultants. It also certifies Proposition 10.6(a) and the signs in Proposition 10.6(c).
- The scripts `axis_lambda.py`, `axis_jet2.py` and `s3_check.py` and their logs. These scripts check the closed forms of Propositions 2.4 and 2.6 in exact arithmetic. The script `deg_restricted.py`, its log and the module `fullmap.py`, which the script imports for one of its floating-point cross-checks. The script checks in exact arithmetic the identities of Section 6.9 that the text cites by the labels of its checks.
- The sources of the Lean formalization, its certificate files, the programs that regenerate them and the SHA-256 hashes of these files.

A README maps the covers of Table 3 to their files and the labels of the bodies to those of the code. It also states the formulas of the region functions and the floating-point constants of the programs. The covers themselves (about 220 MB) are not included, but the programs regenerate them deterministically. The script `cert/run_checks.sh` regenerates them a second time, compares the two and runs all the checks of Section 5.6. In the regenerated covers the arrays of leaves equal those of the stored ones. The computations use FLINT/Arb 3.4.0 [FLI25, Joh17] with gcc 15.2.0 for the C code, and CPython 3.14.4 with numpy 2.5.3, mpmath 1.3.0 [mpm23], `python-flint` 0.9.0 (with its own FLINT 3.6.0), SymPy 1.14.0, Singular 4.4.1 and msolve 0.9.4. For the floating-point cross-checks we also use SciPy 1.18.1.

The computer-assisted part of the proof assumes the correctness of Arb, of the compiler, of the computer algebra systems and the Python libraries listed above, and of our own programs, whose sizes the README lists. The second evaluation of the leaves in Section 5.6 calls the same compiled libraries as the programs that built the covers, so it detects errors in those programs and in the stored covers but not in the formulas that the libraries evaluate. A separately written program derives the type of each leaf of the fold-core, corner and fin covers from the reproduced enclosures. It recomputes the bounds of the band brackets in exact rational arithmetic. Two of the rigorous checks are independent of the compiled formulas: the leaves excluded by the α-test are retested in mpmath, and all inclusions between regions are verified in exact

rational arithmetic. The values computed by the C code are compared with a second rigorous implementation only in chart 1, at 100 points. There the evaluator of Section 9 reproduces the values of K, $\widehat{A}$, P, Q, $\widetilde{J}$, T_1, T_2, T_3 and J_{mir} computed by the C code (Section 9.2). The other quantities that the proof takes from the C code rest on this one implementation: the derivatives $\partial_r T_3$, $\partial_\varphi^2 T_3$ and $\partial_\varphi^2 \widetilde{J}$ of the band certificates (Section 5.4), the quantities of charts 0, 2, 3 and 4, among them those of the umbilic chart, and the quantities of the bulk, corner and fin charts. The floating-point checks of the covers described in the README compute J independently of the compiled formulas, but only at sample points. The certified computations of Section 9 are re-certified by the separately written program of Section 9.2, which shares no code with the programs of Section 9 except the ball arithmetic. The Lean formalization does not depend on the correctness of any of these programs: in place of Proposition 5.2 it uses facts proved by hand or by certificates of its own, which use a different cover and certify different quantities.

Some computations test the proof but are not part of it: the confirmation of the vanishing coefficients of Lemma 2.5 and of the value of $\gamma(s^*)$ in the proof of Proposition 2.6, the test of the vanishing coefficients at p^* in Section 5.1, the enclosure of A at $s_{eq}(1,1,1)$ in the proof of Proposition 5.2(g), the second proof of Lemma 6.7(b) by the covers, the enclosure of the axis point in Section 9.1, the brackets of the crossing parameters, the comparisons of the evaluator of Section 9 with other programs, the independent re-certification in Section 9.2, the msolve and floating-point checks in Section 10.4, the floating-point counts in Section 10.6, the evaluation of the mass ratio at s_a and s_b and the numerical comparison with the deltoid in Section 12, the floating-point checks of the covers described in the README, and three checks that `cert/run_checks.sh` runs: the condition that $\partial_r K > 0$ wherever $K = 0$ on the leaves of types M, P, F and B in charts 1 and 3, lower bounds for $1 - \zeta_i^2$ and for the Hessian of g_α on a box near the axis together with the location of the root boxes of the lower axis cover, and the largest s, 0.5927734375, of a leaf of type M, F or B on which K is not negative throughout.

The formalization is written in Lean 4 [dMU21], version 4.35.0-rc3, with Mathlib [mC20] at the corresponding tag. The main theorem of the formalization states Theorems 1 and 2 and takes no unproved inputs. For Theorem 1 the formal statement contains the radius function R with its properties, the five rows of Table 1, with Θ defined by one order of the outer bodies, and the description of the critical values for one inner body; for Theorem 2 it contains the formula, in which 12 counts the collinear and 6 the convex CCs, and items (a)–(g). Besides definitions of Mathlib, these statements rest on 124 definitions and one structure of the formalization. The README of the formalization lists the files that contain them and matches each part of the two statements with the paper. The main theorem depends only on the axioms `propext`, `Classical.choice` and `Quot.sound`, and no theorem in the 13,562 modules of its import closure, Mathlib included, depends on another axiom. Beyond these axioms, the formal proof assumes the correctness of the Lean kernel, including its arithmetic of natural numbers. Two kernels implemented separately from Lean's, nanoda 0.4.17 and lean4lean, also accept every declaration on which the main theorem depends, read from an export of the compiled formalization (directory `kernel2` of the formalization). Outside the scratch and experiment directories, which nothing in the proof imports and which are not part of the supplement, the Lean files of the formalization contain no `sorry`, `native_decide`, `implemented_by` or `extern`.

The cover of the formalization, with about 1.19 million leaves, shares only the bounds of its regions with the paper, up to rounding. Most leaves enclose the solution of Lemma 2.2 by a Krawczyk test in half-angle tangents of the angles and the other quantities by Taylor models of order 3 with exact dyadic coefficients; the cones of the umbilic ball use first-order slopes along rays, and the remaining leaves exclude their boxes by algebraic tests. Instead of $\widetilde{J}$ and the other quantities of Section 5.1, the leaves certify signs of the function $\det(I - M_{\mathrm{C}})$ of the remark below

and of its derivatives. Further certificates take the place of the computations of Sections 9 and 10 in the proof of Theorem 2; of Section 9 they certify only the counts of Proposition 9.1 and one mass vector or segment of Table 5 for each value of N from 34 to 48. In all, the kernel checks of the certificates take about 240 CPU-hours, and some modules need up to about 27 GB of memory. Regenerating the certificate files takes about 16 CPU-hours. On the tested platform, CPython 3.14.4 on x86-64 Linux with glibc 2.43, the regenerated files are identical to the hashed ones. Elsewhere a regenerated file may differ, since its hints are rounded floating-point values that depend on the math library, and then the kernel check, not the hash, decides whether it is a valid certificate.

Table 7 lists the items of Proposition 5.2 and the other ingredients of Sections 6 and 7 that rest on the certificates of Section 5, with their counterparts in the formal proof.

Remark (the sign of J in the formal proof). For $a \in \Omega_4$ place the configuration with $x_4 = 0$ and x_1, x_2, x_3 in counterclockwise order, and put $\beta_i = S_i/S$. Give each of its six segments b a vector $\gamma_b \in \mathbb{R}^2$ and a weight v_b: for the spoke $i4$, $\gamma_b = g_i$ and $v_b = a_i^2(1 - a_i^3)\beta_i$, and for the outer side jk, $\gamma_b = g_j + g_k$ and $v_b = R_i(R_i^{3/2} - 1)\beta_j\beta_k$. Here $g_i = n_i/h_i$ is the gradient of $\log S_i$ with respect to x_4, where n_i is the unit normal of the side x_jx_k that points into the triangle and h_i is the distance of x_4 from that side. The weights are positive, and the *compliance matrix*

$$M_{\mathrm{C}} = \frac{1}{3}\sum_b v_b\,(\gamma_b - \bar\gamma)(\gamma_b - \bar\gamma)^{\mathsf{T}}, \qquad \bar\gamma = \frac{\sum_b v_b\gamma_b}{\sum_b v_b},$$

is a symmetric 2×2 matrix that depends on a and θ but on no derivative. The formalization proves that on Ω_4

$$J \det \Psi_{\mathrm{C}} \det \Lambda_{\mathrm{C}} = \det(I - M_{\mathrm{C}}), \qquad \det \Psi_{\mathrm{C}} < 0 < \det \Lambda_{\mathrm{C}},$$

hence $\operatorname{sign} J = -\operatorname{sign}\det(I - M_{\mathrm{C}})$ (theorems `CC50.Compliance.J_mul_det_Psi_mul_det_Lam`, `det_PsiC_neg`, `det_LamC_pos` and `sign_J` in `CC50/Compliance/TheoremC.lean`). Here Λ_{C} maps $\varepsilon \in \mathbb{R}^3$ to $\left(\sum_l \varepsilon_l S_l,\ \sum_l \varepsilon_l S_l x_l\right) \in \mathbb{R} \times \mathbb{R}^2$, so that $\det \Lambda_{\mathrm{C}} = 2S_1S_2S_3S$. The matrix Ψ_{C}, `PsiC` in the same file, maps the three parameters of a load to the elongations of the spokes in the elastic response of the framework formed by the six segments, with stiffnesses that are positive where $K < 0$. The proof has three steps. First, M_{C} is the compliance of this framework for the loads S_1c, S_2c, S_3c and $-Sc$ on the four bodies, $c \in \mathbb{R}^2$, and an exact identity for the flexibility of a framework with one self-stress turns it into the covariance above. Second, for every configuration with body 4 strictly inside the triangle of the others and all positive stiffnesses, the matrix that takes the place of Ψ_{C} is invertible, and its determinant is negative, since these pairs form a connected set and the determinant is negative at one of them. Third, differentiating the CC equations along the family of configurations parametrized by a gives a 3×3 matrix $\mathcal{Q}$ with $\Psi_{\mathrm{C}}\mathcal{Q} = I$ and $T\mathcal{Q} = \Lambda_{\mathrm{C}}\,\partial\mu/\partial a$, where T is block triangular with $\det T = \det(I - M_{\mathrm{C}})$; taking determinants yields the identity.

Apart from the certificates, the formal proof follows Sections 2–4 and 6–11 and, like Section 6, needs no degree theory; it derives Theorem 2(g), however, from $J < 0$ at $s_{eq}(1, 1, 1)$ (Proposition 2.4) and Theorem 6.34 instead of Table 1. Dziobek's relations, the absence of CCs with exactly three bodies collinear and the six convex CCs come from the formalization of [Tom26], which is part of the formal proof, and Moulton's count [Mou10] is proved as well. The closed forms of the factors of J on the axis (Proposition 2.4) and the inequality $c(s^*) \neq 0$ of Proposition 2.6, which the paper checks by computer algebra, are proved in Lean. The formal count at a cusp point (Proposition 7.10) needs F only of class C^3, not real-analytic as in Lemma 7.7(c). Besides Theorems 1 and 2, the formalization proves Theorem 10.1, except the 45-digit values of part (3); for the digits printed in Theorem 2(e) it proves that m^{**} and m_f lie in the two

paper	formal proof	argument
Proposition 5.2(a)	`sStar_bounds`: $s_a \le s^* \le s_b$, from $s^{*3} = 3/(6\sqrt{3}-2)$	without a certificate
Proposition 5.2(b): the covers of Table 3	the cover `Final.coverHyp` with about 1.19 million leaves (directories `CC50/Prod`, `CC50/Chart` and `CC50/Band2`), which certify signs of $\det(I - M_{\mathrm{C}})$ and its derivatives in place of $\widetilde{J}$, T_1, T_2 and T_3; `Agg.certFacts_of_cover` and `Agg.critCertFacts_of_cover` derive from it the certified facts that Sections 6 and 7 use	the paper's
Proposition 5.2(c) and the umbilic chart	a cover of the ball of radius 3/4000 about p^* in W by 275 cones, with slopes along the rays from p^*, where $M_{\mathrm{C}} = I$ (`Chart.UmbCov.umbBall_cover`)	different
Proposition 5.2(d) for leaves of types M, F and B, and (e)	the fields `resolved`, `top` and `star` of `Agg.DFacts`, which every leaf of types M, fold and band carries; `Agg.level_star_of_cover`	the paper's
Proposition 5.2(d) for leaves of type P, in the proof of Lemma 6.7(c)	none: the formal counterparts of Lemmas 6.7(c),(d) and 6.8, `Agg.ray_unique_of_cover` and `Agg.ray_exists_of_cover`, need a resolved leaf only at non-physical limits of physical points with $J \le 0$, and such a limit lies in a leaf of type M, fold or band	different
Proposition 5.2(f)	the half-plane condition on each fold leaf (`Fold.foldLeaf_certFacts`) and each band leaf, with directions given by dyadic coefficients, close to u_L and u_U; `Agg.halfplane_L_of_cover` and `Agg.halfplane_U_of_cover`	the paper's
Proposition 5.2(g)	none: (g) serves only the paragraph after Theorem 2	not used
Proposition 5.2(h) and the leaves of type B of the umbilic cover, in Proposition 7.13(c)	`Ex.Cusp.cuspRayCertFacts`: one certified point on each of the four families of mirror points in W, from a mirror solve in a fold leaf or from one of the band leaves `Band2.Test.bandA0` and `Band2.Test.bandA1`	different
the bound (3.1) of the leaves of type B, used as (7.1)	`Agg.BandFacts`, from `Band2.bandLeaf_facts2`, `Band2.bandLeaf_facts3`, `Chart.topBand_leaf_ok` and `Chart.umbBand_leaf_ok`; `Agg.band_of_cover` combines the bounds as in the proof of Lemma 7.8	the paper's, along straight lines

TABLE 7. The items of Proposition 5.2 and the other ingredients of Sections 6 and 7 that rest on the certificates, and their counterparts in the formal proof. The Lean names are relative to the namespace `CC50`, and M_{C} is the compliance matrix of the remark on the sign of J in the formal proof. "The paper's" means that the formal proof follows the argument of the paper, with certified quantities of its own.

intervals of width $5.4 \cdot 10^{-25}$ of Section 10.6. The formalization does not cover Section 12, in particular the constant κ_s and Proposition 12.1. The README of the formalization lists the other differences from the paper.

The code, the formalization and the data are released under the Apache License 2.0.

Use of AI tools

Generative AI tools were used to find and prove the results, to write the programs and the Lean formalization, and to draft the text.

Funding and competing interests

This research received no specific grant from any funding agency. The author has no competing interests to declare that are relevant to the content of this article.

References

[ACS12] A. Albouy, H. E. Cabral and A. A. Santos, *Some problems on the classical n-body problem*, Celestial Mech. Dynam. Astronom. **113** (2012), 369–375.

[AFS08] A. Albouy, Y. Fu and S. Sun, *Symmetry of planar four-body convex central configurations*, Proc. R. Soc. Lond. Ser. A Math. Phys. Eng. Sci. **464** (2008), 1355–1365.

[AK12] A. Albouy and V. Kaloshin, *Finiteness of central configurations of five bodies in the plane*, Ann. of Math. (2) **176** (2012), 535–588.

[Alb95] A. Albouy, *Symétrie des configurations centrales de quatre corps*, C. R. Acad. Sci. Paris Sér. I **320** (1995), 217–220.

[Alb96] A. Albouy, *The symmetric central configurations of four equal masses*, Contemp. Math. **198** (1996), 131–135.

[Bar08] J. F. Barros, *Configurações centrais no problema restrito dos 4-corpos no plano*, Ph.D. thesis, Universidade Federal de Pernambuco, Recife, 2008.

[BL11] J. F. Barros and E. S. G. Leandro, *The set of degenerate central configurations in the planar restricted four-body problem*, SIAM J. Math. Anal. **43** (2011), 634–661.

[BL14] J. F. Barros and E. S. G. Leandro, *Bifurcations and enumeration of classes of relative equilibria in the planar restricted four-body problem*, SIAM J. Math. Anal. **46** (2014), 1185–1203.

[BLP09] J. Bernat, J. Llibre and E. Pérez-Chavela, *On the planar central configurations of the* 4*-body problem with three equal masses*, Dyn. Contin. Discrete Impuls. Syst. Ser. A Math. Anal. **16** (2009), 1–13.

[CCLM15] M. Corbera, J. M. Cors, J. Llibre and R. Moeckel, *Bifurcation of relative equilibria of the* $(1 + 3)$*-body problem*, SIAM J. Math. Anal. **47** (2015), 1377–1404; preprint of December 3, 2014, `https://www-users.cse.umn.edu/~rmoeckel/research/Bifurcations1+3BP.9.pdf` (numbering of this preprint).

[CCR19] M. Corbera, J. M. Cors and G. E. Roberts, *Classifying four-body convex central configurations*, Celestial Mech. Dynam. Astronom. **131** (2019), Paper No. 34.

[Cha18] J. Chazy, *Sur certaines trajectoires du problème des n corps*, Bull. Astron. **35** (1918), 321–389.

[dMU21] L. de Moura and S. Ullrich, *The Lean 4 theorem prover and programming language*, in: Automated Deduction – CADE 28, Lecture Notes in Comput. Sci. **12699**, Springer, Cham, 2021, 625–635.

[Dzi00] O. Dziobek, *Über einen merkwürdigen Fall des Vielkörperproblems*, Astron. Nachr. **152** (1900), 33–46.

[FLI25] The FLINT team, *FLINT: Fast Library for Number Theory*, version 3.4.0, 2025, `https://flintlib.org`.

[FTZ24] J.-Ll. Figueras, W. Tucker and P. Zgliczyński, *The number of relative equilibria in the PCR4BP*, J. Dynam. Differential Equations **36** (2024), 2827–2877.

[Ham02] M. Hampton, *Concave central configurations in the four-body problem*, Ph.D. thesis, University of Washington, Seattle, 2002.

[HM06] M. Hampton and R. Moeckel, *Finiteness of relative equilibria of the four-body problem*, Invent. Math. **163** (2006), 289–312; preprint of December 17, 2004, `https://www-users.cse.umn.edu/~rmoeckel/research/FinitenessRE4BP.rev.pdf` (numbering of this preprint).

[Joh17] F. Johansson, *Arb: efficient arbitrary-precision midpoint-radius interval arithmetic*, IEEE Trans. Comput. **66** (2017), 1281–1292.

[Kra69] R. Krawczyk, *Newton-Algorithmen zur Bestimmung von Nullstellen mit Fehlerschranken*, Computing **4** (1969), 187–201.

[Kul97] W. Kulpa, *The Poincaré–Miranda theorem*, Amer. Math. Monthly **104** (1997), 545–550.

[Lea03] E. S. G. Leandro, *Finiteness and bifurcations of some symmetrical classes of central configurations*, Arch. Ration. Mech. Anal. **167** (2003), 147–177.

[LPRX26] Y. Liu, N. Poudel, R. Raut and Z. Xie, *Concave kite central configurations in the planar four-body problem with three equal masses*, arXiv:2606.19596 (2026).

[LS09] T.-L. Lee and M. Santoprete, *Central configurations of the five-body problem with equal masses*, Celestial Mech. Dynam. Astronom. **104** (2009), 369–381.

[MB03] K. Makino and M. Berz, *Taylor models and other validated functional inclusion methods*, Int. J. Pure Appl. Math. **4** (2003), 379–456.

[MB32] W. D. MacMillan and W. Bartky, *Permanent configurations in the problem of four bodies*, Trans. Amer. Math. Soc. **34** (1932), 838–875.

[mC20] The mathlib Community, *The Lean mathematical library*, in: Proceedings of the 9th ACM SIGPLAN International Conference on Certified Programs and Proofs (CPP 2020), ACM, 2020, 367–381.

[Mir40] C. Miranda, *Un'osservazione su un teorema di Brouwer*, Boll. Un. Mat. Ital. (2) **3** (1940), 5–7.

[MKC09] R. E. Moore, R. B. Kearfott and M. J. Cloud, *Introduction to Interval Analysis*, SIAM, Philadelphia, PA, 2009.

[Moe01] R. Moeckel, *Generic finiteness for Dziobek configurations*, Trans. Amer. Math. Soc. **353** (2001), 4673–4686.

[Moe14] R. Moeckel, *Lectures on central configurations*, lecture notes of a course at the Centre de Recerca Matemàtica, Barcelona, January 2014 (version of March 20, 2014), `https://www-users.cse.umn.edu/~rmoeckel/notes/CentralConfigurations.pdf`.

[Moe15] R. Moeckel, *Central configurations*, in: J. Llibre, R. Moeckel and C. Simó, Central Configurations, Periodic Orbits, and Hamiltonian Systems, Adv. Courses Math. CRM Barcelona, Birkhäuser, 2015, 105–167.

[Moe90] R. Moeckel, *On central configurations*, Math. Z. **205** (1990), 499–517.

[Moo66] R. E. Moore, *Interval Analysis*, Prentice-Hall, Englewood Cliffs, NJ, 1966.

[Moo77] R. E. Moore, *A test for existence of solutions to nonlinear systems*, SIAM J. Numer. Anal. **14** (1977), 611–615.

[Mou10] F. R. Moulton, *The straight line solutions of the problem of n bodies*, Ann. of Math. (2) **12** (1910), 1–17.

[mpm23] The mpmath development team, *mpmath: a Python library for arbitrary-precision floating-point arithmetic (version 1.3.0)*, 2023, `http://mpmath.org/`.

[MS88] K. R. Meyer and D. S. Schmidt, *Bifurcations of relative equilibria in the* 4- *and* 5-*body problem*, Ergodic Theory Dynam. Systems **8*** (1988), 215–225.

[MZ19] M. Moczurad and P. Zgliczyński, *Central configurations in planar n-body problem with equal masses for* $n = 5, 6, 7$, Celestial Mech. Dynam. Astronom. **131** (2019), Paper No. 46.

[Neu90] A. Neumaier, *Interval Methods for Systems of Equations*, Encyclopedia Math. Appl. **37**, Cambridge Univ. Press, Cambridge, 1990.

[Pal73] J. I. Palmore, *Relative equilibria of the n-body problem*, Ph.D. thesis, University of California, Berkeley, 1973.

[Pal75] J. I. Palmore, *Classifying relative equilibria. II*, Bull. Amer. Math. Soc. **81** (1975), 489–491.

[Rob25] G. E. Roberts, *On kite central configurations*, Nonlinearity **38** (2025), no. 7, Paper No. 075001, arXiv:2411.07867.

[RS16] D. Rusu and M. Santoprete, *Bifurcations of central configurations in the four-body problem with some equal masses*, SIAM J. Appl. Dyn. Syst. **15** (2016), 440–458, arXiv:1412.6443 (numbering of the arXiv version).

[Sar42] A. Sard, *The measure of the critical values of differentiable maps*, Bull. Amer. Math. Soc. **48** (1942), 883–890.

[SX10] J. Shi and Z. Xie, *Classification of four-body central configurations with three equal masses*, J. Math. Anal. Appl. **363** (2010), 512–524.

[Shu71] M. Shub, *Appendix to Smale's paper: Diagonals and relative equilibria*, in: Manifolds–Amsterdam 1970, Lecture Notes in Math. **197**, Springer, 1971, 199–201.

[Sim78] C. Simó, *Relative equilibrium solutions in the four body problem*, Celestial Mech. **18** (1978), 165–184.

[Sma98] S. Smale, *Mathematical problems for the next century*, Math. Intelligencer **20** (1998), 7–15.

[SXY25] S. Sun, Z. Xie and P. You, *Degeneracy of planar central configurations in the N-body problem*, arXiv:2510.25649 (2025).

[Tom26] T. S. Tomar, *Uniqueness of four-body convex central configurations for all masses*, arXiv:2609.35632 (2026); Zenodo, doi:10.5281/zenodo.23004306 (all versions).

[Tuc11] W. Tucker, *Validated Numerics: A Short Introduction to Rigorous Computations*, Princeton Univ. Press, Princeton, NJ, 2011.

[Whi55] H. Whitney, *On singularities of mappings of Euclidean spaces. I. Mappings of the plane into the plane*, Ann. of Math. (2) **62** (1955), 374–410.

[Win41] A. Wintner, *The Analytical Foundations of Celestial Mechanics*, Princeton Math. Ser. **5**, Princeton Univ. Press, Princeton, NJ, 1941.

[Xia04] Z. Xia, *Convex central configurations for the n-body problem*, J. Differential Equations **200** (2004), 185–190.

[ZX26] T. Zhou and Z. Xia, *On the degeneracy of the central configuration formed by a regular n-gon with a central mass*, arXiv:2604.04610 (2026).

Independent researcher
ORCID: https://orcid.org/0000-0003-4668-3639